International Benchmark
VeRCoRs 2018

Benchmark workshop
Modeling the behaviour of the VeRCoRs mock-up

Program & Abstracts
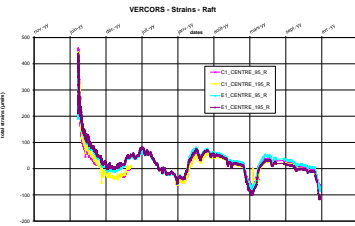
Foreword

Long term operation of its nuclear fleet is the major industrial stake for EDF Group in the coming 20 years. Some major steps forwards on the subject were already accomplished in the UK. In France the EDF objective is to guarantee that it will be possible to operate safely its units up to 60 years. In order to meet this objective, EDF has made the decision to deploy a heavy investment program identified under the name of "Grand Carénage" in order to operate maintenance and upgrade of its plants so has to guaranty a safe operation up to 60 years. This program includes implementation of safety upgrades triggered by the lessons learnt from the Fukushima-Daïchi accident.

In PWR NPPs such as operated by EDF, practically every component can be replaced, with the exception of the reactor vessel and the containment building. Consequently those two components deserve a specific attention as regards aging management.

In France, as well as generally speaking in Western Europe, and according to the IAEA guidance, long term operation approvals are managed, under the control of the nuclear safety authority, through implementation of periodic safety reviews, on a 10 year periodicity. Regarding the containment, its leak-tightness is tested every 10 years through a full-pressure test and is a necessary condition for future operation. Passing the leak-tightness criterion is obviously of crucial importance for the long term operation of the nuclear unit under consideration.

Two types of containment were built in France. The 900 MW units are equipped with single wall containment (concrete wall and steel liner), while for the 1300 and 1400 MW units the containment consists of a double wall building without liner. As a consequence, it is clear that the leak-tightness performance of the double wall containments is much more dependent on the evolution of the concrete structure behaviour with ageing than the single wall with liner might be. Additionally, the experience feedback from the first 30 years of operation indicates that the leak-tightness performance may significantly evolve within a 10 year period of time.

Therefore, understanding the physical phenomena that control leak-tightness is a necessary research effort so as to be able to anticipate the performance of double wall containments for their 4th and 5th 10 yearly periodic safety reviews and take, when necessary, the adequate preventive maintenance actions. Furthermore, accurate predictions of the air leakage through pertinent modelling will allow EDF to optimize the maintenance programs in particular by identifying the areas to be coated to guarantee the leak-tightness performance.

The VeRCoRs mock-up was designed to represent a double wall containment building and instrumented to validate numerical modelling of the physical phenomena occurring in the concrete walls through its whole lifetime. The Vercors results will contribute to the robustness of the leak-tightness model and to the necessary technical justifications for long term operation of the EDF nuclear fleet beyond 40 years.

The VeRCoRs project is now running as planned, as the mock-up has demonstrated his representativeness through multiple pressure tests representative of pre-operation test (Pre-OP), initial test (VCI), 10 years test (VD1) and 20 years test (VD2). The aging factor of the mock-up is 9, which will permit in a few years to soon anticipate results for 30, 40 years and beyond.

Several research programs have used the mock-up which makes VeRCoRs concrete the most studied and documented concrete in the world. EDF is very proud of the success of this second VeRCoRs benchmark, one of the successes being the large participation of the scientific community, even more important than for the previous benchmark.

EDF is thanks sincerely all the institutions and researchers who decided to contribute to the benchmark whether for the first or second time. The mock-up will still be operated for several years. The knowledge gathered on VeRCoRs, regarding materials, laws behaviors and the understanding of the leakage phenomenon will be very useful to manage the lifetime of the containments. Especially the evolution of the leak-tightness at a later age, anticipating the behavior of real containments in the coming decades, is some of the more expected results from the EDF industrial point of view.

It is likely that other benchmarks will be proposed, both on ageing, severe accident or Non Destructive Examinations methodologies. There is no doubt that the international scientific community will continue to contribute to this remarkable research initiative.

Guillaume JACQUART
Deputy Director
EDF – Design and Technology Branch of the Engineering and New Build Projects Direction

Restitution Workshop of the VeRCoRs 2018 benchmark

- ## Monday 27 August

8h30 - 9h30:   Registration

Morning *- chairman: Guillaume Jacquart (EDF-DIPNN-Design and Technology Branch)*

9h30 - 9h50:   Welcome address – *Bernard Salha (Head of EDF Research and Development)*

9h50-10h25:   The VeRCoRs program at mid-term
B. Masson, J. Niepceron (EDF DIPNN-Design and Technology Branch, Lyon, France)

10h25-11h00:   Recent results at Experimental level
M. Corbin (EDF DIPNN-Design and Technology Branch, Lyon, France)

11h00-11h20:   *Break*

11h20-11h55:   From ageing to leak modelling
J. Haelewyn, C. Toulemonde, J-L Adia, A. Cherki El Idrisi (EDF R&D, Paris- Saclay, France)

11h55-12h15:   VeRCoRs benchmark: general organization and participation,
J. Mazars (Grenoble Institute of Technology, France)

Lunch

Afternoon *- chairman: Miguel Azenha (University of Minho, Portugal)*

14h00-14h30:   VeRCoRs benchmark: overview of the results
Theme 1 – Creep modelling,
M. Corbin (EDF Direction Technique, Lyon, France)

14h30-15h30:   Technical presentations on Theme 1

- *Yangsu Kwon, Keun-Kyeong Kim, Myung-Sug Cho, Kyung-Hun Kang, Hong-Pyo Lee, Korea Nuclear & Hydro Power Central Research Institute, Republic of Korea*
Verification of creep model for time-dependent behaviour on VeRCoRs concrete

- *K. Calonius, VTT Technical Research Centre of Finland Ltd, Finland*
Mechanical analysis of a concrete cylinder subjected to a creep test - the VeRCoRs 2018 benchmark case

- *J-M. Torrenti, A Aili, IFSTTAR/Univ. Paris-Est, France*
Modelling of the basic creep of the VeRCoRs concrete

15h30-15h50:   *Break*

15h50-16h50:   Technical presentations on Theme 1

- *M. Ahs, R. Malm, C. Bernstone , Lund University / KTH Royal Inst. of Tech./Vattenfall, Sweden*
Modelling creep in concrete cylinders subjected to different relative humidity levels–the VeRCoRs 2018 benchmark

- *M. Asali, B. Capra, Oxand, France*
Thermo-Hydro-Mechanical Strategy for Forecasting the Leakage Rate of Double-Wall Nuclear Reactor Buildings: Focus on the modeling of VeRCoRs' concrete delayed strains

- *J.R. Hogancamp, M. Sircar – Sandia National Laboratories, Albuquerque/ U.S.Nuclear Regulatory Commission, Washington, D.C., USA*
VeRCoRs Theme I: Creep Modeling

16h50-17h20:   General discussion on Creep Modelling

17h30: *Welcome cocktail*

- **Tuesday 28 August**

Morning - *chairman: Ludovic Jason (CEA- Saclay, France)*

9h00-9h30: VeRCoRs benchmark: overview of the results
Theme 2 – Mechanical behaviour of the containment during pressurization test
Theme 3 – Air leakage
M. Corbin (EDF DIPNN-Design and Technology Branch, Lyon, France)

9h30-10h30: Technical presentations on Theme 2

- *J. Stepan, UVJ Rez, a.s. div. Energoprojekt Praha, Czech Republic,*
Analyses of Behaviour of the Containment Building in Stage 2

- *S. Kevorkian, G. Nahas, J. Clément, IRSN, France*
A numerical model of the VeRCoRs mock-up, pressure tests

- *J. Koskinen, P. Varpasuo, Fortum Power & Heat Ltd/PVA Eng. Services, Finland*
VERCORS Containment Mock-Up test pressure response simulation by MSC/Nastran software

10h30-10h50: *Break*

10h50-12h10: Technical presentations on Theme 2

- *S. Jiménez, A. Cornejo, L.G. Barbu, S. Oller and A.H. Barbat, CIMNE/Technical University of Catalonia Barcelona, Spain*
Analysis of the VeRCoRs mock-up of a reactor containment building by means of a constitutive serial-parallel rule of mixtures

- *J.R. Hogancamp, M. Sircar – Sandia National Laboratories, Albuquerque/ U.S.Nuclear Regulatory Commission, Washington, D.C., USA*
VeRCoRs Theme II: Mechanical Behavior of the Containment during Pressurization Test

- *M. Ahs, R. Malm, C. Brernstone, Lund University/KTH Royal Inst. of Tech./Vattenfall, Sweden* Modelling creep in a pre-stressed mock-up reactor containment – the VeRCoRs 2018 benchmark case

- *J-M. Torrenti, A. Aili, IFSTTAR/Univ. Paris-Est, France*
Modelling of the global delayed behaviour of the VeRCoRs mockup

Lunch

Afternoon - *chairman: Pierre Labbé (ESTP, France)*

13h40-15h40: Technical presentations on Themes 2 & 3

- *M. Asali, B. Capra, OXAND, France*
Thermo-Hydro-Mechanical Strategy for Forecasting the Leakage Rate of Double-Wall Nuclear Reactor Buildings: Application to the VeRCoRs Mock-Up

- *Xu Huang, J. Dury, E. Bentz, O-S. Kwon, University of Toronto, Canada*
Prediction of mechanical behaviour and air leakage of the VeRCoRs benchmark reactor containment structure

- *M. Mazoyan-Kharazi, N. Goujard, INGEROP/Mines Paris-Tech, France*
Development of a numerical model for studying the leakage tight-ness evolution of VeRCoRs experimental containment vessel under aging effect

- *Yangsu Kwon, Keun-Kyeong Kim, Myung-Sug Cho, Kyung-Hun Kang, Hong-Pyo Lee - Korea Nuclear & Hydro Power Central Research Institute, Republic of Korea*
Structural behaviour and air leakage rate prediction for VeRCoRs mock-up by 3D numerical analysis

15h40-16h00: *Break*

16h00-17h50:   Technical presentations on Themes 2 & 3

- *T. Thénint, V. Le Corvec, S. Ghavamian, SIXENCE NECS, France*
  Study of the containment history of the VeRCoRs mock-up and prediction of the leakage rate under pressurization tests

- *K. Calonius, VTT Technical Research Centre of Finland Ltd, Finland*
  Finite element analysis of a pre-stressed mock-up reactor containment - the VeRCoRs 2018 benchmark case

- *D. E.-M. Bouhjiti, J. Baroth, F. Dufour and B. Masson, Ch. Pereniti 3SR Grenoble/EDF, France*
  Predictive probabilistic analysis of the long term ageing of concrete effect on the behaviour of NCBs during pressurization tests: Mechanical and tightness analysis

- *S. Aparicio, M.G. Hernández and J.J. Anaya, ITEFI (CSIC) Madrid, Spain*
  Prediction of the strains and stresses in the gusset using COMSOL Multiphysics

17h50-18h15:   General discussion on Mechanical Behaviour & Air Leakage

- **Wednesday 29 August** (session VeRCoRs is part of TINCE conference)

9h00 -10h00:   TINCE opening ceremony

Session VeRCoRs : *Chairman, Jacky Mazars (Grenoble Institute of Technology - France)*

10h15-10h35:   VeRCoRs program: what is going on, what will go on
B. Masson, M. Corbin, J. Niepceron (EDF DIPNN-Design and Technology Branch, Lyon – France)

10h35-11h10:   How to characterize the airtightness of containment structures. Overview of monitoring techniques tested on VeRCoRs Mock-up
J.M. Henault, P. Laviron, S. Desforges, D. Vautrin, A. Courtois, B. Martin, A. Legrix (EDF-R&D / EDF-DPIH DTG / EDF DI TEGG - France)

11h10-11h45:   VeRCoRs digital twin and its tools
G. Boulant, C. Toulemonde, F. Hamon, J-P Mathieu (EDF-R&D, Lab Paris-Saclay & Lab Les Renardières - France)

11h45-12h10:   Appraisal of the benchmark VeRCoRs 2018
M. Corbin (EDF DIPNN-Design and Technology Branch, Lyon - France)

12h10-12h30:   Conclusions,
N. Herrmann. (Karlsruhe Institute of Technology - Germany)

Lunch

Afternoon : Visit of the Vercors experimental facilities *(EDF-Lab Les Renardières)*

Departure by bus at 1:15 pm from the Saclay campus to the Renardières campus - Return around 5:30 pm

General presentations

- **The VeRCoRs program at mid-term**

  &

- **Recent results at experimental level**

  B. Masson, M. Corbin & J. Niepceron (EDF – Direction Technique, Lyon , France)

- **From ageing to leak modelling**

  J. Haelewyn, L. Charpin, C. Toulemonde, J-L. Adia, A. Cherki El Idrissi (EDF-R&D, Paris-Saclay, France)

The VeRCoRs program at mid term

Results at experimental level

Benoit Masson*, Manuel Corbin and Julien Niepceron

EDF Direction Technique, 19, rue Pierre Bourdeix, 69007 Lyon (France)
[*]Corresponding Author, benoit.masson@edf.fr:

Abstract: This paper summaries the aims of the VeRCoRs project: demonstrate the adequate behavior of a nuclear containment in case of severe accident, improve our understanding of the leakage and its evolution with the ageing, and collect experimental data necessary for the development and validation of numerical models. In order to perform those objectives a mockup at 1/3 scale, widely instrumented with numerous different type sensors was built on the R&D site of EDF in Les Renardières in 2016. This scale allows us to see in the future by accelerating all the ageing phenomena. Besides the ageing measurements (strains, temperatures, hygrometry, humidity of the concrete) and the samples testings (strength, modulus, …), pressure test are carried out as if this building would be part of the nuclear fleet of EDF. Since three years of measurements collected in the databank, it is confirmed that the ageing phenomena are significantly accelerated. The first pressure test has confirmed the representativeness of the mockup, and the leakage rate has increased in the same proportions than a real containment. Some new results has been gathered thanks to optic fiber measurements, leakage collecting boxes, gas pressure in the concrete, have led to a better knowledge of the leakage way in a prestressed wall. The creep, especially before the heating of the mock-up is not at all those attended, but confirm that the thermal activation is important.

Keywords: Ageing, Containment building, Mockup, Leakage

Introduction

The passive leak-tightness function of the French 1300-1450 MWe NPP reactor building is provided by a reinforced and pre-stress concrete inner wall without steel liner, an outer reinforced wall assuring the protection against external effects. The leak through the internal wall is collected in the annular space being permanently maintained slightly below atmospheric pressure.

The technical objective, in term of leak-tightness, is to maintain the rate of gas escape under a legal criterion. The compliance with the rule is evaluated by measuring the quantity of air leak, obtained during a periodical pressure test at ambient temperature.

Numerical models are up to now not sufficiently mature and accurate to predict the evolution of the leakage rate during these pressure tests, nor during standard design-basis accidents. In the frame of NPP life extension perspective, the project of building a reduced scale containment mock-up seemed to be a good way to obtain reliable results. The main objectives were the following:

- to demonstrate in an indisputable way the adequate behaviour of inner wall in situation of severe accident (high pressure and high temperature during two weeks);

- to have a better understanding of the leakage and its evolution with the ageing of the structure. The ageing of the mock-up will be accelerated by the scale effects (reduced thickness, faster drying, faster shrinkage); which allows to anticipate the behavior of the real containments.
- to collect experimental data necessary for the development and validation of numerical models.

The 1/3 scale was chosen to anticipate on the containment behaviour with an accelerating factor of time. As the wall thickness will be reduced, the drying of the structure will be then faster. These will result in faster drying shrinkage and drying creep, which are supposed to be the main phenomena explaining the leak rate evolution. As the thickness is reduced by a factor 1/3, the time accelerating factor is hoped to be 9. As a consequence, extended end-of-life conditions (60 years) of a full size structure may be reproduced on the mock-up only after about 7 years.

In order to facilitate the transfer of the results from the experimental case to the NPP cases, the mock-up has to be as close as possible to the real containment building. That's why it integrates all complexities of the containment structure.

The mock-up or precisely the inner containment building, was built between May 2014 and August 2015 which according to the scale factor of 9 fits well with the real containment building erection time.

The main characteristics of the mock-up are stated below (Fig 1 and Tab 1):

Fig 1: Scheme of the mockup

	1/3 scale model	Full scale
Height from gusset to the top [m]	20.79	62.38
Internal radius of cylinder [m]	7.30	21.90
Thickness of cylinder [m]	0.40	1.20
Internal radius of the dome (tore) [m]	2.67	8.00
Internal radius of the dome (center) [m]	10.67	32.00
Thickness of the dome [m]	0.30	0.90
Free volume inside containment [m^3]	3 160	85 350

Tab 1: Characteristics of the mockup

The pressurization test were intended to be held with the same periodicity as a real containment, but with a time scale of 1/9. So, the pre commissioning test was held in December 2015, the first operational test, after about one year for a real containment, in January 2016 for the mock-up, and the decennial tests (for real containment), every 13 month. However for practical reasons, the decennial test will be held from now every 12 month. A simulation of a severe accident, with an increase of the internal pressure with air and steam is considered at the end of the research program.

To achieve the objectives of the project, VeRcOrs has been wisely and extensively instrumented furthermore numerous sample of concrete, steel rebars, tendons were sampled to characterize the materials. Measurements were taken from the first concreting and will be perform up to the end of the project, without discontinuities. The monitoring system is

composed of:
- 1 meteorological station
- for the ambient air measure : 10 thermometers, 10 relative humidity sensors, 1 atmospheric pressure gage, 1 flow meter
- 12 pendulums (4 plumb lines with each 3 tables of aiming at different heights on 4 vertical lines)
- 4 vertical Invar wires
- 336 Embedded strain sensors
- 211 Thermo-sensors PT100
- 2 km of optic fiber
- 31 TDR (Time Domain Reflectometry) sensors
- 30 « pulse » sensors (permeability measurement)
- 6 dynamometers for instrumented tendons
- 160 strain gauges on rebars

Results of the program up to now

The daily measurements (strain, temperatures, and hygrometry) are available on a very large number of sensor (only few strain gauges are damaged and 80% of the optical fibre length in the wall is operable). The measurement of the global air leakage during the first four tests (pre commissioning, first test, first decennial test and second decennial test) is very accurate and the local measurements of the leakage (with collecting boxes placed on the wall and flow meter to measure the leakage) gives us lot of answer concerning the leakage through the wall. The mock-up, for ageing, for structural behavior and for patterns of leakage defects, is representative of a real containment.
In the next items, we will give you the most interesting results.

Digital twin

When we think of Digital Twin it is often mixed up with BIM (Building Information Modelling). BIM helps to design, to build and perhaps to operate the building, however the purpose of the Digital Twin is far more ambitious. It can use a part of the BIM (drawings, modelling, …), but is ultimate goal is to collect all the data (principally measurements on the structure and on samples, but visual inspections too and other kinds of results interesting for the structure), from the beginning of the erection, in the correct format, to gather the different finite element models and calculations and to aggregate this elements, calculations and data, so that the engineer could easily perform studies with variable hypothesis to better understand the ageing of the structure.
The DT emerged from the necessity to collaborate seamlessly between the specialists of the construction, the measurement, the materials experts and the calculation engineers. The design of the DT was not defined before the beginning of the project, it has significantly progressed from the first air test so that we now have an operating and efficient DT. We are now going to use the DT on real containment buildings.

Materials knowledges

To have a perfect understanding of the mock-up, the materials (cement, concrete, steel rebars, ten-dons) have to be very well defined. This is why numerous (more than 1200) samples were collected. Several laboratories (more than 40 laboratories in the international COST 1404 project for example, more than 10 in the MACENA project which the aim was the behavior in case of severe accident) have tested the samples, at early age, after ageing, and in different environmental conditions. A very large data base has been build and is still gather data today.

All those data is highly valuable for the scientific community and has allowed to complete and improve the material behaviours laws.

Accelerating ageing factor

Fig 2: Accelerating factor in tangential direction

Fig 3: Accelerating factor in vertical direction

Ageing is identified by the delayed strains on the prestressed concrete structures. The expected accelerated factor for delayed strains was 9, based on the Eurocode rules for creep and shrinkage. Modelling gave us other factors, depending of the different creep and shrinkage laws, with lower values (the minor value given was 4). For the aim of the mock-up

and the duration of the research program, it is very important to know the real factor, based on the delayed deformations.

To obtain the accelerating factor, a comparison is performed of the measurements of three real containments and VeRCoRs from the end of prestressing, in both tangential and vertical directions. On the graph below (Fig 2 & 3), the accelerating factor is taken to be 10 for VeRCoRs (yellow curves). It can be noticed that the yellow curves matches well with the greens (our reference). The effect of dead load, that reduce the stress and so the shrinkage in vertical direction for the mock-up, appears not to be significant.

This accelerating factor confirm that creep and shrinkage, and their relationships with water content and temperature, are not perfectly known. Indeed, some models and creep laws gave us values about of 4 or 7, and the Eurocode 9. We intend to continue our work to better understand their interdependency.

Ways of leak

Several types of measurements give us some information.

- Some pulse sensors, used to measure the gas pressure in the wall, located at different places in the thickness of the wall, show us a typical leakage through a porous medium, with an increasing of the pressure in the wall correlated with the distance from the side were pressure is applied. But some other indicated that the leakage found shortcuts in the wall. These sensors were located close to the sheath of the tendons, as it is assumed that this kind of singularity is a weak point (steel sheath is not perfectly adherent). Some tests have been performed in Grenoble INPG which show same phenomena for the rebars.
- Optic fibers are embedded in the wall, at three different thickness. This kind of device allows to see the strains, and the cracks, or more precisely the evolution of the cracks, through the wall. The graph below (Fig 4) represents a horizontal section of the containment wall and in blue, red and green, the evolutions of strain measured with the OF. Where there is an evolution on the three levels, it could be cracks going through the full depth. The black dotted lines indicate leaking cracks, and the length of the line is representative of the leakage.

Fig 4: Strain measured by OF in the depth and leakage measured with boxes

- The leakage on the wall is located by spraying soap water on the wall, and measured thanks to a leak-tight box connected to flow meter on the area where the leakage is targeted. There is a good correlation between the signals perceived by the OF showing a peak of strain through the full depth of the wall, and detected leaking cracks located thank to collecting box, however sometimes signals obtained from OF doesn't necessary lead to leaking cracks. As an explanation it may possible that for small

opening the leak either a) find an easier path, b) or the crack isn't a full depth crack.

- A concrete sample has been saturated with deuterium, and placed in a tomographic device. A water pressure was applied on a face, and the progression of the water in the sample highlighted by tomography. It has appeared that the permeability was higher (so the leakage was higher) along the rebar.

To conclude about the leak, it definitely appears that the leakage, that goes majority directly through the wall, can use sometimes tortuous ways, for example along the tendons or the rebars, and probably in the areas with poor concrete quality (low cement rate, honeycombing …). More investigations must be perform to better understand and quantify this phenomenon.

Technologies benchmarking

The high density of sensors and theirs locations on the structure allow to compare different technologies that gives in theory the same measurement. To validate that the location of a OF sensor vertically on the wall gives the same results as the vertical invar wire or as the integrate measurement of the vertical vibrating wires embedded in the wall, three OF sensors have been anchored on the wall (Fig 5). The results are not coherent, it is possible that the anchorage methodology has to be improved. Another idea is to glue the OF directly on the wall.

Fig 5-a: Position of the added FO sensor (in blue) regarding the Invar wire (in green); 5-b: anchorage

Fig 5-c: displacements measured by invar wire (full curve) and by FO sensors (dashed curve)

Non destructive evaluations

The "Non Destructive Evaluation of containment nuclear plant structures" project (ENDE) is a French project developed with 8 partners. This project aims to control the containment of structures by Non Destructive Testing with ultrasonic, electromagnetic and electric methods. It consists to transfer the NDE technics achieved in laboratory to on site measurements. In situ measurements involved some constraints such as: the proximity of reinforcements and the properties gradients in the concrete. The testing were implemented on the VeRCoRs mock up (Fig 6), during testing stages or in normal running.

Fig 6: a) VeRCoRs containment mock-up developed by EDF, b) Ultrasonic surface wave non-contact scanner, c) Resistivity measurement, d) Diffused utrasonic waves monitoring

The results are widely described by the ENDE project, for example in [1] and [2]. As a conclusion, NDE methods can be successfully used on a nuclear power plant. To improve our understanding of the ageing and leakage phenomenon it is mandatory have to pursue research:

- On determining if a crack is a full depth crack or not on walls up to 1,2 m thickness.
- The knowledge of the water content or humidity in the wall is still not possible. However, it is possible to measure the humidity in the first centimeters of the wall and afterwards, with a numerical model, to deduce the humidity in the entire wall.

Bio healing

Bio healing research is very promising. Tests performed on samples, that the leakage through concrete cracks, could be reduced up to 70%. It has been decided to evaluate this possibility on the mock-up. The bio healing process started 8 weeks before the test, on a vertical crack and on a horizontal construction joint (at each batch of concrete), that were leaking on the test performed the year before. The two areas were just above the gusset. For the vertical cracks, no improvement has been seen. For the horizontal defect, the decrease of the leakage rate was up to 8 times. The research has to continue to understand those promising results, which could be a good way to enhance the leak tightness of the concrete structures.

Prediction of the leakage

The prediction of the leakage is one of the most important aim of the Vercors mockup. A first benchmark has been organized in 2016, and the results have shown a large dispersion of the results, with differences of about 200 times in the predictions, nonetheless nobody gave an accurate results. For the next benchmark, it is expected to obtain more accurate results. Moreover, EDF has developed a methodology that has been very close to the test results, but the physic of the models used has to be consolidated. If the global prediction is satisfying, further progress will have to be performed in order to reach a higher accuracy on each specific areas of the mock-up.

What is going on now

About the measurement devices, the mock-up is still open for new comers to evaluate a new sensor technology, as for OF strain sensor. The next step is to test OF glued directly on the wall to compare with invar wire.

About the NDE technology, further progress are on-going in the concrete moisture content (or water content) measurements. Surface sensor measurements can be quite accurate in the prediction of the water content through the thickness of the wall. This humidity gradient knowledge is of prior importance to calibrate the creep and shrinkage models. Another axis of work is to develop the cracking sensor based on sonic waves, which gave us some hopeful results. NDE technologies are more than necessary in a context of ageing structures.

This is why large samples will be build, with well-known defects, to evaluate sensors that other companies have to propose. The targeted fields are: carbonation, cracks, permeability, stiffness, strength, delamination, corrosion. If the results obtained are valid on the sample, the technology will be evaluated on VeRCoRs and used and eventually on real structures.

The next steps for the experimental program are the periodic pressure tests, every year (thanks to the accelerating factor of 10, so the test performed every ten years on a real containment are performed every year on VeRCoRs). There will be 5 more tests and at the end an ultimate test with air and steam pressure, to simulate a severe accident, could be done. This is not sure, because the representativeness of this kind of test must be demonstrated before the test would be performed.

To better understand the leakage phenomena, the execution of tests at low pressure, with some parts of the containment coated with removable coating, is studied.

Conclusion

The VeRCoRs project is now running as planned, as the mock-up has demonstrated his representativeness. Several research programs have used the mock-up (COST TU 1404 [4], ENDE, MACENA [5], …) which makes VeRCoRs concrete the most studied and documented concrete in the world. Two benchmark were done, so that the different teams can compare theirs results and improve their calculation.

VeRCoRs is still open for tests, especially for NDE tests, because these kind of methodologies will be increasingly useful to demonstrate the capacity of the structure to resist to a severe accident at the end of its life, especially for containments that are not equipped with monitoring devices.

The knowledge gathered on VeRCoRs, regarding materials, laws behaviors and the understanding of the leakage phenomenon, will be very useful to manage the lifetime of the containments, besides the digital twin that will be developed for the real containments.

It is likely that other benchmarks will be proposed, both on ageing, severe accident or NDE methodologies.

REFERENCES

[1] *"Non Destructive Evaluation of the durability and damages of concrete in nuclear power plants"* in 12th European Conference on Non-Destructive Testing (12th ECNDT)

[2] *"Non-destructive evaluation of containment walls in Nuclear Power Plants"* in 43rd Annual Review of progress in Quantitative Non-destructive evaluation, vol 36

[3] VeRCoRs website where data and results of the first benchmark are available: https://fr.amiando.com/EDF-vercors-project.html.

[4] COST TU 1404 website: more than 40 laboratories have made tests and evaluations on the VeRCoRs concrete: https://www.tu1404.eu

[5] MACENA website: https://espaces-collaboratifs-production.grenet.fr/share/page/site/MACENA/documentlibrary

From ageing to leak modelling

J. Haelewyn[*], L. Charpin[*], C. Toulemonde[*], J-L. Adia[*] et A. Cherki El Idrissi[*]

[*]EDF R&D, France, e-mail: jessica.haelewyn@edf.fr

ABSTRACT

1) Introduction and context.

Safety and life extension of Nuclear Power Plants are an EDF priority. To pursue this objective, the VeRCoRs mock-up is a very useful experimental tool.

One of the main objectives of the project is to understand leak tightness evolution under ageing. In fact, at a third scale, drying effects will be nine times faster and hence studies of ageing speeded up.

First, a digital twin of VeRCoRs is developed to follow its life. This numerical model is also necessary to understand ageing of the mock-up by analysing non-measurable quantities such as stresses. The objective is to draw up an inventory of the prediction capacities of digital clone regarding the thermal, drying and mechanical aspects. The numerical results are compared to the available measurements: temperature, strains and displacements.

Numerical results and all measurements are then used to: first, have a better understanding of the leak tightness evolution and, secondly, develop a phenomenological model that is able to predict leak rate.

2) From ageing...

The numerical model of the VeRCoRs mock-up is focused on the inner pre-stressed concrete containment building. The outer concrete containment building is not represented in this study since it has no explicit mechanical role neither in the ageing process of the inner containment nor in its subsequent leak tightness. The mesh used for thermal and hydric computations is the one provided to the benchmark participants.

The pre-stress cables are individually modelled using bar elements which are kinematically linked to the solid concrete elements through Lagrange multipliers. Their deviations around the access hatch and other passages through the walls are explicitly taken into account. The metal elements closing the through-wall passages (pipes, hatches) are also explicitly modelled in 3D in order to correctly take account of their role during the Integrated Leakage Rate Test (ILRT). All computations are performed with *code_aster* which is an open-source FEM solver developed at EDF R&D (www.code-aster.org). Three computations are performed sequentially: thermal, hydric and mechanical computations. The simulation starts at the beginning of prestressing (June 2015) and simulates ten years of VeRCoRs's life.

For thermal computation, the boundary conditions are the fixed temperatures imposed at the surface of concrete. The choice of the imposed temperatures on the internal and outer faces of the mock-up's inner containment is of importance. The best fit is obtained by imposing the temperatures measured at the surface of the concrete wall.

Drying is modelled using the non-linear diffusion equation developed in [1] available in *code_aster* under the name SECH_GRANGER. Drying behavior law parameters are identified on mass loss curves from different sample tests [2], see Figure 1.
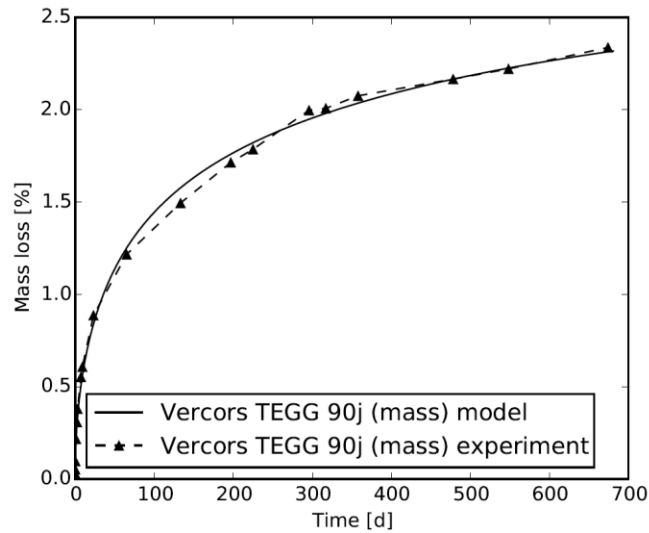
Figure 1: Mass loss fit for a specific drying sample

At this stage, the computed water content can be compared to measures. Some novel devices tested on VeRcoRs [3] provide an estimation of water content in the concrete wall. Comparison between computed and measured water content shows about 20% difference (see Figure 2). Although monitoring is improving, measurement uncertainty remains too high (at about 10%) to assess the accuracy of a set of drying model parameters.
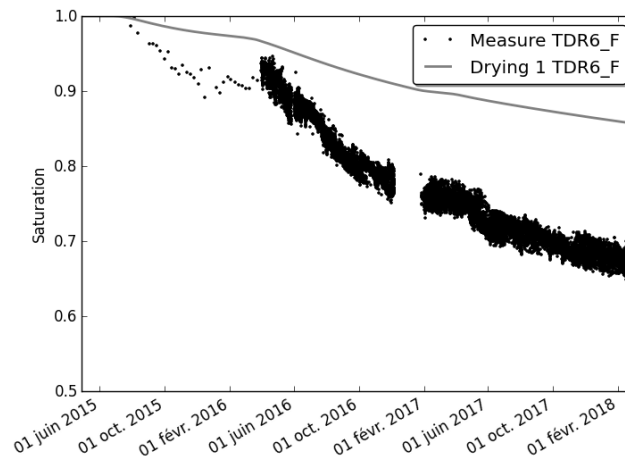

Figure 2: Water content evolution in the cylindrical part far from any singularities

The mechanical model is based on an additive decomposition of the strain into five main contributions: elastic strain, thermal strain, drying shrinkage strain, basic creep strain, and desiccation creep strain. Basic creep strain used is available in *code_aster* in BETON_BURGER model. All creep parameters used on the VeRCoRs mock-up computation have first been identified on sample tests [4]. Results are then compared to other measurements to validate the digital twin. For example, a comparison on strains is shown on Figure 3.
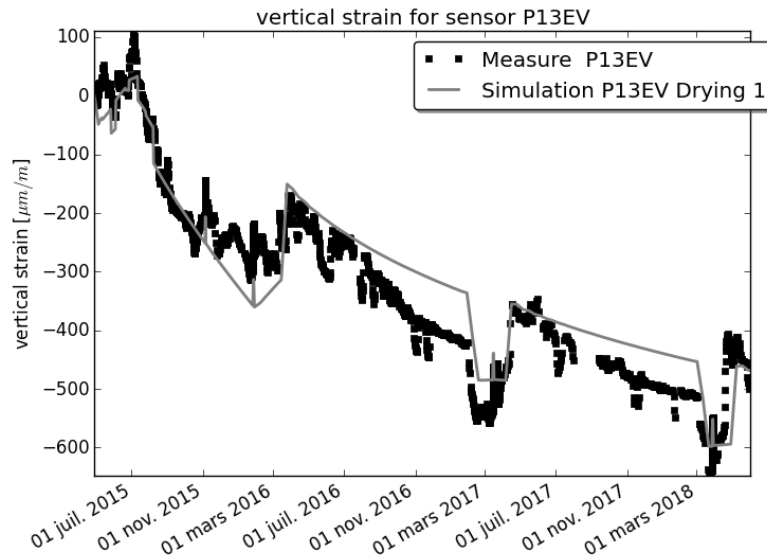
Figure 3: Strain time history (VeRCoRs mock up) compared with numerical model

3) … to leak prediction

EDF aims at developing a phenomenological model that is able to predict leak rate of containment buildings. It is meant to be simple and macroscopic. To do so, the first part of the work is to capitalise on most of the leakage data and the numerical results of the digital twin. The leakage related data are of two kinds: local and global. To analyse the evolution of leaks between two pressure tests, local leaks are interpreted as a leak field that is displayed on a developed view of the containment building. Figure 4 shows the evolution of local leakage between the 3rd and 4th pressure tests (called "VD1" and "VD2"). The fact that the gusset is the most evolving area is highlighted by the evolution field.
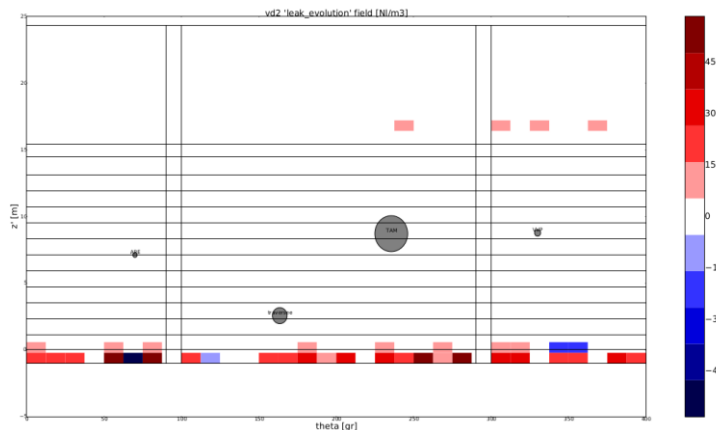
Figure 4: Leak evolution field between the 3rd and 4th pressure tests

Then, comparing global leakage and the sum of local leakage, we notice that there is a part of leakage which is not measured locally. If it is assumed that all leakage that passes through cracks is measured, then the complementary part can be likened to porous leakage, which passes through concrete pores. Our phenomenological model is based on this hypothesis, and global leakage is thus divided into two parts: local leakage and porous leakage.

To evaluate porous leakage, our current practice is to model it as a porous medium via a thermo-hydro-mechanical model. For a given water content in a concrete wall, a gas pressure is applied to the inner face and the leakage rate is calculated. Among the most influential parameters are permeability and water content. The computed water content profile given by the digital twin is used as an input parameter. Permeability is identified based on the previous pressure test in order to predict porous leakage during the next test.

Prediction of local leakage is performed globally. Local leaks evolution is based on several assumptions related to the ageing of concrete. Concrete cracking is likely to take place mainly at early

age, prior to prestressing. At prestressing, most defects are closed and compressed. Then, the ageing acts, concrete relaxes, cracks propagate and/or re-open. The first hypothesis is that there is a physical quantity related to ageing that drives the evolution of local leakage. The second hypothesis is that initiation of a leak (or the initial state of cracking) is not only controlled by this quantity but also by other mechanisms (a priori mainly the young age shrinkage and drying). Prestressing loss was chosen, as it is the most relevant physical quantity to correlate with the sum of the local leaks of each test (Figure 5). Therefore, this correlation has been used to predict the local leakage during the next test.
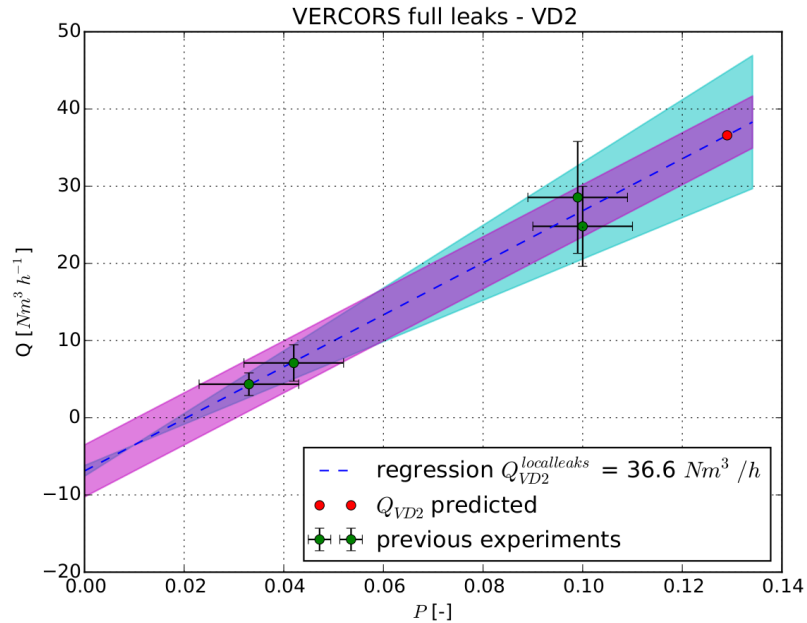
Figure 5: Sum of local leaks relative to pre-stress loss

This method was applied in the blind prediction of the leakage rate of the VD2 test and shows good results with 6% error on the overall leak.

REFERENCES

[1] Granger, L. Comportement différé du béton dans les enceintes de centrales nucléaires : analyse et modélisation. *Ph. D. thesis*, Laboratoire Central des Ponts et Chaussées ,(1995)

[2] Charpin L.; Courtois A.; Taillade F.; Martin B. ; Masson B.; Haelewyn J. Identification of the parameters of concrete drying constitutive laws: benefit of using profiles in addition to mass loss of samples, application to VeRCoRs concrete - *TINCE* (2018)

[3] Haelewyn J., Guihard V., Courtois A., Taillade F., Balayssac J-L, Placko D., Sanahuja J. Relevance and means for measuring water content in concrete structures. An illustration with PWR concrete containment- *TINCE* (2018)

[4] Charpin, L., Sow T., d'Estève de Pradel X., Hamon F., Mathieu J.-P. Numerical simulation of 12 years long biaxial creep tests. Efficiency of assuming a constant Poisson's ratio. *In 6th BIOT conference*, Champs sur Marne, France (2017)

Theme 1: Creep modelling

Micromechanics and/or Multiphysics approaches

- **Yangsu K., Keun-Kyeong K., Myung-Sug C., Kyung-Hun K., Hong-Pyo L.** Korea Nuclear & Hydro Power Central Research Institute (KHNP CRI), Daejeon, Republic of Korea,

  Verification of Creep Model for Time-dependent behaviour on VeRCoRs Concrete

- **K. Calonius** – *VTT, Finland*

- **J-M. Torrenti, A Aili** - IFSTTAR / Univ. Paris-Est – France,

  Modelling of the basic creep of the VeRCoRs concrete

- **M. Ahs, R. Malm, C. Bernstone** - Lund University / KTH Royal Inst. of Tech. / Vattenfall AB, Sweden

  Modelling creep in concrete cylinders subjected to different relative humidity levels–the VeRCoRs 2018 benchmark

- **M. Asali**, **B. Capra** - Oxand, France

  Thermo-Hydro-Mechanical Strategy for Forecasting the Leakage Rate of Double-Wall Nuclear Reactor Buildings: Focus on the modeling of VeRCoRs' concrete delayed strains

- **J. R. Hogancamp, M. Sircar** – Sandia National Laboratories Albuquerque / U.S. Nuclear Regulatory Commission Washington, D.C., USA

  Vercors Theme 1 – Creep modelling

Verification of Creep Model for Time-dependent behaviour on VeRCoRs Concrete

Yangsu Kwon [*] **, Keun-Kyeong Kim** [†] **, Myung-Sug Cho** [††] **, Kyung-Hun Kang** [†††] **and Hong-Pyo Lee** [††††]

[*] Korea Nuclear & Hydro Power Central Research Institute (KHNP CRI), Daejeon, Republic of Korea, e-mail: yangsu.kwon@khnp.co.kr

[†] Korea Nuclear & Hydro Power Central Research Institute (KHNP CRI), Daejeon, Republic of Korea, e-mail: kenk.kim@khnp.co.kr

[††] Korea Nuclear & Hydro Power Central Research Institute (KHNP CRI), Daejeon, Republic of Korea, e-mail: mscho621@khnp.co.kr

[†††] Korea Nuclear & Hydro Power Central Research Institute (KHNP CRI), Daejeon, Republic of Korea, e-mail: kangcrete@khnp.co.kr

[††††] Korea Nuclear & Hydro Power Central Research Institute (KHNP CRI), Daejeon, Republic of Korea, e-mail: hongpyo.lee@khnp.co.kr

ABSTRACT

The main objective of this paper is the more accurate evaluation of creep behavior on early-age concrete material. The creep deformation, representative time-dependent behavior, could cause the damage including cracks during the construction stage of a containment vessel. It is necessary to consider it appropriately in design and construction level. The numerical analysis by finite element analysis is one of the solutions for the prediction of time-dependent behavior; however, there are many difficulties in model configuration. In this paper, viscoelastic model in ABAQUS was applied to calculate the degree of hydration from the VeRCoRs test results. Finally, three-dimensional finite element analysis was conducted to creep of deformation of cement paste, basic creep, drying creep varying humidity condition of concrete.

Creep model for numerical analysis

The modeling for creep behaviors of concrete was applied as a viscoelastic material in ABAQUS[1]. In order to consider the creep behavior as viscoelastic material properties, it is required that the normalized shear and/or bulk moduli, $g_r(t)$ and $k_r(t)$, as function of time (hour or day in this paper). In a consideration of the time-dependent creep coefficient, $\phi(t,t0)$, the normalized relaxation moduli($g_r(t)$ and $k_r(t)$) could be simplified as a function of the creep coefficient of which the Poisson's ratio is assumed to be constant in time. The normalized relaxation moduli were as follows:

$$g_r(t) = \frac{G_R(t)}{G_0} = \frac{\dfrac{E_0}{2(1+v_0)(1+\varphi(t,t_0))}}{\dfrac{E_0}{2(1+v_0)}} = \frac{1}{(1+\varphi(t,t_0))} \tag{1}$$

$$k_r(t) = \frac{K_R(t)}{K_0} = \frac{\dfrac{E_0}{3(1-2v_0)(1+\varphi(t,t_0))}}{\dfrac{E_0}{3(1-2v_0)}} = \frac{1}{(1+\varphi(t,t_0))} \quad v \tag{2}$$

where, $G_R(t)$ and $K_R(t)$ are the time dependent shear relaxation modulus and bulk relaxation modulus.

These two variables are obtained by multiplying the instantaneous relaxation moduli with some dimensionless relaxation function as $1/(1 + \phi(t, t_0))$. Through the non-linear least-squares fit, the Prony series parameters are calculated automatically.

In order to improve the accuracy of the viscoelastic model for creep behavior, the degree of hydration was also calculated using material test results of VeRCoRs concrete such as hydration heat release curve, strength and elastic modulus development curve of early-age concrete. The time-dependent hydration degree equation is as below:

$$\alpha_e = \alpha_1(1 - e^{-r_e t_e}) + (1 - \alpha_1) \exp\left[-\lambda_1 \left(\ln\left(1 + \frac{t_e}{t_1}\right)\right)^{-k_1}\right] \tag{3}$$

Where α_e is the degree of hydration of concrete, α_1 is the initial hydration degree, t_e is the equivalent age of concrete, r_e is the reaction velocity (1/hr) and λ_1, k_1, t_1 are the values that could be obtained by experiments.

The first term of hydration degree equation is related to very early-age behavior and second term is expressed to after early-age of concrete. By regression analysis of the equation to real test results, the coefficient was determined (See Table 1 and Fig. 1). The hydration degree – mechanical properties (elastic modulus and compressive strength) relation also was determined (see Fig. 2).
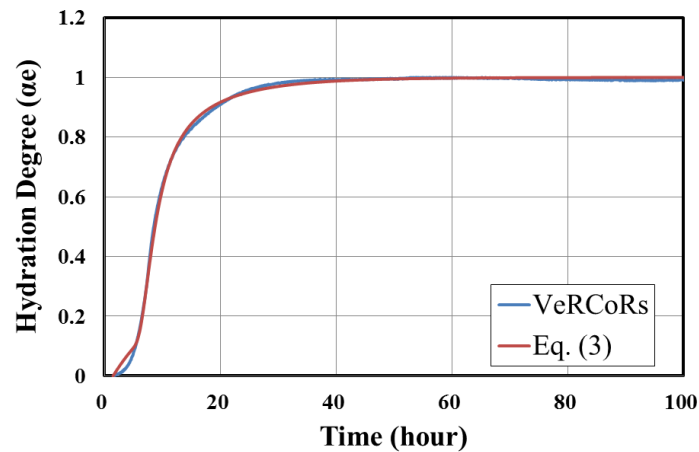
Fig. 1. Evolution of hydration degree as a function of concrete age

| (a) Elastic modulus | (b) Compressive Strength |
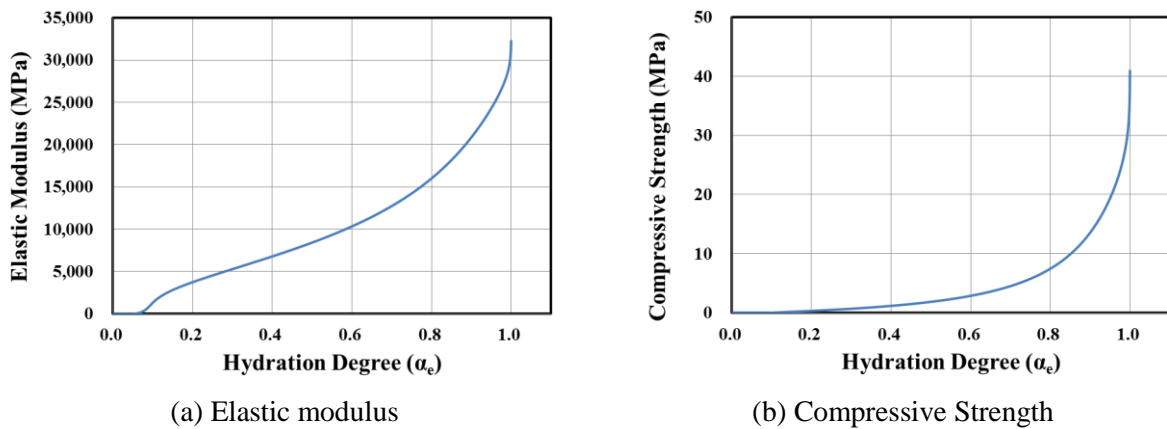
Fig. 2. Prediction of (a) elastic modulus and (b) compressive strength as a function of hydration degree

Table 1. Regression results of hydration degree coefficient

α_1	r_e	λ_1	$k_1,$	t_1
0.33	0.095	203	8.69	1.5

Analysis results of creep behavior

To predict the creep deformation in Theme 1-1 and Theme 1-2(see Fig. 3), the three-dimensional finite element analysis was conducted. The size of cylinder (radius and height), load and other related conditions were reflected as VeRCoRs basic and drying creep tests (See Fig. 4).

The results of the creep test specimens are shown in Fig. 5 and 6. Based on the analysis results of cement paste in Theme 1-1 (Fig. 5), there are no clear differences in creep strain from 1 to 7 day. This result seems that the temporal resolution in this analysis model is not enough to consider early-age behavior. However, the results of Theme 1-2 (Fig. 6) show the clear differences by concrete aging and outer condition. For more accurate analysis of early-age behavior, it is necessary to perform the time setting including loading step and the material properties should be considered in a fine manner.

Fig. 3. Concrete creep measurement (VeRCoRs Theme 1)
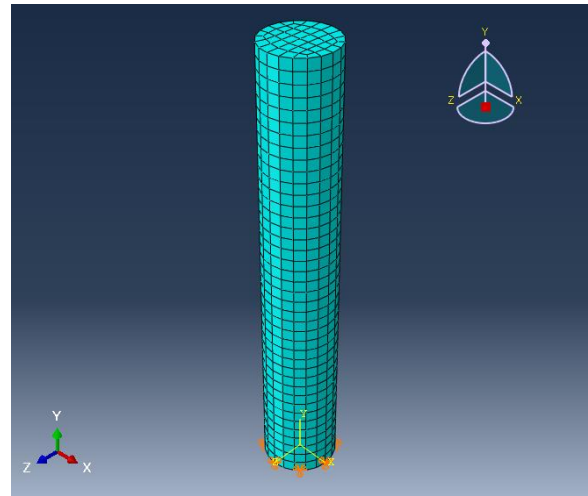
Fig. 4. FEM Model
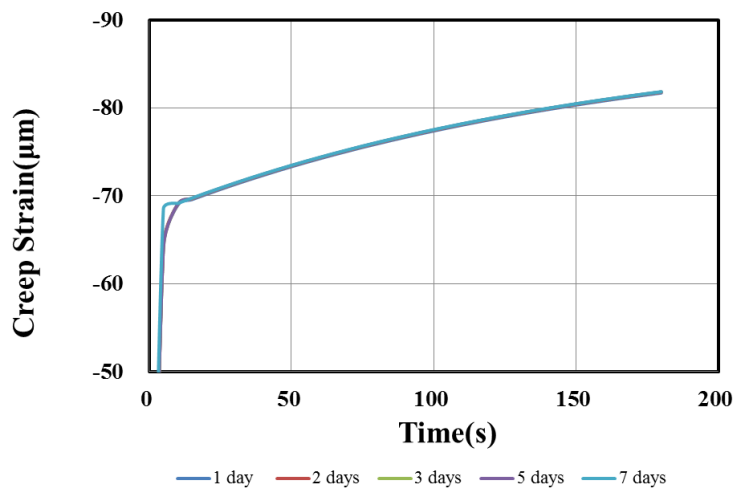
Fig. 5. Analysis results of creep test on cement paste (Theme 1-1)
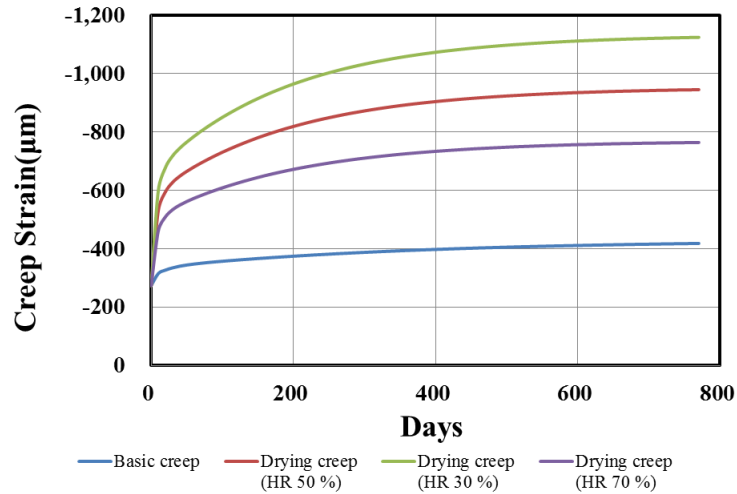
Fig. 6. Analysis results of basic and drying creep test (Theme 1-2)

REFERENCES

[1] *ABAQUS*, "ABAQUS *User Manual* 6-14", Dassault Systèmes(2013)

[2] ACI Committee 209, "Guide for Modeling and Calculating Shrinkage and Creep in Hardened Concrete (ACI 209.2R-08)," American Concrete Institute, Farmington Hills, MI(2008)

[3] CEB, "CEB-FIP Model Code 1990," CEB Bulletin d'Information No. 213/214, Comité Euro-International du Béton, Lausanne, Switzerland, 33-41(1993)

[4] CEB, "Structural Concrete—Textbook on Behaviour, Design and Performance. Updated Knowledge of the CEB/FIP Model Code 1990," fib Bulletin 2, V. 2, Federation Internationale du Beton, Lausanne, Switzerland, 37-52(1999)

[5] M. Irfan-ul-Hassan, B. Pichler, R. Reihsner, and Ch. Hellmich, "Elastic and creep properties of young cement paste, as determined from hourly repeated minute-long quasi-static tests", Cement and Concrete Research, 82, 36-49 (2016)
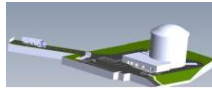
Mechanical analysis of a concrete cylinder subjected to a creep test - the VeRCoRs 2018 benchmark case (Theme 1)

Kim M. Calonius[*]

[*]VTT Technical Research Centre of Finland Ltd, Finland, e-mail: kim.calonius@vtt.fi

ABSTRACT

This paper presents mechanical analysis of a concrete cylinder subjected to a creep test. It is a part of the new VeRCoRs benchmark 2018 arranged by EDF. The results from the analyses have been preliminarily compared with actual measurements performed on a concrete cylinder subjected to a certain experimental set up. The creep and shrinkage of concrete test samples is calculated here according to Eurocode. The experimental and calculation results correspond to each other rather well, but the main problem is that the Eurocode does not assess the drying creep. However, the drying creep is calculated from the experimental results. This is just a preliminary study of this theme and the results will be reviewed and improved.

INTRODUCTION

As part of EDF's continuous effort on the safety and life extension of its Nuclear Power Plants, an experimental mock-up of a reactor containment building at 1/3 scale has been built near Paris (France) [1]. The main objectives of the project are to study the behaviour at early age, the evolution of the leak tightness under the effect of aging and the behaviour under severe accident conditions. VTT took part in the first international calculation benchmark called VeRCoRs 2015 and focused mainly on cracking and leakage under a test pressure of 0.52 MPa abs [1]. The previous results have been reported [2], [3], [4].

This paper presents mechanical analysis of a concrete cylinder subjected to a creep test. It is a part of the new VeRCoRs benchmark 2018 arranged by EDF. The results from the analyses have been preliminarily compared with actual measurements performed on a concrete cylinder subjected to a certain experimental set up.

CREEP TEST CALCULATIONS

The creep and shrinkage of concrete test samples is calculated here according to Section 3 and ANNEX B of EC2: European Committee for Standardization, CEN, EN 1992-1-1. Eurocode 2: Design of concrete structures - Part 1 -1: General rules and rules for buildings, 2004 [5]. The test specimen or any geometry is not modelled. The calculations are purely analytic and based on the equations in the Eurocode. The test for the cement paste (Theme 1-1) is not analysed here. The small hollow specimen are neither analysed. The Eurocode calculations are not described here.

The cylindrical test specimen had a height of 1 m and a diameter of 0.16 m. The specimen was first covered (sealed) by a leak-tight coating. There were two types of tests. Either the coating was used for the whole duration of the test (basic creep test) or it was removed after 90 days (drying creep test). In both tests, an almost constant mechanical axial load of 12 MPa load was applied after 90 days. The tests were also done without mechanical loading. The test arrangement is shown in Figure 1.

Figure 1. Test arrangement (detail of the center part on the right) [7].

For Theme 1-1, it was asked to give the concrete basic creep axial strains without strains due to shrinkage. For Theme 1-2, it was also asked to give the so-called drying creep in relative humidities of 30%, 50% and 70%. Eurocode does not even mention the Picket effect or drying creep, so it does not directly give that component. Drying creep is well described in an article by Benboudjema, Meftah and Torrenti [6]:

Predicting delayed strains in concrete proves to be critical to a large number of pre-stressed concrete structures, such as containment vessels of nuclear power plants. These delayed strains include:

- autogeneous shrinkage, as deformation related to the water consumption during the hydration reaction in early-age concrete: ε_{as}

- drying shrinkage, as deformation related to the moisture diffusion from the inner core to the outside of the concrete member: ε_{ds}

- basic creep strains, as time-dependent deformation of a loaded specimen, without drying: ε_{bc}

- drying creep strains, as additional deformation, which occurred in a drying and loaded specimen (Pickett effect): ε_{dc}

Drying creep strains cannot be directly separated from the other components of the delayed strains. Indeed, a drying test, a basic creep test and a total creep test need to be performed, in order to get the drying creep strains (Figure 2). Therefore, the drying creep strains reads:

$$\varepsilon_{dc} = \varepsilon_T - \varepsilon_e - \varepsilon_{bc} - \varepsilon_{as} - \varepsilon_{ds} \tag{1}$$

where ε_T is total strain and ε_e is elastic strain due to loading.
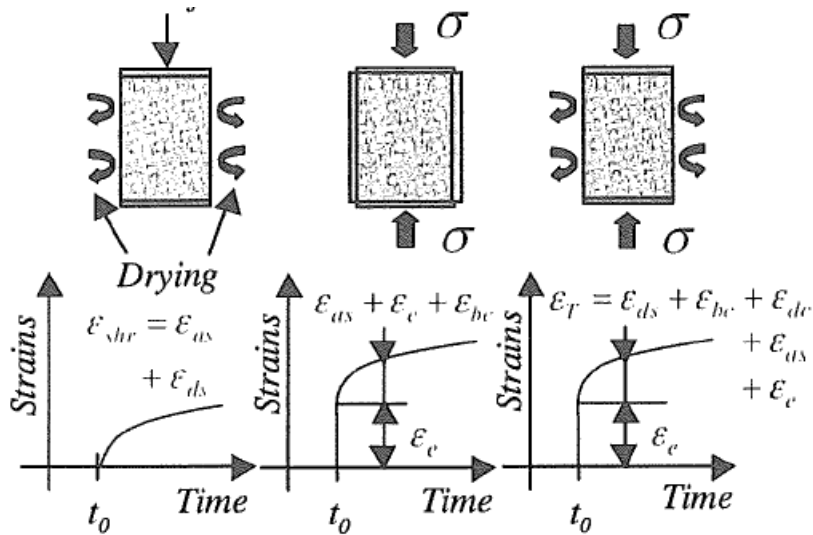
Figure 2. Experimental procedure to get the drying creep strains [6].

Strain components measured in the several different creep tests are shown in Figure 3 [7]. The author of this paper is not completely sure about these experimental results and how they have been obtained. That is why these results are not discussed throroughly in this paper. Elastic strain (if approx. 300 microns) is included in the total strain and in the basic creep strain results. During the other measurements, there was not any loading present. The highest curve is obtained in the drying creep test and actually contains all the possible strain components. The actual drying creep is calculated by subtracting basic creep and drying shrinkage (after 91 days) from the total strain. This drying shrinkage also has to contain the autogeneous shrinkage (non-drying shrinkage), since it is always present in concrete regardless of the conditions.
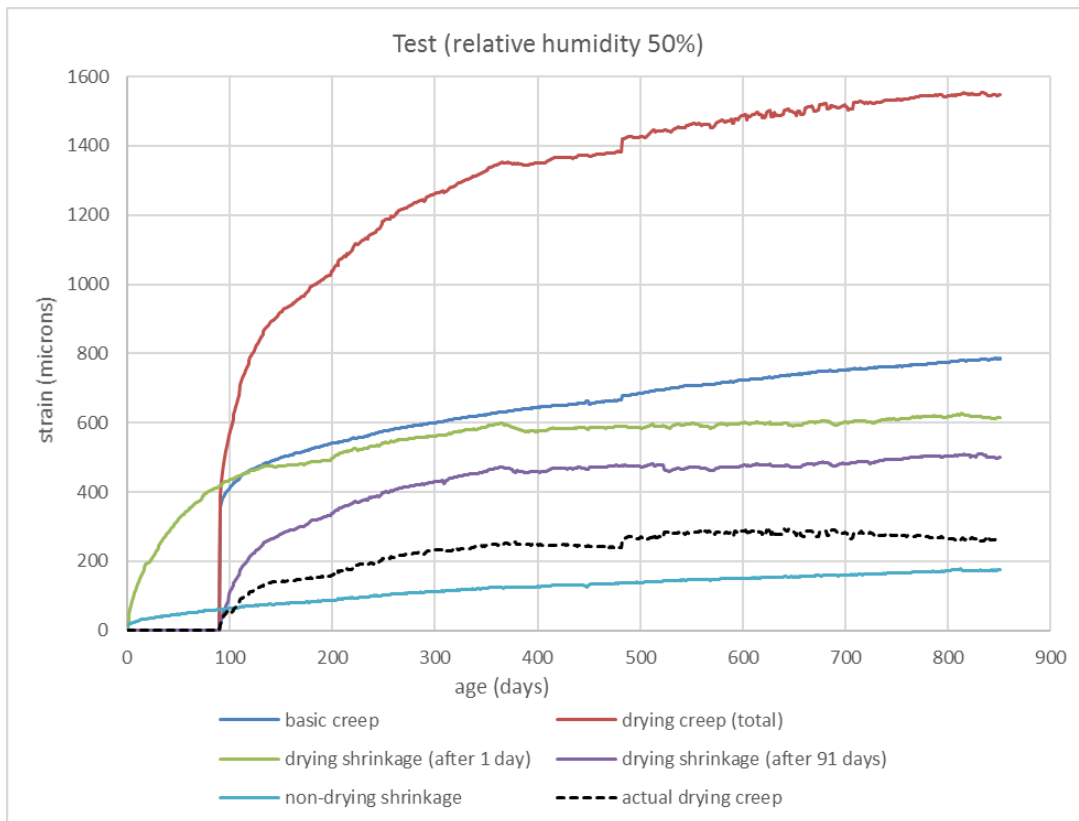
Figure 3. Strain components measured in the creep tests [7].

Strain components in the drying creep test according to Eurocode [5] are shown in Figure 4. In basic creep test, where the specimen was sealed throughout the test, there is no drying shrinkage. These components do not include elastic stain, but it is shown separately. Now, at least the calculated basic creep can be compared to the measured one in a straightforward manner. The elastic strain just has to be superposed to it. It can be seen that they correspond to each other really well. Also, the shrinkage strains correspond to each other relatively well.
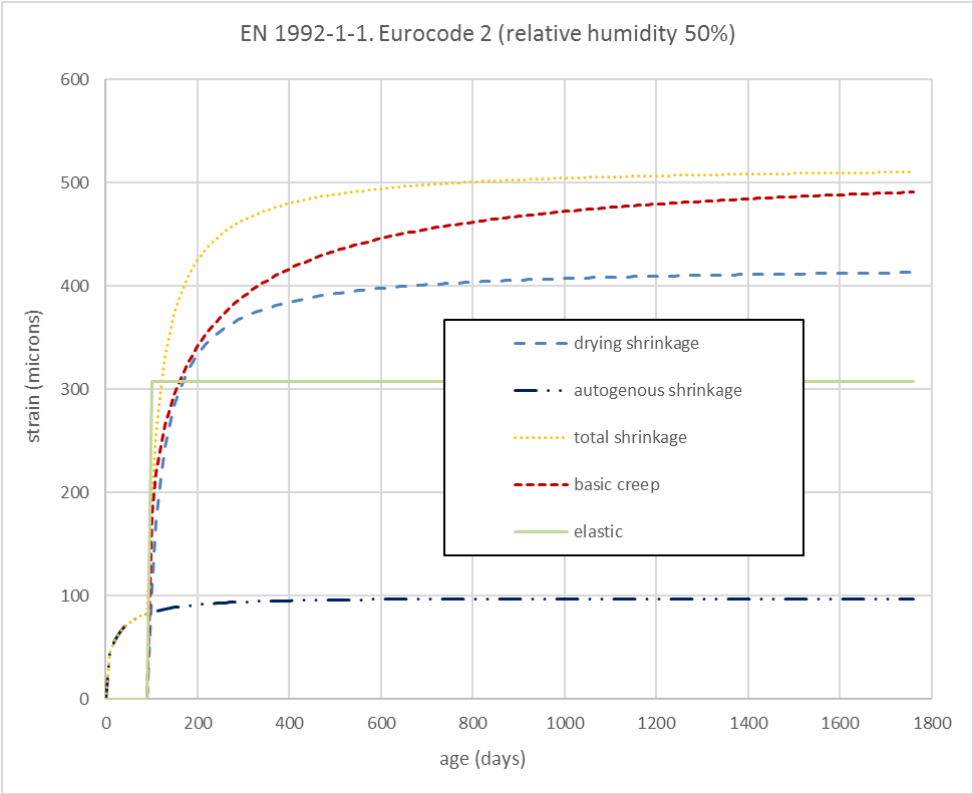
Figure 4. Strain components in drying creep test according to Eurocode [5].

The problem is that Eurocode does not include the drying creep. The author provided drying creep results to the benchmark exercise as a difference between basic creep and drying shrinkage, but that is not the right way. The provided results are shown below, but it has to be noted that regarding the drying creep they are wrong.
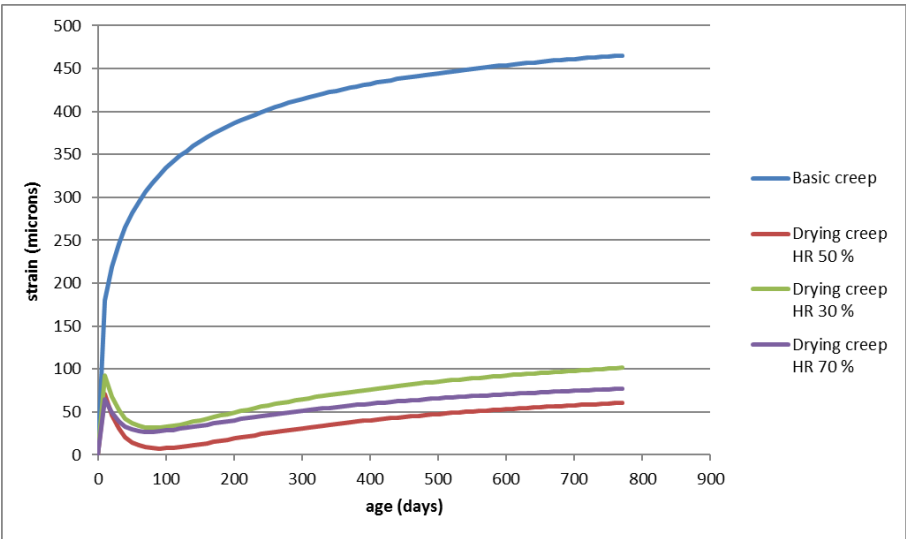
Figure 5. Basic creep strain (RH 50%) and drying creep strains for different RHs.
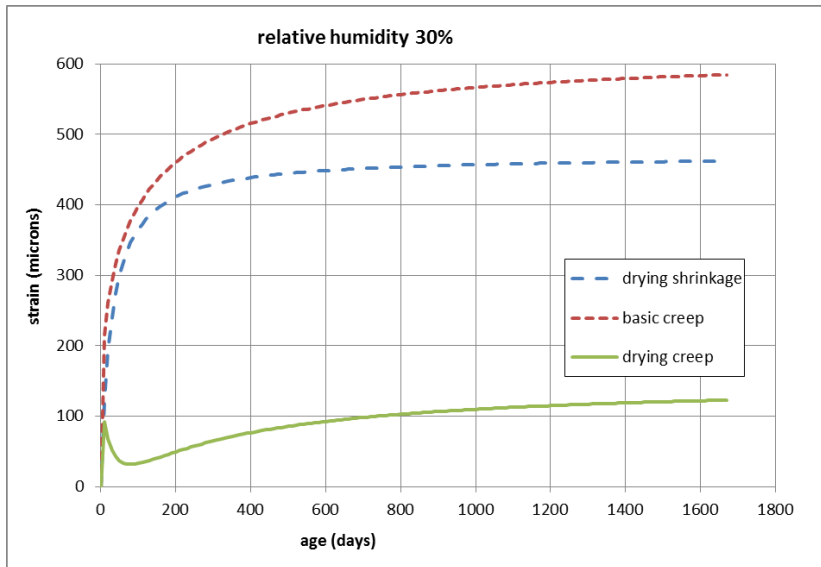
Figure 6. Strains for RH = 30%.
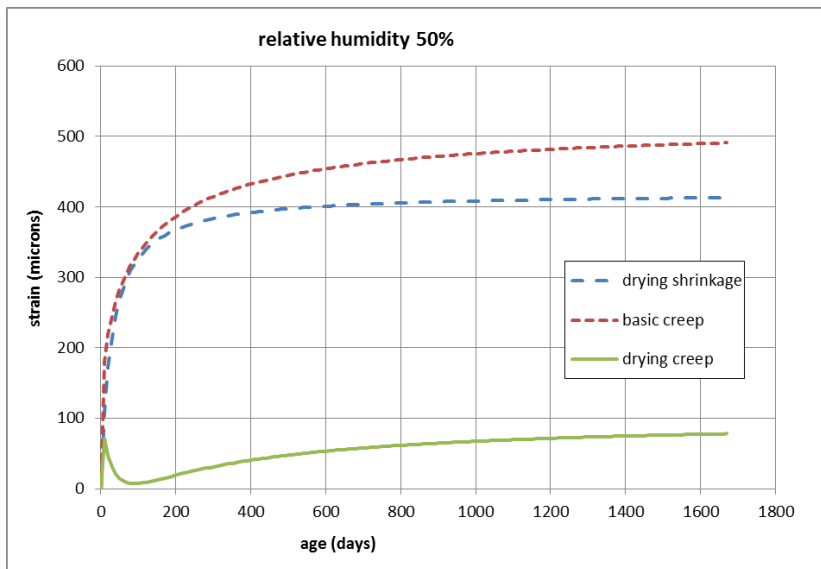
Figure 7. Strains for RH = 50%.
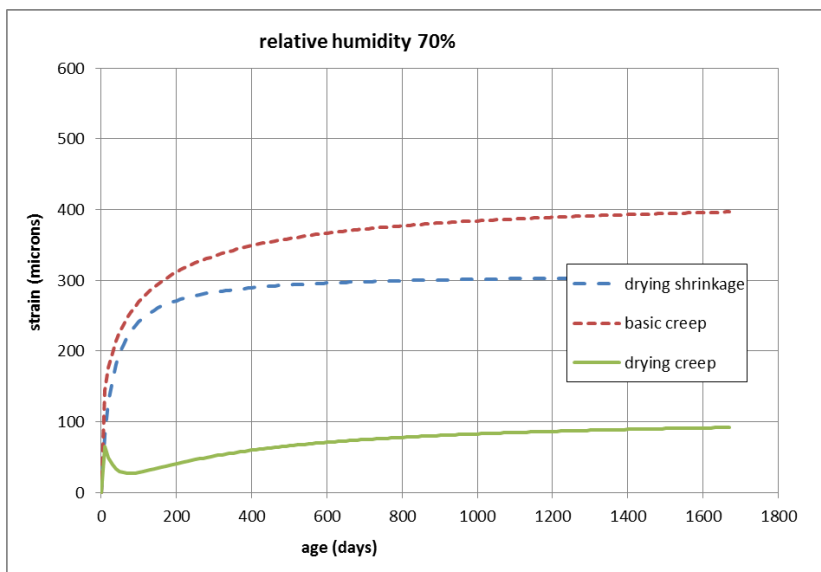
Figure 8. Strains for RH = 70%.

CONCLUSIONS

Eurocode gives creep and shrinkage results close to the measured ones even though it is a simple approach and does not take into account the geometry or other details of the specimen in any way. It does not assess the drying creep which is one of the requested calculation results. This is just a preliminary study of this theme and the results will be reviewed and improved.

ACKNOWLEDGEMENTS

REFERENCES

[1] Corbin, M. and Garcia M. International Benchmark VeRCoRs 2015 - Overview, synthesis and les-sons learnt. (2016).

[2] Calonius, K., Nilsson, T., Elison, O. and Lehmann, S. EDF VERCORS Project – Benchmark 1: Themes 1, 2 and 3. Research Report VTT-R-00016-16. (2016).

[3] Calonius, K., Nilsson, T., Elison, O. and Lehmann, S. Theme 2 and 3 of the international benchmark VeRCoRs, paper for the VeRCoRs Workshop in Les Renardières, France, 7-9 March 2016.

[4] Calonius, K. VERCORS Project – Benchmark 1: Themes 2 and 3 – improved model. VTT Research Report VTT-R-01041-17. (2017).

[5] European Committee for Standaridization, CEN, EN 1992-1-1. Eurocode 2: Design of concrete structures - Part 1 -1: General rules and rules for buildings, 2004.

[6] Benboudjema, F., Meftah F. and Torrenti J. M. "Drying creep: an elasto-plastic damage approach of the structural effect". Fracture Mechanics of Concrete Structures, de Borst et al (eds), 2001 Swets & Zeitlinger, Lisse, ISBN 90 2651 825 O. (2001)

[7] Experimental results and photographs provided by EDF. (2018)

Modelling of the basic creep of the VeRCoRs concrete

Jean Michel Torrenti[*] and Abdushalamu Aili[†]

[*] Université Paris-Est, MAST, IFSTTAR, F-77447 Marne-la-Vallée, France, e-mail: jean-michel.torrenti@ifsttar.fr

[†] Université Paris-Est, Laboratoire Navier (UMR 8205), CNRS, Ecole des Ponts ParisTech, IFSTTAR, F-77455 Marne-la-Vallée, France

ABSTRACT

The prediction of the long term behaviour of prestressed concrete structures is important in order to assess and/or extend the service life of such structures. In the case of nuclear power plants where the internal vessel is a biaxially prestressed structure, the prediction of the delayed deformations is also a safety concern. Here, the relations proposed by MC2010 [1] for autogenous shrinkage and basic creep are used and compared to experimental results provided for the benchmark Vercors.

Autogenous shrinkage

In MC2010, autogenous shrinkage is expressed as

$$\varepsilon_{cbs} = \xi_{cbs1}\, \alpha_{bs} \left(\frac{0,1\, f_{cm}}{6+0,1\, f_{cm}}\right)\left(1 - e^{-0,2\xi_{cbs2}\sqrt{t}}\right) \tag{1}$$

where α_{bs} is a parameter depending on the cement type, f_{cm} is the mean compressive strength and ξ_{cbs1} and ξ_{cbs2} parameters adjusted to experimental results.

Figure 1 shows the comparison of this expression when the parameters are adjusted to experimental results.
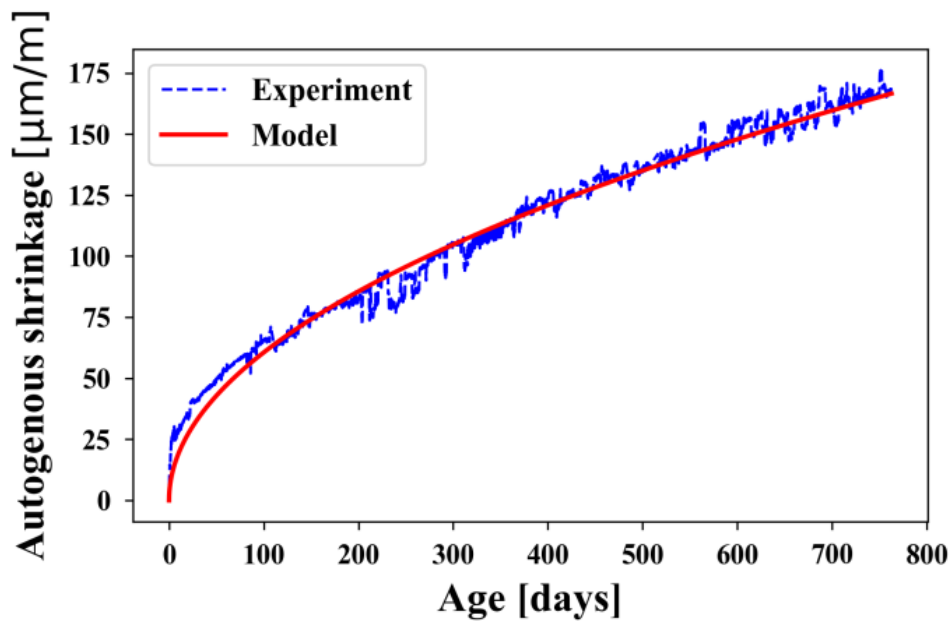
Figure 1: autogenous shrinkage - comparison between experimental results and equation 1 with $\xi_{cbs1} = 152$ and $\xi_{cbs2} = 0,0024$

Basic creep

Several comparisons with experimental results [2, 3] shows that basic creep could be estimated with the relation proposed by MC2010:

$$\varphi_{bc}(t, t_0) = \frac{\xi_{bc1}}{C} ln\left(1 + \frac{t - t_0}{\tau(t_0)\xi_{bc2}}\right) \tag{2}$$

with C a constant under isothermal conditions, t_0 is the age of concrete at loading and $\tau(t_0)$ a parameter depending on the age of loading. ξ_{bc1} and ξ_{bc2} are parameters adjusted to experimental results.

The deformation corresponding to the basic creep is then:

$$\varepsilon_{cbs} = \frac{\sigma}{E_{28}} \varphi_{bc}(t, t_0) \tag{3}$$

where σ is the applied stress and E_{28} the Young modulus at 28 days.

To compare the model with experimental results, the instantaneous deformation and autogenous shrinkage are removed from the total deformation. Figure 2 shows the comparison between the experimental results and equation 3 when the parameters are adjusted.
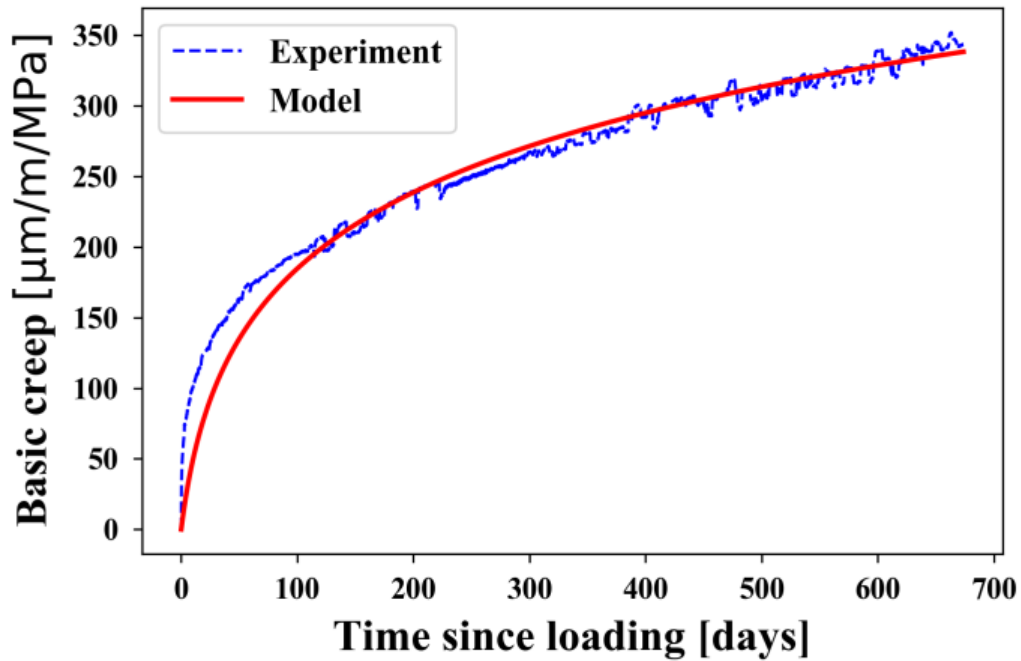
Figure 2: basic creep - comparison between experimental results and equations 2 and 3 with $\xi_{bc1} = 1,6$ and $\xi_{bc2} = 3,4$

These models will be used to predict the global behaviour of the mockup (see contribution to theme 2).

REFERENCES

[1] fib model code for concrete structures MC2010, Ernst und sohn, 2013

[2] R. Le Roy, F. Le Maou, J.M. Torrenti (2017), Long term basic creep behavior of high performance concrete. Data and modelling, Materials and structures, 50:85.

[3] J.M. Torrenti, R. Le Roy (2018), Analysis of some basic creep tests on concrete and their implications for modelling, Structural Concrete, 19; 483–488.

Modelling creep in concrete cylinders subjected to different relative humidity levels–the VeRCoRs 2018 benchmark

M. ÅHS[*], R. MALM[†] AND C. BERNSTONE[††],

[*]Lund University, Lund, Sweden, e-mail: magnus.ahs@byggtek.lth.se

[†]KTH Royal Institute of Technology, Stockholm, Sweden, e-mail: richard.malm@byv.kth.se

[††]Vattenfall AB, Solna, Sweden, e-mail: christian.bernstone@vattenfall.com,

ABSTRACT

In this study, a multiphysics model is presented that predicts creep in three months old concrete cylinders subjected to drying. The model includes concrete hydration, and a moisture transport model with relative humidity as the driving potential. These parameters are important to include in order to simulate creep. The model was implemented in the finite element software COMSOL Multiphysics. The calculated axial deformation of the cylinder was compared with measurements performed on an experimental set-up. The model was found to be able to predict the axial deformations with reasonable accuracy. This study is a part of the VeRCoRs 2018 benchmark provided by the Electricité de France, EDF.

INTRODUCTION

This study presents mechanical analyses of a concrete cylinder subjected to a creep test. It is a part of the VeRCoRs benchmark 2018 arranged by Electricité de France, EDF. The results from the analyses have been compared with actual measurements performed on a concrete cylinder subjected to a certain experimental set up. In this study, the focus has been to use a model available for professional designers, Eurocode 2, and not to develop a model that only researchers is able to use and to show the magnitude of error that may be expected by using such a model in a laboratory test set up.

A number of different studies have been initiated by the Swedish power industry with an objective to develop advanced calculation tools to analyse mechanics and transport mechanisms in nuclear power and hydropower concrete structures [1, 2].

HYDRATION MODEL

Material properties of concrete change significantly during the first month. In order to correctly describe the behaviour of young concrete it is therefore vital to use a model that describes such material changes. As most of the material properties are related to the hydration degree of cement this is used as a method to address the changes with time.

The model of hydration, used in this study, was developed by Byfors [3] and it describes the hydration of concrete through time, $\alpha(t)$, Eq. 1

$$\alpha(t) = e^{A\log(\frac{t}{3600})^B} \quad (1)$$

where A and B are curve fitting parameters, in this study A=-7 and B=-2.7 was used. These parameters were determined by using the provided temperature development from VeRCoR at adiabatic conditions from the actual used concrete together with the maximum heat release from hydration.

Hydration in an early age concrete is described by adopting a model presented by Norling Mjörnell [4]. The mathematical formulation of hydration rate of concrete $\frac{\partial \alpha(t)}{\partial t}$ is shown in Eq. (2)

$$\frac{\partial \alpha(t)}{\partial t} = \beta_{WC}\beta_T\beta_\varphi \left(\frac{\partial \alpha(t_e)}{\partial t}\right)_{ref} \tag{2}$$

where $\beta_{WC}, \beta_T, \beta_\varphi$, are parameters dependent on the water to cement ratio, the temperature and the relative humidity, RH, respectively and $\left(\frac{\partial \alpha(t_e)}{\partial t}\right)_{ref}$ is the hydration rate in a reference climate 20 °C and at fully saturated conditions.

The expression used to calculate the water to cement ratio parameter is shown in Eq. (3)

$$\beta_{WC} = \left(\frac{\alpha_{max} - \alpha}{\alpha_{max}}\right)^{A_{betaWC}} \tag{3}$$

where α_{max}, here 0.98, is equal to the maximum possible hydration degree, and A_{betaWC}, here 1.9, which is a parameter used to fit the current hydration development to a reference hydration development on a concrete with a reference water to cement ratio. This takes into account that the amount of unreacted cement is reduced with time.

The temperature dependency on hydration rate is based on the Arrhenius equation for thermal activation and is described by the maturity function shown in Eq. (4)

$$\beta_T = e^{\left(\frac{1}{T_{ref}} - \frac{1}{T}\right)\theta} \tag{4}$$

where T_{ref} is the reference temperature, in our case 293.15 [K], T is the actual temperature in [K], and θ is the temperature dependency of the activation temperature. This temperature dependency is described by Eq. (5)

$$\theta = \theta_{ref} \left(\frac{30}{T + 10 - 273.15}\right)^{\kappa_3} \tag{5}$$

where θ_{ref}, here 4700 and κ_3, here 0.54 are empirical constants derived from experimental adaptations.

Finally, β_φ, is a parameter determined by the proportion of capillary pores filled with water, as it is mainly the liquid water in the pores that contributes to the formation of hydration products. The capillary pore volume P_{cap_p} is determined by using Eq. (6)

$$P_{cap_p} = \frac{\frac{W_0}{C} - .39 \cdot \alpha(t)}{0.32 + \frac{W_0}{C}} \tag{6}$$

where $\frac{W_0}{C}$, is the water to cement ratio in [kg/kg]. And parameter β_φ is then described by Eq. (7)

$$\beta_\varphi = \frac{\frac{W_e(\varphi)}{C} - P_{cap_p} \cdot \alpha(t)}{\frac{W_0}{C} - .19\alpha(t) - P_{cap_p} \cdot \alpha(t)} \tag{7}$$

where, $W_e(\varphi)$, is the moisture content at a certain RH.

HEAT TRANSFER MODEL

The temperature condition inside the concrete cylinder was determined by solving the conventional energy-balance Eq. (8)

$$\rho \cdot C_p \cdot \frac{\partial T}{\partial t} = \nabla(k\nabla T) + Q \tag{8}$$

where ρ represents the density 2350 [kg/m³], C_p the specific heat capacity 880 [J/(kgK)], T the temperature in [K] and k the heat conductivity 1.8 [W/(mK)]. The heat released from the cement hydration reaction Q, was also included as a function of the hydration rate see Eq. (9)

$$Q = \frac{d\alpha(t)}{dt} \cdot q_u \cdot C \tag{9}$$

where q_u represents the maximum heat released by hydration and C represents the cement content in the concrete mixture, 320 [kg/m³]. The initial concrete temperature of the concrete cylinder was assumed to be 293 [K]. The cement used in the actual concrete mixture, CEM I 52,5 N CE CP2 NF Gaurain, has a maximum heat release of 376 [kJ/kg], and this was used in the model.

MOISTURE TRANSPORT MODEL

Moisture transport may be modelled by using a number of different transport potentials, such as air vapour content, air vapour pressure or capillary pressure. This model used relative humidity as a driving potential and was previously developed in the Nugenia-Acceppt project. Results from using this model were verified qualitatively with measurements from Swedish nuclear reactor Ringhals 4 performed in another study [5]. The moisture transport, J, was modelled by using the relative humidity as the driving potential, see Eq. (10)

$$J = -\delta_\varphi \frac{\partial \varphi}{\partial x} \tag{10}$$

where φ [-], is the ratio between actual and saturation vapour content, which is the RH in the pores of the material and δ_φ [m²kg/(sm³)] is the moisture dependent transport coefficient with RH as the transport potential.

The moisture transport in the proposed model [6], is based on the mass conservation equation, Fick's second law, Eq. (11)

$$\frac{\partial W_e}{\partial t} = \frac{\partial W_e}{\partial \varphi} \frac{\partial \varphi}{\partial t} = \nabla(\delta_\varphi \nabla \varphi) + Q_2 \tag{11}$$

where $\frac{\partial W_e}{\partial \varphi}$ represents the moisture capacity derived from the sorption isotherm, δ_φ represents the moisture transport coefficient with relative humidity as a driving potential, φ is the relative humidity, and Q_2 represents the self-desiccation of concrete. Self-desiccation was evaluated by using Eq. (12)

$$Q_2 = \frac{\partial \alpha(t)}{\partial t} \cdot C \cdot 0.25 \tag{12}$$

where $\frac{\partial \alpha(t)}{\partial t}$ represents the hydration rate, C, represents the cement content [kg/m³] in the concrete mixture and 0.25, which represents an assumed maximum possible amount of water chemically bounded by the cement.

THERMAL EXPANSION, SHRINKAGE AND CREEP MODEL

The thermal expansion, ε_{th}, was included by using, Eq. (13)
$$\varepsilon_{th} = \alpha \cdot (T - T_{ref}) \tag{13}$$
where α, is the thermal coefficient $(1,1 \cdot 10^{-5})$ [1/K], T represents the temperature [K] and T_{ref} represents the reference temperature 293 [K].

The drying shrinkage was included by using Eq. (14)
$$\varepsilon_{sh}(t) = \frac{W_i - W(t)}{W_i - W_\infty} \cdot \varepsilon_{sh,\infty} \tag{14}$$
where $\varepsilon_{sh}(t)$, represents the shrinkage strain at time t, W_i, is the initial moisture content, $W(t)$ is the moisture content at time t, W_∞ is the moisture content when in equilibrium with the current humidity exposure, and $\varepsilon_{sh,\infty}$ represents the final shrinkage strain which is estimated to 0.05%.

Creep was modelled by using the model described in Eurocode 2. In this model, the creep coefficient, $\varphi_c(t, t_0)$, is described by Eq. (15)

$$\varphi_c(t, t_0) = \varphi_0 \cdot \beta_c(t, t_0) \tag{15}$$

where the φ_0 is the notional creep coefficient and $\beta_c(t, t_0)$ is a coefficient to describe the development of creep with time after loading. A thorough description is found in in Eurocode 2[7].

The creep strain, ε_{cr}, is included by using Eq. 16

$$\varepsilon_{cr} = \varphi_c(t, t_0) \cdot \frac{\sigma}{E} \tag{16}$$

where σ, represents the stresses in the concrete and E represents the modulus of elasticity which was assumed constant 31.8 [GPa].

The total strain is then described by Eq. 17

$$\varepsilon_{tot} = \varepsilon_{el} + \varepsilon_{th} + \varepsilon_{sh} + \varepsilon_{cr} \tag{17}$$

where ε_{el} is the elastic strain from the mechanical loads.

CASE STUDY

The above presented model was applied to various laboratory test set-ups on a number of concrete cylinders subjected to various boundary conditions with the finite element software COMSOL. The diameter of each cylinder was 0.08 m and the length was 1.0 m. In Figure 3 and Figure 2, the geometry and the finite element mesh are shown.
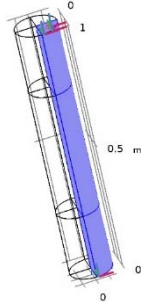
Figure 1 Geometry of the concrete cylinder, 1 m long and 0.16 m in diameter
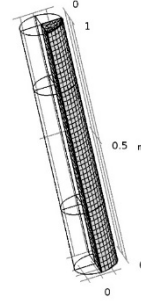
Figure 2 Illustration of the finite element mesh of the concrete cylinder

Only one forth of the cross section of the cylinder was modelled. The mesh consisted of around 2000 hexahedral elements and the degrees of freedom used were around 220 000.

The surrounding temperature was set as 293 K. A convective heat flux was used at the vertical concrete surfaces. The humidity during the drying shrinkage test was set to 50% RH 24 hours after casting. In the creep test, the surface was assumed to be totally sealed for 90 days, before loading the concrete cylinder. At the time of the exerted axial load the sealing was removed and the surface exposed to a relative humidity of 50 % RH. The simulations were performed by setting the climate to 30, 50 and 70 % RH.

The surface mass transfer resistance with RH as a driving potential, k_{RH},was modelled by using Lewis relation [8], Eq. (18)

$$k_{RH} = \frac{h \cdot v_s}{\rho_{air} \cdot C_{p(air)}} \tag{18}$$

where, h, is the convection heat transfer coefficient [W/(m²K¹)], v_s is the saturation vapour content [kg/m³], ρ_{air}, is the air density [kg/m³], and $C_{p(air)}$, is the heat capacity of air [J/(kgK)]. This model is an estimation of the surface mass transfer resistance.

The exerted axial load was modelled as a constant boundary load of 60.25 kN on the surface perpendicular to the length of the cylinder. The creep test was controlled by a hydraulic jack, and a pressure cell was used to monitor the applied pressure. Because of creep and shrinkage, the applied force continuously decreased from the initial force of 241 kN. When the force decreased 10 %,to 216 kN the force was adjusted and increased to 241 kN again.

RESULTS AND DISCUSSION

Results from calculations performed by using the presented model, are shown in Figure 3 to Figure 5. In Figure 3, the results from the simulated axial deformation is presented together with the measurements performed on the concrete cylinder during drying. Figure 4 shows the actual basic creep of the concrete cylinder, in addition to the results from the applied creep model.
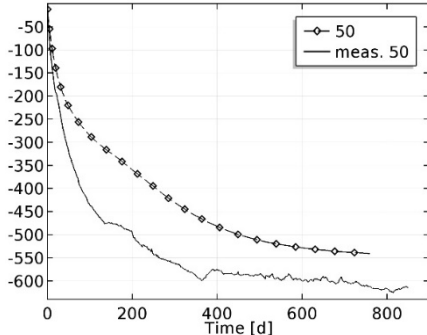

Figure 3 Drying shrinkage axial strains (10^{-6} m/m)
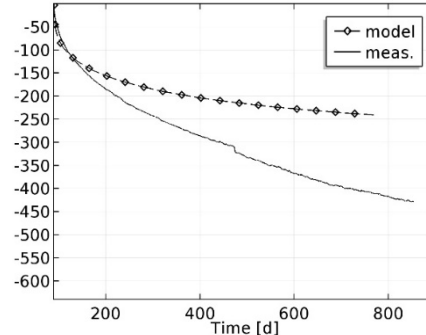
Figure 4 Basic creep axial strains (10^{-6} m/m)

During the first 150 days, the actual, measured, shrinkage is larger than the simulated. After 200 days, the measured shrinkage is about 500 micro strains compared to 375 micro strains obtained by the simulation, see Figure 3. This difference may be an effect of underestimated drying caused by an underestimation of the moisture transport property of the early age concrete. Another possible reason for this difference may stem from underestimation of the maximum shrinkage coefficient. In addition, the difference could partly be explained by the fact that the modulus of elasticity is assumed to be constant during the simulation. This overestimates the modulus of elasticity during early ages. The actual shrinkage in the range between 400-800 days is of a similar magnitude compared with the results from the model. The calculated basic creep of the concrete cylinder, see Figure 4, is not as large as the actual basic creep. During the first few days the simulated creep is larger than the calculated creep but afterwards the actual axial deformations are larger. This indicates that the Eurocode underestimates the actual basic creep of concrete on a long-term basis. The fact that Eurocode underestimates creep has been shown by other authors, i.a. Lundqvist [9] and Raphael et al. [10].

Calculated drying creep for three different exposure humidities, 30, 50 and 70% RH, are shown in Figure 5 including measurements performed on one concrete cylinder exposed to 50% RH.
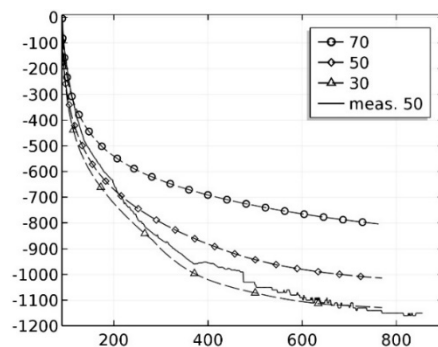
Figure 5 Drying creep axial strains (10^{-6} m/m)

The calculated drying creep clearly shows that low humidity increases the deformations with time, see Figure 5. Furthermore, it is shown that the applied model from Eurocode underestimates the actual creep. The underestimation is around 10 % after some 750 days. After that amount of time deformations caused by shrinkage are reduced to a large extent and the major contribution should originate from creep alone.

CONCLUSIONS

A method to model axial deformation in COMSOL was developed. The Eurocode model to estimate creep is underestimating the actual creep compared to the measurements. This means that practitioners using the established Eurocode model underestimates creep in this type of application which may have an impact on the design of new structures.

ACKNOWLEDGEMENT

REFERENCES

1. Åhs, M. and S. Poyet, *The prediction of moisture and temperature distribution in a concrete reactor containment*. 2015, Lund university. p. 72.
2. Eriksson, D., R. Malm, and H. Hansson, *Nugenia Acceppt - Analysis of stress concentrations and crack risk*. 2015, KTH Royal Institute of Technology.
3. Byfors, J., *Plain concrete at early ages*. 1980, KTH, Royal Institute of Technology: Stockholm, Sweden.
4. Norling Mjörnell, K., *Moisture Conditions in High Performance Concrete. Mathematical Modelling and Measurements*. 1997, Institutionen för byggnadsmaterial, Chalmers tekniska högskola.
5. Oxfall, M., P. Johansson, and M. Hassanzadeh, *Moisture Profiles in Concrete Walls of a Nuclear Reactor Containment after 30 Years of Operation*, in *XXII Nordic Concrete Research Symposium, 2014-08-13*. 2014, Norsk Betongforening.
6. Åhs, M., S. Poyet, L.-O. Nilsson and V. L'Hostis, *A model to predict moisture conditions in concrete reactor containments*, in *Fontevraud 8, Contribution of materials investigations and operating experience to LWRs' safety, performance and reliability*. 2014: Avignon, France.
7. *Eurocode 2: Design of concrete structures Part 1-1: General rules for Buildings*, in *EN 1992-1-1 Appendix B*. 2004, European committee for standardization: Brussels. p. 225.
8. Lewis, W., *The evaporation of a liquid into a gas*. International Journal of Heat and Mass Transfer, 1962. **5**(1-2): p. 109-112.
9. Lundqvist, P., *Assessment of Long-Term Losses in Prestressed Concrete Structures - Application for Nuclear Reactor Containments*, in *Division of Structural Engingeering*. 2012, Faculty of engineering, Lund University: Lund.
10. Raphael, W., E. Zgheib, and A. Chateauneuf, *Experimental investigations and sensitivity analysis to explain the large creep of concrete deformations in the bridge of Cheviré*. Case Studies in Construction Materials, 2018. **9**: p. e00176.

Thermo-Hydro-Mechanical Strategy for Forecasting the Leakage Rate of Double-Wall Nuclear Reactor Buildings:
Focus on the modeling of VeRCoRs' concrete delayed strains

M. Asali[*] and B. Capra[†]

[*] OXAND France, 49 av. Franklin Roosevelt, Avon-Fontainebleau, France, mehdi.asali@oxand.com
[†] OXAND France, 49 av. Franklin Roosevelt, Avon-Fontainebleau, France, bruno.capra@oxand.com

ABSTRACT

In order to compute the total air leakage rate of the VeRCoRs mock-up, we propose a chained weakly-coupled thermo-hydro-mechanical (THM) strategy which aims at assessing the temperature, saturation degree, stress and strain fields and damage state within the structure under operating conditions (long-term operation). Thus, early age behavior of concrete during erection and accidental situations with high and quick variations of pressure and temperature are out of the scope of this study.

This paper focuses on the delayed strains modeling for the inner containment concrete structure and on the identification of associated material and modeling parameters.

THERMAL MODEL

In a first step, the temperature field $T(\boldsymbol{x}, t)$ (in K) is computed independently of all other phenomena. Heat transfer is governed by thermal conduction within concrete's volume and follows the classical heat equation (1):

$$\rho_b C_p \frac{\partial T(\boldsymbol{x}, t)}{\partial t} + \boldsymbol{\nabla} \cdot [-\lambda(T)\boldsymbol{\nabla}T(\boldsymbol{x}, t)] = 0 \tag{1}$$

Where ρ_b is the concrete density (in kg·m⁻³), C_p is the concrete thermal capacity (J·kg⁻¹·K⁻¹) and λ is the concrete thermal conductivity field (in W·m⁻¹·K⁻¹) depending on temperature T. In a classical way, boundary conditions of the thermal problem can be expressed with imposed temperatures, convective exchanges or thermal radiations.

HYDRIC MODEL

In a second step, the water saturation field $S_l(\boldsymbol{x}, t)$ in concrete is computed. Humidity staying above 40% in concrete during inner containments operation, the following assumptions are typically considered ([1], [2]):
- Drying is mainly due to liquid water movements within concrete porosity,
- Drying/wetting cycles during the pre-operational phase only impact surface concrete, not core concrete,
- Air pressure is negligible compared to water pressure.

In that case, a classical non-linear diffusion equation (2) is used, where the humidity diffusion coefficient $D(S_l, T)$ depends on temperature as proposed by [1]:

$$\frac{\partial S_l(\boldsymbol{x}, t)}{\partial t} + \boldsymbol{\nabla} \cdot [D(S_l, T)\boldsymbol{\nabla}S_l(\boldsymbol{x}, t)] = 0 \tag{2a}$$

$$D(S_l, T) = \frac{K_{int}^l k_{rl}(S_l)}{\eta_l \phi} \frac{\partial P_c}{\partial S_l} \frac{T(\boldsymbol{x}, t)}{T^{ref}} \exp\left(\frac{E_a}{R}\left(\frac{1}{T^{ref}} - \frac{1}{T}\right)\right) \tag{2b}$$

Where K_{int}^l is the water intrinsic permeability of concrete (in m²), k_{rl} is the water relative permeability field (values between 0 and 1), η_l is the water viscosity (in Pa·s), ϕ is the concrete porosity, P_c is the capillary pressure field (in Pa), T^{ref} is the reference temperature (in K) at which all hydric properties of equation (2) are defined or measured, E_a is the thermal activation energy of concrete (in J·mol⁻¹), R is the universal gas constant (in J·mol⁻¹·K⁻¹).

The capillary pressure is defined with Van Genuchten's retention model [3]:

$$P_c(S_l) = P_r\left(S_l^{-1/m} - 1\right)^{1/n} \tag{3}$$

Where P_r (in Pa) and n (> 1) are model parameters and $m = 1 - 1/n$. The water relative permeability follows Mualem's model [4]:

$$k_{rl}(S_l) = \sqrt{S_l}\left[1 - \left(1 - S_l^{1/m}\right)^m\right]^2 \tag{4}$$

MECHANICAL MODEL

In a third step, delayed strains in concrete are computed. Prestressing losses in tendons are modeled according to ETC-C formulae [5] considering a perfect bond between concrete and steel cables. Passive reinforcement bars are not explicitly considered. The total strain field $\boldsymbol{\varepsilon}(\boldsymbol{x}, t)$ is split into five main components representative of operating conditions:

$$\boldsymbol{\varepsilon}(\boldsymbol{x}, t) = \boldsymbol{\varepsilon}^{\mathbf{el}} + \boldsymbol{\varepsilon}^{\mathbf{bc}} + \boldsymbol{\varepsilon}^{\mathbf{dc}} + \boldsymbol{\varepsilon}^{\mathbf{ds}} + \boldsymbol{\varepsilon}^{\mathbf{th}} \tag{5}$$

Where $\boldsymbol{\varepsilon}^{\mathbf{el}}$ is the damaged elastic strain tensor, $\boldsymbol{\varepsilon}^{\mathbf{bc}}$ is the basic creep tensor, $\boldsymbol{\varepsilon}^{\mathbf{dc}}$ is the drying creep tensor, $\boldsymbol{\varepsilon}^{\mathbf{ds}}$ is the drying shrinkage tensor and $\boldsymbol{\varepsilon}^{\mathbf{th}}$ is the thermal expansion tensor.

Thermal expansion and drying shrinkage are considered as isotropic and proportional to temperature and saturation respectively ([6], [1]):

$$\boldsymbol{\varepsilon}^{\mathbf{th}}(\boldsymbol{x}, t) = \alpha_{th}\big(T(\boldsymbol{x}, t) - T(\boldsymbol{x}, 0)\big)\mathbf{I_3} \tag{6}$$

$$\boldsymbol{\varepsilon}^{\mathbf{ds}}(\boldsymbol{x}, t) = \kappa_{ds}\big(S_l(\boldsymbol{x}, 0) - S_l(\boldsymbol{x}, t)\big)\mathbf{I_3} \tag{7}$$

Where α_{th} is the thermal expansion coefficient (in K⁻¹), κ_{ds} is the drying shrinkage coefficient (no unit) and $\mathbf{I_3}$ is the 3D identity matrix.

Drying creep is considered as proportional to the effective stress $\widetilde{\boldsymbol{\sigma}}$ (in Pa) and saturation states of concrete as suggested by [7] and [8] to model Pickett's effect [9]:

$$\dot{\boldsymbol{\varepsilon}}^{\mathbf{dc}}(\boldsymbol{x}, t) = \kappa_{dc}\big|\dot{S}_l(\boldsymbol{x}, t)\big|\widetilde{\boldsymbol{\sigma}}(\boldsymbol{x}, t) \tag{8}$$

Where κ_{dc} is the drying creep coefficient (in Pa⁻¹).

Basic creep is modeled with an ageing Burger's rheological chain (9), as suggested by [7]. This choice enables to consider biaxial creep effects (10, 11), a logarithmic evolution of creep strains over time (12) and the impact of pre-computed temperature and saturation fields on creep parameters (12, 13):

$$\boldsymbol{\varepsilon}^{\mathbf{bc}}(\boldsymbol{x},t) = \boldsymbol{\varepsilon}^{\mathbf{rev}}(\boldsymbol{x},t) + \boldsymbol{\varepsilon}^{\mathbf{irr}}(\boldsymbol{x},t) \tag{9}$$

$$\hat{\eta}_{irr}(t)\dot{\boldsymbol{\varepsilon}}^{\mathbf{irr}} = (1+v_{bc})\boldsymbol{\sigma} - v_{bc}\mathrm{tr}(\boldsymbol{\sigma})\mathbf{I_3} \tag{10}$$

$$\hat{\eta}_{rev}\dot{\boldsymbol{\varepsilon}}^{\mathbf{rev}} + \hat{k}_{rev}\boldsymbol{\varepsilon}^{\mathbf{rev}} = (1+v_{bc})\tilde{\boldsymbol{\sigma}} - v_{bc}\mathrm{tr}(\tilde{\boldsymbol{\sigma}})\mathbf{I_3} \tag{11}$$

$$\hat{\eta}_{irr}(t,T,S_l) = \frac{k_{irr}t}{S_l}\exp\left(\frac{E_a}{R}\left(\frac{1}{T}-\frac{1}{T_{ref}}\right)\right) \tag{12}$$

$$\hat{\Xi}_{rev}(T,S_l) = \frac{\Xi_{rev}}{S_l}\exp\left(\frac{E_a}{R}\left(\frac{1}{T}-\frac{1}{T_{ref}}\right)\right), \qquad \Xi \in \{k,\eta\} \tag{13}$$

Where $\boldsymbol{\varepsilon}^{\mathbf{rev}}$ is the reversible basic creep strain field, $\boldsymbol{\varepsilon}^{\mathbf{irr}}$ is the non-reversible creep strain field, $\boldsymbol{\sigma}$ is the total stress tensor field in concrete, v_{bc} is the basic creep Poisson's ratio, k_{irr} is the stiffness associated to the non-reversible ageing dashpot (in Pa), k_{rev} is the stiffness associated to the reversible creep strains (in Pa), η_{rev} is the viscosity associated to the reversible creep strains (in Pa·s).

Concrete's post-peak behavior is modeled thanks to damage theory used in the μ-model [10] in order to take into account a unilateral effect (crack closing and reopening) that could occur with cycling internal leakage rate tests:

$$E\boldsymbol{\varepsilon}^{\mathbf{el}}(\boldsymbol{x},t) = (1+v)\tilde{\boldsymbol{\sigma}} - v\,\mathrm{tr}(\tilde{\boldsymbol{\sigma}})\mathbf{I_3} \tag{14}$$

$$\boldsymbol{\sigma}(\boldsymbol{x},t) = (1-d)\tilde{\boldsymbol{\sigma}}(\boldsymbol{x},t) \tag{15}$$

$$d(\boldsymbol{x},t) = 1 - \frac{(1-A)Y_0}{Y(\boldsymbol{\varepsilon}^{\mathbf{el}})} - A\exp\left(B\left(Y_0 - Y(\boldsymbol{\varepsilon}^{\mathbf{el}})\right)\right) \tag{16}$$

Where E is the Young's modulus of concrete (in Pa), v its Poisson's ratio, d is the scalar effective damage variable field (values between 0 and 1, a non-null value meaning active cracking either in tension or compression), A and B are coefficients depending on the stress state of concrete and defined from post-peak responses of concrete in pure tension and pure compression, Y is a driving variable for damage evolution and Y_0 is the initial threshold of variable Y. To limit mesh sensitivity due to the softening behavior of concrete, parameter B is adjusted together with element sizes [11].

IDENTIFICATION OF MODELING PARAMETERS

The concrete delayed strain model (5-16) is implemented as an external user behavior law with TFEL/MFront v2.0.1 [12] within the general framework of Code_Aster [13].

If available, concrete parameters are preferably mean values of on-site measurements for each lift (density, porosity, Young's modulus, tensile strength, thermal expansion coefficient). If not, some identifications are directly provided by EDF for the benchmark (thermal capacity, thermal conductivity, activation energy, fracture energy).

The last parameters are then identified from specific laboratory tests (cylindrical concrete specimen: 1 m height, 16 cm diameter) that were carried out by EDF for the benchmark. Van Genuchten's coefficients P_r and n are first identified from the desorption isothermal curve of concrete (Figure 1), then the water intrinsic permeability K_{int}^l from the weight loss curve (Figure 2).

Knowing those three desiccation parameters, the drying shrinkage coefficient κ_{ds} is identified from the 1D drying shrinkage test (including autogenous shrinkage, Figure 3) and the three rheological coefficients k_{rev}, η_{rev} and k_{irr} are identified from the 1D basic creep test (corrected from autogenous shrinkage, Figure 4).
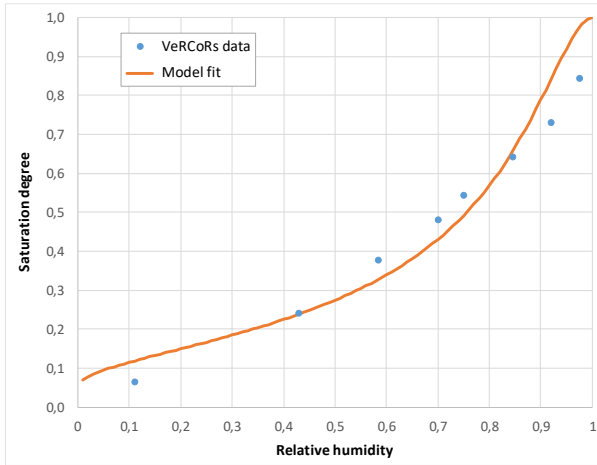
Figure 1: Van Genuchten's coefficients identification from desorption isotherm measurements
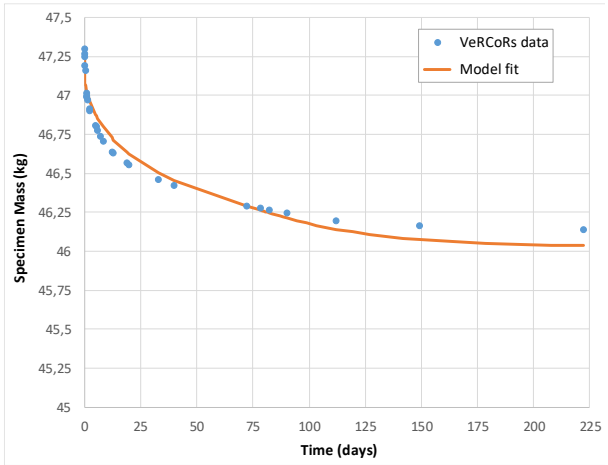

Figure 2: Water intrinsic permeability identification from weight loss measurements
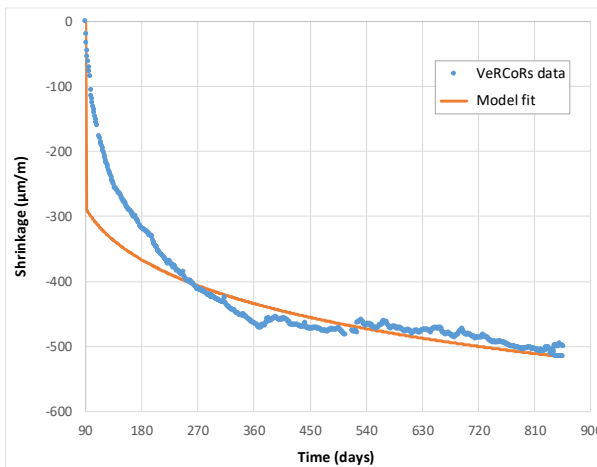

Figure 3: Drying shrinkage coefficient identification from 1D laboratory test
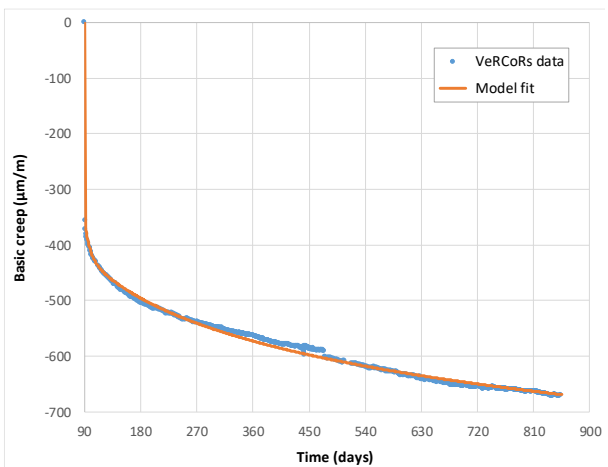
Figure 4: Basic creep coefficients identification from 1D laboratory test

Knowing the drying shrinkage and basic creep components of delayed strains, the drying creep coefficient is finally identified from the 1D total creep test (Figure 5).
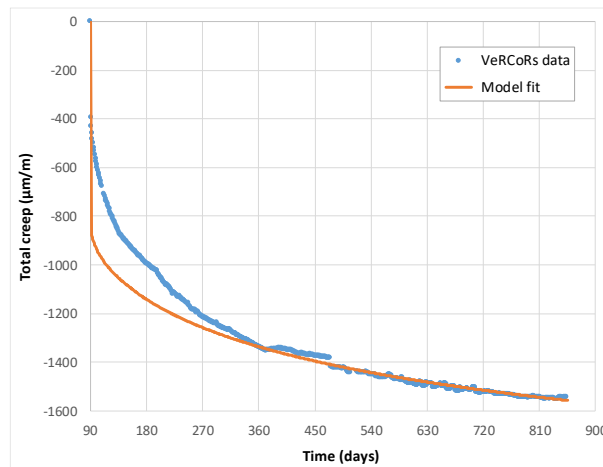
Figure 5: Drying creep coefficient identification from 1D total creep laboratory test

CONCLUSIONS

Based on available laboratory testing (mainly uniaxial samples), chosen models can well reproduce the long-term behavior of VeRCoRs reconstituted concrete. Some extra specific testing would be needed to identify the biaxial creep behavior and a possible differential creep behavior between tension and compression, thus those effects have not been considered in the structural computation submitted to the benchmark. Completed with on-site lift measurements, a full-scale computation has been performed with the proposed modeling strategy (see detailed results in Themes 2 & 3).

REFERENCES

[1] L. Granger, "Comportement différé du béton dans les enceintes de centrales nucléaires: analyse et modélisation", Thèse de l'ENPC (1995)

[2] E. Drouet, "Impact de la température sur la carbonatation des matériaux cimentaires – Prise en compte des transferts hydriques", Thèse de l'Ecole Normale Supérieure de Cachan (2010)

[3] M. T. Van Genuchten, "A closed-form equation for predicting the hydraulic conductivity of unsaturated soils", *Soil Science Society of America Journal*, **44**:892-898 (1980)

[4] Y. Mualem, "New model for predicting hydraulic conductivity of unsaturated porous media", *Water Resources Research*, **12**:513-522 (1978)

[5] "EPR Technical Code for Civil works", AFCEN (Association Française pour les règles de Conception, de construction et de surveillance en exploitation des matériels des Chaudières Electro Nucléaires), Lyon, 2010

[6] Z. P. Bazant, F. H. Wittman, "Creep and shrinkage of concrete structures, chapter 'Creep and shrinkage mechanisms'", *Wiley*, Chichester (1982)

[7] A. Hilaire, "Etude des déformations différées des bétons en compression et en traction, du jeune âge au long terme", Thèse de l'Ecole Normale Supérieure de Cachan (2014)

[8] Z. P. Bazant, J. C. Chern. "Concrete creep at variable humidity: constitutive law and mechanism", *Materials and Structures*, **18**:1-20 (1985)

[9] G. Pickett, "The effect of change in moisture-content on the creep of concrete under a sustained load", *ACI Journal Proceedings*, vol. **38** (1942)

[10] J. Mazars, F. Hamon and S. Grange, "A new 3D damage model for concrete under monotonic, cyclic and dynamic loadings", *Materials and Structures*, **48**:3779-3793 (2015)

[11] A. Hillerborg, M. Modeer and P. E. Petersonn, "Analysis of crack formation and growth in concrete by mean of fracture mechanics and finite elements", *Cement and Concrete Research*, **6**:773-782 (1976)

[12] http://tfel.sourceforge.net/, MFront website, "A code generation tool dedicated to material knowledge"

[13] http://web-code-aster.org/spip.php?rubrique2, "Code_Aster website, "Structures and Thermomechanics Analysis for Studies and Research"

VeRCoRs Theme I: Creep Modeling

Dr. Joshua R. Hogancamp[*], **Madhumita Sircar**[†]

[*]Sandia National Laboratories, Albuquerque, USA, e-mail: jhoganc@sandia.gov
[†]U.S. Nuclear Regulatory Commission, Washington, D.C., USA, e-mail: Madhumita.Sircar@nrc.gov

PRIMARY FEATURES

Concrete creep is dependent on many factors including but not limited to volume to surface area ratio, temperature, load, time, aggregate type and content, humidity, and moisture content. Concrete subjected to a constant load with no addition or loss of moisture, i.e. a completely sealed specimen, undergoes what is known as basic creep. If concrete is exposed to a dry environment, the specimen undergoes a volume change from drying shrinkage. Similar to a drying sponge, water evaporating from concrete pores creates capillary suction forces that causes the concrete to shrink. Concrete that is subjected to creep (concrete under load) while exposed to a dry environment undergoes a compounded effect called drying creep. Drying creep has a larger magnitude than the combination of basic creep with drying shrinkage; experts are still unsure as to the exact mechanisms behind basic creep and drying creep. Tests measure drying creep by utilizing the same experiment as for basic creep but exposing the specimens to a dry environment, typically 50% relative humidity (RH). Figure 1 shows the basic and drying creep test results for the specimen setup shown in Figure 2. The elastic strain immediately jumps to ~0.0003 when the load is applied, and the creep strain is the gradual increase in axial strain vs time.
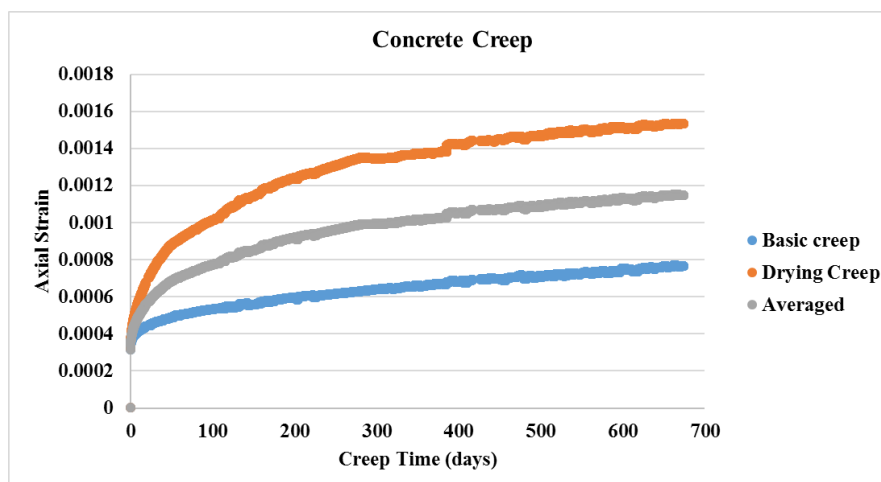
Figure 1: Basic (bottom line) and drying (top line) creep tests with an averaged value (middle line). Temperature: 50°C. RH: 50%.

Figure 2: Concrete creep measurement apparatus.

Large structures like those found at nuclear power plants may be more susceptible to basic creep since the surface area-to-volume ratio is low. However, the *VeRCoRs* posttensioned concrete containment vessel is 1/3 scale and is expected to be susceptible to drying creep. Therefore, the creep strain utilized in developing the models for the *VeRCoRs* simulation was taken as the average between the measured basic and drying creep strains.

The concrete was modeled as an isotropic homogeneous material using a viscoelastic Prony series model in ABAQUS (ABAQUS 6.14, 2018). A Prony series is a set of exponential decay terms that can replicate exponentially decaying data such as stress relaxation or concrete creep. An isotropic homogeneous material model was chosen since the concrete was predicted to act as a single material rather than a conglomerate of aggregates held together with cement paste. A viscoelastic Prony series model was chosen because of the Prony series' robust capability to capture viscoelastic behavior. No damage was expected to occur in the concrete over the course of the simulation, so a purely viscoelastic model was deemed adequate to capture long-term deformation over time. The Prony series equation used by ABAQUS is a string of exponential terms as described in Table 1.

The parameters G_i and τ_i are determined from experimental data using the following algorithm:
1. Compute Young's modulus by dividing stress / strain at each time point. Note that stress is constant while strain continues to increase, resulting in a decreasing modulus with time.
2. Convert Young's modulus to the shear modulus at each point in time using Young's modulus as calculated in Step 1 and Poisson's ratio (assumed constant).
3. Compute the Prony series with initial assumed values that give the general shape of the curve.
4. Compute and square the difference at every data point between the experimental values and the Prony values. The difference is squared to ensure that every difference value is positive.
5. Sum the squared difference values over the entire curve.
6. Run an in-built algorithm in a numerical software (Excel, Mathematica, MATLAB, etc.) to minimize the sum of the squared difference values by manipulating the Prony series constants G_i and τ_i.
7. Perform steps 1-6 for Prony series equations with $i = 2, 3, 4, 5$ terms to determine the smallest number of Prony terms that can minimize the sum of the squared difference values.

Table 1: Prony series equation and details.

Equation	Description
$$G(t) = G_0 \left(1 - \sum_{i=1}^{N} G_i \left(1 - e^{-\frac{t}{\tau_i}} \right) \right)$$	Prony series equation used to fit Prony parameters/constants to experimental data
$$G = \frac{E}{2(1 + \nu)}$$	Conversion of Young's modulus E and Poisson's ratio ν to shear modulus G
Variable	**Definition**
$G(t)$	Shear modulus with respect to time
G_0	Instantaneous shear modulus
G_i	Shear material constant
τ_i	Time constant (unit must match t)
t	Time (seconds, minutes, etc.)
E	Young's modulus
ν	Poisson's ratio

The Prony series parameters were combined in ABAQUS with the elastic response of the material, and a uniaxial compression creep test simulation was run in ABAQUS using a cylinder the same size as in the actual experiment.

RESULTS

Using the algorithm described in the PRIMARY FEATURES section, the Prony series parameters G_i and τ_i are determined from experimental data as shown in Figure 3. The two lines (experimental instantaneous shear modulus and Prony series fit) are almost identical. In this simulation, four terms ($i = 4$) were used in the Prony series. The robust capabilities of the Prony series lie in the ability to add exponential terms to match an exponential decay if required. In essence, each term of the Prony series captures a different time scale. For example:

- The first term of the Prony series can accurately capture the first several days of the creep function.
- The second term can add the ability to capture the first several weeks.
- The third term can add the ability to capture the first several months.
- The fourth term can add the ability to capture the first several years.

One, two, and three-term equations did not accurately capture creep behavior; the five-term equation did not further minimize the sum of the squared difference values between the experimental values and the Prony series values.
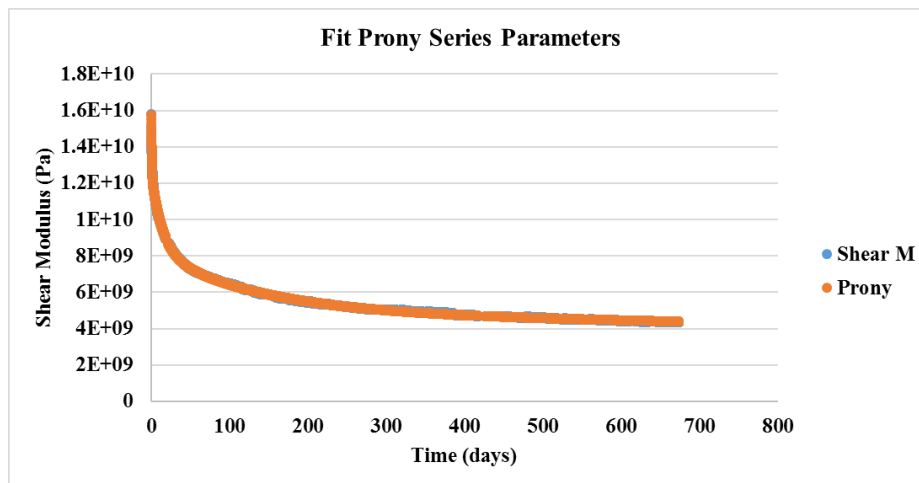
Figure 3: Fit Prony series parameters to shear modulus.

The results of the creep cylinder ABAQUS simulation are shown in Figure 4. The ABAQUS cylinder axial strain results agree well with the 'averaged' creep data.
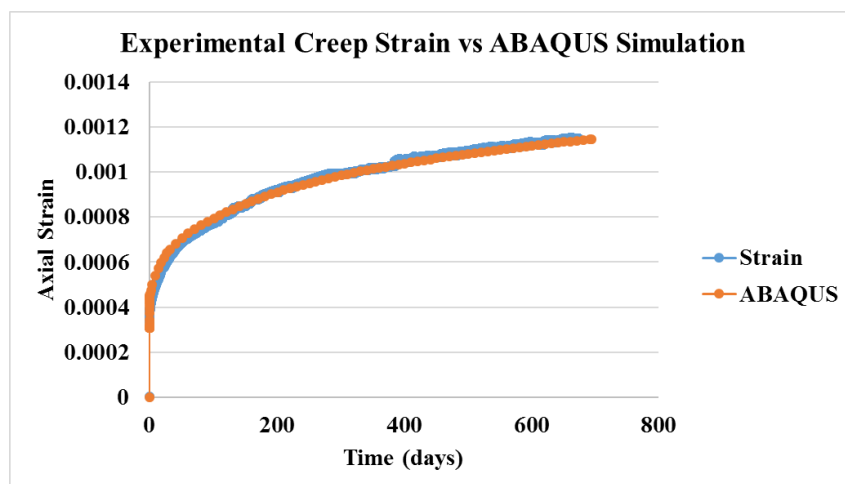
Figure 4: ABAQUS simulation creep strain results compared to 'averaged' experimental creep presented in Figure 1.

CONCLUSIONS

- Four terms in the Prony series were able to precisely capture the degrading shear modulus vs time of the experimental creep test data.
- The isotropic homogeneous viscoelastic Prony series model in ABAQUS can replicate uniaxial concrete compression cylinder creep strain.
- The ABAQUS uniaxial concrete compression cylinder creep test replicated the axial strain vs time of the experimental data.

REFERENCES

ABAQUS 6.14. (2018). Dassault Systèmes.

DISCLAIMERS

Theme 2: Mechanical behavior of the containment during pressurization test

- **J. Stepan -** UVJ Rez, a.s. div. Energoprojekt Praha, Czech Republic

  Analyses of Behaviour of the Containment Building in Stage 2

- **S. Kevorkian**, **G. Nahas, J. Clément -** IRSN, France,

  A numerical model of the VeRCoRs mock-up, pressure tests

- **J. Koskinen, P. Varpasuo -** Fortum Power & Heat Ltd/PVA Eng. Services, Finland

  VERCORS Containment Mock-Up test pressure response simulation by MSC/Nastran software

- **S. Jiménez, A. Cornejo, L.G. Barbu, S. Oller and A.H. Barbat** CIMNE/Technical University of Catalonia Barcelona, Spain

  Analysis of the VeRCoRs mock-up of a reactor containment building by means of a constitutive serial-parallel rule of mixtures

- **J. R. Hogancamp, M. Sircar** - Sandia National Laboratories, Albuquerque / U.S.Nuclear Regulatory Commission, Washington, D.C., USA

  VeRCoRs Theme II: Mechanical Behavior of the Containment during Pressurization Test

- **M. Ahs, R. Malm, C. Brernstone -** Lund University/KTH Royal Inst. of Tech./Vatenfall, Sweden

  Modelling creep in a pre-stressed mock-up reactor containment –the VeRCoRs 2018 benchmark case.

- **J-M. Torrenti, A. Aili -** IFSTTAR/Univ. Paris-Est, France ,

  Modelling of the global delayed behaviour of the VeRCoRs mock-up

- **S. Aparicio**, **M.G. Hernández, J.J. Anaya** - *ITEFI, CSIC, Madrid, Spain*

  Prediction of the strains and stresses in the gusset using COMSOL Multiphysics

Analyses of Behaviour of the Containment Building in Stage 2

J. Stepan[*]

[*] UJV Rez a.s., div. Energoprojekt Praha, Prague, Czech Republic, e-mail: jan.stepan1@ujv.cz

INTRODUCTION

Presented analyses were focused on behaviour of the containment building during prestressing and pressure tests including effects of shrinkage and creep of concrete (Stage 2 of VerCoRs 2018 benchmark).

The history of structure construction was included into the analyses considering these simplifications:

- The time history of structure construction was simplified into three basic steps – concreting of foundation slab and pedestal (used representative date 27.8.2014), concreting of cylindrical part (used representative date 25.11.2014), concreting of dome part (used representative date 22.4.2015).

- Prestressing in 16 Phases was simplified into 11 time steps, shrinkage and creep of concrete were taken into account between individual time steps.

- Distributions of forces in the tendons along their length were considered as variable due to friction but bonded tendons were considered since the beginning of analyses. The prestressing losses caused by friction were calculated based on the data published in the summary table on VerCoRs web site.

- Pressure tests were considered as instantaneous loading without effects of time dependent material properties.

Abaqus code was used for calculations. Concrete was modelled by solid elements, tendons by rod elements embedded into the solid elements. Visco-elastic material model is used for concrete with time dependent parameters corresponding to creep. No concrete cracking is included due to limitation of Abaqus code. Shrinkage of concrete was considered by prescribed strain deformation depending on time. Likewise, material model used for tendons is visco-elastic taking into account relaxation. Material data were set according test results available on VerCoRs web site.

Due to the significant influence of temperature on deformation response of structure, measured temperature history was considered and idealized changes of temperature was prescribed in calculations as a boundary condition. Unfortunately, measured temperatures are presented just for limited period of structure life-time – see Fig.1. No data are open for stage of construction and prestressing, therefore temperature of structure in these stages is considered as constant. Simplified temperature of containment structure used in calculation is presented in Fig.2. Based on measured temperatures, typical temperature of internal and external surface was determined. Temperature on the surfaces was considered uniform for all structure, no gradient of temperature with height was taken into account. Since starting of air-conditioning of internal area of containment, internal temperature is mainly independent on external environment whereas temperature of external surface in still affected by season changes of outer temperature.
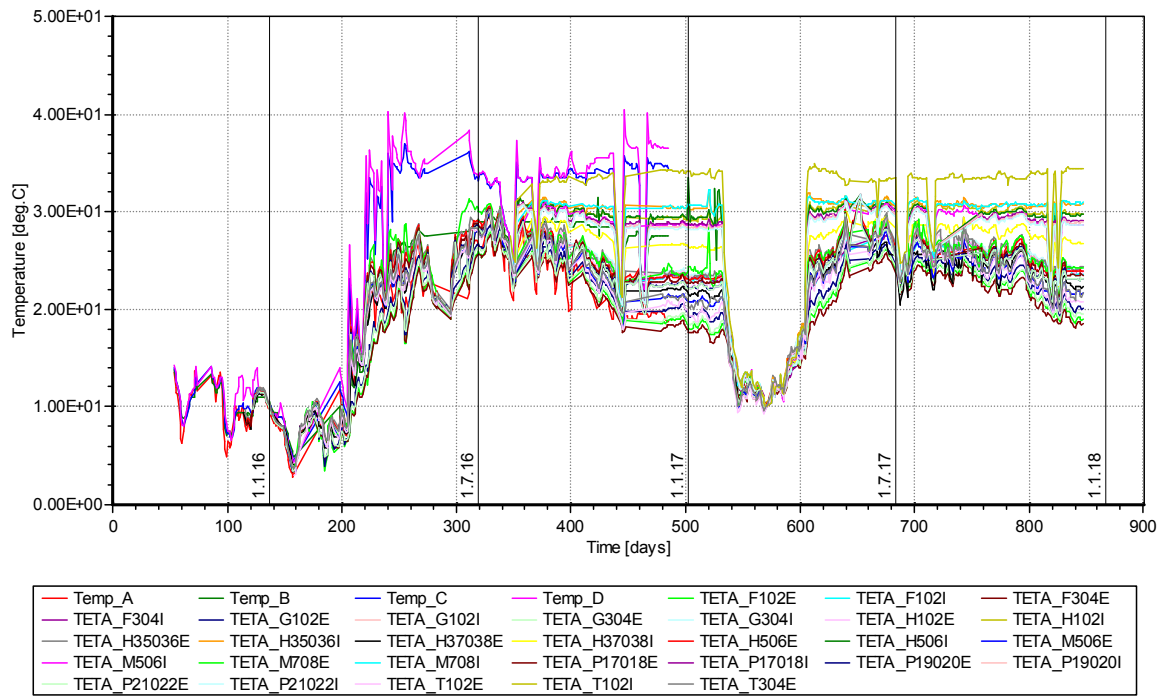
Fig. 1 – Measured temperature of containment structure, time 0 corresponds to the end of prestressing
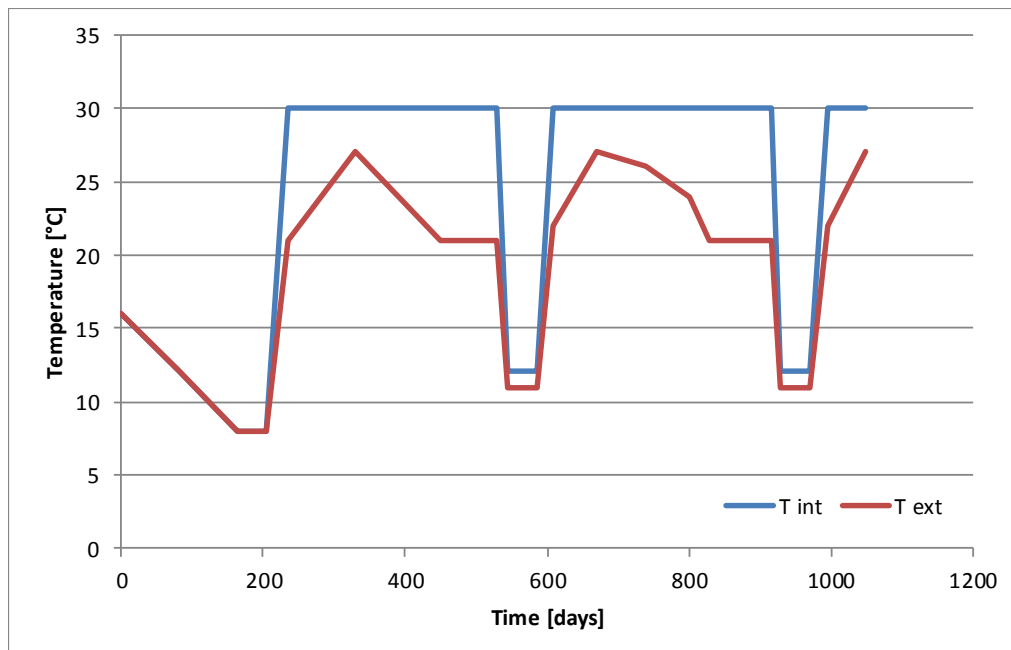

Fig. 2 – Idealized temperature of containment structure used in calculation, time 0 corresponds to the end of prestressing

RESULTS

Application of above described mechanical and temperature loadings led to 45 calculation steps combining instantaneous changes of loading and time dependent effects. Results were evaluated using two main criteria – relatively rapid change of deformation due to presence of internal pressure during pressure tests and long-term increase of deformation.

The comparison of calculated and measured changes of deformation due to action of pressure showed that elastic material properties set according results of material tests are valid for structure as well.

In case of long-term increase of deformation due to shrinkage and creep of concrete, early analyses showed slower increase of deformation. Therefore, input parameters used for calculation of shrinkage and creep of concrete were modified with the aim to fit measured data. Comparison of calculated and measured strain for final calculation is presented in Fig. 3 and in more detail for period between prestressing and 3rd pressure test in Fig.4.
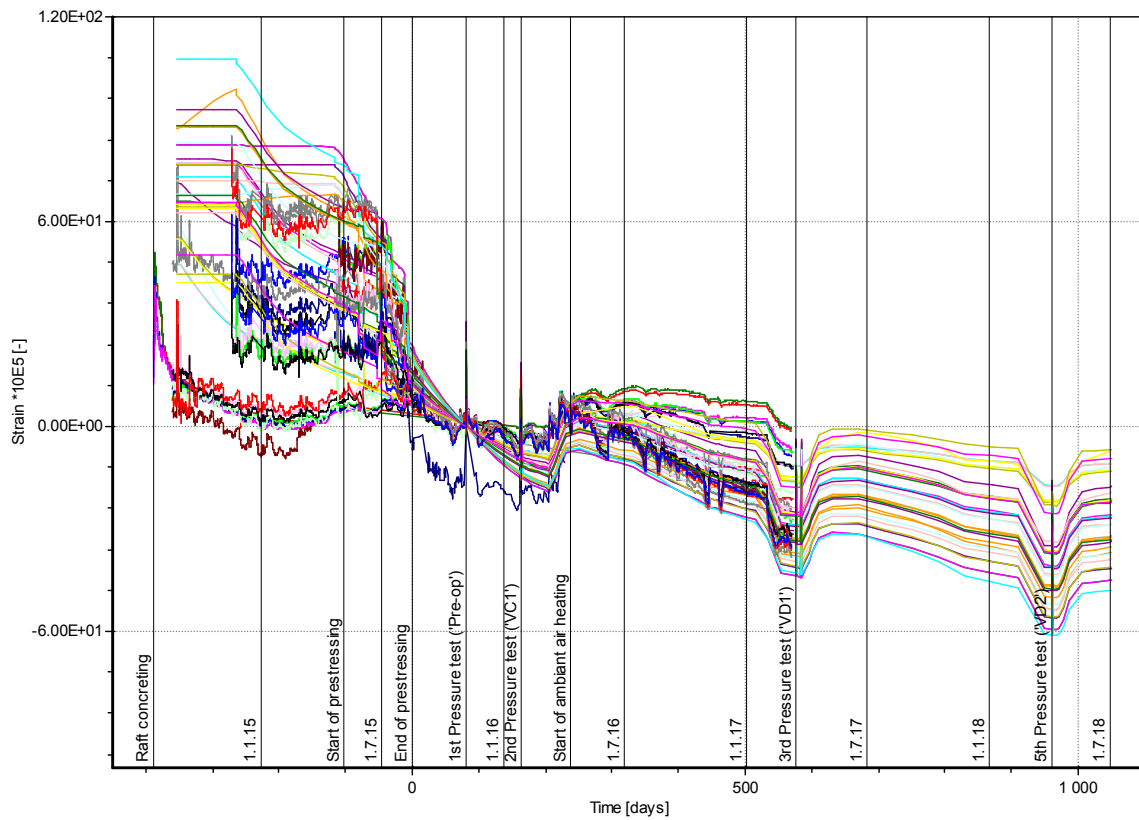
Fig. 3 – Comparison of measured and calculated strain, time 0 corresponds to the end of prestressing, strain 0 corresponds to the beginning of Pre-op test
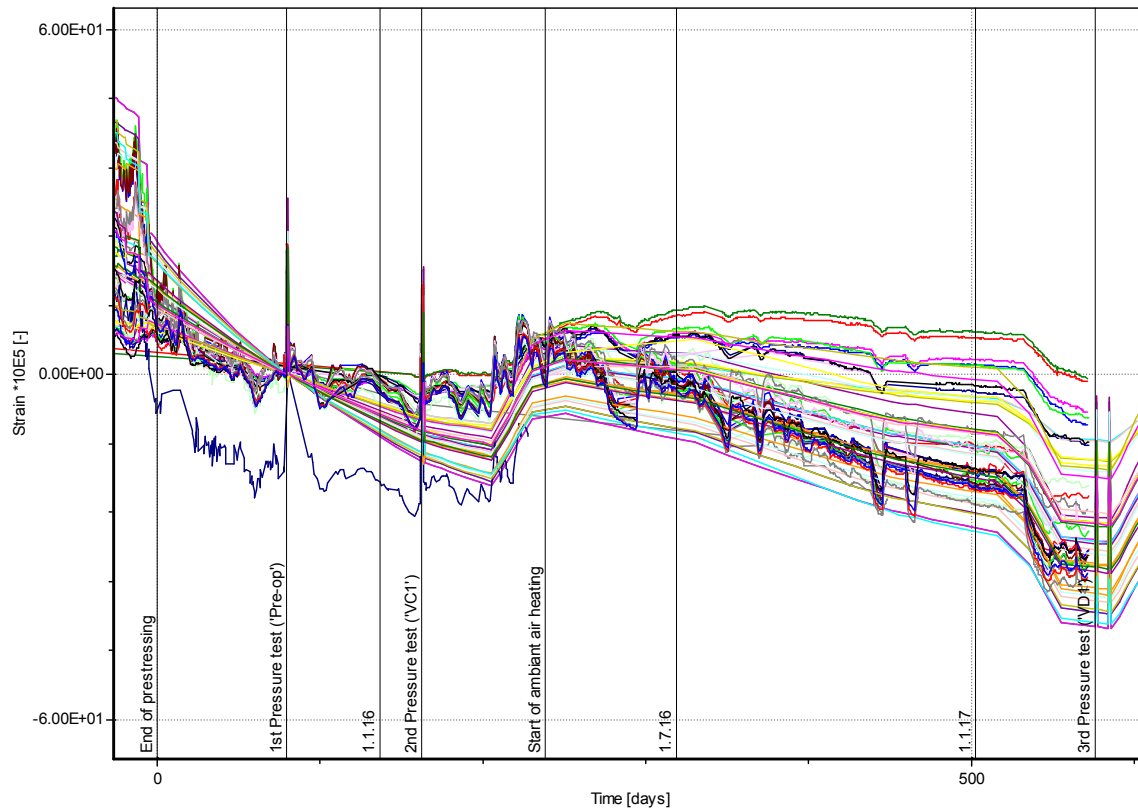
Fig. 4 – Detail of comparison of measured and calculated strain, time 0 corresponds to the end of prestressing, strain 0 corresponds to the beginning of Pre-op test

CONCLUSIONS

Starting position for analyses done within the scope of VerCoRs-2018 was based on experience obtain in the previous stage of VerCoRs benchmark. Prestressing was divided into individual steps taking into account creep of concrete during time period of prestressing. In addition, knowledge of time history of temperature of the structure enabled to include influence of temperature changes into calculations. These more specific input data for calculation enabled direct comparison of results with measured strains. Results showed good agreement in instantaneous response but there were differences in long-time increase of deformation. After a change of boundary conditions used for calculation of shrinkage and creep of concrete, results fit measured strains relatively well.

For future improvement of analyses, bringing of following additional data into the open would help:

- measured temperature history of the containment structure during construction and prestressing till the 1st pressure test

- measured prestressing forces in tendons, both during prestressing and long-term monitoring

In case of measured prestressing forces in tendons, based on our experience, it is expected that there are differences between theoretical formulas used for calculation of prestressing losses (friction and relaxation) and real behaviour of tendons. Knowledge of real time history of prestressing forces in tendons would enable to divide the loading and the response of structure (loaded mainly by prestressing) and that way address additional gaps in presumptions of analyses.

A numerical model of the VeRCoRs mock-up, pressure tests.

S. KEVORKIAN[*], G. NAHAS[†] and J. CLEMENT[††]

[*] IRSN, Fontenay-aux-Roses, France, e-mail: sandrine.kevorkian@irsn.fr.

[†] IRSN, Fontenay-aux-Roses, France, e-mail: georges.nahas @irsn.fr.

[††] IRSN, Fontenay-aux-Roses, France, e-mail: julien.clement @irsn.fr.

ABSTRACT

The mesh of the mock-up Vercors was made by IRSN using the software Cast3m [1]. Based on the real geometry provided by the VeRCoRs organising committee, it takes into account all the lifts of the mock-up, the pre-stressing tendons, the rebars and the precast shells of the dome.

The basemat is modelled with volumic finite elements and clamped at its bottom.

A first calculation was presented at the first workshop (2015), taking into account the lifts and the rebars of the current part of the mock-up in order to test the feasibility of computations on that model. This calculation was made with the software Cast3m [1].

The constitutive law of the concrete used is OTTOSEN model [2].

According to the fictitious crack model approach, OTTOSEN model is well adapted for brittle material such as concrete or ceramic, it uses the Hillborg approach for the modelling of crack.

For a reason of simplification, the concrete was considered as homogeneous in the first calculation.

The new calculation presented in this workshop takes into account:

- the mechanical characteristics of each lift ;

- the rebars in prestressing ribs and equipment hatch are added ;

- the door and the sleeve of the equipment hatch are added in order to apply the pressure ;

- the penetrations are sealed with volumic elements (super elements) in order to consider the pressure applied on the concrete ;

- the stirrups are added in the dome and the current part of the mock-up.

The pictures 1 to 5 represent the stirrups, the super elements, the door and the sleeve of the equipment hatch added to the model.
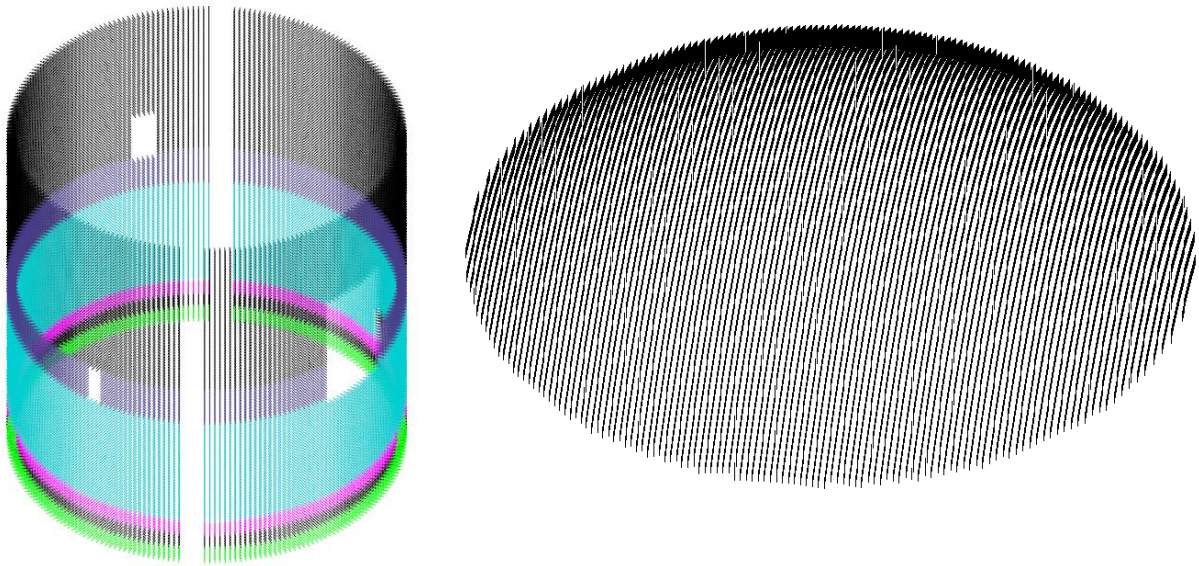
Figure 1 : Stirrups

Figure 2 : Elements used to seal penetrations.
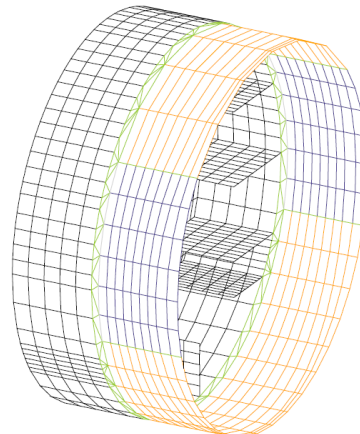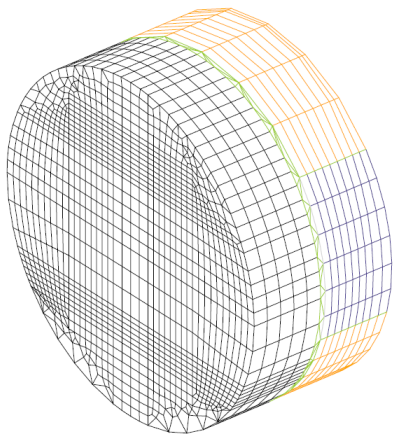
Figure 3 The door and the sleeve of the equipment hatch
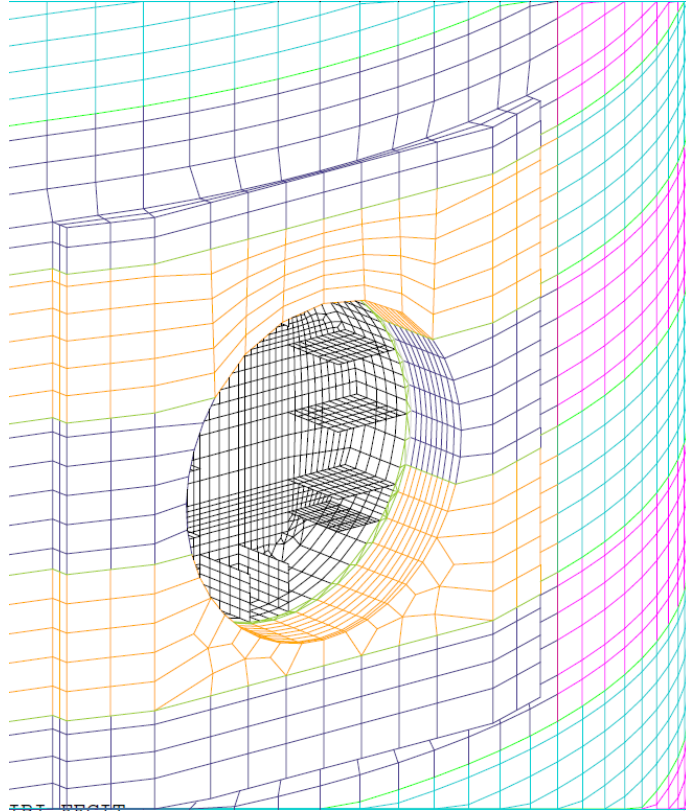
Figure 4 : The equipment hatch
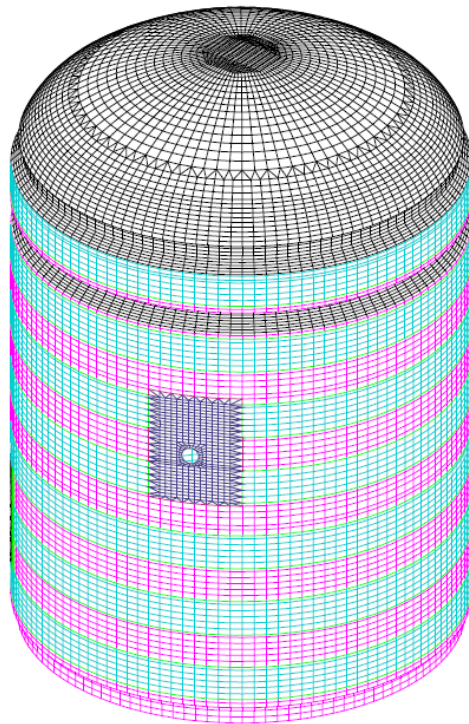
Figure 5 : Internal surface where the pressure is applied

The stress state of the mock-up before the pressure tests is obtained at different times :
- at the end of construction ;
- at the end of the tensioning of tendons for a concrete structure ;
- at the dates when the pressure will be applied.

Those differed stress states are due to the long term behaviour of concrete (creep and shrinkage)
The deformed state of the structure at the end of tensionning of tendons is presented in Figure 6
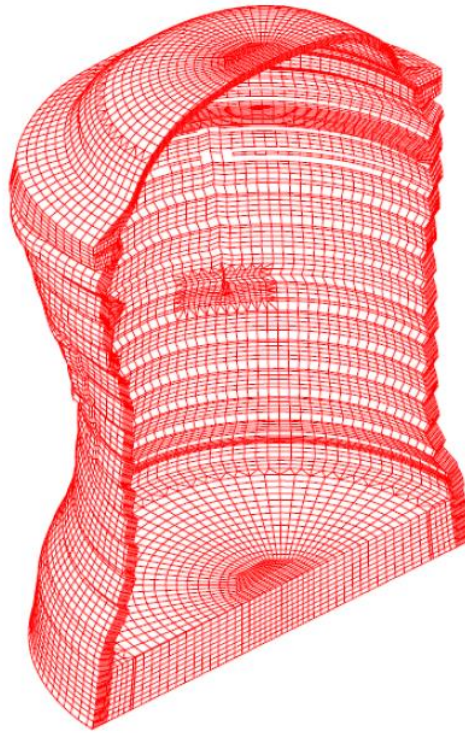
Figure 6 : Prestressed structure at the end of tensioning of tendons

Then the mechanical behaviour of the model submitted to an internal pressure is calculated.
For each of the pressure test considered, the stress state which was calculated as shown above, is applied on the structure.
Then the internal air pressure is applied. The evolutions of differed displacements and the pressure are presented in the figures 7 and 8.
On these figures, the time of each pressure test is presented :
- t= 0 for the first air pressure test, Pre Operationnal (VpreOp) ;
- t= 81 for the second air pressure test VC1;
- t= 495 for VD1;
- t= 502 for VD1 bis;
- t= 879 for VD2.
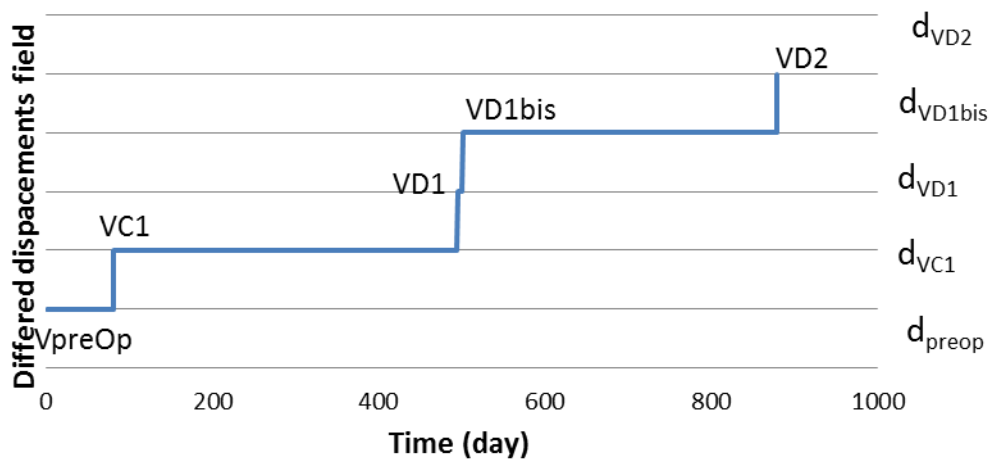
Figure 7 : The differed displacements field in function of time
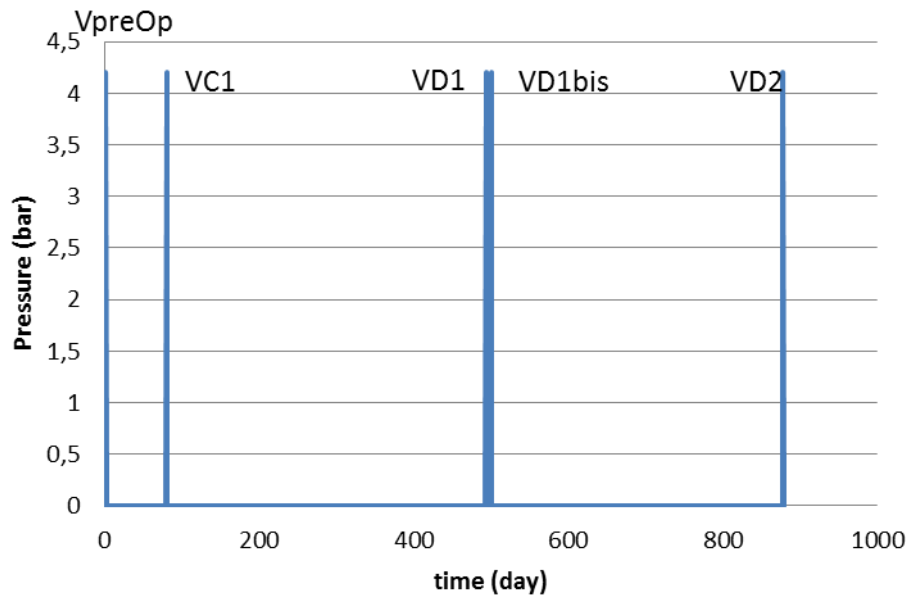
Figure 8 Evolution of the internal pressure in function of time

Figure 9 represents the deformations of the mock-up just before the first pressure test (in red) and at the peak of pressure (in green). The coefficient of amplification is taken equal to 500.
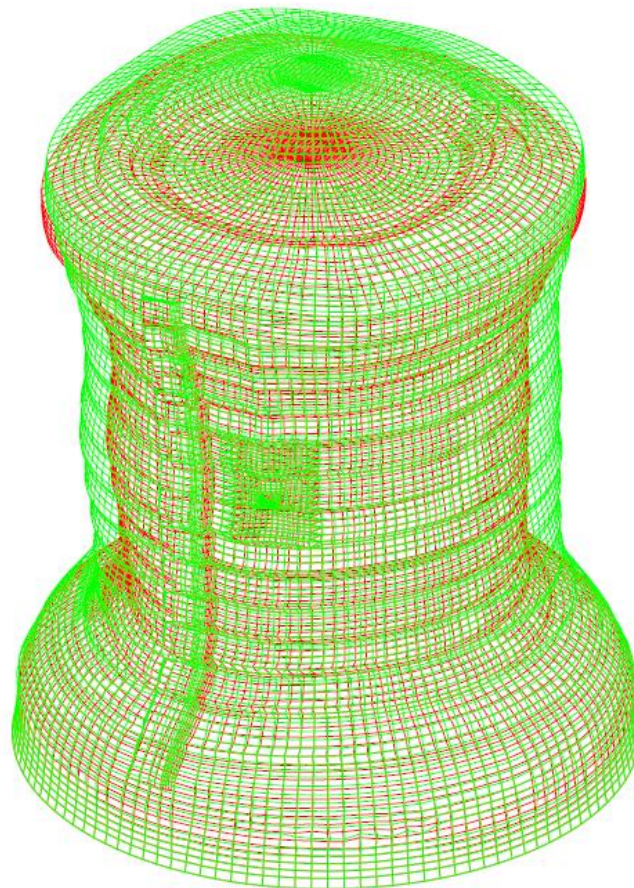

Figure 9 : Deformation before pressure (red) and during the peak of pressure (green) Amplitude ×500

The Figure 9 represents an usual result, pre-stressed concrete containments : the long term differed deformations do not balance the deformation due to a pressure test.

REFERENCES

[1] *Cast3m version 15 http://www-cast3m.cea.fr*

[2] Rapport DMT/94-705, "Introduction du modèle OTTOSEN dans CASTEM2000 Formulation Implantation"

VERCORS Containment Mock-Up test pressure response simulation by MSC/Nastran software

Joonas Koskinen[*], Pentti Varpasuo[†]

[*] Fortum Power and Heat Ltd Keilalahdentie 2-4, Espoo, Finland
[†] PVA Engineering Services, Runeberginkatu 42A35, 00260 Helsinki, Finland
e-mail: pentti.varpasuo@partners.fortum.com

ABSTRACT

The finite element model of the VERCORS mock-up was developed by using the Bentley/Microstation CAD – software and PATRAN preprocessor for MSC/Nastran software. The model geometry contained 454638 points, 123134 curves and 59015 surfaces. The corresponding finite element mesh contained 104507 nodes and 182292 rod and shell elements The tendons were explicitly modeled by two node rods and the concrete was modeled by four node shells. The reinforcing bars were not modelled. The number of degrees of freedom in the model was 627042. The execution of one load case using Lenovo Power Laptop Model p5-4/5585 with 8 CPUs, 16 gigabytes of RAM and 5585 MHz clock frequency took ten minutes in wall clock time. In figure 1 the displacement response of the model shown for test pressure load case:

Figure 1. The displacements of of the VERCORS mock-up for the test pressure load case, units are meters.

The Fortum contribution consisted of the concrete strain results denominated as Theme 2 by organizers.

Analysis of the VeRCoRs mock-up of a reactor containment building by means of a constitutive serial-parallel rule of mixtures

S. Jiménez[*], A. Cornejo[*], L.G. Barbu[*], S. Oller[†] and A.H. Barbat[†]

*Centre Internacional de Mètodes Numèrics en Enginyeria (CIMNE), Campus Norte UPC, 08034 Barcelona, Spain, e-mail: sjimenez@cimne.upc.edu
†Universidad Politécnica de Cataluña (UPC), Campus Norte UPC, 08034 Barcelona, Spain

INTRODUCTION

The performed analysis is based on a finite element (FE) mesh of the containment building and a linear description of the tendons. The prestressed concrete is modelled as a composite material whose behavior is described by using the serial-parallel rule of mixtures (S/P RoM). The prestressing is applied as an initial strain imposed only in the steel material used to model the tendons. By means of the S-P RoM [1,2], equilibrium is reached, at each integration point, between the reinforcing and prestressing steel and concrete and the strain tensor of the steel is updated with the contribution of the concrete. An important advantage of this methodology is that each material behaves following its own constitutive law (elasticity, damage, plasticity, viscoelasticity, etc.). Next, the displacement field is updated until the global convergence of residual forces is achieved. Regarding the stress relaxation of the tendons, the model is capable of predicting the time evolution of the stress tensor (triaxial stress state) with only two parameters: the viscoelastic coefficient and the delay time. In order to simulate the degradation of the concrete due to the pre-stressing or the pressurization, an isotropic damage model has been used.

SERIAL-PARALLEL RULE OF MIXTURES

The Serial-Parallel rule of mixtures (S-P RoM) defines two different compatibility conditions between the strain a stress states of the composite constituent materials: it states an iso-strain condition on the parallel direction, usually the fiber direction, and it defines an iso-stress condition on the serial direction, usually the remaining directions. Using these compatibility equations in a composite made of matrix and fiber, if the matrix structural capacity is lost due to excessive shear stresses, the iso-stress condition also reduces the shear capacity of fiber, and consequently the composite serial strength is also reduced. Since the behavior of the composite is different depending on the serial or parallel direction, one must split the strain and stress tensors in its serial and parallel parts. This is done with two complementary fourth order projector tensors, one corresponding to the serial direction (P_S) and the other to the parallel direction (P_P).

The S-P RoM assumes the following hypothesis in order to take into account the strain-stress states defined in the previous paragraphs:

1. The composite is composed by only two components: fibre and matrix
2. Component materials have the same strain in parallel (fibre) direction.
3. Component materials have the same stress in serial direction.
4. Composite material response is in direct relation with the volume fractions of compounding materials.
5. Homogeneous distribution of phases is considered in the composite.
6. Perfect bounding between components is considered.

In order to state the stress equilibrium and the strain compatibility, one must analyse the hypothesis previously exposed:

Parallel behaviour:
$$^{c}\varepsilon_P = ^{f}\varepsilon_P = ^{m}\varepsilon_P$$
$$^{c}\sigma_P = ^{f}k \cdot ^{f}\sigma_P + ^{m}k \cdot ^{m}\sigma_P$$
(7)

Serial behaviour:
$$^{c}\varepsilon_S = ^{f}k \cdot ^{f}\varepsilon_S + ^{m}k \cdot ^{m}\varepsilon_S$$
$$^{c}\sigma_S = ^{f}\sigma_S = ^{m}\sigma_S$$
(8)

where superscripts c, m and f stand for composite, matrix and fibre, respectively and ^{i}k corresponds to the volume fraction coefficient of each constituent in the composite and

$$\begin{bmatrix} ^{i}\sigma_P \\ ^{i}\sigma_S \end{bmatrix} = \begin{bmatrix} ^{i}C_{PP} & ^{i}C_{PS} \\ ^{i}C_{SP} & ^{i}C_{SS} \end{bmatrix} : \begin{bmatrix} ^{i}\varepsilon_P \\ ^{i}\varepsilon_S \end{bmatrix}$$
(5)

C_{pp}, C_{ps}, C_{sp} and C_{ss} depend on the elastic constitutive tensors and on the two complementary fourth order projector tensors, one corresponding to the serial direction (P_S) and the other to the parallel direction (P_P).

The known variable that enters the algorithm (input) is the strain state $^{c}\boldsymbol{\varepsilon}$ of the composite material at time $t + \Delta t$. From this input, the S-P RoM has to find a pair of strain/stress tensors for each component that fulfills the equilibrium, compatibility and the constitutive equations in each integration point. The first thing done by the algorithm is to split the strain tensor into its parallel and its serial parts, in order to compute the strain state in the matrix and the fiber. The parallel strain component is, according to equation (7), the same for both materials and for the composite. The procedure used to obtain the strains and stresses for each material component is similar to any Newton-Raphson strategy in which the serial part of the strain of the matrix is the main unknown while the rest can be computed depending on its value. In order to see more details about the formulation, it is suggested to check the [3]. This iterative methodology has to update the serial-parallel components of the strains and stresses until the serial stresses between the material components are equal (as expected by the 3rd hypothesis).

SINGULARITIES OF THE IMPOSED STRAIN PROCEDURE

The previous numerical formulation is capable of simulating the behaviour of reinforced concrete as a composite material composed by concrete and reinforcing steel. If one wants to take into account the case of the prestressing steel, both for the pre and the post-tensioned case, it is necessary to rewrite the compatibility condition of the S-P RoM because now the relative movement between the components is allowed if and only if an imposed strain condition exists over one of them. Equations (7) must therefore be rewritten taking into account the imposition of an initial strain for the fiber in order to represent the pre-tensioning or post-tensioning of the prestressing steel. In the first iteration of the S-P RoM algorithm, the parallel component of the strain tensor of the prestressing steel is fixed to the imposed pre-stress value. Knowing the composite strain tensor and the parallel component of the strain of the fiber, one can obtain the total strain tensor of the fiber and, depending on the desired fiber constitutive model, the integrated stress tensor is computed.

$$incr = 1; iter = 1; \qquad \begin{array}{l} ^{m}\varepsilon_P = ^{c}\varepsilon_P \\ ^{f}\varepsilon_P = \varepsilon_{imp} \end{array}$$

$$incr \geq 1; iter > 1; \qquad \begin{array}{l} ^{m}\varepsilon_P = ^{c}\varepsilon_P \\ ^{f}\varepsilon_P = ^{c}\varepsilon_P + \varepsilon_{imp} \end{array}$$
(14)

TIME-DEPENDENT MODELS

One of the behaviors responsible for the nonlinearity in the materials' response over the time field is due to viscoelasticity. Viscoelasticity studies the rheological behavior of materials, in other words, behaviors affected by the course of time. There is extensive literature available on this subject, especially in books that deal with the influence of time on these materials [4]. The spring-damper scheme for the Generalized Maxwell model can be seen in the Figure 1.
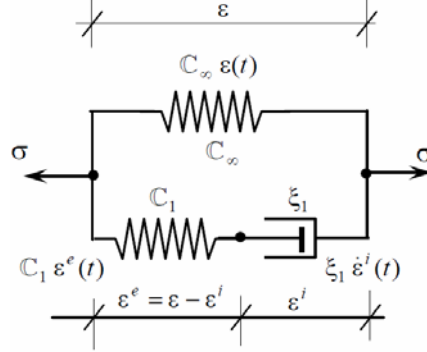

Fig. 1. The generalized Maxwell Model.

The algorithm used can be seen in Table 1. The complete mathematical description of the formulation can be found in [3].

1- Obtaining the strain

$$[\varepsilon_{ij}]^{t+\Delta t}$$

2- Stress integration

$$[\sigma_{ij}]^{t+\Delta t} = [\sigma_{ij}]^{t} \cdot e^{-(\Delta t)/r_1} - C_{ijkl}[\varepsilon_{kl}]^{t} \cdot e^{-(\Delta t)/r_1}\left[1 + \frac{C_1}{C_0\xi}\frac{\Delta t}{2}\right] + C_{ijkl}[\varepsilon_{kl}]^{t+\Delta t} \cdot \left[1 - \frac{C_1}{C_0\xi}\frac{\Delta t}{2}\right]$$

Table 1. Generalized Maxwell algorithm used.

ISOTROPIC CONTINUOUS DAMAGE

The damage of a continuous solid (stiffness degradation) is an alteration of the elastic properties during load application due to a decrease of the effective strength area. This effective area loss is normally caused by the increase of voids and/or micro fractures.

For the isotropic damage model, the material degradation is developed in all directions alike and only depends on one scalar damage variable d, and the equation of isotropic damage is then

$$\sigma_0 = \frac{\sigma}{1-d} \tag{29}$$

Where d is the internal variable of damage, σ is Cauchy's stress tensor and σ_0 is the effective Cauchy's stress tensor measured in the "non-damaged" space. This internal variable is a measure of the material's stiffness loss and its higher or lower limits are given by $0 \leq d \leq 1$. In order to know if the material has reached the non-linear behaviour, the damage models use the so called "damage threshold criterion". This criterion depends on the type of material and is defined in the same way as the plasticity problems,

$$F(\sigma_0; q) = f(\sigma_0) - c(d) \, , \, with \, q \equiv d \tag{29}$$

And once this threshold is fulfilled, one must define an evolution law of the internal damage variable which, for the exponential softening case, is expressed as,

$$G\big(f(\boldsymbol{\sigma_0})\big) = 1 - \frac{f^0(\boldsymbol{\sigma_0})}{f(\boldsymbol{\sigma_0})} e^{A\left(1 - \frac{f(\boldsymbol{\sigma_0})}{f^0(\boldsymbol{\sigma_0})}\right)} \tag{29}$$

where A is a parameter that depends on the fracture energy of the material and $f^0(\boldsymbol{\sigma_0})$ corresponds to the initial threshold that initiates the non-linear behaviour.

In order to predict the crack opening the following expression has been used:

$$u_{cr} = \big(d \cdot \varepsilon_{eq}\big) \cdot l_f \tag{29}$$

where ε_{eq} is the equivalent strain of the Gauss point and l_f is the characteristic length of the element. The equivalent strain is computed as:

$$\varepsilon_{eq} = \frac{\boldsymbol{\sigma} : \boldsymbol{\varepsilon}}{f(\boldsymbol{\sigma})} \tag{29}$$

GENERATION OF THE COMPOSITE MATERIALS

In order to take into account the effect of the prestressing steel, a new and reliable technique has been developed. This methodology only requires a linear description of the steel tendons and a FE mesh for the volumes of the other materials (see Figure 2). Once these entities are defined, the software intersect the linear elements with the solid elements and creates a file with the intersection coordinates which, afterwards, it is used to generate the different composite materials (in terms of volumetric participation of steel and its fibre direction). In Figure 2 one can see the FE discretization of one tendon and the local axes of the prestressing steel computed.
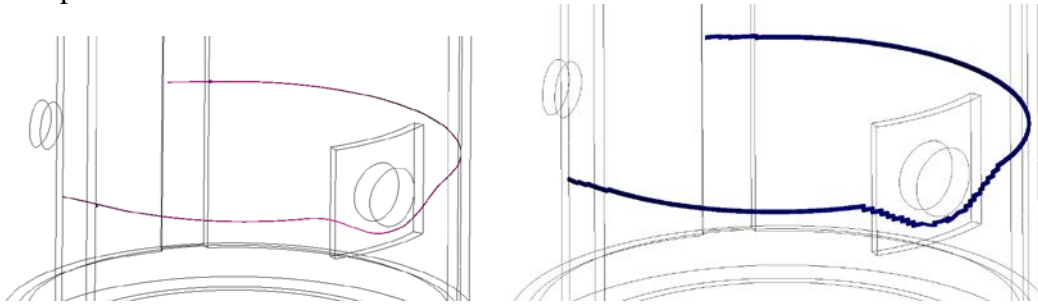
Fig. 2. Linear description of the steel tendon and its FE discretization.

FINITE ELEMENT MESH

The FE mesh has been generated using GiD [5]. Figure 3 shows the final model used for the calculations made up of 199600 8-noded hexahedra with linear shape functions.
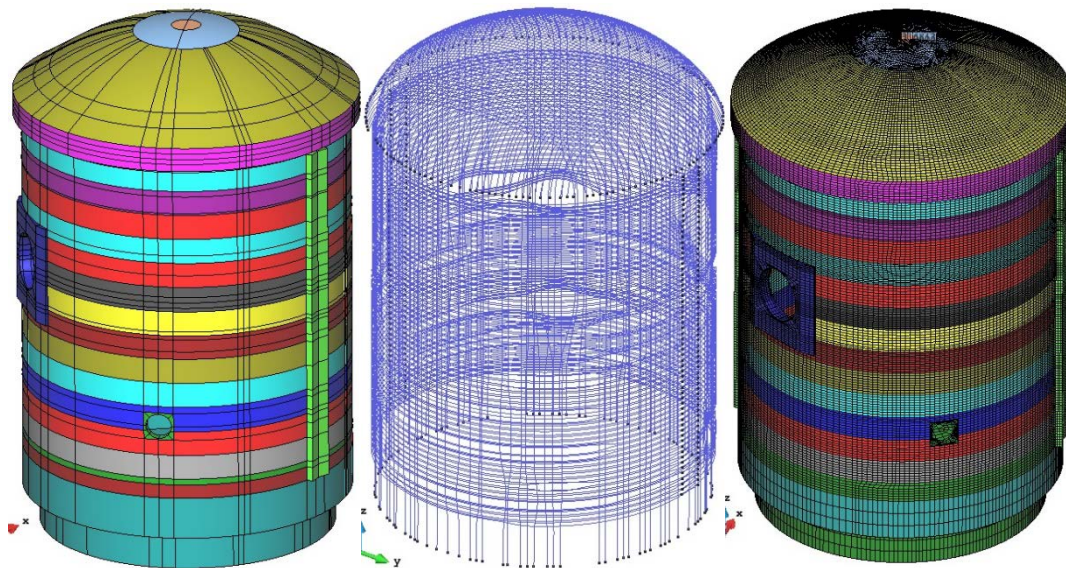
Fig. 3. Containment model (left), prestressing steel system (centre) and FE model (right) in GiD.

MODEL CALIBRATION: STRAIN CURVES

The strain curves obtained from the containment monitoring done after construction have been used for the calibration of the model. Figure 3 shows the final results for 4 sensors distributed in the mock-up where the red points are the predictions obtained with the numerical simulation.
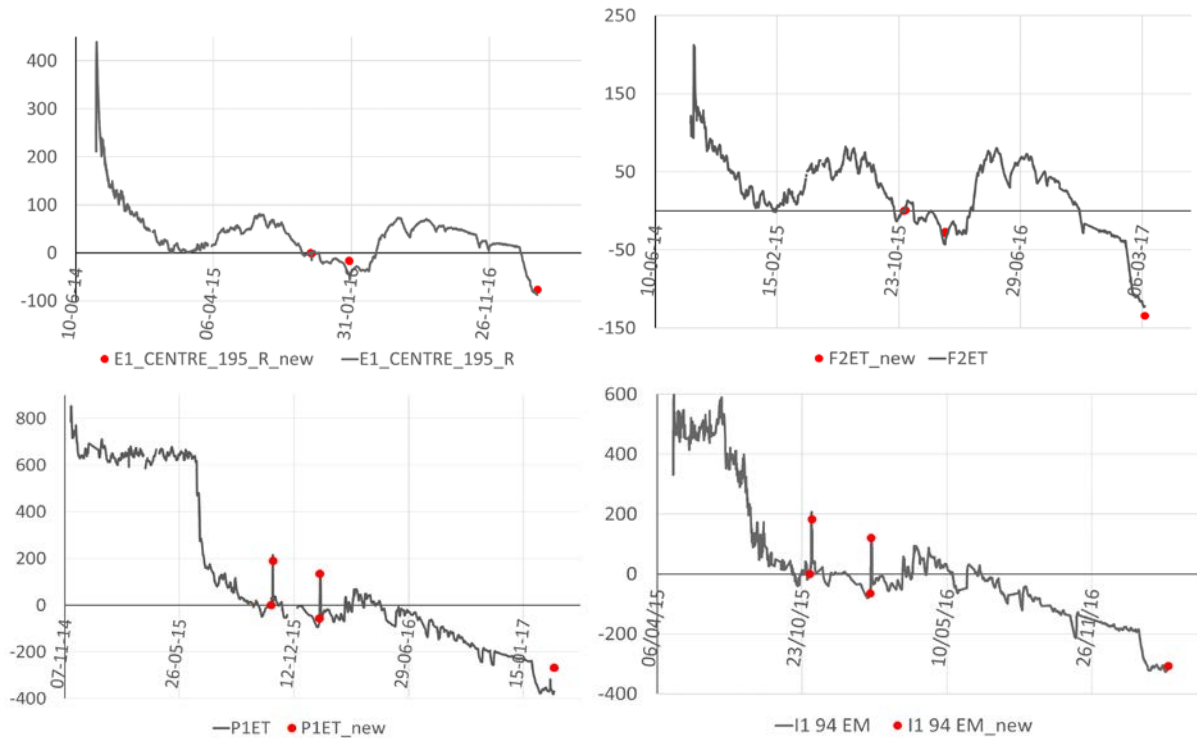

Fig. 3. Strain curves [μm/m] in the period between the end of the containment construction and the start of VD1. Raft (top left), gusset (top right), cylinder (bottom left) and dome (bottom right) sensors.

RESULTS OF THE NUMERICAL ANALYSIS

Figures 4 to 6 show the results obtained through the numerical analysis performed with PLCd [6]. Only VD2 pressure test results are provided to show the type of output obtained through the S-P RoM approach.
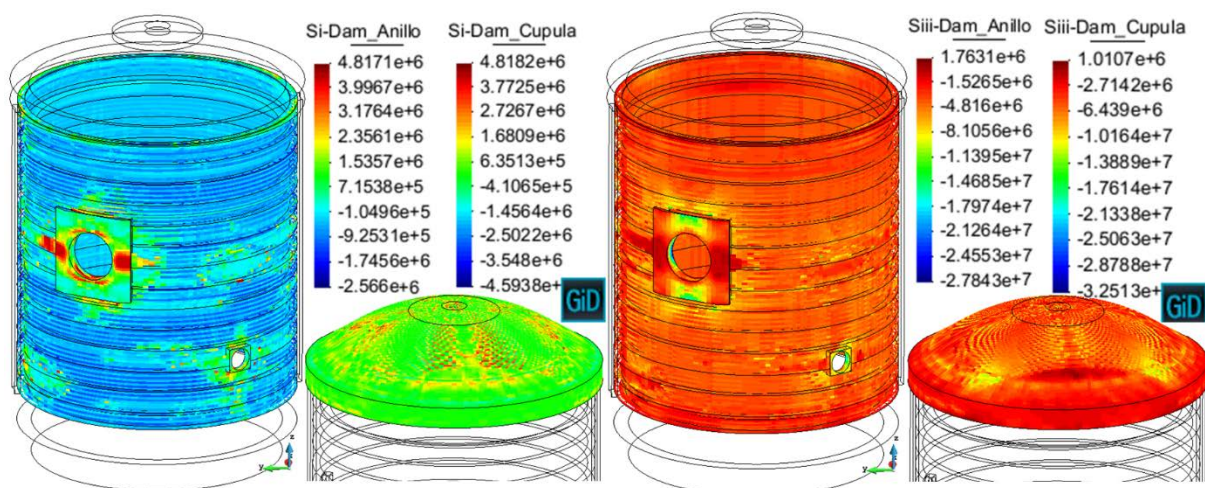

Fig. 4. Principal stresses [Pa] for the maximum inner pressure during VD2 test. Tensions (left) and compressions (right) for the cylinder (*Anillo*) and the dome (*Cúpula*)
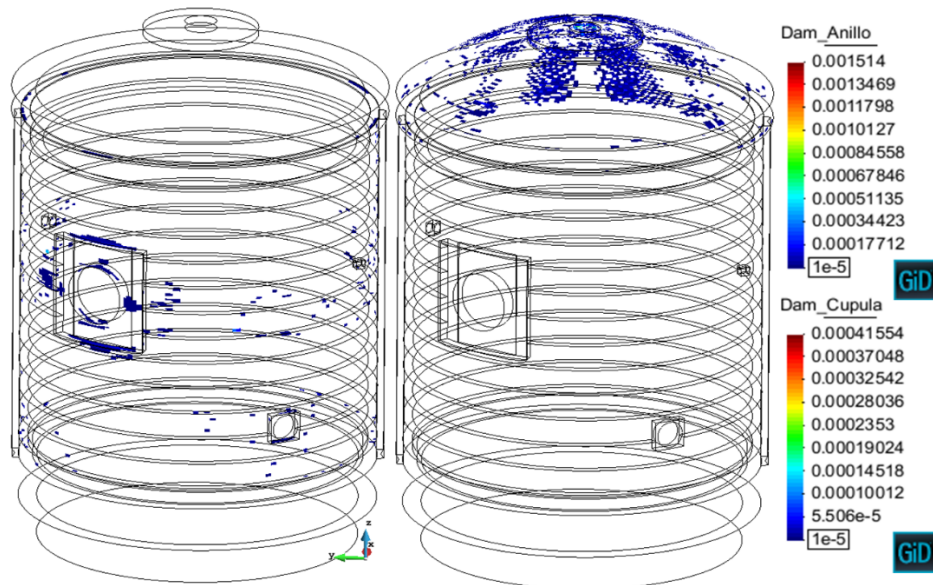
Fig. 5. Crack opening displacement [m] for the maximum inner pressure during VD2 test for the cylinder (*Anillo*) and the dome (*Cúpula*)
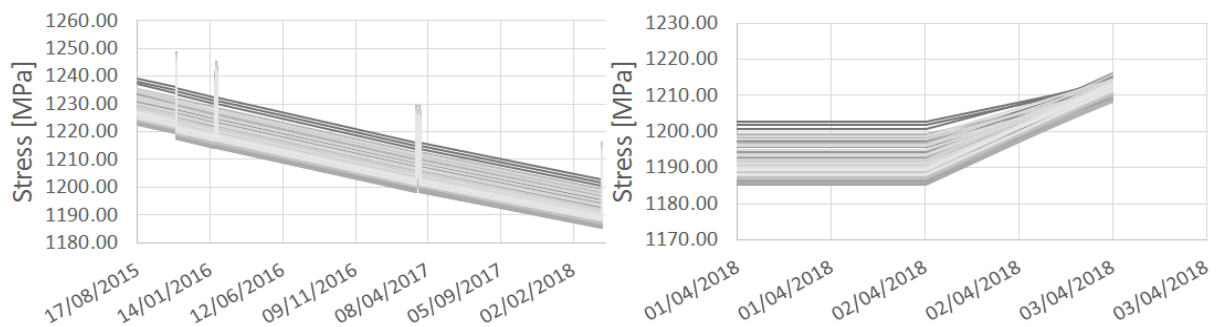

Fig. 6. Prestressing tension [MPa] evolution for Gamma tendons. General view of the whole period of analysis (left) and VD2 test detail (right).

REFERENCES

[1] Rastellini, F., Oller, S., Salomon, O., Oñate, E., 2008. Composite materials non-linear modelling for long fibre reinforced laminates: Continuum basis, computational aspects and validations. Computers and Structures 86(9), 879-896.

[2] Martinez, X., Oller, S., Rastellini, F. and Barbat, A.H., 2008. A numerical procedure simulating RC structures reinforced with FRP using the serial/parallel mixing theory, Computers and Structures, 86(15-16):1604-18.

[3] Cornejo, A., Barbu, L.G., Escudero, C., Martinez, X., Oller, S. and Barbat, A.H., 2018. Methodology for the analysis of post-tensioned structures using a constitutive serial-parallel rule of mixtures. Composite Structures.

[4] E. J. Barbero, F. A. Cosso, X. Martinez (2014). Identification of Fracture Toughness for Discrete Damage Mechanics Analysis of Glass-Epoxy Laminates. Applied Composite Materials. 21(4): 633-650. DOI: 10.1007/s10443-013-9359-y.

[5] GiD. The personal pre and post processor. URL: https://www.gidhome.com/

[6] PLCd Manual. Non-linear thermo-mechanic finite element code oriented to PhD student education. Code developed at CIMNE; 1991–to present. URL: http://www.cimne.com/plcd>.

VeRCoRs Theme II: Mechanical Behavior of the Containment during Pressurization Test

Dr. Joshua R. Hogancamp[*], Madhumita Sircar[†]

*Sandia National Laboratories, Albuquerque, USA, e-mail: jhoganc@sandia.gov
[†]U.S. Nuclear Regulatory Commission, Washington, D.C., USA, e-mail: Madhumita.Sircar@nrc.gov

PRIMARY FEATURES

The containment vessel concrete and posttensioning tendon geometries and mesh were provided by EDF. The finite element rebar mesh was created utilizing the geometry and meshing software Cubit (CUBIT 15.3, 2018). The finite element analysis was performed utilizing ABAQUS (ABAQUS 6.14, 2018).

The concrete was modeled using a homogenous linear viscoelastic Prony series model in ABAQUS with a Young's modulus of 34.3 GPa. A Prony series is a set of exponential decay terms that can replicate exponentially decaying data such as stress relaxation or concrete creep. Four terms were used for the Prony series in the viscoelastic material model to replicate the creep data provided by EDF. Concrete cylinder creep uniaxial compression test simulations in ABAQUS showed that the chosen material model replicated the creep test results provided by EDF. All steels in the simulation were modeled as linear elastic with a Young's modulus of 200 GPa since no steel is expected to stress beyond yield.

Rebar area was calculated from the drawings provided by EDF and to the simulation added as 4-noded surface elements. The rebar layers are represented in ABAQUS as surface elements with orthotropic properties depending on reinforcement ratios in each direction representing hoop and vertical rebars. Surface layers of steel reinforcement bars are located 0.040 m from the surface of the concrete. The pedestal and containment base contain seven layers of rebar combined corresponding to actual rebar in the CV. Additional rebar around the openings are applied as separate surface layers. Containment base mat rebar and dome rebar has been applied as an X-Y grid in lieu of the combined X-Y grid and hoop-radial rebar in the mockup.

The bottom-most nodes in the CV are assumed fixed in all directions. The pressure load is applied to the entire inner surface of the containment vessel. Gravity is in effect throughout the entire simulation. The 2-noded bar element tendon posttensioning is simulated as an initial stress of 1400 MPa. The initial tendon stress of 1400 MPa was determined by accounting for initial stress at the jacking location, relaxation losses, friction losses, and pull-in at wedge blocking. Posttensioning was applied simultaneously to all tendons at the beginning of the simulation.

The VeRCoRs simulation load history used by SNL/NRC is presented in Table 1. Time between pressurizations is described as 'dormant period'; gravity and posttensioning are still active in the dormant periods.

Table 1: SNL/NRC VeRCoRs simulation load history.

Step Title	Date Begin	Date End	Total Time (days)	Description
Initialize	N/A	N/A	10 seconds	Ramp gravity and posttensioning loads
0	8/17/2015	11/2/2015	77.00	Posttensioning complete, await first pressurization
1	11/2/2015	11/4/2015	2.253	Strains reference date 11/2/2015
2	11/4/2015	11/6/2015	2.411	Pressurization 'Pre-op'
3	11/6/2015	1/25/2016	80.00	Dormant period
4	1/25/2016	1/28/2016	2.411	Pressurization 'VC1'
5	1/28/2016	3/14/2017	411.2	Dormant period
6	3/14/2017	3/16/2017	2.411	Pressurization 'VD1'
7	3/16/2017	3/21/2017	4.611	Dormant period
8	3/21/2017	3/23/2017	2.411	Pressurization 'VD1 bis'
9	3/23/2017	4/2/2018	374.6	Dormant period
10	4/2/2018	4/4/2018	2.411	Pressurization 'VD2'

Stress and strain measurements are taken at every time step in ABAQUS. ABAQUS utilizes an implicit solver and solves the finite element simulation at varying time steps depending on the precision required. The details of the ABAQUS time step increments are listed in Table 2.

Table 2: ABAQUS time step increments.

Step	Initial Time Step	Minimum Time Step	Maximum Time Step
Initialization	2.0 seconds	0.01 seconds	10.0 seconds
Pressurization	1.5 hours	0.5 hours	3.0 hours
Dormant period	5.0 days	0.25 days	50.0 days

Stresses are recorded in elements defined in each of the following locations:
- Gusset
- Containment wall
- Dome
- Center of the floor of the containment

RESULTS

Selected results are presented herein. Strain gage results are presented with respect to strain accumulated after November 2, 2015 (the strain zero-reference date). The figures do *not* include strain accumulated during posttensioning. Strains in the simulation were accrued beginning on August 17, 2015, and include gravity post-tensioning, and creep effects. The graphs shown in this section show only the strains accrues since November 2, 2015, since the organizing committee has requested that the strain be zeroed on November 2, 2015. Each spike in the strain is a CV pressurization: Pre-op, VC1, VD1, VD1-bis, and VD2. At ~500 days, VD1 and VD1-bis are only a few days apart.
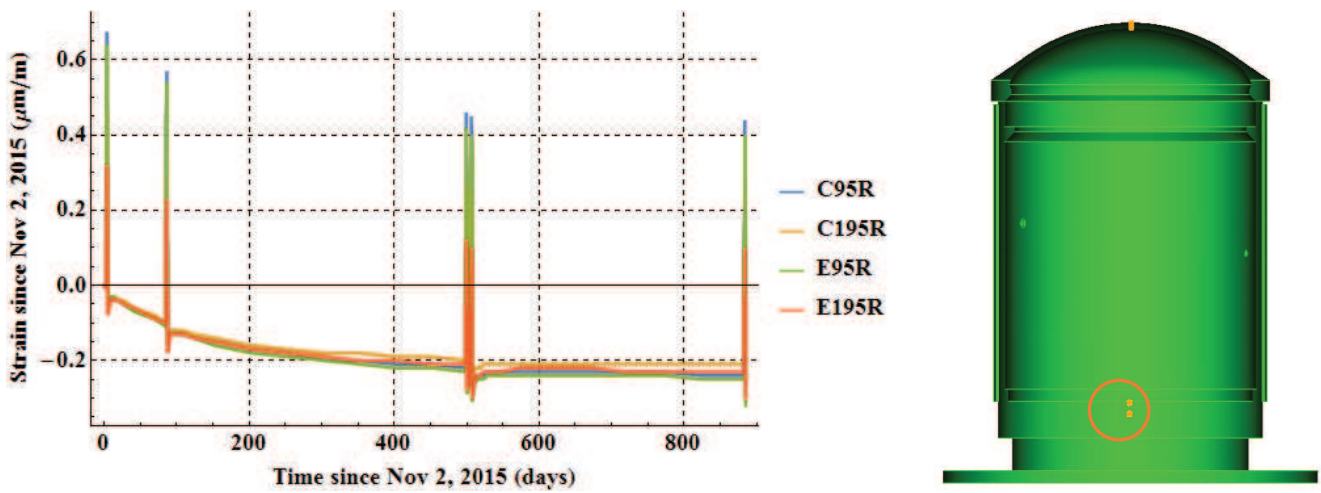
**Figure 1: C95R, C195R, E95R, E195R strains.**
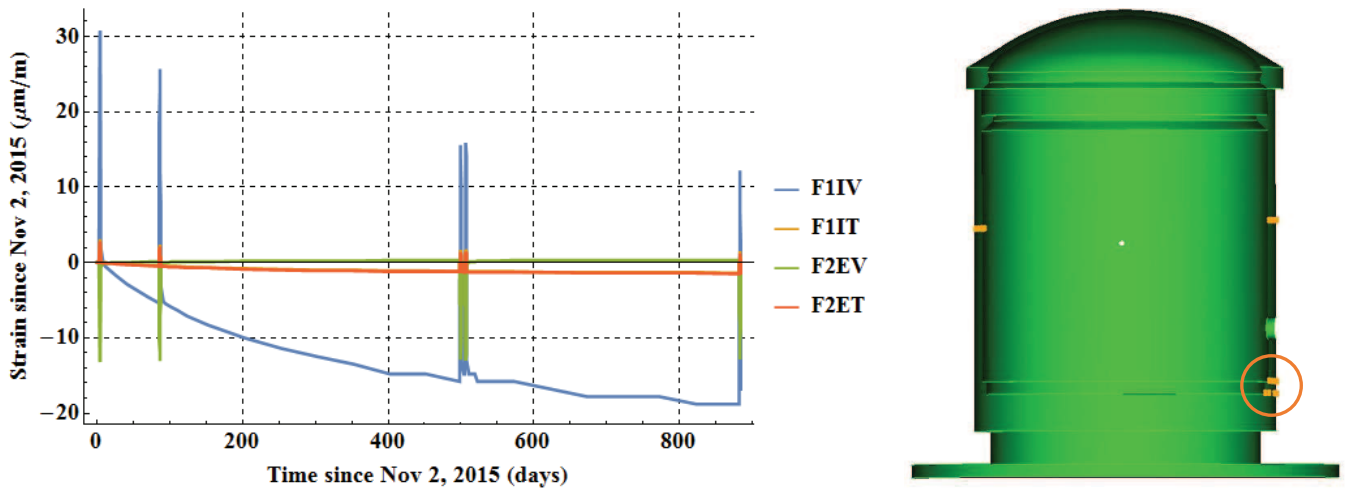
Figure 2: F1IV, F1IT, F2EV, F2ET strains.

Strain gages C95R, C195R, E95R, and E195R experienced far less strain than the rest of the gages because they were located in the center of the base of the containment vessel surrounded by mass concrete and reinforcement. However, Figure 1 does show that creep effects of the viscoelastic material model were readily apparent in the simulation. Strain gage F1IV experienced large creep strains compared to the other gages in Figure 2 due to its position in the CV. F1IV is located near the inner surface of the CV where the cylinder meets the base; this location is subject to large compressive strains during posttensioning, and is subsequently subject to large creep strains.

Figure 3 shows the deformation and maximum compressive stresses in the CV due to post-tensioning. Stresses are shown in Pa. The exaggerated deformation clearly shows the result of posttensioning in the hoop direction and in the dome.
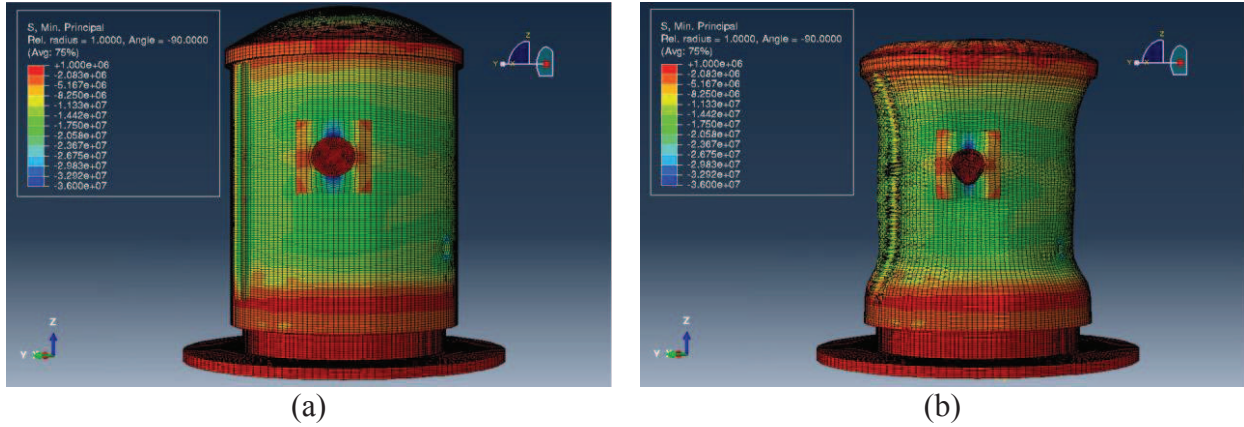
Figure 3: Maximum CV compressive stresses in ABAQUS simulation in (a) undeformed shape and (b) deformed shape. Deformation scale: 2000.

Figure 4 shows results for stresses at locations of strain gages F1IV, F1IT, F2EV, and F2ET. Strain gage F2EV experienced tensile stresses due to being on the outside of the CV where the cylinder meets the base. Neither posttensioning nor pressurizations increased stresses beyond yield, as expected. Figure 5 shows the stress histories of strain gages F2EV and F2ET zoomed to show the effects of concrete creep on stress in the containment. For these particular strain gages, concrete creep altered the stress by 7.8% and 4.8% for gages F2EV and F2ET, respectively.
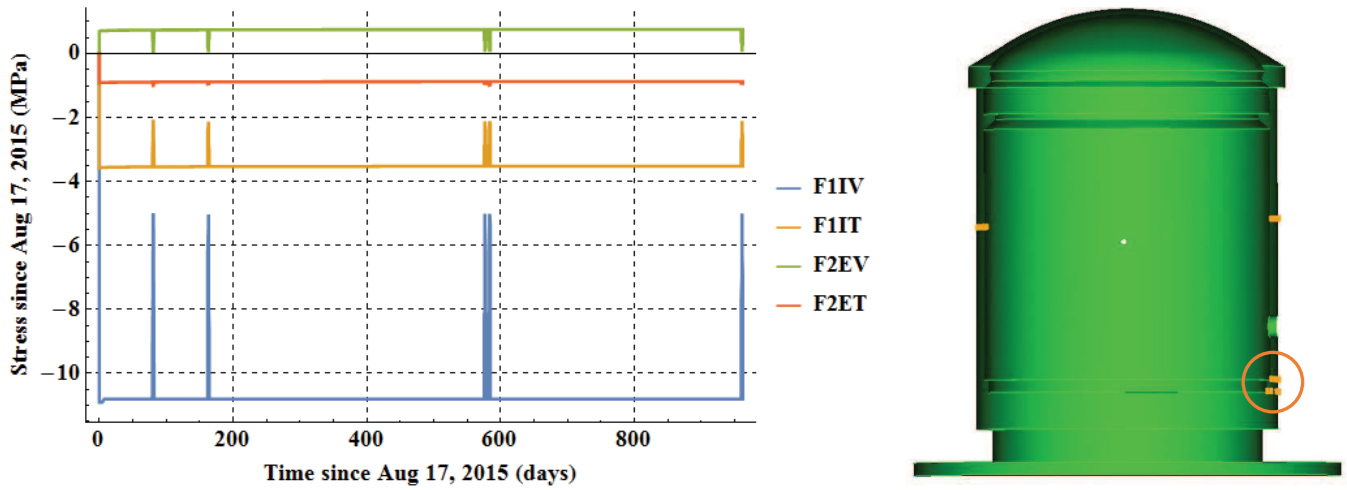

**Figure 4: Stress histories of F1IV, F1IT, F2EV, and F2ET.**

4
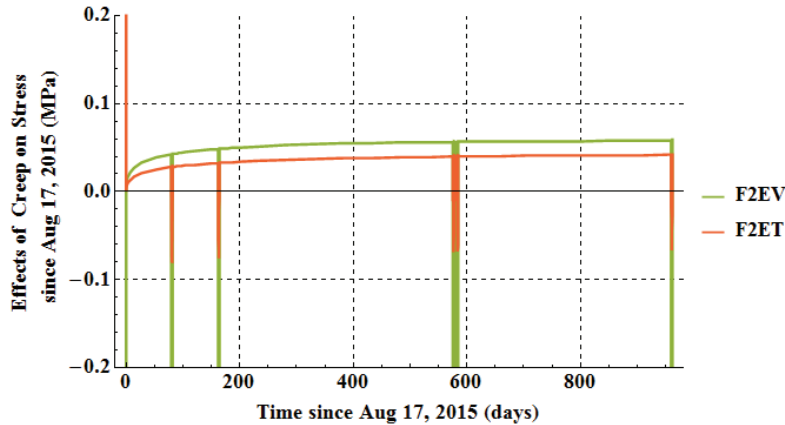
Figure 5: Stress histories of F2EV and F2ET zoomed to show the effects of creep on stress.

CONCLUSIONS

- The simulation adequately captured posttensioning and creep effects. Future comparisons with experimental results will determine accuracy and/or precision of the simulation results.
- From these results, long-term creep strain is in the same range of strain magnitude that was caused by applied 4.2 bar pressurizations in posttensioned containment vessels.
- Pressurizations in the simulation did not create tensile stresses in the containment vessel. The region represented by gage F2EV actually reduced stress to almost zero during pressurization. All stresses were lower than the respective (tensile or compressive) concrete strength.
- Creep effects of concrete are predicted to alter stresses in the containment as shown by strain gages F2EV and F2ET which had changes in stress of 7.8% and 4.8%, respectively, due to concrete creep.

REFERENCES

ABAQUS 6.14. (2018). Dassault Systèmes.
CUBIT 15.3. (2018). Sandia National Laboratories.

DISCLAIMERS

Modelling creep in a pre-stressed mock-up reactor containment –the VeRCoRs 2018 benchmark case

M. ÅHS[*], R. MALM[†] AND C. BERNSTONE[††],

[*]Lund University, Lund, Sweden, e-mail: magnus.ahs@byggtek.lth.se

[†]KTH Royal Institute of Technology, Stockholm, Sweden, e-mail: richard.malm@byv.kth.se

[††]Vattenfall AB, Solna, Sweden, e-mail: christian.bernstone@vattenfall.com,

ABSTRACT

This study is a part of the VeRCoRs 2018 benchmark arranged by the Electricité de France, EDF. Theme 2 in this benchmark is focused on calculating the deformations caused by changes in temperature, humidity and creep of an experimental reactor containment (RC) built in 1/3 scale. In this study the Eurocode model for creep is applied by using the finite element software COMSOL Multiphysics. The results from the calculations are compared with actual measurements performed on the experimental RC. A series of pressurization tests have been analysed during a time period of 1.5 years which have been simulated with the model.

INTRODUCTION

A number of different studies have been initiated by the Swedish power industry with an overall objective to enhance and develop advanced calculation tools to analyse mechanics and transport mechanisms in nuclear power and hydropower concrete structures [1]. These studies have had focus on analysing the structural performance by scrutinizing deformation, strains, strength, fracture and cracking. In other projects, research have been focused on transport mechanism analysis including mass and heat transport within the concrete [2]. Furthermore, a few studies have been conducted where both of these disciplines have been investigated simultaneously by combing these areas of research [3].

This study presents mechanical analyses of a prestressed concrete RC subjected to a series of well-defined pressurization test. It is a part of the VeRCoRs benchmark 2018 arranged by Electricité de France, EDF. The results from the analyses have been compared with actual measurements performed i a number of positions in a real 1/3 scale pre-stressed concrete RC. The main features of the model are presented together with results from the case study on how the RC structure responds to the applied loads. The focus has been to use a model that is available to professional designers in order to investigate how well these models are able to predict creep in large concrete structures.

HEAT TRANSFER MODEL

Heat transfer was modelled by using the commonly used diffusion equation described by Eq. (1)

$$\rho \cdot C_p \cdot \frac{\partial T}{\partial t} = \nabla(k\nabla T) \tag{1}$$

where ρ, is the density of concrete (assumed to be 2350 (kg/m^3)), C_p, is the specific heat capacity 880 (J/kgK), and T is the temperature in (K), k is the heat conductivity for concrete assumed to be 1.8 (W/mK). The heat released from the reaction between the cement and mixing water was not included in the analysis.

MOISTURE TRANSPORT MODEL

The model used for moisture transport is based on the conservation of mass and is described by using Eq. (2)

$$\frac{\partial W_e}{\partial t} = \frac{\partial W_e}{\partial \varphi}\frac{\partial \varphi}{\partial t} = \nabla(\delta_\varphi \nabla \varphi) \tag{2}$$

where $\frac{\partial W_e}{\partial \varphi}$ is the moisture capacity derived from the slope of the sorption isotherm expressed as moisture content (kg water/m³ of material), δ_φ represents the moisture transport coefficient with relative humidity as a driving potential, φ is the relative humidity (-). Self-desiccation was not included in the moisture transfer model.

DEFORMATIONS

Deformations attributed to changes in the climate (temperature and humidity), internal loads (pre-stressing of tendons) and external loads (Pressurization test) were included in the model.

Thermally induced strains, ε_{th}, i.e. contraction and expansion, were modelled by using Eq. (3)

$$\varepsilon_{th} = \alpha \cdot (T - T_{ref}) \tag{3}$$

where α, is the thermal coefficient of concrete (assumed to $1.1 \cdot 10^{-5}$ (1/K)), T, is the temperature in K, and T_{ref} is the reference temperature in (K).

Furthermore, humidity induced strains, i.e. swelling and shrinkage, were modelled by using Eq. (4)

$$\varepsilon_{sh}(t) = \frac{W_i - W(t)}{W_i - W_\infty} \cdot \varepsilon_{sh,\infty} \tag{4}$$

where $\varepsilon_{sh}(t)$, is the shrinkage strain at time t, W_i, is the initial moisture content, $W(t)$ is the moisture content at time t, W_∞ is the moisture content when in equilibrium with the current humidity exposure, and $\varepsilon_{sh,\infty}$ represents the final shrinkage strain which was estimated to 0.05%.

Creep was modelled by using Eurocode 2. In this model the creep coefficient, $\varphi_c(t, t_0)$, is described by Eq. (5)

$$\varphi_c(t, t_0) = \varphi_0 \cdot \beta_c(t, t_0) \tag{5}$$

where φ_0, is the notional creep coefficient and $\beta_c(t, t_0)$ is a is a coefficient to describe the development of creep with time after loading. A detailed description of the applied creep model is found in Eurocode [4].

The creep strain was modelled by using Eq. (6)

$$\varepsilon_{cr} = \varphi_c(t, t_0) \cdot \frac{\sigma}{E} \tag{6}$$

where σ, is the compressive strength of the concrete and E, is the elastic modulus.

The total strain ε_{tot}, is described by Eq. (7)

$$\varepsilon_{tot} = \varepsilon_{el} + \varepsilon_{th} + \varepsilon_{sh} + \varepsilon_{cr} \tag{7}$$

where ε_{el} is the elastic strain from the mechanical loads.

CASE STUDY

The model was applied to analyse a pre-stressed concrete RC, which was about 21 m high and had a radius of about 7.6 m. The concrete compression strength and the modulus of elasticity 50.8 MPa and 31.8 GPa respectively was provided by Vercors 2018 Benchmark. The geometry used in this study represents 1/8th (45 degrees sector) of the RC and this is shown in Figure 1. It was redrawn from the original geometry data from the Vercors 2018 benchmark. The pre-stressed tendons of the geometry are shown in Figure 2. The tendons configuration was provided by the Vercors 2018 benchmark.
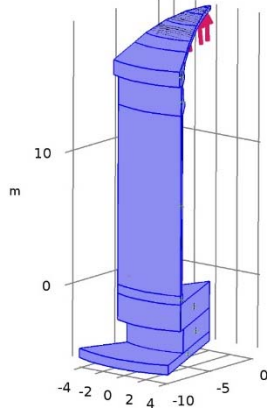

Figure 1 Geometry of the concrete reactor containment adopted from Vercors 2018 benchmark
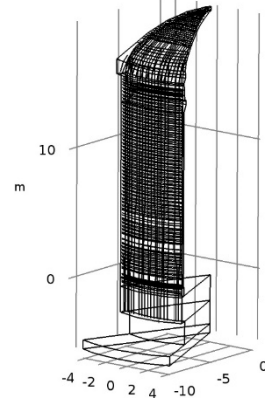

Figure 2 Geometric configuration of the pre-stressed tendons provided by Vercors 2018 benchmark

The tendons pre-stressing sequence was simplified in the model, and took place during 1 day where all tendons were assumed to be stressed simultaneously during that time. The pre-stressing force including pre-stress losses, was estimated to 613 kN per tendon, were calculated by using the model presented by Eriksson et al.[3] . The tendons modelled by using truss-elements with the assumption of no slip between concrete and tendons. Four pressurization tests with maximum 4.2 bar over pressure have been performed and those are simulated according to the time schedule provided by Vercors 2018 benchmark. Each test follows the test pressure sequence shown in Figure 3. In Figure 4, the actual temperature conditions inside (dashed line) and outside (solid line) of the RC are shown.
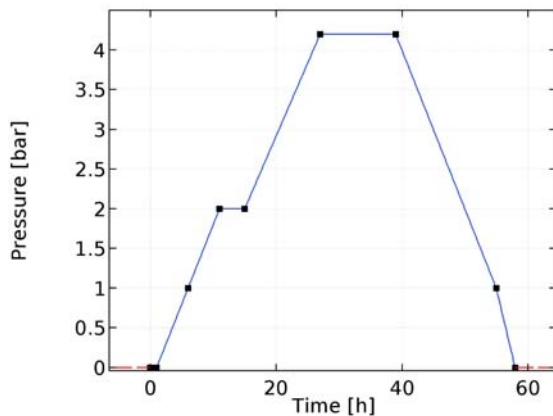

*Figure 3 Pressure test sequence of the pre-stressed concrete RC.*
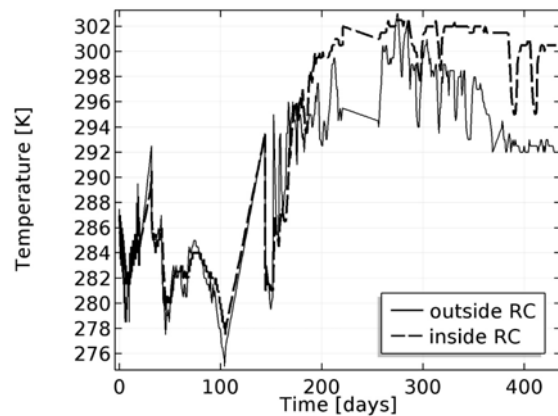
Figure 4 Temperature inside and outside of the pre-stressed concrete RC.

The thermal and humidity boundary conditions on the concrete surfaces were applied differently in two separate cases. In one case they were assumed as constant and in the other case the actual conditions were used. The actual conditions were determined at four different locations of which one was used for outside conditions and one was used for inside conditions, provided by Vercors 2018 for a part of the time period. A convective heat flux and moisture flux was used at the concrete surfaces as a boundary condition. The initial temperature and humidity in the concrete were assumed to be uniform and set to the surrounding temperature and 90 % RH respectively.

The surface mass transfer resistance with RH as a driving potential, k_{RH}, was modelled by using Lewis relation [5], se Eq. (8)

$$k_{RH} = \frac{h \cdot v_s}{\rho_{air} \cdot C_{p(air)}}$$

(8)

where, h, is the convection heat transfer coefficient [W/(m²K)], v_s is the saturation vapour content [kg/m³] at the current temperature, ρ_{air}, is the air density [kg/m³] assumed constant, and $C_{p(air)}$, is the heat capacity of air [J/(kgK)]. This model is an estimation of the surface mass transfer resistance.

RESULTS AND DISCUSSION

In this section results are evaluated at a specific point, H1EV, located at a level of +8.43 m and a radius of 7.58, which is located in the RC concrete wall. This point is located 0.12 cm from the external surface of the 0.4 m concrete wall. The results from the simulations performed by using the presented model, are shown in Figure 5 to Figure 6. In Figure 5, the predicted strains in vertical direction (dashed with diamond markers) are presented together with the measurements performed on the actual concrete containment (solid line), when a constant climate in temperature and relative humidity was set at the boundaries. The deformations were set to zero at the time of the first pressurization test. Figure 6 show the predicted vertical strains from the applied model (dashed line with diamond markers) when the actual climate conditions were set at the boundaries and the measured strains (solid line).
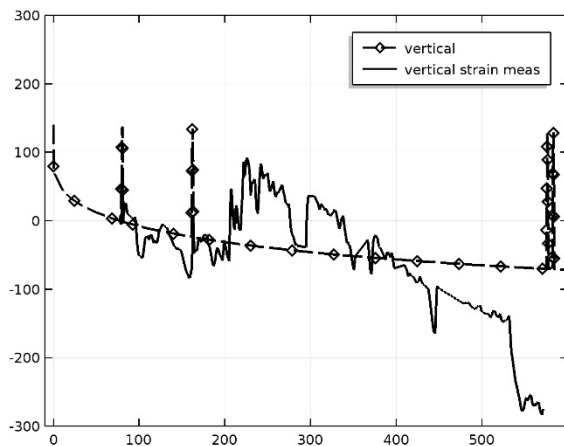

Figure 5 Vertical strains at +8.43 m in an undisturbed cross-section (10⁻⁶ m/m) point of reference before the first pressurization test.
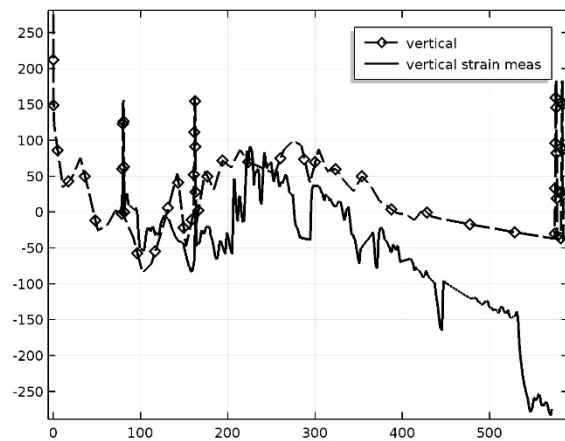
*Figure 6 Vertical tangential strains at +8.43 m in an undisturbed cross-section (10⁻⁶ m/m) point of reference before the first pressurization test.*

The predicted vertical strains, dashed line with diamonds, when assuming constant boundary conditions, follows a smooth curve, see Figure 5. Such a prediction is in agreement what could be expected. The magnitude of the predicted creep seems to be underestimated compared to the measured vertical strains, cf. slope between 200 and 500 days. The actual measured vertical strains, solid line, determined in that position are not in a good agreement with the prediction. However, the measured vertical strains in that particular point may be affected by the actual climatic conditions and therefore show a rather complicated deformation pattern. In addition, some of the sudden peaks in the actual vertical strain, cf. days 440 and 550, could be a result from cracking in the vicinity of the point. Such an event may result in sudden stress redistribution. In Figure 6 there is a better agreement between the predicted and the actual measured vertical strains. The overall shape of the strain curve from simulation and measurement are alike. It is clear that the predicted strains are underestimated compared with the actual strains, such findings are in agreement with Lundqvist [6] and Raphael et al. [7]. It is also clear that the environmental conditions have a large impact of the actual strains in this particular case.

CONCLUSIONS

A method to model axial deformation in COMSOL Multiphysics was developed. It is clear that the applied model is underestimating the creep. It is also clear that the impact of the environment on deformations may be large and it may therefore be useful to put some effort into predicting the climate as good as possible.

ACKNOWLEDGEMENTS

REFERENCES

1. Malm, R., *Guideline for FE analyses of concrete dams*. 2016.
2. Åhs, M. and S. Poyet, *The prediction of moisture and temperature distribution in a concrete reactor containment*. 2015, Lund university. p. 72.
3. Eriksson, D., R. Malm, and H. Hansson, *Nugenia Acceppt - Analysis of stress concentrations and crack risk*. 2015, KTH Royal Institute of Technology.
4. *Eurocode 2: Design of concrete structures Part 1-1: General rules for Buildings*, in *EN 1992-1-1 Appendix B*. 2004, European committee for standardization: Brussels. p. 225.
5. Lewis, W., *The evaporation of a liquid into a gas.* International Journal of Heat and Mass Transfer, 1962. **5**(1-2): p. 109-112.
6. Lundqvist, P., *Assessment of Long-Term Losses in Prestressed Concrete Structures - Application for Nuclear Reactor Containments*, in *Division of Structural Engingeering*. 2012, Faculty of engineering, Lund University: Lund.
7. Raphael, W., E. Zgheib, and A. Chateauneuf, *Experimental investigations and sensitivity analysis to explain the large creep of concrete deformations in the bridge of Cheviré.* Case Studies in Construction Materials, 2018. **9**: p. e00176.
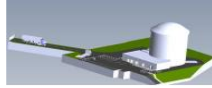
Modelling of the global delayed behaviour of the VeRCoRs mockup

Jean Michel Torrenti[*] and Abdushalamu Aili[†]

[*] Université Paris-Est, MAST, IFSTTAR, F-77447 Marne-la-Vallée, France, e-mail: jean-michel.torrenti@ifsttar.fr

[†] Université Paris-Est, Laboratoire Navier (UMR 8205), CNRS, Ecole des Ponts ParisTech, IFSTTAR, F-77455 Marne-la-Vallée, France

ABSTRACT

In this paper, a modelling of the delayed strains (creep and shrinkage of concrete and relaxation of steel) based on the MC2010 [1] is used to predict the behaviour of a representative part of the mock-up (strains at mid-height in the cylindrical part). The parameters of the relations giving the evolution of shrinkage and creep of concrete and of relaxation of steel are fitted to measurements made on laboratory samples. This modelling takes also into account the influence of the temperature and of the relative humidity (varying under service conditions). Finally, the predicted delayed strains are compared with the measurements.

Long term behaviour of concrete

The delayed strains of concrete are classically decomposed in four components: autogenous shrinkage, drying shrinkage, basic creep and drying creep. The relations of the fib model code 2010 [1] are used with a fitting of the parameters on experimental results as indicated in EC2-2 and proposed by the CEOS.fr project [2]. The effect of relative humidity is included in these relations. For temperature, the thermoactivation of the strains is taken into account by means of relations of the model code 2010.

Autogenous shrinkage and basic creep are already presented in the abstract concerning theme 1. For drying shrinkage the following relation is used:

$$\varepsilon_{cds} = \xi_{cds1}\left[(220 + 110\alpha_{ds1})e^{-\alpha_{ds2}f_{cm}}\right]\beta_{RH}\left[\frac{(t-t_s)}{0{,}035\xi_{cds2}h^2+(t-t_s)}\right]^{0,5} \tag{1}$$

where α_{ds1} and α_{ds2} are parameters depending on the cement type, h is the notional size and ξ_{cds1} and ξ_{cds2} parameters adjusted to experimental results. β_{RH} is a function of the relative humidity:

$$\beta_{RH} = 1{,}55\left[1 - \left(\frac{RH}{RH_{eq}}\right)^3\right] \tag{2}$$

where

$$RH_{eq} = 72[-0{,}046(f_{cm} - 8)] + 75 \tag{3}$$

The best fit of model of drying shrinkage to experimental results is obtained with $\xi_{cds1} = 0{,}829$ and $\xi_{cds2} = 0{,}417$. While the relative humidity for the experiment is constant at 50%, the relative humidity around the VeRCoRs mock-up is not constant (see Fig.4). We consider approximately that the relative humidity drops from 80% to 50% on 9th of March 2016. The influence of variation of relative humidity on drying shrinkage is taken into account by the concept of equivalent time as following. Before the time t_h where the relative humidity drops, the drying shrinkage is computed with relative humidity of 80%:

$$\varepsilon^{ds} = \varepsilon^{ds}(t - t_0, h_r = 80\%), \text{for } t \le t_h \tag{4}$$

The drying shrinkage ε_h^{ds} at time t_h is used to compute the equivalent time t_{eq} at which we would obtain the same drying shrinkage ε_h^{ds} if the relative humidity was 50%, i.e., $\varepsilon^{ds}(t_{eq}, h_r = 50\%) = \varepsilon^{ds}(t_h - t_0, h_r = 80\%)$. Then, for the time $t > t_h$, we compute the drying shrinkage as following:

$$\varepsilon^{ds} = \varepsilon^{ds}(t - t_0 - t_{eq}, h_r = 50\%), for\ t \ge t_h \tag{5}$$
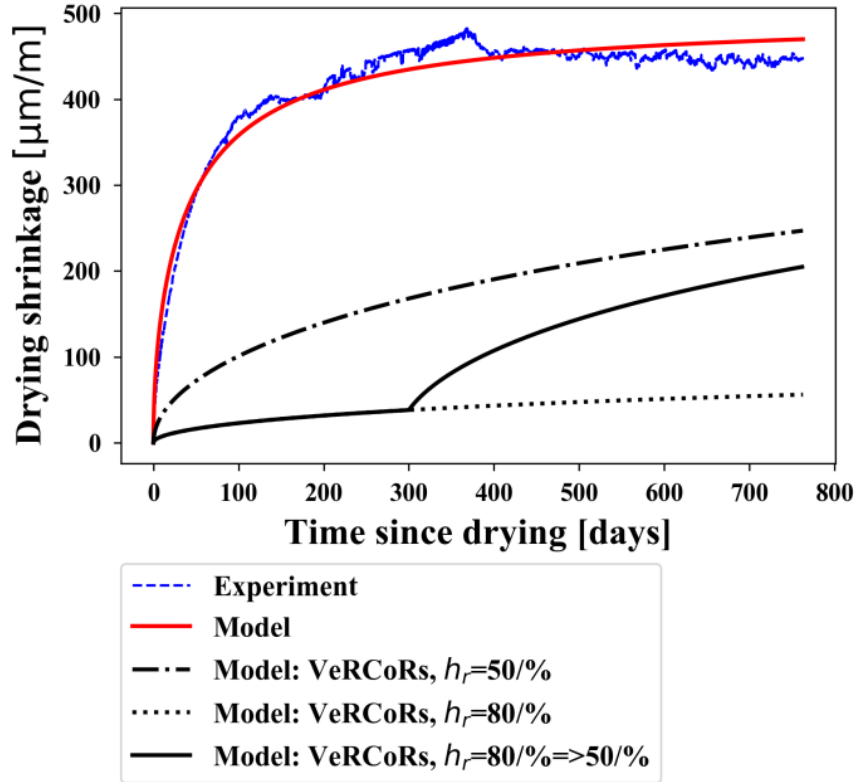

Figure 1 Experiment measurement of drying shrinkage, calibration of model and its application to VeRCoRs mock-up

The drying creep function is expressed as:

$$\varphi_{dc}(t, t_0) = \xi_{dc1} \beta_{dc}(f_{cm}, RH, t_0)\, \beta_{dc,t-t0} \tag{6}$$

with:

$$\beta_{dc,t-t0} = \left[\frac{t - t_0}{\xi_{dc2}\beta_h + t - t_0}\right]^{\gamma(t0)} \tag{7}$$

ξ_{dc1} and ξ_{dc2} are parameters that could be adjusted to experimental results. β_h is a function of the notional size. The best fit for drying creep is obtained with $\xi_{dc1} = 1,558$ and $\xi_{dc2} = 3,404$. Figure 2 shows also the drying creep of VeRCoRs mock-up at 50% and 80% of relative humidity respectively (calculated with the notional size of the mock-up which is different from the notional size of the sample used for the laboratory test). The variation of relative humidity is taken into account by superposition principle.

Long term behavior of the prestressing steel

Relaxation of creep is taken into account using the relation proposed by the model code 2010. The acceleration of the relaxation due to an elevated temperature which is an important effect [3] is also

taken into account. The parameters of the relations for relaxation are fitted on relaxation tests performed within the ANR MACENA project.
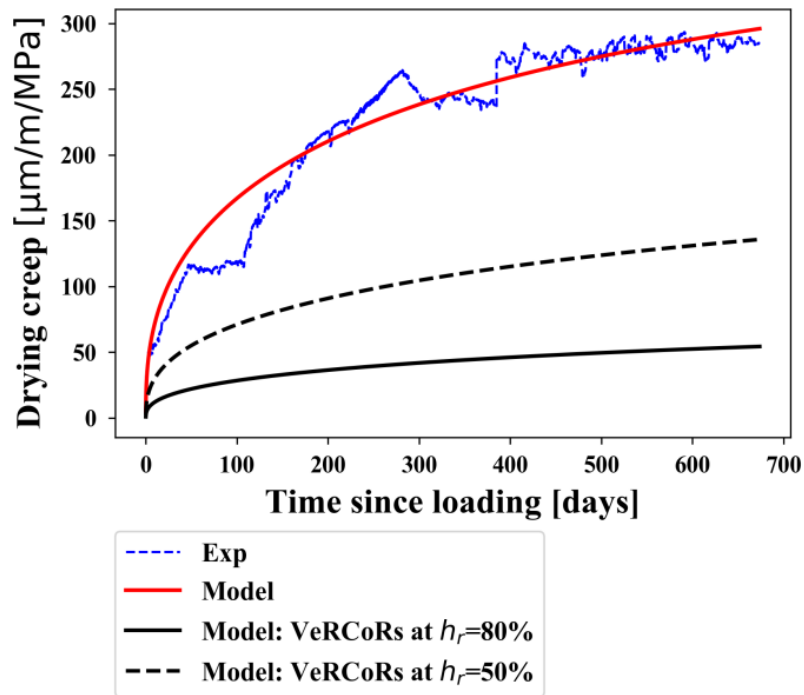

Figure 2 Experimental measurement of drying creep, calibration of model and its application to VeRCoRs mock-up

The evolution $\rho(t)$ of relaxation loss of prestressing over time may be assumed according to equations 10 and 11 where ρ_{100} is the relaxation loss in % after 100 hours and ρ_{1000} is the relaxation loss in % after 1000 hours. These parameters are depending on the stress level and on the temperature.

$$k = \log(\rho_{1000}/\rho_{100}) \tag{8}$$

$$\rho(t) = \rho_{1000} \left(\frac{t}{1000}\right)^{k} \tag{9}$$

Influence of temperature

An elevated temperature during service conditions (around 40°C) is observed in a NPP. This temperature will affect the delayed strains. For shrinkage this effect is neglected (despite the fact that the kinetics of desiccation shrinkage is certainly affected). Basic creep is affected by a thermo-activation using the following relation [4, 5]:

$$C(T) = C \exp\left(Q\left(\frac{1}{T} - \frac{1}{293}\right)\right) \tag{10}$$

where C is a parameter of basic creep (see equation 2 in the abstract of theme 1) and Q is the activation energy of water viscosity.

For drying creep, the temperature affects both kinetics and magnitude. In our application the relations proposed by MC2010 are used. For kinetics, the term β_h in equation 7 is multiplied by:

$$\beta_T(T) = \exp\left(\frac{1500}{273 + T} - 5.12\right) \tag{11}$$

For magnitude, the drying creep function φ_{dc} is multiplied by:

$$\varphi_{dc,T}(T) = \left(\exp(0.015(T - 20)) \right)^{1.2} \tag{12}$$

For steel relaxation, the relation proposed by the fib MC2010 is used. The stress relaxation $\rho(t)$ is multiplied by a factor AT that depends on the temperature:

$$AT(T) = AT(T = 20°C) \cdot \frac{T}{20°C} \tag{13}$$

Using tests performed at Ifsttar [6], the parameters of prestressing relaxation are adjusted at 20°C and at 40°C. Based on the tests performed at 20°C and a stress level of 70%, the Eqs. 8 and 9 are calibrated against the experimental relaxation data. Knowing ρ_{100}, we chose the ρ_{1000} to fit the curve. The best fit is obtained with $\rho_{1000} = 0,893$. For T=40°C the equation 13 is used directly and compared to experimental data (figure 3).
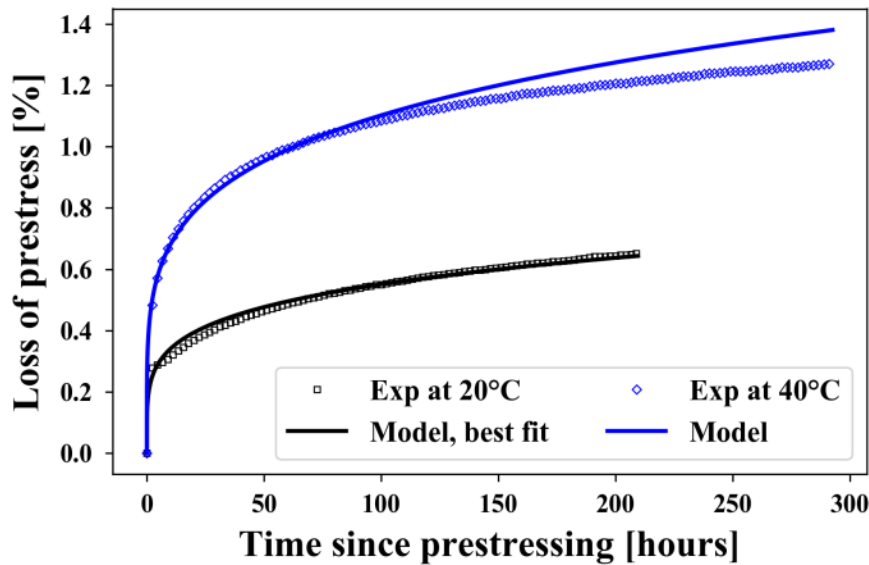

Figure 3 Experimental measurement of relaxation in prestressing cables and calibration of model

Superposition principle

The stresses, the strains, the relative humidity and the temperature are varying with time in the mock-up. Figure 4 presents the simplified history of temperature and relative humidity that will be used for the calculations.

To estimate the evolution of the delayed strain, the following assumptions are done:
- The strains of concrete and prestressing steel are the same,
- The superposition principle could be applied assuming that at each time step we consider a complete unloading and a re-loading i.e. a vertical decomposition of the stress history and not the classical horizontal decomposition [7],
- Biaxial loading: several definitions of the Poisson ratio in the case of creep exist. Nevertheless Aili et al. [8] have shown that, in the case of concrete, considering the Poisson ratio as constant is a good choice. For drying creep the Poisson ratio is assumed equal to -1 in order to obtain the observed behavior i.e. the difference between vertical and orthoradial strains is rapidly constant (see figure 7).

Finally, measured strains in the central part of the containment are compared to the strains obtained with the modelling. A good agreement is observed (Figures 5, 6 and 7).
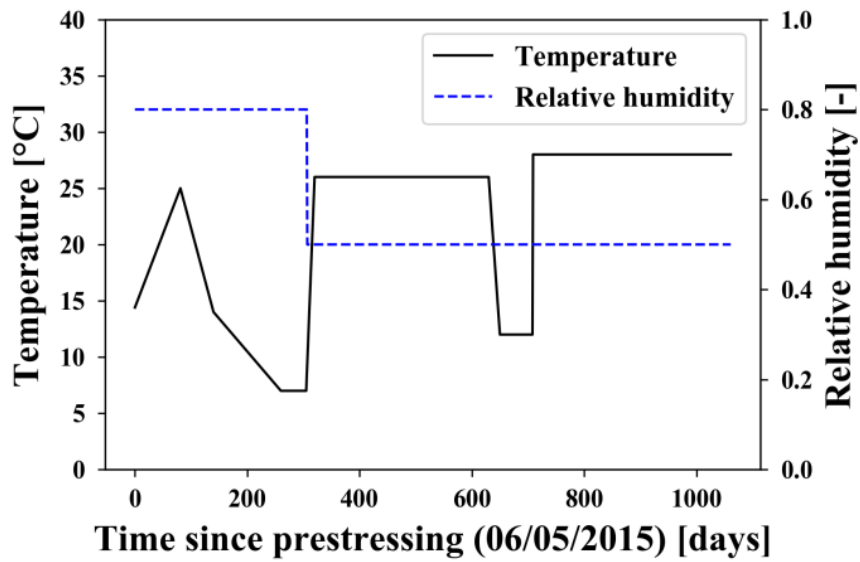
Figure 4: Simplified history of temperature and relative humidity of VeRCoRs mock-up
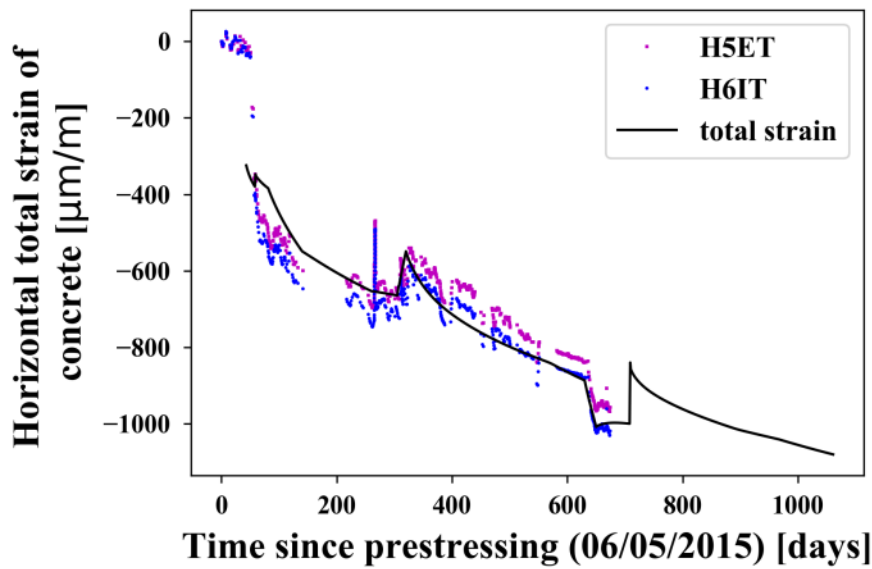
Figure 5: Comparison of on-site measurement of horizontal (tangential) total strain with model prediction
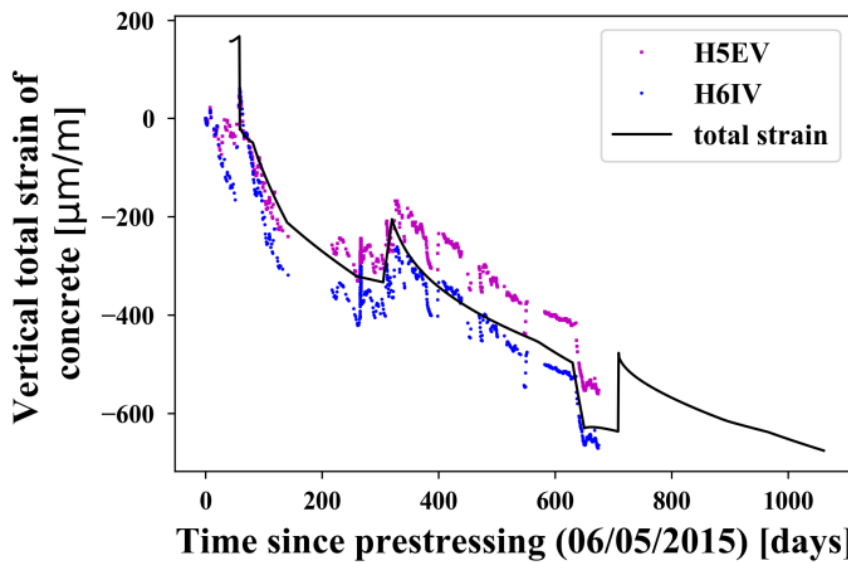

Figure 6: Comparison of on-site measurement of vertical total strain with model prediction
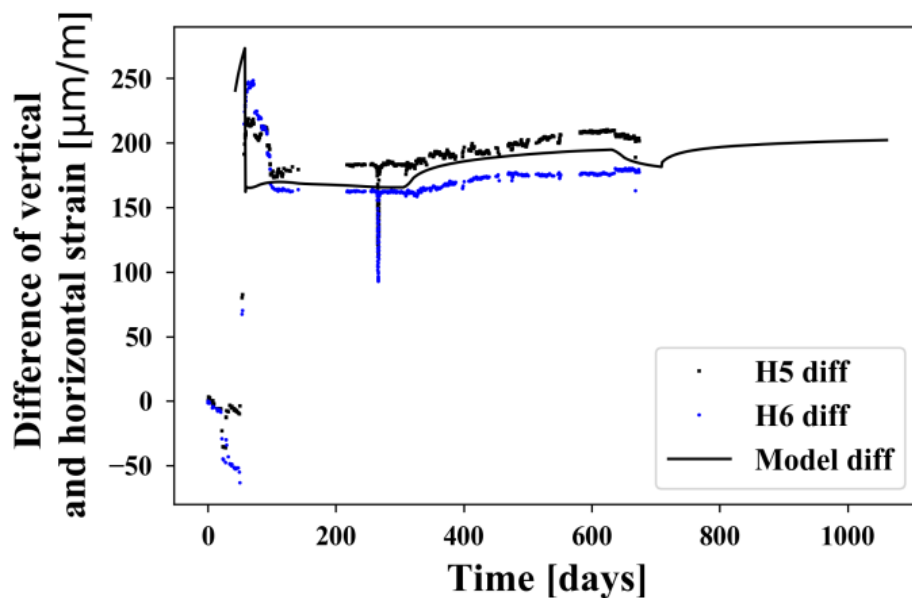
Figure 7: Comparison of on-site measurement of difference between vertical total strain and horizontal total strain against model prediction

REFERENCES

[1] fib model code for concrete structures MC2010, Ernst und sohn, 2013

[2] CEOS, Guidelines for the control of cracking in reinforced concrete structures, Wiley-ISTE, 2016

[3] Anderson P., Thirty years of measured prestress at Swedish nuclear reactor containments, Nuclear Engineering and Design, 235, 2005

[4] Sellier, A., Multon, S., Buffo-Lacarrière, L., Vidal, T., Bourbon, X., & Camps, G. (2016), Concrete creep modelling for structural applications: Non-linearity, multi-axiality, hydration, temperature and drying effects. Cement and Concrete Research, 79, 301–315

[5] J.M. Torrenti (2017), Basic creep of concrete-coupling between high stresses and elevated temperatures, Euro-pean Journal of Environmental and Civil Engineering, DOI:10.1080/19648189.2017.1280417

[6] W. Toumi Ajimi et al. (2016), Experimental Investigations on the Influence of Temperature on the Behavior of Steel Reinforcement (Strands and Rebars), Key Engineering Materials, Vol. 711, pp. 908-915.

[7] J. Walraven, J.H. Shen (1991), On the applicability of the superposition principle in concrete creep. In: Mechanics of Creep Brittle Materials 2. Springer, Dordrecht, p. 282-295

[8] A. Aili, M. Vandamme, J.M. Torrenti, B. Masson, J. Sanahuja, Time evolutions of non-aging viscoelastic Poisson's ratio of concrete and implications for creep of C-S-H, Cement and Concrete Research, 90 (2016) 144–161

Prediction of the strains and stresses in the gusset using COMSOL Multiphysics

S. Aparicio[*†], M.G. Hernández[†] and J.J. Anaya[†]

[†]Instituto de Tecnologías Físicas y de la Información "Leonardo Torres Quevedo" (ITEFI), CSIC, Madrid, Spain, e-mail: sofia.aparicio@csic.es.

ABSTRACT

1. Main features

In this work we present the results of Theme 2: Prediction of the strains, stresses and cracking of the whole containment wall. Our work has been centred in the prediction of strains and stresses in the gusset during several pressurization tests.

We have analysed the behaviour of temperature and strain until March of 2016 and we have performed the simulation of the stresses and strains under several pressurization tests at 0, 2.2 and 4.2 bars of pressure in the gusset part of the mock-up. Each test was performed during 5 days and we have considered the positions E1, C1, G1, F1, G2, and F2. See the red circles in Fig. 1. For that purpose we have used COMSOL Multiphysics 5.3a [1]. COMSOL Multiphysics is a cross-platform finite element analysis, solver and multiphysics simulation software. It allows conventional physics-based user interfaces and coupled systems of partial differential equations (PDEs). COMSOL provides an IDE and unified workflow for electrical, mechanical, fluid, and chemical applications.
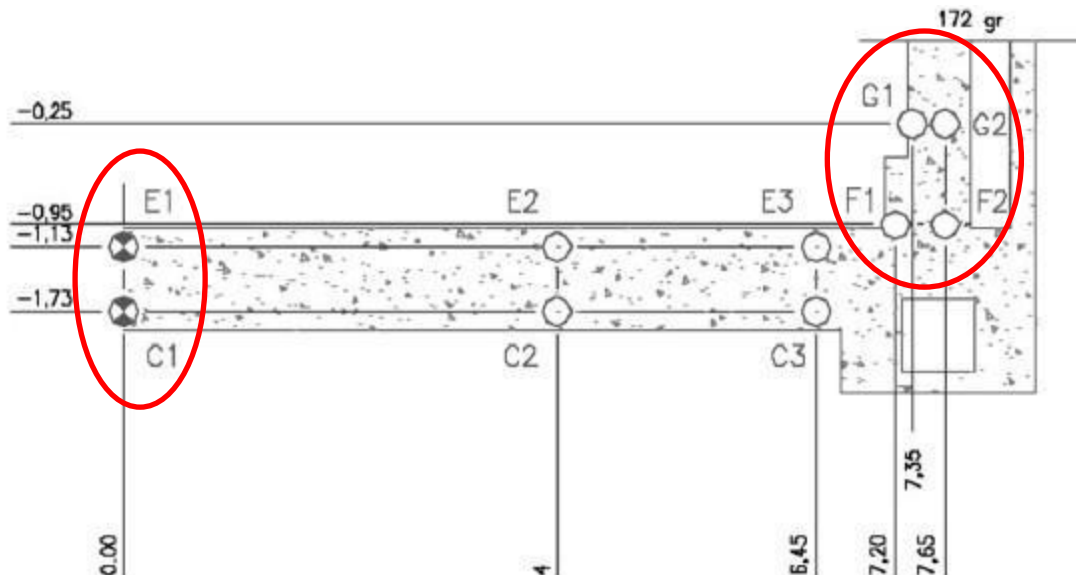
Figure 1. Strains gauges and thermometers at the Base slab- Gusset of the mock-up Section BB [2].

2. Behaviour of temperature and strain in the Gusset

The data provided by EDF [3] was analysed during the first pressurization tests. Strain raw data, temperature and total strain data corrected with temperature in the gusset during t0 and the second pressurization test can be seen in Fig. 2. The behaviour of temperature is very similar for all

considered sensors, only the G1 vertical strain sensor was affected by the tests. A dilation of the material was measured during the tests.
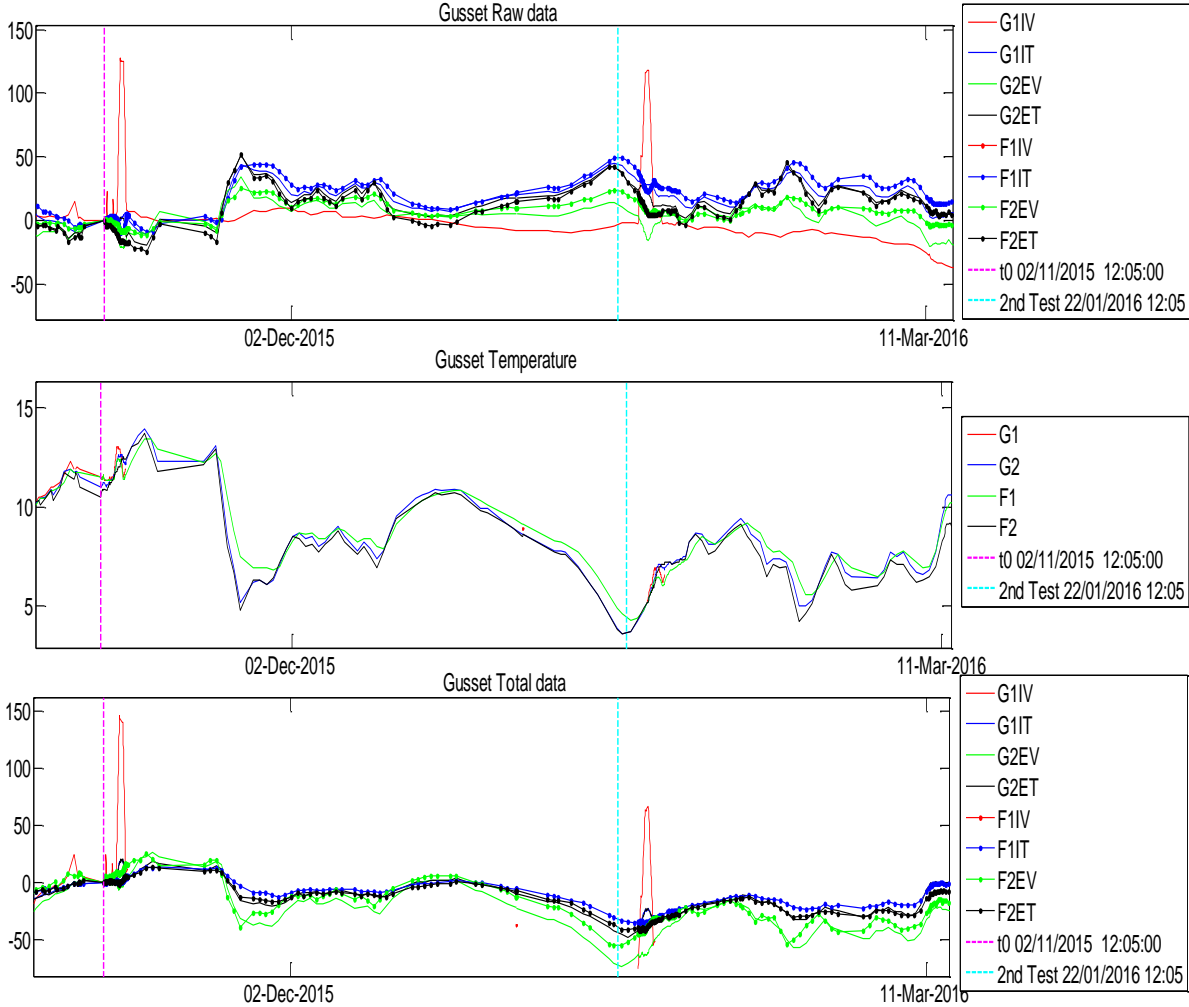
Figure 2. Strain raw data, temperature and total strain data corrected with temperature in the gusset.

A comparison between the temperatures measured in the gusset with the strains sensor and the sensor b of the raft was also analysed. A linear fit was performed obtaining very good values of R2, see Fig. 3. This indicates that there is a linear relationship between the temperature in the Gusset and the ambient temperature in the raft.
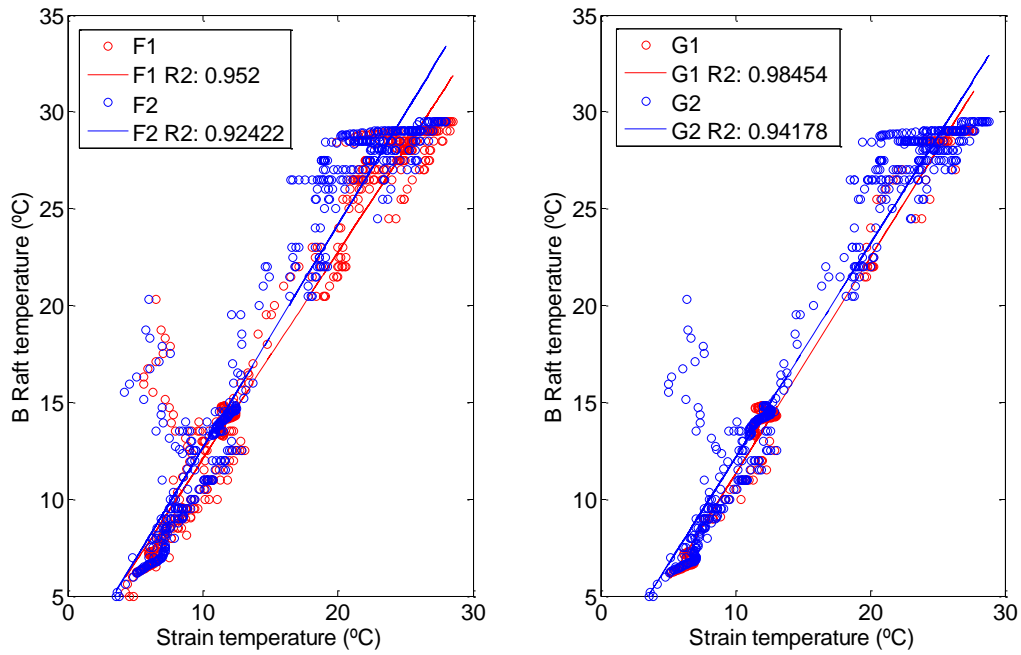
Figure 3. Comparison between the temperatures measured in the gusset with the strains sensor and the sensor b of the raft.

3. Gusset Modelling

To construct the model with COMSOL, a 2D surface representing the gusset and raft in the XY plane was rotated to generate a 3D surface, see grey figure in Fig. 4.

Figure 4. 2D surface representing the gusset and raft in the XY plane.

We have considered a mesh of 20334 tetrahedrons, considering 8250 triangles and 1371 edges elements. The number of vertices elements was 60 and 4584 of mesh vertices.
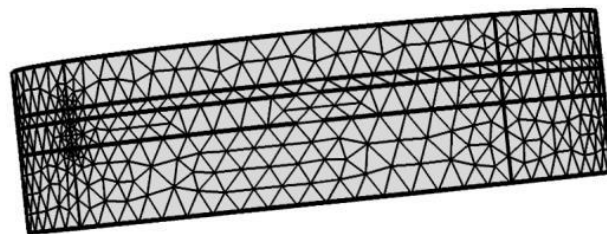
Figure 5. Mesh used for the simulation model.

We have used the heat transfer and structural mechanic modules supplied by COMSOL. A concrete material without reinforcements or tendons was used. The concrete modelled was considered as a

homogeneous material with a Young's modulus of 33.8 GPa, data from EDF. The air temperature and inner/outer face temperature supplied by EDF data and the stress effect of the cylinder and dome on the gusset surface were considered as boundary conditions. In the heat transfer simulation, the initial temperature value assigned was 288.15ºK. For the solid mechanics, it was considered that the interior surface of the gusset was fixed and the upper ring had a compression load of 11MPa, equivalent to the weight of the structure without the reinforcements.

4.   Results of modelization

The radial, shear and Tresca stress obtained after the simulated pressurization test at 0 and 4.2 bars are shown in Fig. 6 and 7.
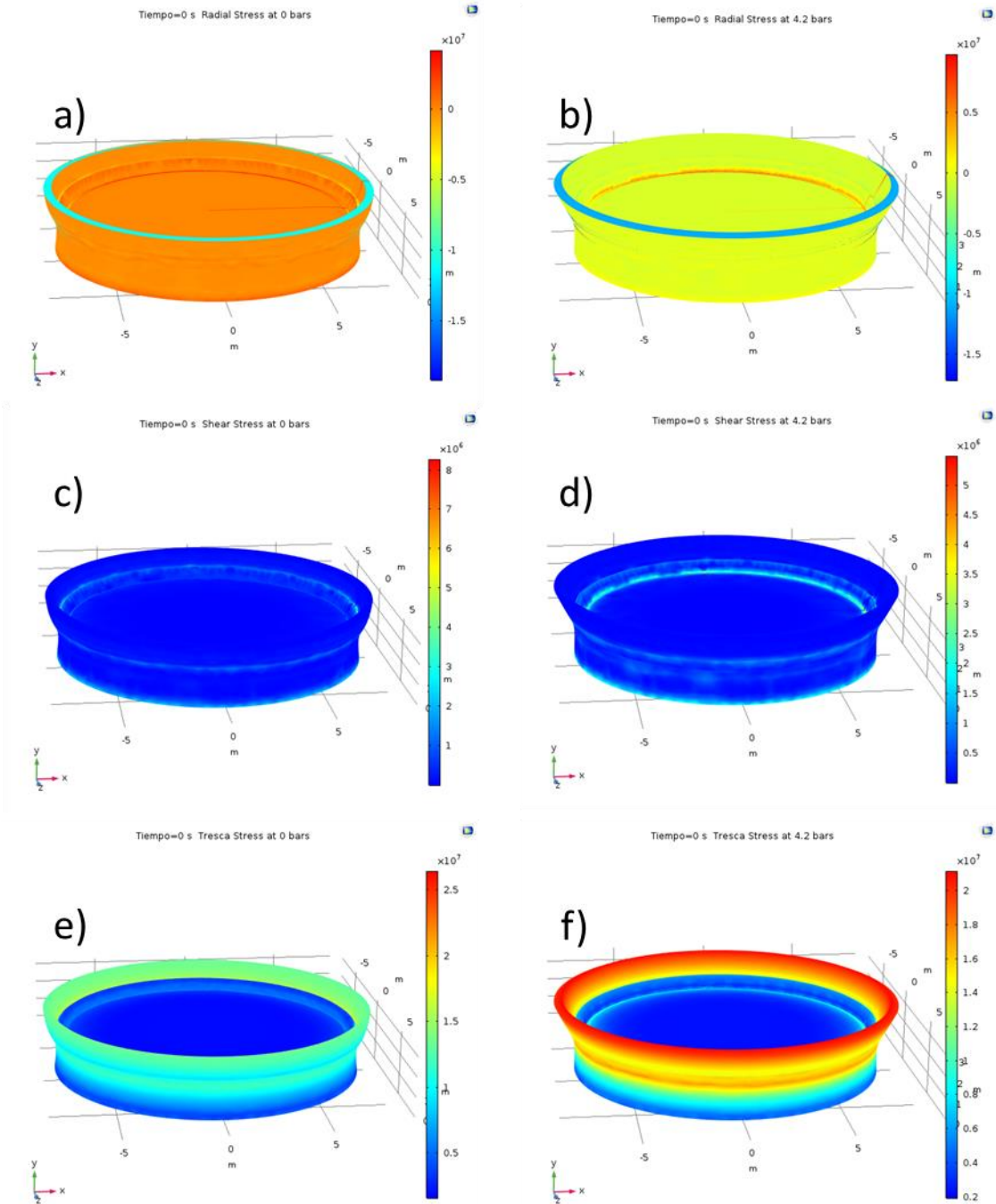
Figure 6. a) and b) Radial, c) and d) shear and e) and f) Tresca stresses colormaps obtained with the model after the simulated pressurization test at 0 and 4.2 bars.
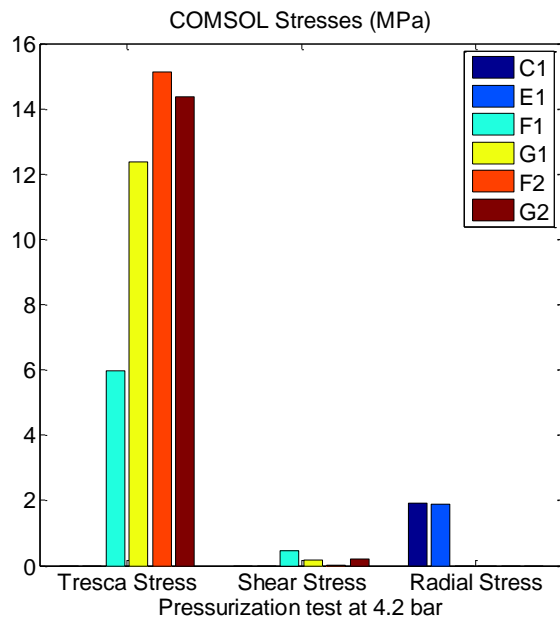
Figure 7. Tresca, shear and radial stresses values obtained with the model after the simulated pressurization test at 4.2 bars.

The total displacement colormaps obtained after the simulated pressurization tests at 0 and 4.2 bars with COMSOL is shown in Fig. 8.
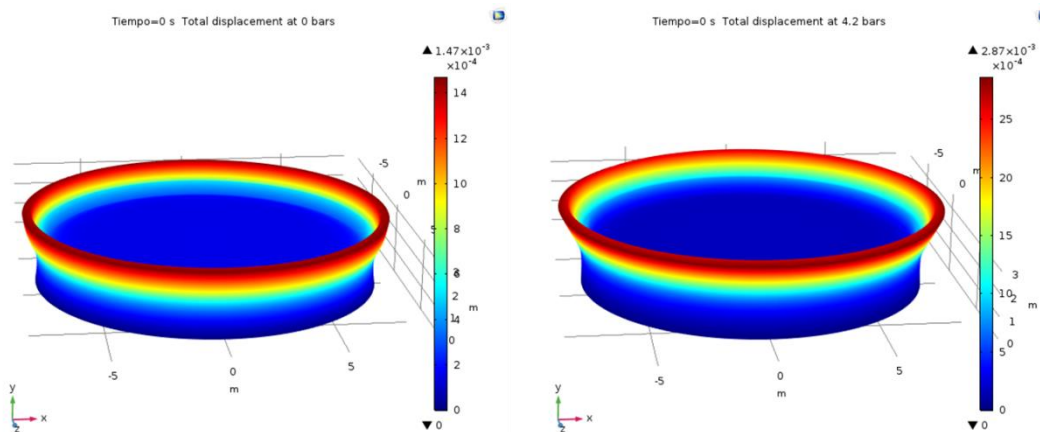
Figure 8. Total displacement obtained with the model after the simulated pressurization tests at 0 and 4.2 bars.

A comparison between the vertical and tangential strains obtained with COMSOL and the real results obtained during the different pressurization tests can be seen in Fig. 9.
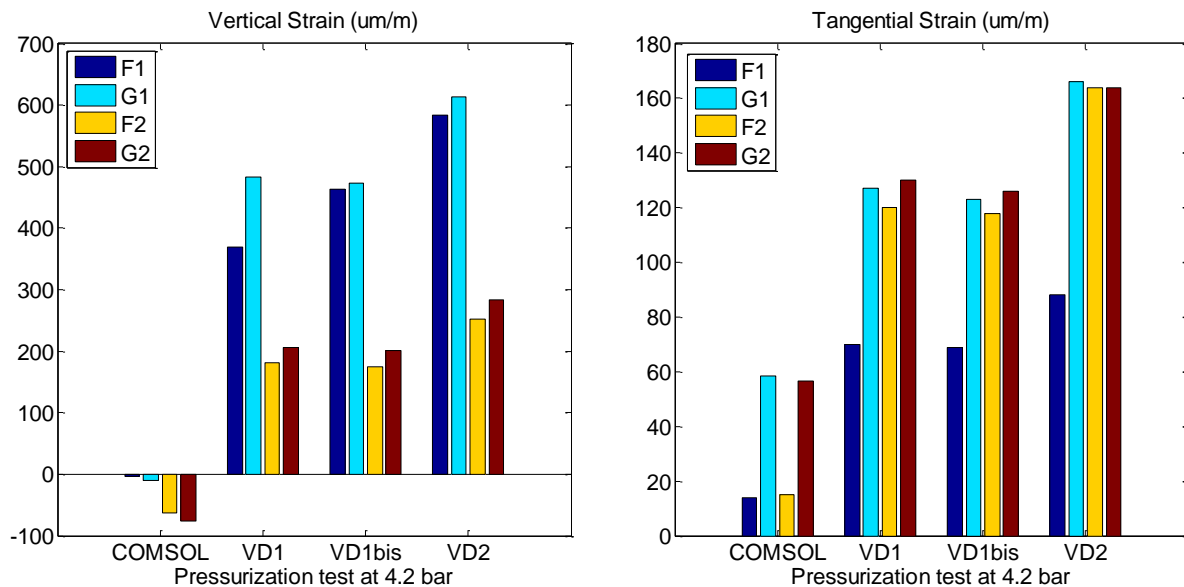
Figure 9. Comparison between the vertical and tangential strains obtained with COMSOL and the real results obtained during the different pressurization tests.

5. Conclusions

The results obtained with COMSOL show that the radial stress is very similar for both sensors C1 and E1. In the case of the other sensors the Tresca stress is much higher than the shear one, being the F2 and G2 sensors the ones affected with more stress.

The vertical strains simulated with COMSOL are quite different to the real values obtained during the pressurization tests. The simulation shows shrinkage in the gusset while in the real tests dilation was observed.

The tangential strains simulated in the gusset with COMSOL shows a similar behaviour as the real values obtained during the pressurization tests. Dilations are observed in these simulations but the strains values are lower than the real ones.

ACKNOLEDGMENTS

REFERENCES

[1] https://www.comsol.com/

[2] M. Corbin and M. Garcia. Overview, synthesis and lessons learnt. International Benchmark VerCoRs 2015.

[2] https://fr.xing-events.com/OLD-EDF-vercors-project.html?page=1320867
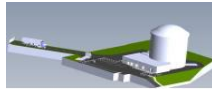
Theme 2 & 3 : Mechanical behavior of the containment during pressurization test - Air leakage

- **M. Asali**, **B. Capra** - *OXAND, France*

  Thermo-Hydro-Mechanical Strategy for Forecasting the Leakage Rate of Double-Wall Nuclear Reactor Buildings: Application to the VeRCoRs Mock-Up

- **Xu Huang, J. Dury, E. Bentz, O-S. Kwon**, University of Toronto, Canada

  Prediction of mechanical behaviour and air leakage of the VeRCoRs benchmark reactor containment structure

- **M. Mozayan Karazi, N. Goujard**, INGEROP / Mines Paris-Tech, France

  Development of a numerical model for studying the leakage tight-ness evolution of VeRCoRs experimental containment vessel under aging effect

- **Yangsu K., Keun-Kyeong K., Myung-Sug C., Kyung-Hun K., Hong-Pyo, L.** Korea Nuclear & Hydro Power Central Research Institute (KHNP CRI), Daejeon, Republic of Korea

  Structural behaviour and air leakage rate prediction for VeRCoRs mock-up by 3D numerical analysis

- **T. Thénint, V. Le Corvec and S. Ghavamian,** SIXENCE NECS, France

  Study of the containment history of the VeRCoRs mock-up and prediction of the leakage rate under pressurization tests

- **K. M. Calonius**, VTT Technical Research Centre of Finland Ltd, Finland

  Finite element analysis of a pre-stressed mock-up reactor containment - the VeRCoRs 2018 benchmark case

- **D. E.-M. Bouhjiti, J. Baroth, F. Dufour and B. Masson**, Chair PERENITI, Lab3SR, Univ. & INP Grenoble / EDF, France

  Predictive probabilistic analysis of the long term ageing of concrete effect on the behaviour of NCBs during pressurization tests: Mechanical and tightness analysis

Thermo-Hydro-Mechanical Strategy for Forecasting the Leakage Rate of Double-Wall Nuclear Reactor Buildings:
Application to the VeRCoRs Mock-Up

M. Asali[*] and B. Capra[†]

[*]OXAND France, 49 av. Franklin Roosevelt, Avon-Fontainebleau, France, mehdi.asali@oxand.com
[†]OXAND France, 49 av. Franklin Roosevelt, Avon-Fontainebleau, France, bruno.capra@oxand.com

ABSTRACT

In order to compute the total air leakage rate of the VeRCoRs mock-up, we propose a chained weakly-coupled thermo-hydro-mechanical (THM) strategy which aims at assessing the temperature, saturation degree, stress and strain fields and damage state within the structure under operating conditions (long-term operation). Those fields are used as inputs for a final post-treatment using a finite element especially developed for leakage computations. Complete details on the numerical methodology can be found in [1] and [2].

Numerical results presented in this paper correspond to the first computation submitted to the benchmark. Since then, experimental results and new data are available and will be considered in an updated computation, results of which will be discussed during the workshop.

MAIN ASSUMPTIONS, BOUNDARY CONDITIONS AND LOADINGS

No early-age evolution of the structure is considered in the proposed work. Thus, only hardened concrete behavior is considered from the starting point of the computation. Material parameters are kept constant over time.

Even if the mock-up represents a simplified version of a real inner containment of double-wall reactor building, the overall structure remains subject to a changing external environment as well as a complex construction phasing process. Main assumptions are the following:

- Erection is done at once; the starting date of all computations is on 30 November 2014.
- Due to water aspersion, the structure begins to dry on 1 April 2015.
- Prestressing occurs between 6 May and 12 August 2015 with a reduced number of tensioning sequences (14 steps lasting 24 hours each) compared to the original planning (36 groups of cables in 16 phases). The initial tension is 848 kN for all cables.
- Two main life phases of the structure are occurring: pre-operational until 28 January 2016 during which the mock-up is subject to its external environment, then operational starting on 1 April 2016. The transition between both phases is linearized.
- The first four internal leakage rate tests (ILRT) of the mock-up are considered in the present study: two pre-operational tests (VC_0 and VC_1) occurring during 4-6 November 2015 and 25-28 January 2016 respectively, and the two first decennial test (VD_1, VD_{1bis}, and VD_2) during 14-16 March 2017 (repeated 21-23 March 2017) and 2-4 April 2018 respectively. They all last 2.5 days and the pressure evolution is shown in Figure 1. The raft being submerged during ILRT, it is not considered as a possible leakage pathway (null flux).
- During the pre-operational phase, evolutions of air temperature and relative humidity (RH) are defined linearly between their extremal seasonal values. Air temperature and RH are kept constant during the operational phase. Both evolutions are shown in Figure 2 and Figure 3 following mean benchmark measurements.
- Soil temperature is kept constant at 10 °C. Soil RH is kept constant at 99%.

- Reinforcement bars are not explicitly modeled but participate in the dead weight of the global structure (+100 kg·m⁻³).
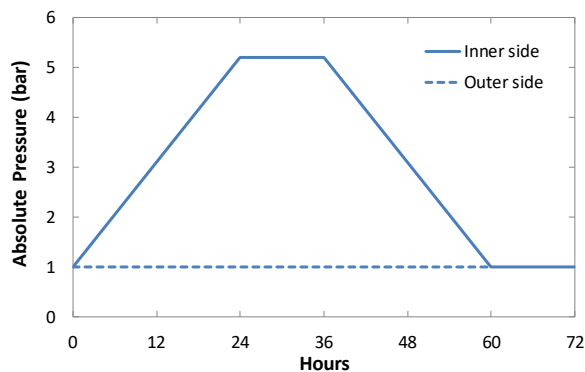
Figure 1: Absolute air pressure imposed during ILRT
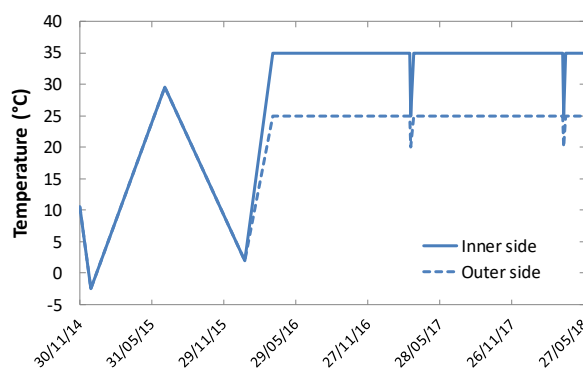
Figure 2: Evolution of imposed air temperature
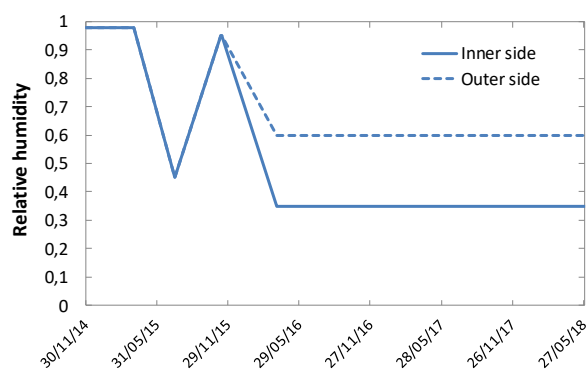
Figure 3: Evolution of imposed air RH

MODELING PRINCIPLES OF CONSIDERED PHENOMENA

Considering the size of the studied structure and the complexity of all interacting phenomena, it is very difficult from a computational perspective to build an industrial and operational tool finely and fully modeling all the strong couplings. To simplify the problem, a chained weakly-coupled methodology has been implemented. It is based on a 3D macro finite element discretization and aims at representing at lower numerical cost the physical behavior of an inner containment under operating conditions.

The main goals of this simplified - but not simplistic - approach are to:
- Compute air leakage through porous and cracked concrete in a practical way,
- Be able to consider variability and uncertainty of the main material parameters while keeping acceptable computation times for industrial use,
- Increase the value of field data, either monitored occasionally (e.g. total leakage rate) or continuously (e.g. delayed strains), by using this data as input to adapt or calibrate the tool and improve forecasts over time.

The main components of the chained weakly-coupled THM modeling have been presented in Theme 1. Associated temperature, saturation and mechanical states are then post-treated during each ILRT to compute the inner containment leakage rate. Although cracks in concrete are small and localized for large structures as inner containments, they could represent a preferential pathway for air leakage. Thus, a dedicated 3D finite element has been developed that introduces an equivalent cracking state without explicitly meshing those defects. Its principle (Figure 4) is to superimpose a Darcy's flow (2) within the unsaturated porous concrete matrix of size Ω_e (in m³) and a Poiseuille's flow (3) within a perfectly plane crack of area Σ_e (in m²), opening w_e (in m) and normed normal vector $\mathbf{n_e}$. Considering a stationary and compressible laminar flow and air as a perfect gas, mass conservation leads to solve the non-linear diffusion equation (1):

$$\nabla \cdot \mathbf{q_D} + \nabla \cdot \mathbf{q_P} = 0 \tag{1}$$

$$\mathbf{q_D}(\pmb{x},t) = -\frac{M_g}{RT(\pmb{x},t)}\frac{K_{int}^g k_{rg}(S_l)}{2\eta_g}\nabla P_g^2(\pmb{x},t) \tag{2}$$

$$\mathbf{q_P}(\pmb{x},t) = -\frac{M_g}{RT(\pmb{x},t)}\frac{\zeta \Sigma_e w_e^3}{24\Omega_e \eta_g}(\mathbf{I_3} - \mathbf{n_e}{\otimes}\mathbf{n_e})\nabla P_g^2(\pmb{x},t) \tag{3}$$

Where $\mathbf{q_D}$ and $\mathbf{q_P}$ are air flux fields within the matrix and the crack respectively (in kg·s^{-1}·m^{-2}), K_{int}^g is the air intrinsic permeability of concrete (in m^2), k_{rg} its air relative permeability field (defined by a modified Mualem's law), η_g is the air viscosity (in Pa·s), M_g is the air molar mass (in kg·mol^{-1}), P_g is the air pressure field (in Pa), n (and $m = 1 - 1/n$) is one coefficient of Van Genuchten's model and ζ a flow reduction factor to represent tortuosity, roughness or turbulence effects (values between 0 and 1).

Crack openings and orientations in each finite element are obtained according to [3] and [4] (Figure 5). A crack-effective strain tensor field $\pmb{\varepsilon_{cod}}$ is defined from the damaged elastic behavior of concrete (4). Its maximal eigenvalue in tension (if any) is used to compute the crack opening (5) and the associated eigenvector defines the crack surface normal.

$$\pmb{\varepsilon_{cod}}(\pmb{x},t) = \pmb{\varepsilon^{el}} - \frac{1}{E}[(1+\nu)\pmb{\sigma} - \nu\,\mathrm{tr}(\pmb{\sigma})\mathbf{I_3}] \tag{4}$$

$$w_e = \sqrt[3]{\Omega_e}\,\max[\max(\mathrm{Sp}(\pmb{\varepsilon_{cod}})),0] \tag{5}$$

Where $\pmb{\varepsilon^{el}}$ is the damaged elastic strain tensor, E is the Young's modulus of concrete (in Pa), ν its Poisson's ratio and $\pmb{\sigma}$ is the stress tensor (in Pa).
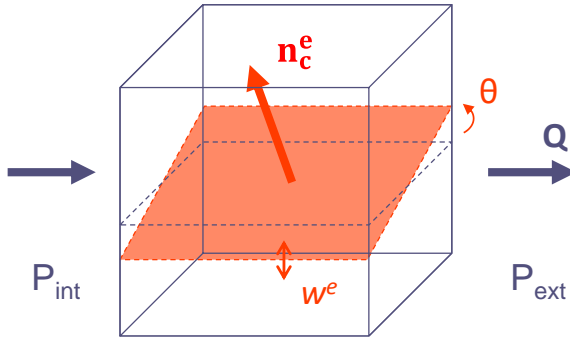
Figure 4: Principle of the cracked finite element
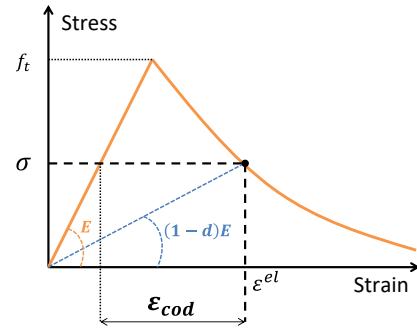
Figure 5: 1D principle to define the crack effective strain

Total leakage corresponding to the quantity of air leaving the internal volume of the inner containment, the total mass leak rate Q_M (in kg·s^{-1}) is computed by projecting nodal air fluxes and integrating over the whole internal surface. To compare leakage rates of all NRB independently of each ILRT temperature and pressure conditions, EDF converts mass flow rates into volumetric flow rates expressed at normal temperature and pressure conditions:

$$Q_V^{norm} = 3600\,\frac{R}{M_g}\frac{T^{norm}}{P^{norm}}Q_M \tag{6}$$

Where Q_V^{norm} is the volumetric total leakage rate (in Nm^3·h^{-1}) at normal temperature T^{norm} (0 °C) and normal pressure P^{norm} (101315 Pa).

IDENTIFICATION OF MATERIAL AND MODELING PARAMETERS

As much as possible material parameters are defined according to data available within the benchmark (lab tests, construction site measurements or design values). Cable parameters come from design and manufacturer values. Mean values are considered when available for each concrete lift. A fitting procedure has been set up for parameters not directly accessible, in the following order: Van Genuchten's parameters are identified on the isothermal desorption curve, water intrinsic permeability

on the weight-loss curve, the shrinkage coefficient on the drying shrinkage curve (with autogenous shrinkage), the three basic creep rheological coefficients on the non-drying creep curve (corrected from autogenous shrinkage) and the drying creep coefficient on the total creep curve.

From visual inspections a set of 12 equidistant going-through cracks has been manually patched on the gusset during the first ILRT computation (VC_0, see Figure 6). Assuming the cracks have the same unknown opening and a prefixed flow reduction factor $\zeta = 0.1$, it is possible to identify both intrinsic gas permeability of concrete and gusset cracks opening knowing the global and local leakage rates.

Air flux density (kg·s^{-1}·m^{-2})
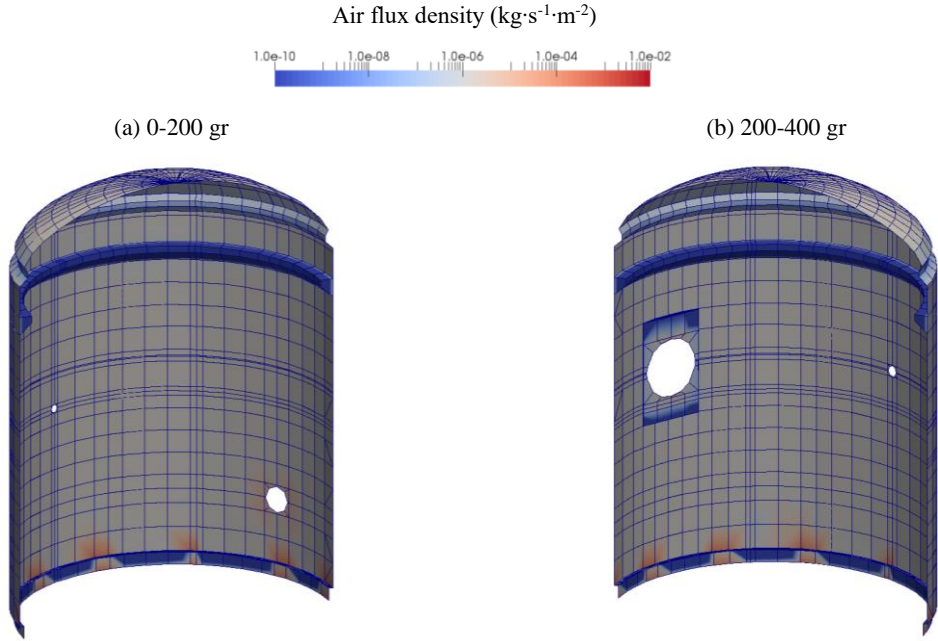
Figure 6: Air nodal mass fluxes computed at the inner side of the mock-up during VC_0 (with 12 cracks in the gusset)

MAIN RESULTS, ANALYSIS AND DISCUSSION

The presented THM strategy is implemented within TFEL/MFront v2.0.1 [5] (for the delayed strains modeling) and Code_Aster v12.3 [6] (for the global THM computations). All models use the coarser mesh available in the previous benchmark and linear finite elements.

Core concrete saturation at mid-height of the inner wall (H1-H2 sensors), at the maximal pressure plateau of each ILRT, is shown on Figure 7.
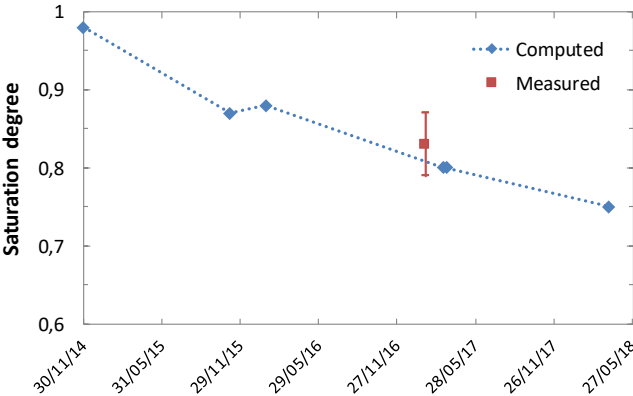
Figure 7: Evolution of computed saturation at mid-height and mid-thickness of the cylindrical part

According to Figure 7, the drying kinetics of concrete identified from reconstituted laboratory experiments (desorption and weight-loss curves) is in a good agreement with the unique data available on the mock-up. The increase of saturation during winter 2015-2016 is due to cycling environmental RH until VC_1.

Evolutions of concrete total strains at mid-height of the inner wall are shown in Figure 8.
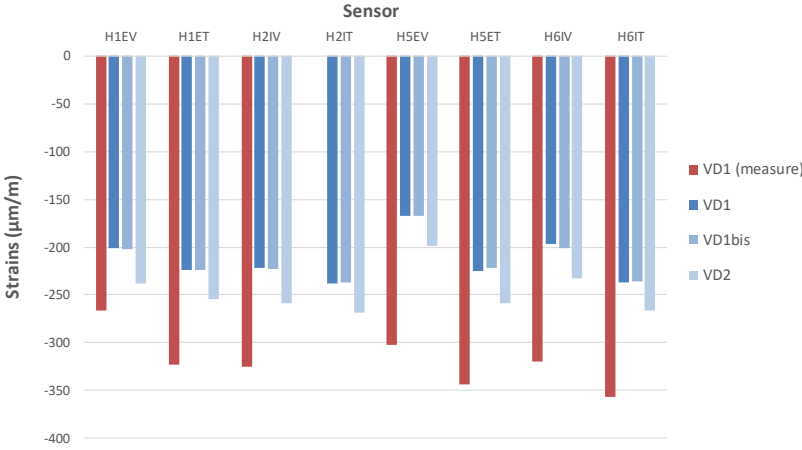
Figure 8: Evolution of computed strains at mid-height of the mock-up's cylindrical part

From previous results (see [1] and previous benchmark), kinetics of delayed effects is well reproduced in both tangential and vertical directions. According to Figure 8, compressive strain levels are globally underestimated by the model, especially at points H5 and H6. This gap may be explained by two factors:

- only uniaxial creep tests are available to calibrate a biaxial creep model leading to a homogeneous behavior of concrete in the vertical and tangential directions,
- concrete Young's modulus is considered as homogenous in this computation.

Evolutions of differential strains between the start and the end of the plateau of each ILRT are shown in Figure 9 for the four points of interest at mid-height of the inner containment.

According to Figure 9, the impact of inflation on the mechanical state of concrete is well reproduced by the model in standard areas.
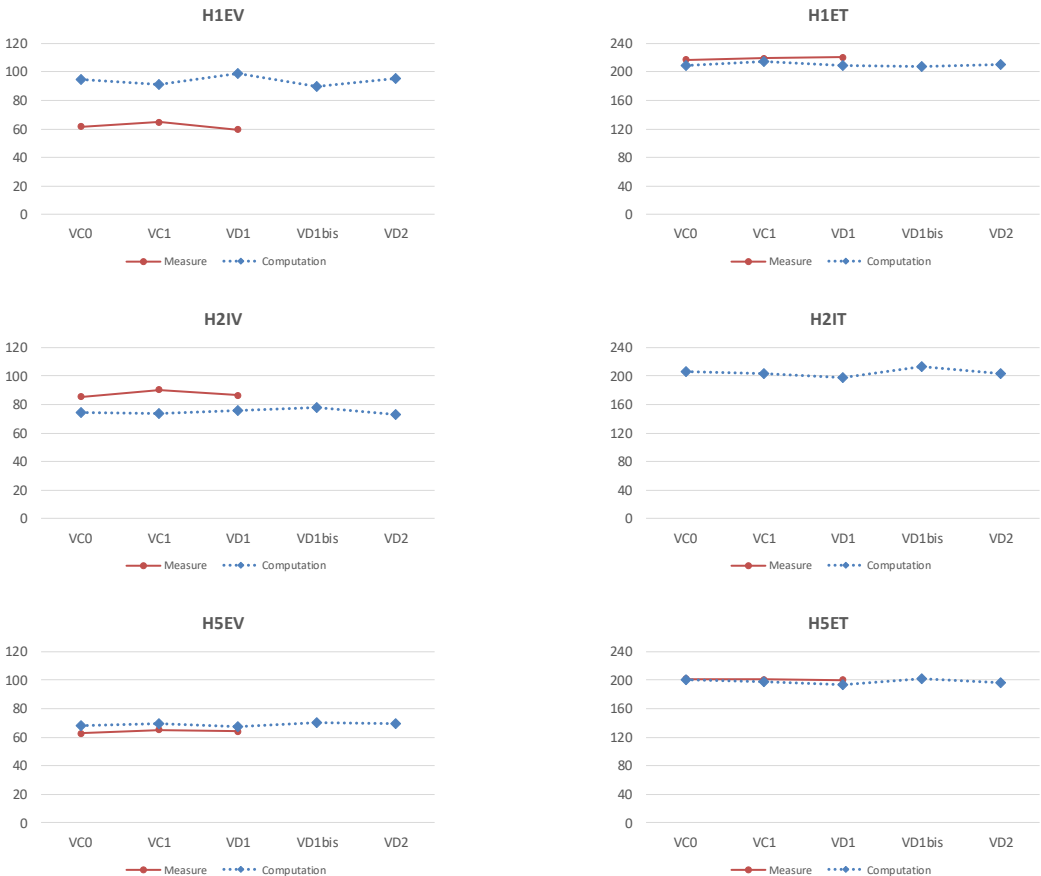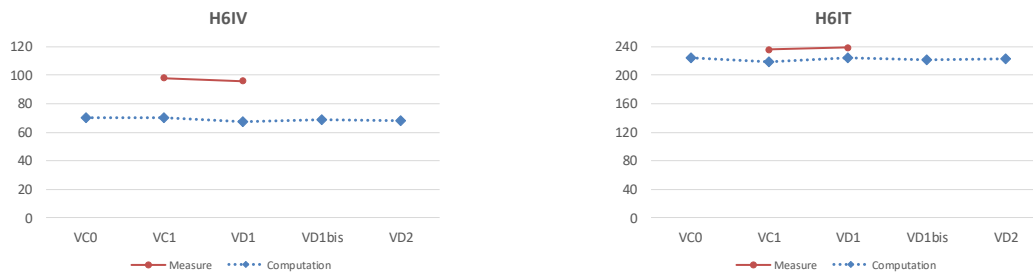
Figure 9: Evolution of computed differential strains during ILRT

Evolution of the total leakage flow rate of the mock-up is shown in Figure 10.
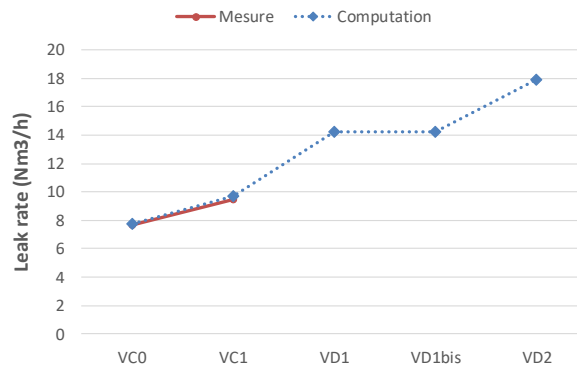
Figure 10: Evolution of computed total leak rate of the mock-up

According to Figure 10, the fitting procedure of leakage parameters on the first ILRT VC_0 provides a very good leak rate forecast for the second ILRT VC_1 mainly subject to drying compared to VC_0. As no sensitive damage and drying evolution is computed between VD_1 and VD_{1bis}, the global (and local) leakage rates stay the same for both IRLT.

Forecasts made for VD_1 and VD_2 use the same crack opening as the one identified during VC_0 (manual patching on the leak rate computation and not impacting the mechanical one). This assumption needs to be verified with results obtained during decennial tests and the possible evolution of gusset crack opening with time and prestressing losses.

Another assumption that needs to be verified with experimental data is the value chosen for the flow reduction factor. The proposed computation uses a mean value from literature, but an inverse computation with local measurements (when cracks are measurable, i.e. their width is over 100 µm) could help fixing a representative value to better estimate crack openings in the mock-up.

REFERENCES

[1]   M. Asali, "Modélisation et prévision du comportement thermo-hydro-mécanique d'une paroi en béton: application au cas des enceintes de confinement des bâtiments réacteurs nucléaires", Thèse de l'Université Lille 1 (2016)
[2]   M. Asali, B. Capra, J. Mazars, J.-B. Colliat, "Numerical Strategy for Forecasting the Leakage Rate of Inner Containments in Double-Wall Nuclear Reactor Buildings", *Journal of Advanced Concrete Technology*, **14**:408-420 (2016)
[3]   X. Jourdain, "Etude numérique méso-macro des propriétés de transfert des bétons fissures", Thèse de l'Ecole Normale Supérieure de Cachan (2014)
[4]   M. Matallah, C. La Borderie and O. Maurel, "A practical method to estimate crack openings in concrete structures", *International Journal for Numerical and Analytical Methods in Geomechanics*, **34**:1615-1633 (2010)
[5]   http://tfel.sourceforge.net/, MFront website, "A code generation tool dedicated to material knowledge"
[6]   http://web-code-aster.org/spip.php?rubrique2, "Code_Aster website, "Structures and Thermomechanics Analysis for Studies and Research"
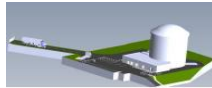
Prediction of mechanical behaviour and air leakage of the VeRCoRs benchmark reactor containment structure

Xu Huang[†], Julia Dury[††], Evan Bentz[*] and Oh-Sung Kwon[**]

[†]University of Toronto, Toronto, Canada, e-mail: xu.huang@mail.utoronto.ca
[††]University of Toronto, Toronto, Canada, e-mail: julia.dury@mail.utoronto.ca
[*]University of Toronto, Toronto, Canada, e-mail: bentz@civ.utoronto.ca
[**]University of Toronto, Toronto, Canada, e-mail: os.kwon@utoronto.ca

ABSTRACT

This paper investigated the long-term performance of the VeRCoRs benchmark nuclear containment structure from the first pressurization test to the recent pressurization test started on April 2, 2018. Theme-2 and Theme-3 of the benchmark are considered in this study. In the Theme-2, a three-dimensional finite element model was built using VecTor4 to evaluate the strain changes due to the internal pressure as well as concrete creep and shrinkage. In the Theme-3, data from the experimental tests performed at the University of Toronto were used to predict the air leakage during the pressurization tests.

INTRODUCTION

With the success of the first VeRCoRs benchmark carried out in 2015, the second benchmark on the same containment structure was proposed with the following three themes:

- Theme-1: prediction of basic creep taking into account the mix design.

- Theme-2: mechanical behaviour of the containment structure during the pressurization tests. This theme involves the prediction of strains, stresses and cracking history of the mock-up during the pressurization tests.

- Theme-3: prediction of air leakage during the pressurization tests.

The Theme-2 and the Theme-3 are considered in this study. The prediction methods for each theme are presented in the following sections.

THEME-2 PREDICTION

Numerical model

A detailed VecTor4 model of the containment structure was built with necessary simplifying assumptions to reduce modelling and computing time. These assumptions have been used in similar studies for a CANDU nuclear containment structure [1] as well as the first VeRCoRs benchmark prediction [2]. Only the key assumptions are summarized in the following:

- The perimeter wall is prismatic, and the buttresses are not included in the numerical model.

- Reinforcing bars are continuous and the irregular layout of the reinforcement and tendons due to permanent opening and support bracket are ignored.

- The containment is assumed to be axisymmetric and the containment structure is represented by a quarter model in VecTor4.

- While there is a sharp geometric change in the ring beam and gusset, the mesh is developed

such that the transitions are smooth without sharp changes as shown in Figure 1(a). This assumption is necessary to avoid numerical errors at the connections.

- To consider the deformation of the raft foundation due to shrinkage and the forces transmitted from the perimeter wall, nodes at the bottom of the perimeter wall are connected to the axis of symmetry using truss element. The stiffness of the truss elements is determined based on the estimated stiffness of the raft foundation. The strain change of the raft foundation due to shrinkage is applied as a pre-strain in the truss elements. Creep of the foundation is ignored.

- Strain changes due to concrete creep and shrinkage are modelled by applying equivalent temperature loads to the internal and external surfaces of the containment.

- Concrete stresses used for the creep calculations are obtained from an initial static analysis where the containment is subjected to dead load and initial prestressing forces.

Based upon the numerical model used in the first benchmark, this study improved the model in the following aspects:

- The hole at the top of the dome in the previous model has been avoided by rearranging the mesh as shown in Figure 1 (b).

- The average temperature and relative humidity used for creep and shrinkage predictions are assumed to be 15°C and 60%, respectively, based on the data provided by the benchmark committee.

- The CEB/FIP 90 model code [3] used for modelling concrete creep was replaced with the up-to-date MC2010 model [4].

- The ACI 209R-08 model [5] was used for modelling concrete shrinkage at the dome while the MC2010 shrinkage model was used for the ring beam and the perimeter wall. This assumption is based on the experimental study on concrete shrinkage conducted by the authors. It was found that the ACI 209R-08 model can more accurately estimate the long-term shrinkage strains for specimens with small volume-to-surface (V/S) ratios. However, for specimens with high V/S ratios such as the VeRCoRs benchmark containment with V/S ratios larger than 300 mm at the perimeter wall and the ring beam, the ACI 209R-08 model predicts unrealistically small shrinkage.
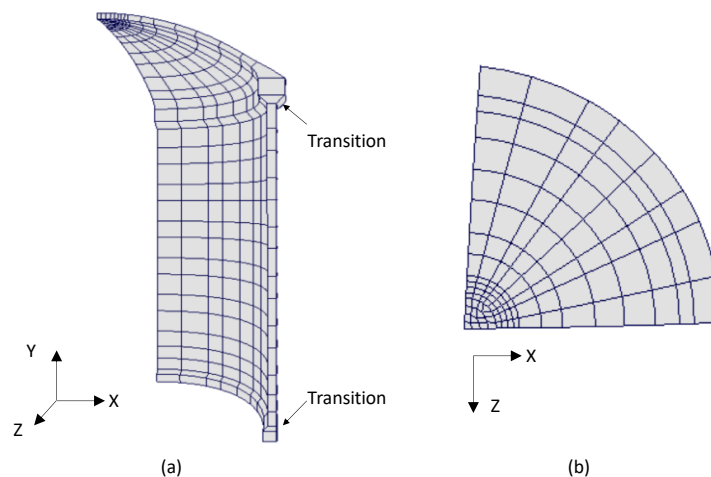
Figure 1. Mesh scheme

Numerical results

Analysis results are reviewed and are compared with measured results in this section. Table 1 shows the long-term strain differences between the dates of interest (the third pressurization test, VD1, and the fifth pressure test, VD2) and the reference date. The reference date is defined as November 2, 2015, right before the start of the first pressurization test. It can be seen that the predicted strain changes are significantly less than the measurements. For the dome elements with the smallest V/S ratio, the differences between the predicted and the measured strain changes are relatively small. With the increase

of the V/S ratios from the perimeter wall to the gusset, the discrepancies increase significantly. This is mainly due to the inaccuracy of the MC2010 model for long-term shrinkage prediction with large V/S ratios. Further study should be conducted to investigate the effect of large V/S ratio on shrinkage of concrete.

Table 1. Long-term strain differences (μm/m)

Zone	Strain gauge	Direction	Start of VD1	Start of VD2	Start of VD1
			prediction		measurement
Gusset	F1	Vertical	-71	-102	not available
	F1	Horizontal	-11	-15	-73
	F2	Vertical	-82	-113	-181
	F2	Horizontal	-9	-32	-119
	G1	Vertical	-72	-102	-344
	G1	Horizontal	-54	-76	-117
	G2	Vertical	-119	-168	-206
	G2	Horizontal	-53	-74	-114
Perimeter wall	P1	Vertical	-128	-161	-360
	P1	Horizontal	-116	-178	-334
	P2	Vertical	-127	-169	-348
	P2	Horizontal	-122	-178	-266
	H1	Vertical	-109	-164	-323
	H1	Horizontal	-118	-179	-326
	H2	Vertical	-128	-168	not available
	H2	Horizontal	-120	-178	-303
Dome	I1	Radial	-255	-336	-301
	I2	Radial	-262	-344	-321
	J1	Radial	-194	-270	Not available
	J1	Circumferential	-161	-216	Not available
	J2	Radial	-194	-271	-258
	J2	Circumferential	-159	-214	-231

Table 2. Strain changes during the pressure tests between 0 bar and 4.2 bar (μm/m)

Zone	Strain gauge	Direction	VD1	VD1
			Prediction	Measurement
Gusset	F1	Vertical	58	not available
	F1	Horizontal	43	-3
	F2	Vertical	81	0
	F2	Horizontal	31	1
	G1	Vertical	114	139
	G1	Horizontal	106	10
	G2	Vertical	145	0
	G2	Horizontal	103	16
Perimeter wall	P1	Vertical	88	73
	P1	Horizontal	218	216
	P2	Vertical	86	88
	P2	Horizontal	229	234
	H1	Vertical	77	60
	H1	Horizontal	223	220
	H2	Vertical	90	86
	H2	Horizontal	227	not available
Dome	I1	Radial	243	158
	I2	Radial	254	170
	J1	Radial	253	not available
	J1	Circumferential	35	not available
	J2	Radial	265	176
	J2	Circumferential	41	10

The strain changes due to the internal pressure increase are shown in Table 2. The predicted strain changes of the perimeter wall are in good agreement with the measurements. However, the strains in the gusset are not well predicted due to the simplified boundary condition made in the numerical model. The strain changes at the strain gauges in the dome are also overestimated. Since these strain gauges are either located at the axisymmetric axis of the dome or close to the simplified transition between the dome and the ring beam, numerical predictions at these locations with the simplifying assumptions are

inaccurate. The containment structure was predicted to be linear elastic and no cracks were predicted during the pressurization tests.

THEME-3 PREDICTION

Modelling assumptions

Although the analysis results from Theme 2 predict that no cracking will occur in the structure, a prediction was made for the flow rate through cracks in the four specified areas of the containment structure. In order to determine the crack lengths and widths through which to predict leakage, the results of the previous benchmark test were analyzed to estimate the total length of through cracks present. Calculated flow rates from the VeRCoRs mockup were compared with experimental flow rates from the University of Toronto [6] in order to validate the predictions made using the experimental value. The leak rate experiment carried out at the University of Toronto is briefly summarized in the next section.

At the peak pressure, the flow rate through the measured cracks in the previous benchmark was calculated to be 0.11 m3/hr/meter of crack for the measured crack widths, which did not exceed 0.05mm through the full depth of any crack. Data from the University of Toronto experiments suggest that for the geometry of the VeRCoRs specimen, a flow of 0.18 m3/hr/meter of crack is to be expected through the cylinder area, assuming a crack width of 0.05 mm. This flow rate was determined by normalizing the data collected from the experiments at the University of Toronto and allowing for a linear relationship between flow and wall thickness, as suggested by the Poiseuille equation which was first used to predict flow rate through cracks in concrete in previous research by Rizkalla et al. [7]. The experimental program at the University of Toronto did not reach levels of overpressure as high as those in the VeRCoRs tests, however, it was observed that the flow rate varied linearly with increases in pressure, therefore this also allowed for extrapolation of the experimental results for application to the VeRCoRs structure.

The discrepancy between the two flow rates (one measured from the previous VeRCoRs benchmark test, and the other one measured at the University of Toronto) is likely due to differences in reinforcement properties and aggregate sizes. The predicted flow rate additionally does not separate the porosity of the concrete, although some airflow through the solid concrete material was observed during the experiments.

From the previous benchmark report, an estimated length of through cracks was measured and the experimental flow rate of 0.18 m^3/hr/meter of crack was multiplied by this length in order to determine the predicted flow rates. Additionally, although it is assumed that no new cracks form due to loading, flow rates are expected to increase due to residual deformation. Between VeRCoRs pressure tests Pre-op and VC1, a 23% increase in global leakage was observed. The large increase in flow rate is understandable for the first loading. Of interest, however, is how the leakage varies during pressure tests after the initial test, VC1. From the experiments at the University of Toronto, it is expected that a 13% increase in flow will occur for the same deformation if the specimen is loaded in cycles, as the VeRCoRs specimen is. For a cyclically loaded specimen at the University of Toronto, increases in flow rate for corresponding deformations and pressures ranged from 10% to 16%.

Predicted results

Table 3 provides a summary of the theoretical crack lengths and predicted initial flow rates. Subsequent flow rate predictions are found in Table 4, and are calculated under the assumption that repeated loading will induce a 13% increase in flow rate. All flow rates given are for the pressure at 4.2 bar relative to atmospheric pressure.

Table 3.Theoretical crack values and predicted flow rates

Area	Flow Rate (Nm^3/hr/meter of crack)	Theoretical Crack Length (m)	Predicted Flow Rate (Nm^3/hr)
Gusset	0.18	21.7	3.9
Hatch	0.18	6.1	1.1
Cylinder	0.18	10.0	1.8
Dome	0.14	1.5	0.2

Table 4.Predicted flow rates (Nm^3/hr) due to repeated pressurization

Area	VD1	VD1bis	VD2
gusset	3.9	4.4	5
hatch area	1.1	1.2	1.4
cylindrical part (wall)	1.8	2	2.3
dome	0.2	0.23	0.26

Experimental procedures

Laboratory experiments were performed at the University of Toronto in order to further investigate the flow of air through cracks. A scaled-down and simplified containment structure was fabricated and tested. Previous research has investigated air flow through flat walls or concrete panels. These experiments were developed to better represent the behavior of a hollow containment vessel that is pressurized internally. This allows for a reduction in uncertainty at the boundary of cracks and the possibility of air flowing out the sides of concrete panels.

Two concrete specimens were cast with a nominal height of 750 mm and wall thickness of 75 mm. The inner and outer diameters of the circular sections were 315 mm and 504 mm, respectively. Both specimens were reinforced with 16 longitudinal steel bars. One specimen was reinforced with 10M rebar and the other with threaded rod of similar diameter.

The testing protocol involved loading the specimen in tension via the reinforcement in set increments of displacement after first cracking. At each load stage, the internal pressure was increased in 0.137 bar increments up to 1.03 bar or up to the capacity of the flow meters. Time was allowed for the flow rate to stabilize before the flow was measured. It was assumed that the total flow into the specimen would equal the total flow out of the specimen.

Sample loading sequences and displacements can be seen in Figure 2. Cracks were measured individually, however, LVDT measurements were taken over the height of the specimen in four locations. The measured LVDT displacements indicate more clearly the deformation of the entire specimen and allow for a nearer calculation to the actual average crack width.

The two concrete specimens exhibited similar results. The specimens showed significant cracking, up to 4 meters in total length for one specimen. A view of a specimen in the loading configuration is shown in Figure 3(a). The relationship between crack width and leakage rate for specimen 2 can be observed in Figure 3(b). The mean crack width was found by averaging the LVDT displacements over the number of cracks observed at the particular load stage.
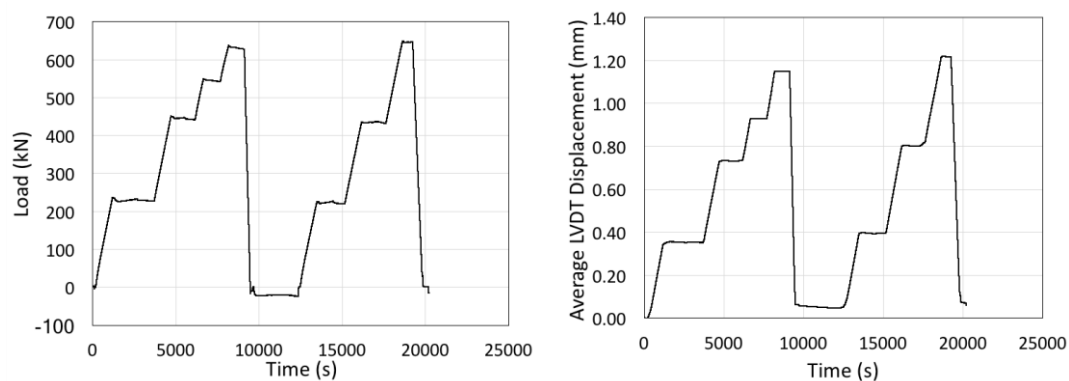

Figure 2. Load and displacement history
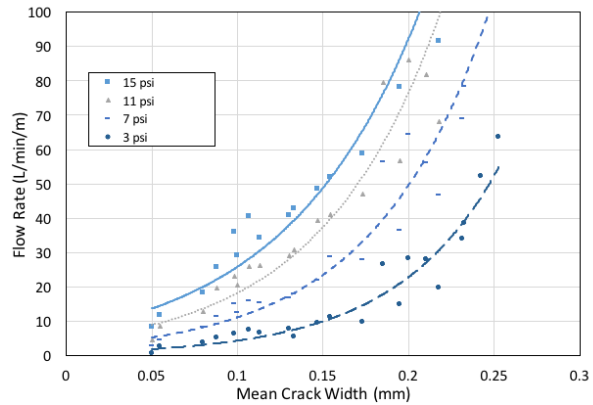
| (a) Test specimen | (b) Test results |

Figure 3. Leak rate test

CONCLUSION

This study presented the analysis methods for Theme-2 and Theme-3 of the VeRCoRs benchmark. The analysis results show that the numerical model for Theme-2 can accurately capture the strain changes of the perimeter wall due to internal pressure increase. However, the influence of the time-dependent parameters such as concrete creep and shrinkage cannot be fully captured mainly due to the limitation in current MC2010 and ACI 209R-08 shrinkage models. For Theme-3, experimental tests were performed at the University of Toronto in order to characterize leakage of air through cracks in pressurized containment structures. Data from these tests was used with information from previous VeRCoRs Benchmark results to make a prediction for leakage rates measured during pressurization tests VD1, VD1bis, and VD2. Calculated flow rates normalized by crack length agree moderately well with results from pressurization test VC1.

REFERENCES

[1]   Huang, X., Kwon, O.-S., Bentz, E., and Tcherner, J., 2017, "Evaluation of CANDU NPP Containment Structure Subjected to Aging and Internal Pressure Increase," Nucl. Eng. Des., **314**, pp. 82–92.

[2]   Huang, X., Kwon, O.-S., and Bentz, E., 2016, "Prediction of Shrinkage and Creep Strains of the VeRCoRs Benchmark Reactor Containment Structure," *The Benchmark Workshop: Modeling the Behaviour of the VeRCoRs Mockup*, Renardières, France.

[3]   CEB-FIP, 1978, *Model Code for Concrete Structures: CEB-FIP Recommendations*, Paris.

[4]   Fédération Internationale du Béton, 2013, *Fib Model Code for Concrete Structures 2010*.

[5]   ACI Committee 209, ed., 2008, *Guide for Modeling and Calculating Shrinkage and Creep in Hardened Concrete*, American Concrete Institute, Detroit.

[6]   Dury, J., 2018, "Analyzing the Long-Term Performance of Concrete in Containment Structures: Shrinkage and Leakage," University of Toronto, Canada.

[7]   Rizkalla, S. H., Lau, B. L., and Simmonds, S. H., 1984, "Air Leakage Characteristics in Reinforced Concrete," J. Struct. Eng., **110**(5), pp. 1149–1162.
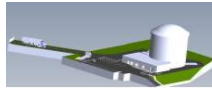
Development of a numerical model for studying the leakage tight-ness evolution of VeRCoRs experimental containment vessel under aging effect

M. Mozayan Kharazi[1], N. Goujard[1,2]

[1]INGEROP, Rueil Malmaison, France, e-mail: mahsa.mozayan@ingerop.com
[2]MINES ParisTech, Paris, France, e-mail: nicolas.goujard@ingerop.com

ABSTRACT

The purpose of this paper is to present the improvements brought to the thermo-hydro-mechanical model of the pre-stressed concrete pressure containment vessel mockup VeRCoRs, since last EDF benchmark in 2015 [5]. The thermos-hydro-mechanical calculation has been refined to take into account the in situ measures. A Truncated Newton Algorithm is implemented to fit creep parameters. The early age behavior of the concrete vessel is taken into account by considering the macro cracks appeared during the first months of the mockup and integrating them as initial state, which improved the flow calculation results. Finally, numerical improvements are made on the flow calculation to increase its stability. The new developments integrated into this work remain adapted to the study of full size engineering applications, and more specifically nuclear power plant reactor buildings.

Geometry and mesh

The VeRCoRs PCCV is composed by a pre-stressed concrete vessel of 20.79 m height. The inner radius of the cylinder part is 7.3 m. The thickness of the cylinder wall is 0.4 m. The containment vessel has several openings. The entire containment vessel is pre-stressed with 295 tendons running in two perpendicular directions: horizontal and vertical. The full 3D containment vessel is considered in the finite element model. The concrete part is modeled with 3D solid elements (linear shape function). The pre-stressing tendons are modeled by truss elements. The reinforcement rebar is not considered directly in the finite element model. However it should be mentioned that the influence of the reinforcement bars is taken into account using a simplified approach based on Eurocode cracking formulations and Hillerburg homogenization method [4].

In order to refine the model, the first step was to create more mesh groups in order to be able to impose the appropriate loadings and boundary conditions to each group. For each of the 17 concrete sections was created a group of volume meshes (figure 1), and a group of 2D meshes for its inner and outer surfaces. Were also added groups of volume meshes for areas with a different porosity and permeability from the rest of the concrete wall:

- for lift joints, between two concrete levels,
- for tendons ducts neighborhood.

a – the 17 concrete levels   **b – concrete meshes with vertical tendons**
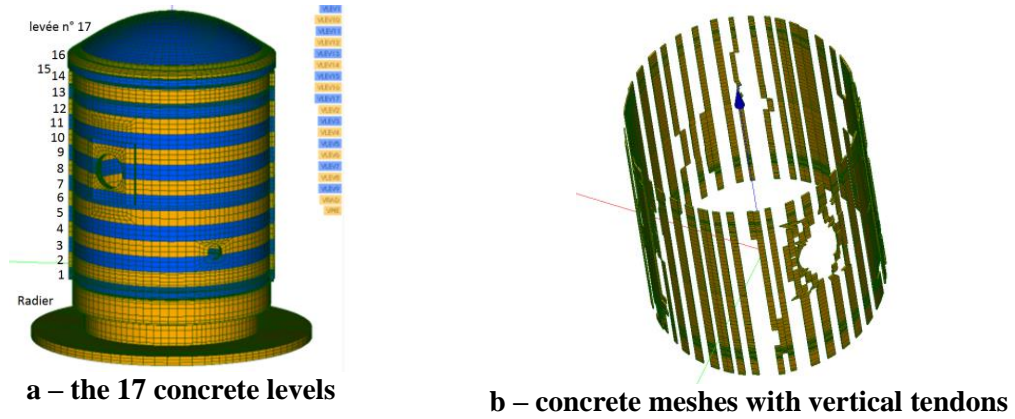
Figure 1 - Mesh refinement examples

Mechanical loading

The mechanical loads applying to the vessel are body weight, pre-stressing and the integrity test pressure gradient. The initial pre-stressing tension in the tendons is 0.827 MN. An atmospheric pressure (0.1 MPa) is applied to the outer surface of the vessel during all its lifetime. On a standard reactor containment building, integrity test are made every decade. As VeRCoRs is at scale 1/3, areas are 1/9 of standard areas, and so the moisture flow is 9 times quicker: integrity tests are made each year, during which the inner of the vessel is inflated to 5.2 bars.

The vertical and the horizontal displacements of the vessel are constrained at the bottom surface of the basement.

Thermal and drying calculations

For the thermal calculation, thanks to the precise monitoring of the mock up, detailed boundary conditions are applied. First, by observing thermal evolution on the sensors, we selected thermal instants representative of all important temperature changes. Then, for the inner and outer surfaces of each concrete level, we took the average of all the corresponding sensors to define the boundary condition to apply. For instance, on figure 2, one can observe a gap of the inner temperature due to a stop of the heating system.
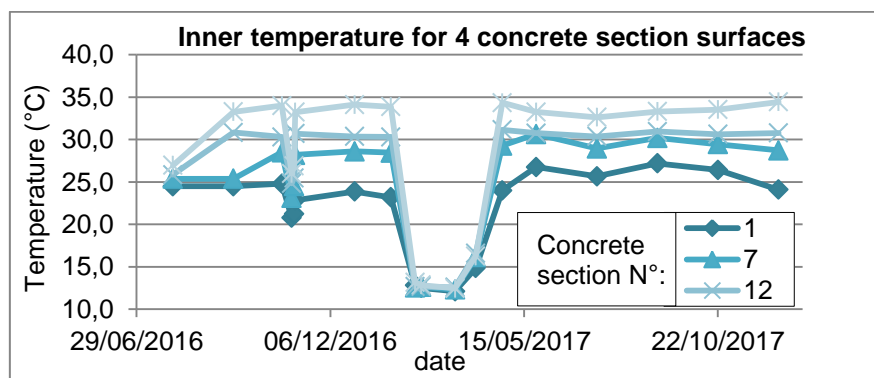
Figure 2 – Thermal boundary condition study

As expected, inner temperature is higher for upper concrete levels, with up to 10 degrees of difference between the top and the bottom of the vessel. This temperature refinement allows getting a more precise temperature evolution in the concrete (figure 3), which will then let us to obtain a more realistic thermal strain and thus better model the mechanical state of the structure.

| a – before temperature refinement | b – after temperature refinement |
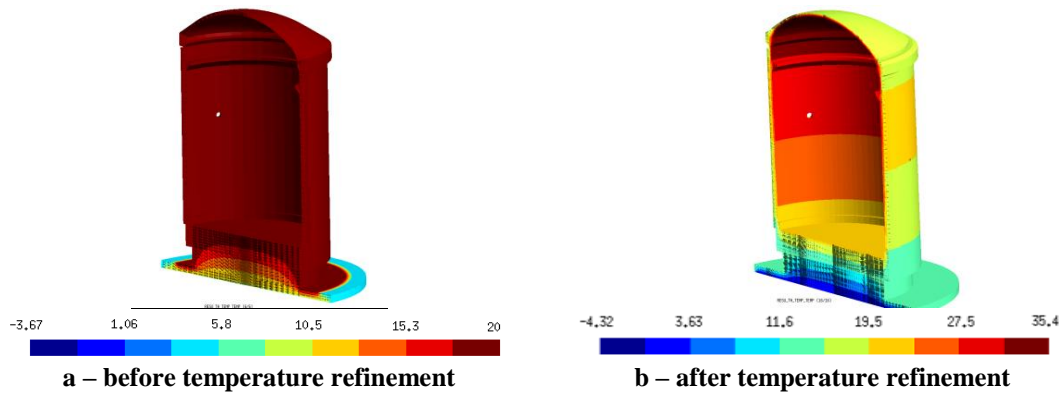
Figure 3 - Temperature results

For the drying calculation, there are less hygrometry sensors than thermal ones on the mock up, so the refinement is a bit less exhaustive. As boundary condition, the surface water concentration was imposed; we use the model of Granger [2] for the drying calculation. As expected, the surfaces of the vessel wall dry much more than its core (figure 4).

| t = 0 | t = 500 days | t = 1000 days |
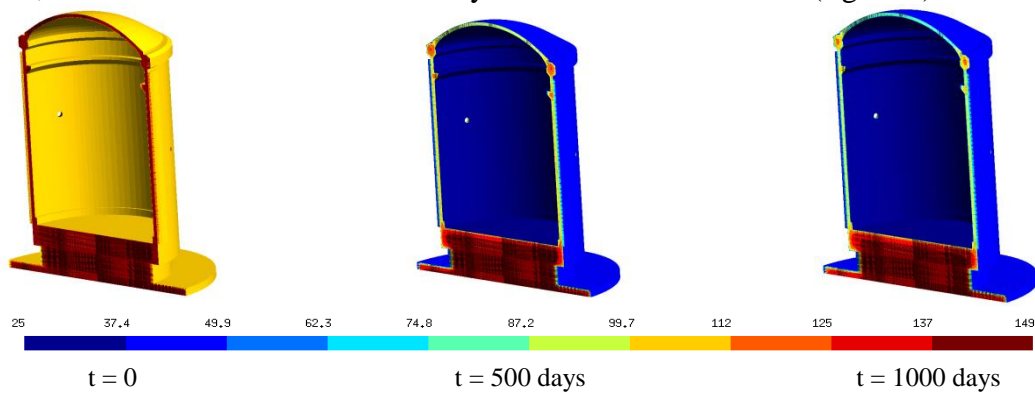
Figure 4 – water concentration evolution

Mechanical calculations

As for the temperature, mechanical parameters such as Young modulus and Poisson coefficient are refined for each concrete level, thanks to the samples taken during the construction of the building.

To get a model as accurate as possible, the pre-stressing is divided into three time steps, following the given pre-stressing sequence (figure 5). This allows a more correct loading history, which better model the mechanical state of the vessel. Moreover it is necessary to ensure an efficient creep-parameters fitting.

| a – before pre-stressing | b – after vertical pre-stressing | c – after bottom-half horizontal pre-stressing | d – after complete pre-stressing |
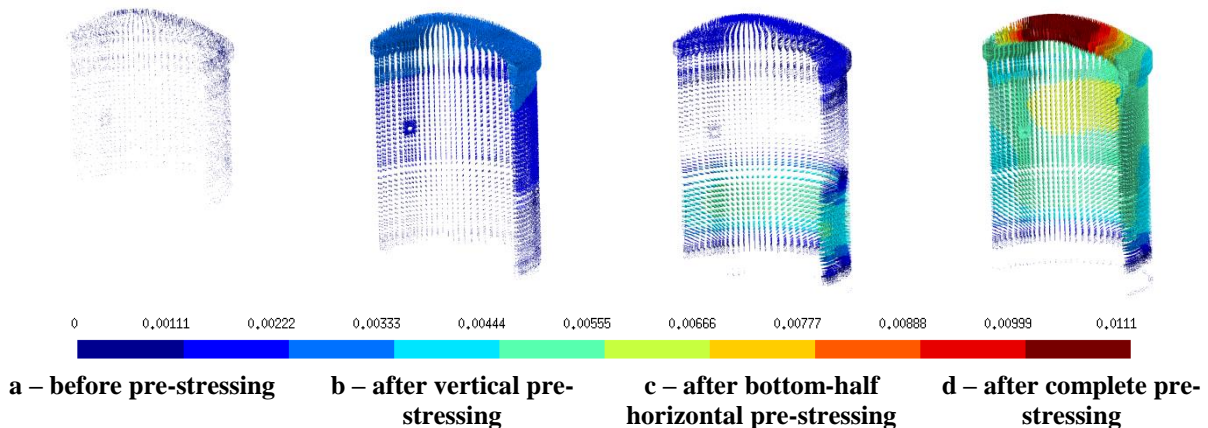
Figure 5 - Displacement evolution during pre-stressing phases

Creep parameters fitting

Creep models are based on many parameters (seven for UMLV model [1]) which describe the model's creep behavior under time dependent loadings. In order to get the parameters values the most representative of the VeRCoRs building; we used a minimization algorithm (the Truncated Newton Algorithm) to fit the parameters so that numerical strains are as close as possible from the experimental strains, and so solve the inverse problem. To guarantee realistic results, the optimization was bound-constraints, by values issued from existing nuclear plants [1], with margin factors.

To proceed, we use a multi scale fitting approach (figure 6). After a first global calculation of the thermo-hydro-mechanical state of the model, we carry out a scale reduction by isolating the thermo-hydric results and the mechanical boundary conditions for selected nodes. Then, we use that reduced model at any iteration, changing only the creep parameters, to compute the calculated strains and compare them to the measured one. The fitting would not be possible without this multi-scale approach, as the global model is too big to be computed at any iteration.

$$\varepsilon_{measured} = \begin{pmatrix} \varepsilon_{meas}(inst_1) \\ ... \\ \varepsilon_{meas}(inst_n) \end{pmatrix}$$
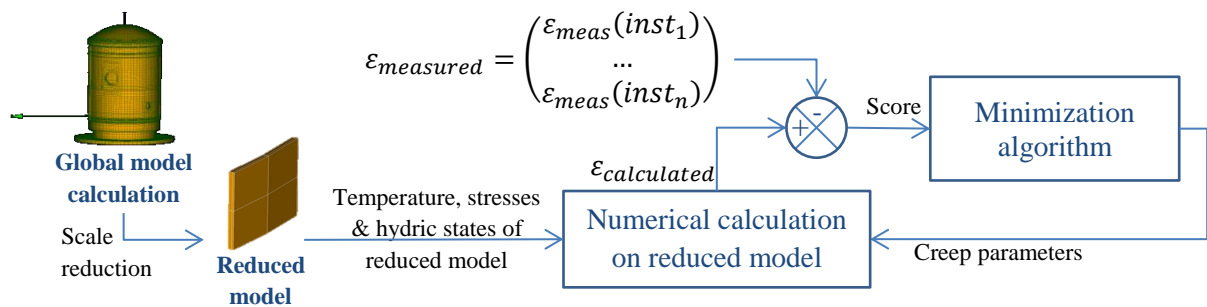
Figure 6 - Creep parameters fitting algorithm

After having applied the algorithm, one can make sure that numerical strains are closed to experimental for long term behavior of the vessel (after 600 days) as well as short term behavior of it (during the pressure test), and so that the creep parameters obtained are representative of the mock up behavior (figure 7).
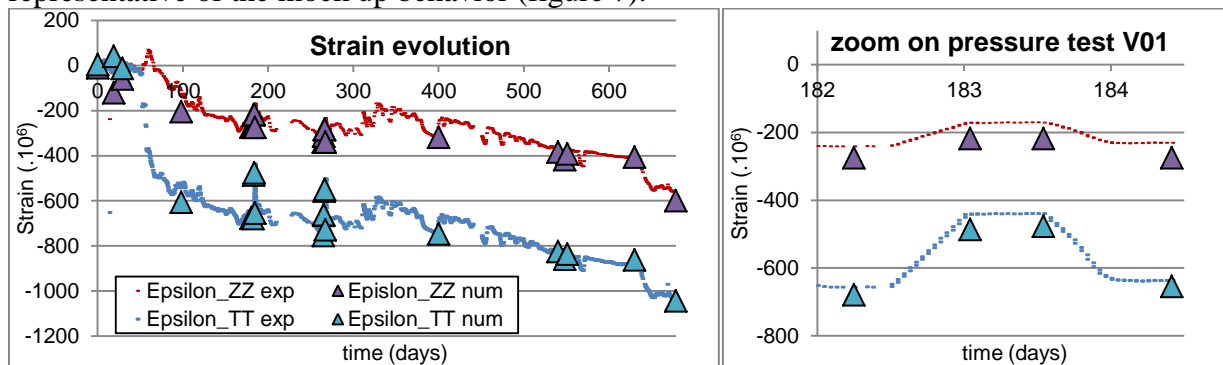
Figure 7 - Strain evolution after numerical fitting algorithm

Damage and crack opening post processing calculation

We choose not to model the early-age behavior of the building so that our method is adapted to large scale calculation. Moreover, this modelling approach let us to have a flexible model which allows us to study the long term behavior of the power plant of nuclear park by integrating their actual state and visual inspections. So, we need to integrate to the model the initial macro cracks in order to get the real cracking state of the building, which is mandatory to get correct flow values.

The initial cracks in the vessel were selected by identifying the cracks from visual inspections which seemed to cross the wall (visual crack on the inner and outer surfaces), and which were leaking. From those identifications were determined the position, length, orientation and opening of those cracks. Then, groups of meshes containing those cracks were created and corresponding materials characteristics were added to the model (figure 8).
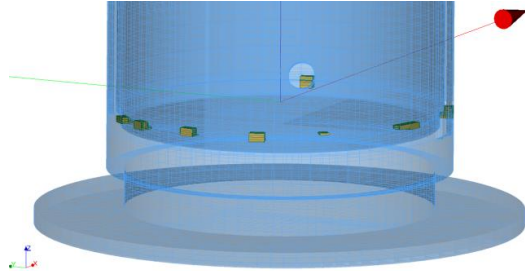
Figure 8 - Meshes containing initial cracks (in yellow)

The macro-crack calculation algorithm, based on Mazars' model [3], has to be rearranged, so that initial cracks are correctly added, and the crack opening updated at each time step. The new structure of the algorithm is represented on figure 9.
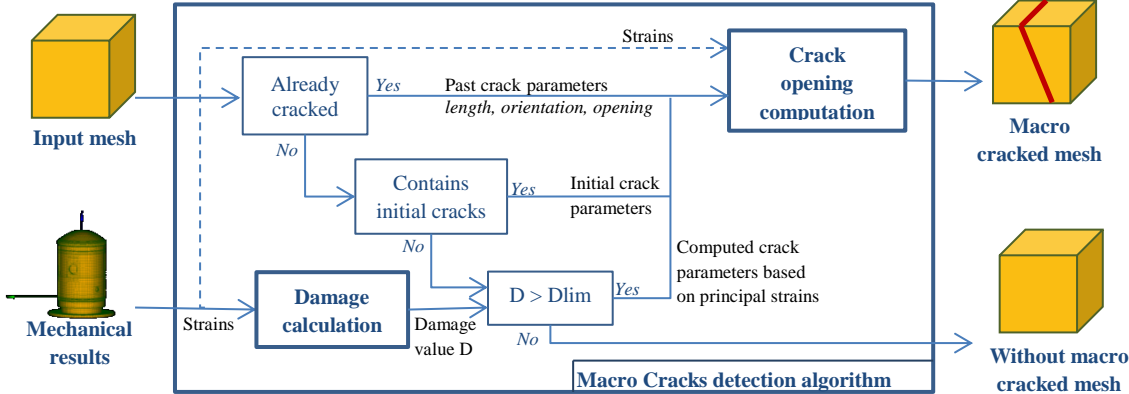
Figure 9 - Macro crack detection algorithm

Hydraulic calculation

The hydraulic calculation is also improved: the hydraulic parameters are calibrated for different zones and different concrete levels, and depend on the concrete damage state.
First, for each concrete level, the site porosity and permeability has been used. Then, for each early age crack, the flow coefficient is calibrated with the in situ measures, applying the inverse of the Poiseuille law. In the same way the permeability of lift joints are calibrated with the in situ measure. Finally, the hydraulic parameters of meshes containing pre-stressing tendons were adjusted.
Besides, as the hydraulic calculation computes the pressure, and then takes it gradient to get the flow. In order to be independent from mesh refinement in high gradient values area, we use quadratic elements for that calculation, which increases the calculation time but also the stability and the pertinence of the results.
Finally, all those improvements allows to get results closer to the one given on last benchmark report; on figure 10, we can notice that using these improvements in the model and taking into account the initial states and early age cracking, we have more realistic numerical results. The local flow through the vessel is represented on figure 11. As expected, the early age cracks and the inter-concrete sections leaking the most are recognizable.

Part	Experimental results		Numerical results before early age cracks integration		Numerical results after early age cracks integration	
	Values (Nm³/h)	Ratio /total	Values (Nm³/h)	Ratio /total	Values (Nm³/h)	Ratio /total
Gusset	2,439	32%	0.05	1%	2.68	37%
Total	7,62		4.2		7.19	

Figure 10 - Hydraulic calculation results

RESUHYDR_FLUX_NOEU_FLURR (2/2)

-1.49e-06 6.66e-06 1.48e-05 2.3e-05 3.11e-05 3.93e-05 4.74e-05 5.56e-05 6.37e-05 7.19e-05 8e-05
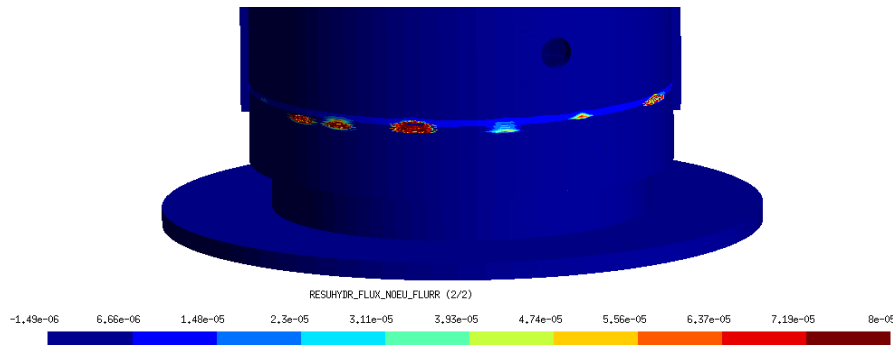
Figure 11 - Local flow on the vessel in the gusset part

REFERENCES

[1] Benboudjema, F., (2002), "Modélisation des déformations différées du béton sous sollicitations bi axiales. application aux enceintes de confinement de bâtiments réacteurs des centrales nucléaires," Ph.D thesis, UMLV, France.
[2] Granger, L. (1995)., "Comportement différé du béton dans les enceintes de centrales nucléaires: analyse et modélisation," Ph.D thesis, ENPC, France.
[3] Mazars, J. (1984)., "Application de la mécanique de l'endommagement au comportement non linéaire et à la rupture du béton de structure," Ph.D thesis, Université de Paris 6, France.
[4] Mozayan, M., (2013). "Une méthodologie de modélisation pour l'évaluation de l'étanchéité des enceintes de confinement des centrales nucléaires," PhD thesis, Ecole normale supérieure de Cachan, France.
[5] EDF website of VeRCoRs benchmark (https://fr.amiando.com/EDF-vercors-project.html?page=1320865)
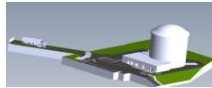
Structural Behaviour and Air Leakage Rate Prediction for VeRCoRs Mock-Up by 3-D Numerical Analysis

Yangsu Kwon [*], **Keun-Kyeong Kim** [†], **Myung-Sug Cho** [††] and **Hong-Pyo Lee** [†††]

[*] Korea Nuclear & Hydro Power, Central Research Institute (KHNP CRI), Daejeon, Republic of Korea, e-mail: yangsu.kwon@khnp.co.kr

[†] Korea Nuclear & Hydro Power, Central Research Institute (KHNP CRI), Daejeon, Republic of Korea, e-mail: kenk.kim@khnp.co.kr

[††] Korea Nuclear & Hydro Power, Central Research Institute (KHNP CRI), Daejeon, Republic of Korea, e-mail: mscho621@khnp.co.kr

[†††] Korea Nuclear & Hydro Power, Central Research Institute (KHNP CRI), Daejeon, Republic of Korea, e-mail: hongpyo.lee@khnp.co.kr

ABSTRACT

In this paper, a three-dimensional finite element analysis (3-D FEA) has been conducted for Theme 2 and 3 in VeRCoRs benchmark 2018. The static analysis and viscoelastic analysis were performed for each pressure test and waiting stages, respectively. The analysis input, including material properties, prestressing force and related conditions, was determined by provided data. With the analysis data and theorical calculation, the location, width, and length ware derived. And, finally, the leakage rate and main leakage path were determined. In the initial stage, the crack around the gusset (or connection between basemat and cylinder structure) seems to be the main cause of air leakage. After 5 pressure tests, however, the leakage through crack on equipment hatch area, increased more than other leakage paths.

Analysis model

The VeRCoRs containment (EDF's 1/3 scale prestressed concrete containment) consists of a prestressed concrete cylinder and a dome with several openings such as E/H and so on. The inner radius of the cylinder structure is 7.3m, thickness of wall is 0.4m and, the total height of containments including dome is 20.79m. Total number of 45,895 three-dimensional quadratic solid elements (named C3D20R in ABAQUS) are based on the numerical modeling of the containment from the dome to the basemat, and the passive reinforcements embedded in the concrete matrix are considered as a additional stiffness and strength calculated by Hsu[1] methods. On the other hand, the internal tendons are described by the truss element (named T3D2 in ABAQUS) maintaining the placing space and Fig. 1(b) shows the 3D finite element idealization of the VeRCoRs mock-up.

The material properties of concrete, reinforcing steel and tendon arethe same as those a VeRCoRs provided, and other not mentioned material properties are determined on the basis of the MC90[2]. Especially the relation corresponding to the interaction between tendon and concrete is constructed through the iteration procedure adopted to take into account the slip effect along the length. In Fig. 2, it can be found that there is a difference in the average stress-strain relations between hoop tendon and vertical tendon, and larger slip effect can be expected at the vertical tendon. More details related to the iteration procedure for the un-bonded internal tendons can be found elsewhere[3].

The modeling for time-dependent behaviors of concrete was applied as a viscoelastic material in ABAQUS[4] determined by Theme 1 results. Analysis procedure for each internal pressure tests applied as "static, general" option in ABAQUS. On the other hand, the "visco" option was applied for the long term waiting stage between each pressure test (see Table 1).

Table 1. Analysis step procedure

Step	Description	Day	Cumulative Date (Day)	Analysis Type (ABAQUS)
Step 1	End of prestressing	103	0 to 103	Static, General
Step 2	Waiting - 1	79	182	Visco
Step 3	1st Pressure test ('Pre-op')	2.417	184.417	Static, General
Step 4	Waiting - 2	80	264.417	Visco
Step 5	2nd Pressure test ('VC1')	2.417	266.834	Static, General
Step 6	Waiting - 3	471	737.834	Visco
Step 7	3rd Pressure test ('VD1')	2.417	740.251	Static, General
Step 9	4th Pressure test ('VD1 bis')	2.417	742.668	Static, General
Step 10	Waiting - 4	314	1056.668	Visco
Step 11	5th Pressure test ('VD2')	2.417	1059.085	Static, General
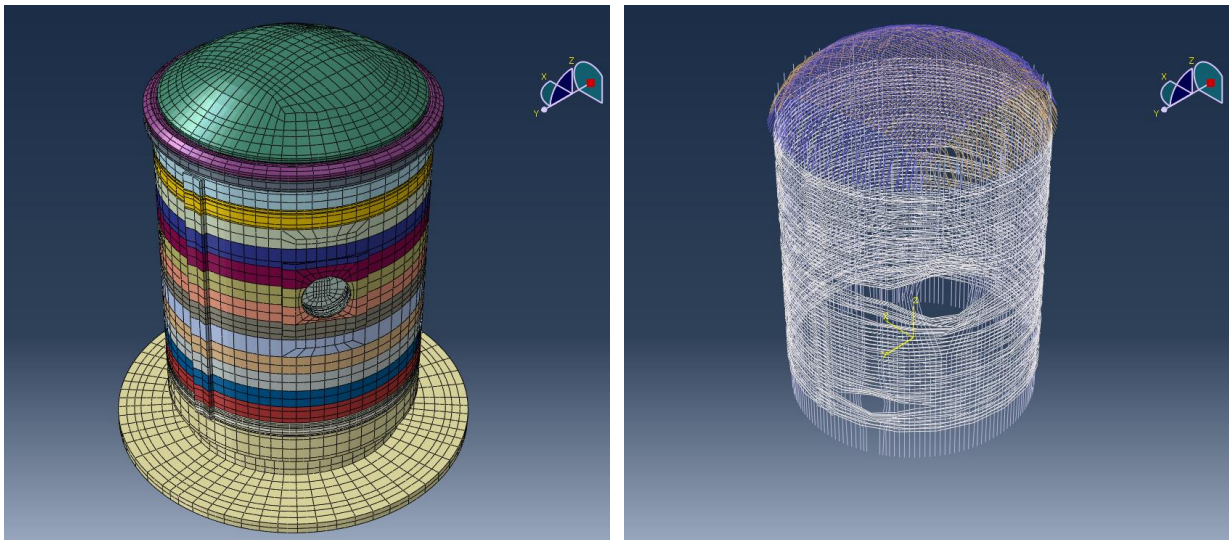
(a) Concrete (Lv. 17)   (b) Prestressing Tendon

Fig. 1. Finite Element Idealization of VeRCoRs Mock-up
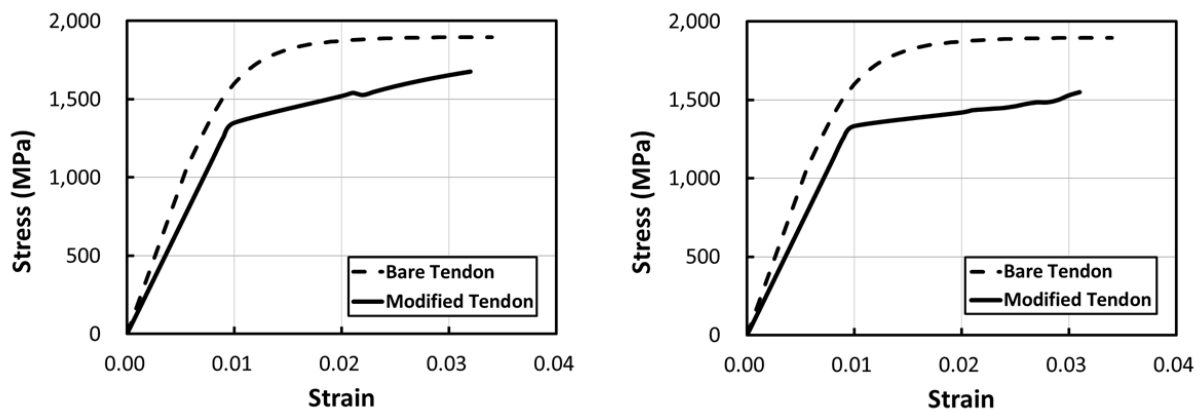
(a) Hoop tendon   (b) Vertical Tendon

Fig. 2. Modified stress-strain relationships of prestressing tendon[3]
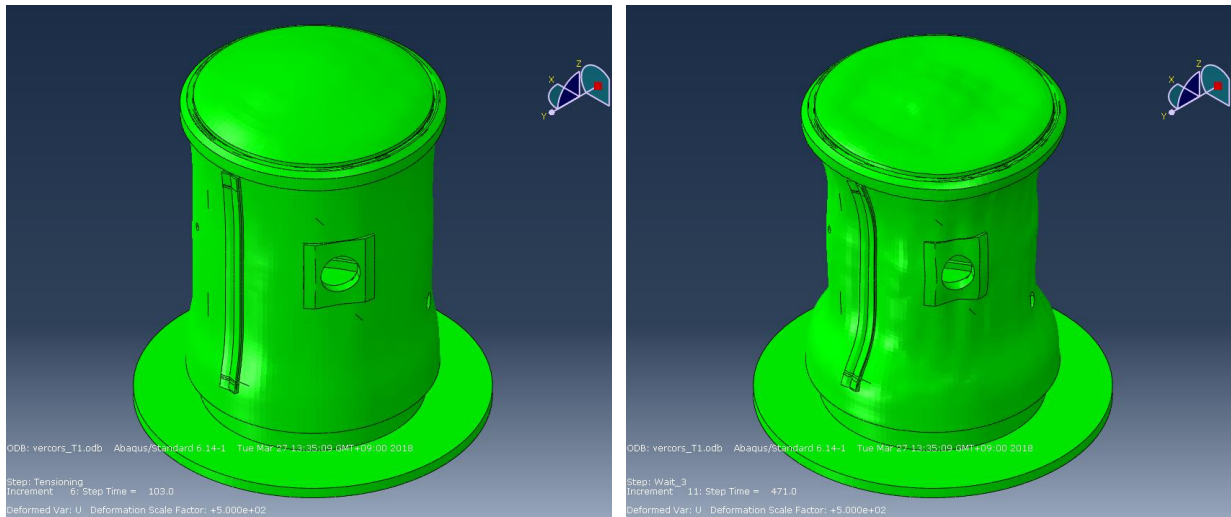
(a) after tensioning(construction finished)   (b) just before pressure test
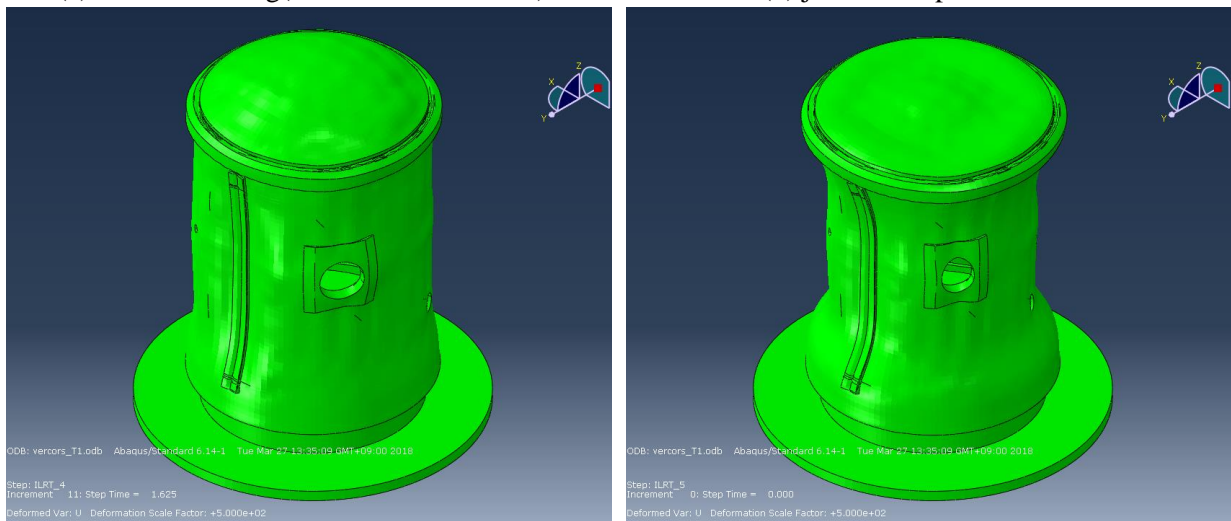
(a) Maximum pressure in pressure test   (b) Unloading

Fig. 3. Deformation shape of containments during pressure test(Scale : ×500)
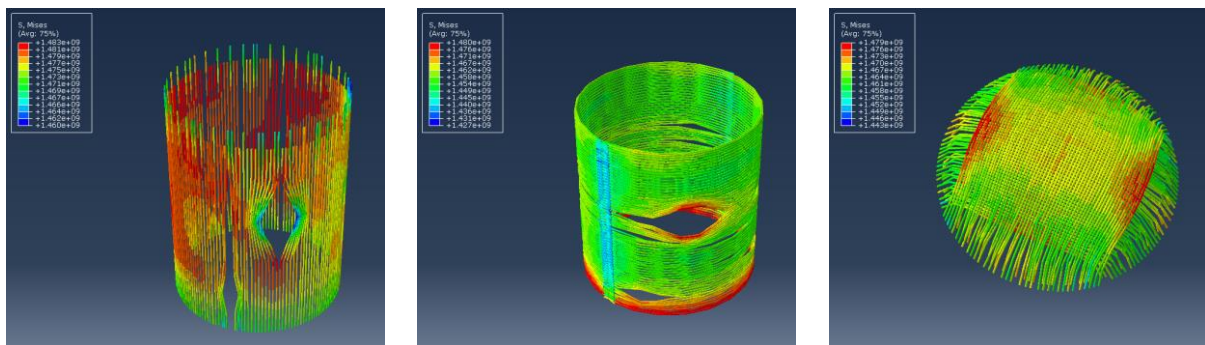
(a) Vertical tendon   (b) Horizontal tendon   (c) Dome tendon

Fig. 4. Mises stress distribution during pressure test(Scale : ×500)

Analysis results

The prediction of the leakage rate during each internal pressure test is based on the equation of Rizkalla et al. [5]. The crack width and length were calculated in each area (gusset, hatch area, cylinder wall, and dome) using the principle stress and strain. After 5 pressure tests, the leakage rate of final test would be two times higher than the initial test results. This is because there are more cracks around E/H, and the main leakage path would also be changed to this side from the gusset area.

Table 2. Results of leakage prediction

Step	Total (Nm³/h)	Leakage path(Nm³/h)			
		gusset	hatch area	cylindrical wall	dome
3rd Pressure test ('VD1')	12.3	7.845	1.012	3.283	0.16
4th Pressure test ('VD1 bis')	16.9	8.099	1.055	7.496	0.25
5th Pressure test ('VD2')	22.5	8.161	1.121	12.868	0.35
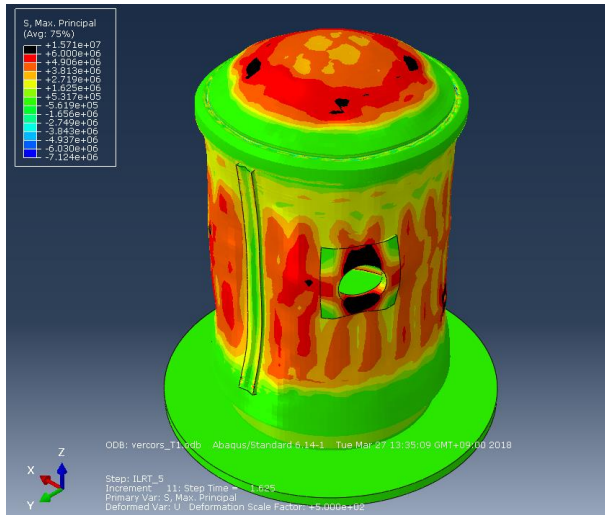
(a) Outer views of entire part
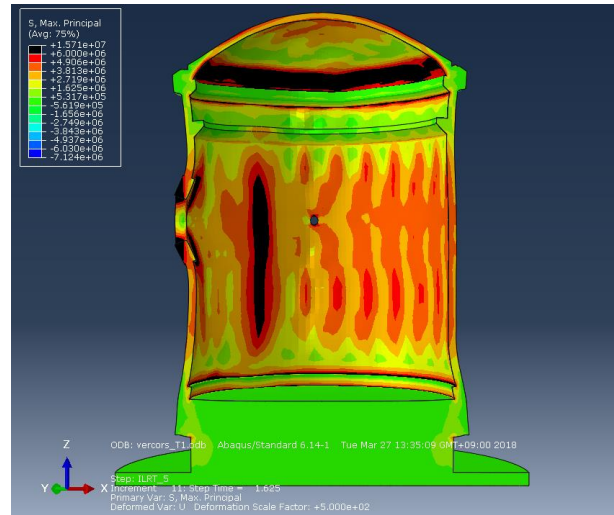
(b) Inner views of entire part
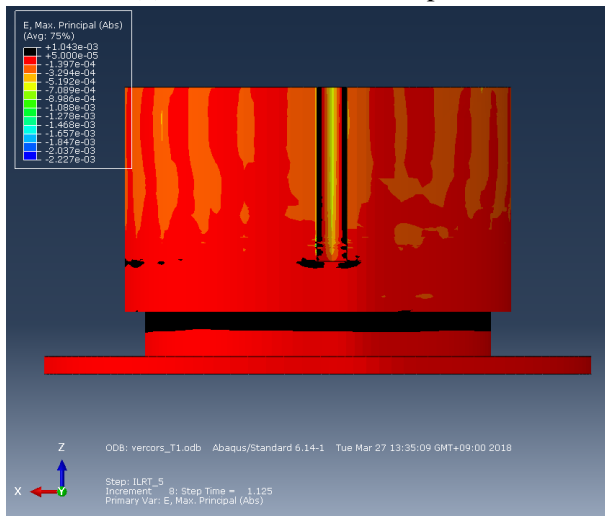
(c) Outer views of basemat and gusset
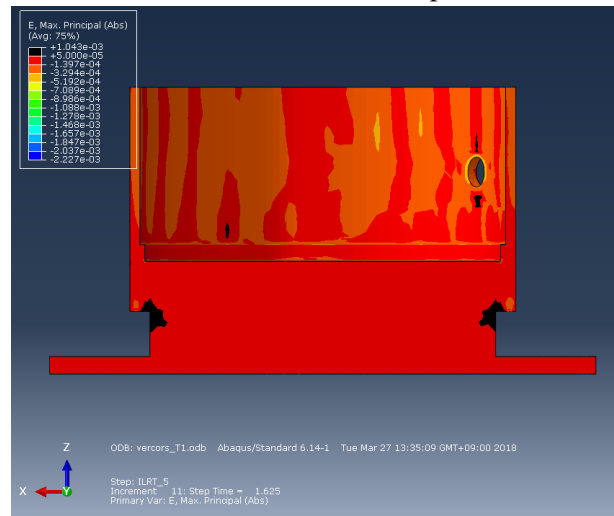
(d) Inner views of basemat and gusset

Fig. 5. Prediction of crack location; black area(Scale : ×500)

REFERENCES

[1] T.T.C Hsu, "Unified theory of reinforced concrete", Routledge (2017)
[2] CEB, "CEB-FIP Model Code 1990," CEB Bulletin d'Information No. 213/214, Comité Euro-International du Béton, Lausanne, Switzerland, 33-41(1993)
[3] H.-G. Kwak, and Y. Kwon, "Nonlinear analysis of containment Structure based on modified tendon model," *Annals of Nuclear Energy*, **92**, 113-126 (2016)
[4] *ABAQUS*, "ABAQUS *User Manual* 6-14", Dassault Systèmes(2013)
[5] S. M. Rizkalla, B. L. Lau and S. H. Simmonds, "Air leakage characteristics in reinforced concrete," *Journal of Structural Engineering*, **10**, 1149-1162 (1984)

Study of the containment history of the VeRCoRs mock-up and prediction of the leakage rate under pressurization tests

Thibaud Thénint[†*], **Véronique Le Corvec**[†] **and Shahrokh Ghavamian**[†]

[†] SIXENSE NECS
196, rue Houdan, 92330 Sceaux, France
{thibaud.thenint, veronique.lecorvec, shahrokh.ghavamian}@necs.fr

ABSTRACT

Our experience on leakage tightness behaviour of pressure containment vessel without steel liner is that prediction of its future capacity to withstand an internal pressure event requires a certain level of knowledge of its construction and the aging process. Considering the complexity of the construction and the numerous physical phenomena involved at the early age of concrete casting and its evolution over several decades of operation with periodic tests, the numerical modelling shall be based on simplifications, assumptions and calibrations.

As part of EDF's study program for the safety and life extension of its Nuclear Power Plants fleet, an experimental mock-up of a reactor containment building at 1/3 scale has been built at "EDF Lab Les Renardières". The construction has been completed at the end of 2015. Because of the scaling effects the drying effects on the mock-up are about 9 times faster than in a full scale containment vessel. The mock up's behaviour is monitored from the beginning of the construction. More than 700 captors and 2 km of optic fibre cables have been positioned in the concrete, both on the steel reinforcement and prestressing cables. Since the concrete pouring and for the duration of the research program extensive data are collected.

Hundreds of samples have been prepared and tested in order to determine their material behaviours and parameters, and especially: hydration, elastic properties, drying, creep (basic and drying) and permeability. The experimental campaign consists of a daily measurement of the whole sensors and in a periodic air pressure test of the mock-up every year. During this test, the containment is pressurized at 5,2 bar absolute.

This paper presents the approach developed at NECS to study the VeRCoRS mock-up for themes 2 (containment history) and 3 (leakage prediction) of the VeRCoRS 2018 benchmark. Some notable improvements in the methodology have been implemented compared to previous works ([1], [2] and [3]).The behaviour of the containment building is modelled since its concreting followed by the prestressing cables tensioning and the 5 pressurization tests (PreOp, VC1, VD1, VD1bis and VD2). All numerical analyses are carried out with an in-house version of Code_Aster software edited by EDF [4].

Methodology of the leakage prediction

Leakage rate prediction is made by solving five chained problems: thermal state, hydric state, mechanical state, crack state, hydraulic state. An effort has been made to model each phenomenon with state of the art models; some notable improvements are taken into account compared to previous works ([1], [2] and [3]):

- drying shrinkage is proportional to the relative humidity and not to the water saturation,

- creep model is inspired by Burger Ageing behaviour, as described in (EDF [5] and Benboudjema [6]): temperature, water saturation and age of the concrete modify creep rate,

- concrete cracking is modelled in the mechanical constitutive law (and no more computed *a posteriori* from linear elastic computations): cracks open and close following the pressure conditions, creep and prestressing losses, damaged concrete lead to force redistribution, constitutive law is orthotropic,

- some cracks can be introduced in the initial state, to deal with cracks observed *in situ* and not reproduced in our numerical simulations (no early age behaviour),

- leakage rate is now deduced from an orthotropic gas flow, computed from all the information given by the non-linear constitutive law.
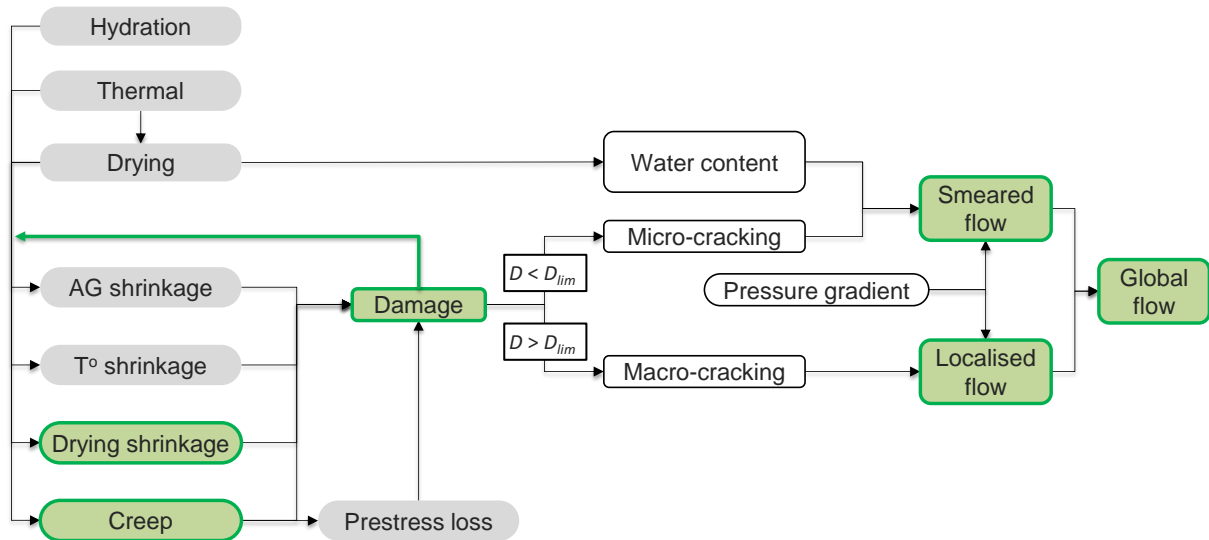
Figure 1.   Steps of leakage rate prediction (green steps have been improved)

FE model

The hydro-thermal model is calculated based on linear volume elements with a mass lumped modelling. This model allows calculating the temperature, the hydration and the drying. The hydration is taken into consideration only by the heat provided. Indeed, the mechanical properties are independent of this magnitude because the concrete is supposed to be perfectly hydrated when it is demoulded.

The mechanical model is calculated with linear volume elements. For the purposes of this study, the mesh is discretized with a variable size element in the thickness of the cylindrical wall. The mechanical model depends on the temperature and drying fields via thermal expansion and long-term strains (shrinkage, creep). Creep and cracking are taken into account.

The prestressing tendons are composed of class 1860 MPa strands. Each tendon was tensioned at 1488 MPa at active extremities before anchorage slip, as in full scale structures. They are modelled as truss elements and are perfectly bounded with the surrounding concrete.

Reinforcement is introduced in the numerical model as unidirectional shell elements, perfectly bounded with the surrounding concrete.

The concrete parameters are supposed to be equal in all the structure and equal to the mean property of all lifts following properties given by EDF.

10 initial cracks are introduced in the model: internal variables of the constitutive law are initialised to represent closed cracks with a (past) crack opening of 0.1 mm. These cracks are vertical and localised in the gusset.
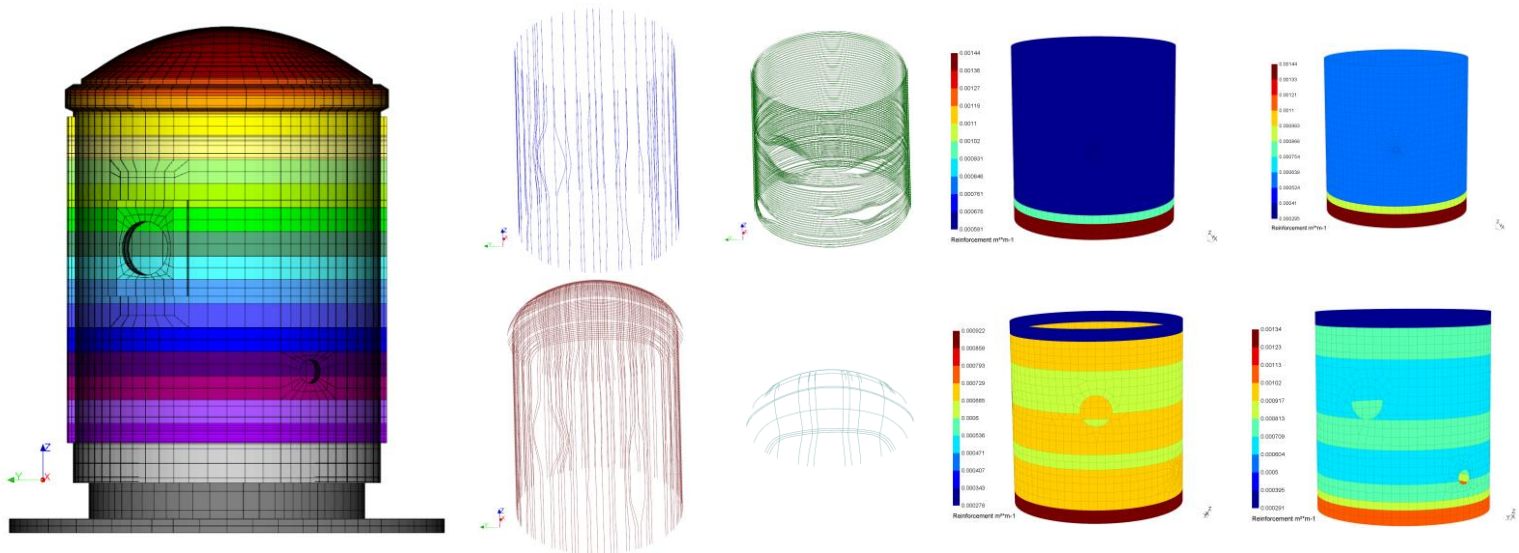
Figure 2.   Views of the numerical model: concrete, prestressing cables and reinforcements

Updating of parameters

Material properties are updated following experimental results on concrete specimens given by EDF (5478-F1, 5478-F3, 5478-F4 and 5478-F7). The implemented models (water loss, drying shrinkage, creep, drying creep), with updated parameters, lead to numerical results in very good agreement with experimental measures (Figure 3). Long term behaviour of concrete is thus simulated with a very satisfactory precision.
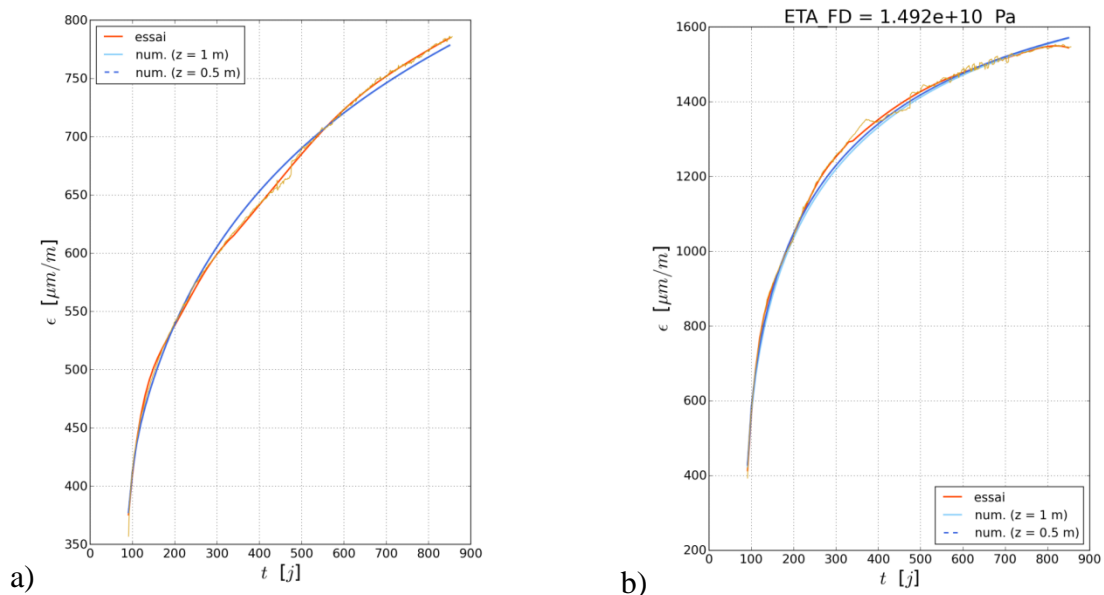
Figure 3.   Comparison of experimental (orange) and numerical (blue) results
a) creep strain, b) total creep strain

Numerical results

The first computed quantities are temperature and water concentration (Figure 4). As long as the external shell is open, there is no variation of these quantities in the thickness of the inner wall; the retained hypothesis for water concentration implying no activation of the drying process. After 400 days, imposed water concentration on the inner and outer skins of the containment wall leads to a water saturation of the wall. After 620 days, atmosphere control is activated: temperature and water saturation are imposed to constant values on inner and outer skins, which leads to spatial gradients. Temperature water concentration evolutions have different characteristic speeds: temperature is constant since 800 days whereas drying process is not finished after 1 400 days (water concentration has not reached a stationary state).
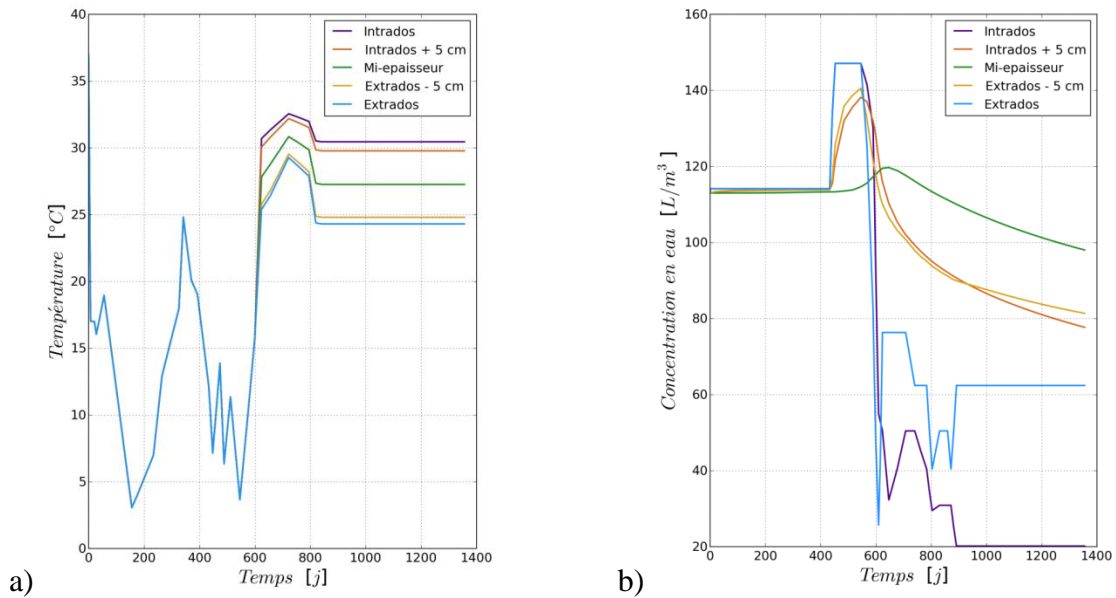
Figure 4.   Time history of temperature (a) and water concentration (b) for different points in the thickness of the cylindrical wall

Mechanical state is then computed, using temperature and water concentration results. Creep is activated as soon as prestressing is applied to the model, which leads to a smaller global stiffness of the mock-up as time goes by (see Figure 5). The magnitude of the displacement is coherent with previous analyses (NECS [3], for example). It is important to remark that concrete cracking is taken into account in this computation but that it does not seem to modify the global behaviour of the containment.
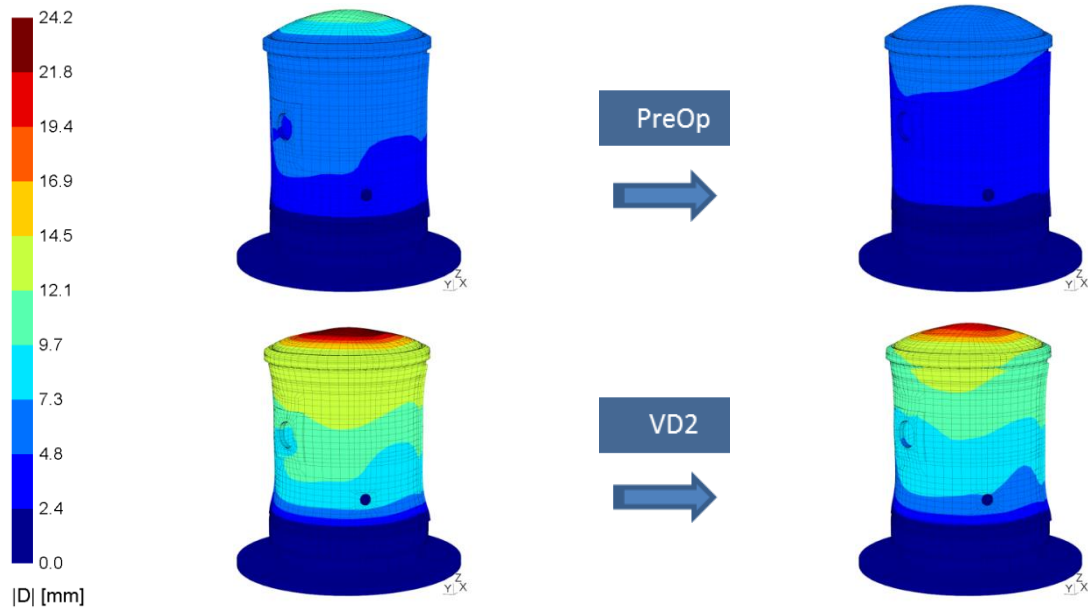
Figure 5.   Deformed shape before and at the end of pressure plateau: comparison of PreOp and VD2

VeRCoRs mock-up experimental strains have been given by EDF. Comparison of these measures with numerical results has been done on all the available points (see example in Figure 6). We can draw the following conclusions: global behaviour is similar between experimental mock-up and numerical model but spatial discrepancy is observed between numerical strains at exact sensor location and among surrounding points. This discrepancy is under investigation (mesh element size effect? proximity with a cable element?). On Figure 6, measure of the temperature at the location of the sensor is also shown (thin red curve). The comparison of total strain and temperature explains the decrease of total strains after 600 days: creep strain is cancelled by thermal expansion.
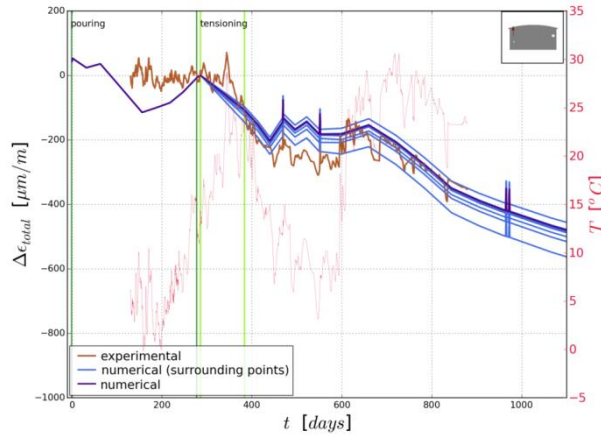
Figure 6.   Comparison of experimental (brown) and numerical (blue) total strains for one sensor

Cracking state obtained from the mechanical resolution (crack width, open/closed state) is post-processed to build a nonlinear orthotropic hydraulic model: pressure and gas flow are then computed. Total flow is shown in Figure 7 for inner and outer skin during PreOp and VD2. Maximal flow is respectively 1.9 Nm^3/h and 12.7 Nm^3/h. The kinetics and localisation of air flow give precious information. In VD2, contrary to PreOp, inner flow is equal to outer flow which is a consequence of crack opening (gas kinetics is instantaneous through cracks, not through sound or micro-damaged concrete). Moreover, the proportion of gas flow through the gusset is more important during VD2: open cracks seem to be localised in the gusset.
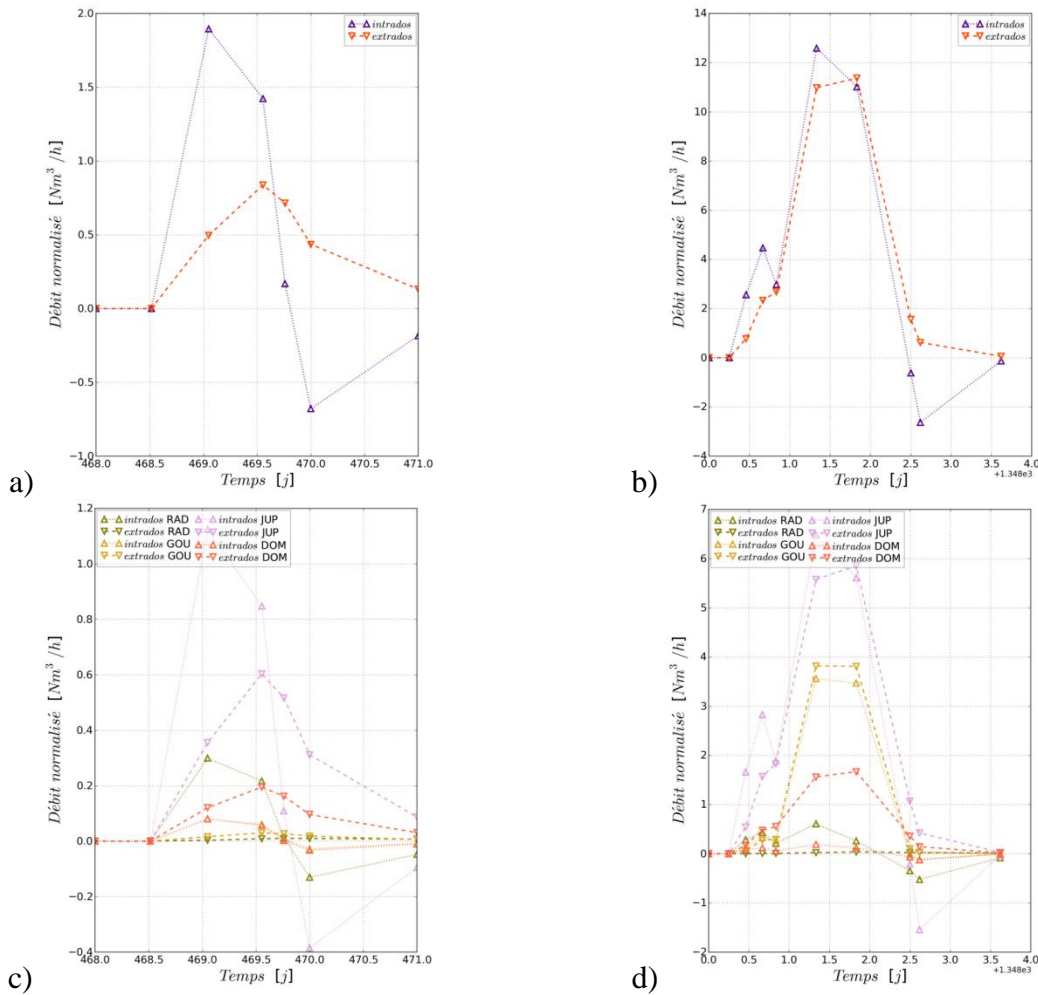
Figure 7.   Leakage rate during PreOp (a and c) and during VD2 (b and d)
Comparison of total flow (a and b)
Contribution of raft (RAD), gusset (GOU), wall (JUP) and dome (DOME) (c and d)

Local quantities of interest give additional information. Gas flow is shown in Figure 8 for VD2 and presents some very localised maximums: elements of the gusset where an initial crack has been introduced. If we look at the cracking state (blue: sound concrete, red: closed crack, green: open crack), we can identify through-wall cracks at the junction between raft and gusset (open crack from inner to outer skin).
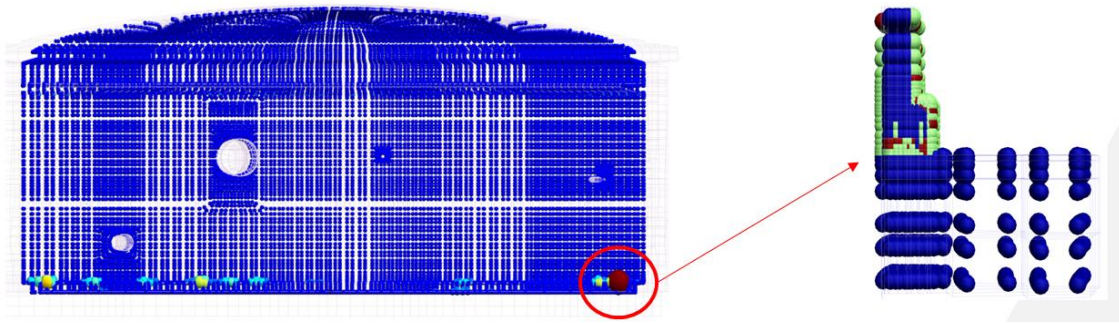
Figure 8.　Gaz flow (left) and cracking state (right) during VD2

Conclusions and perspectives

The implementation and updating of state of the art models in the five chained computations give very satisfactory results in the prediction of leakage rate. Global flow is in agreement with VeRCoRs measures. Adequate post-processing gives meaningful information to better understand mechanical state and its consequence on gas flow. Initial crack state is identified as a key parameter. Correlation between measures and numerical results (strains) is to be improved and better understood.

This work is being continued to finish validating the model and extract increasing knowledge from numerical simulations. As parameters are numerous (>50) and boundary conditions sometimes unknown, some sensitivity analyses are to be made (see example below): for example, initial cracking state and material parameters (tensile stress or desorption curve) may modify significantly global gas flow.

Global flow [Nm³/h]	Measure	No initial crack	Reference	Initial crack +	Max f_t	Min f_t	Measured desorption curve
PreOp	7.7	1.9	1.9	1.9	1.9	2.0	4.5
VC1	9.5	1.0	1.0	1.0	1.0	1.0	6.0
VD1	-	7.0	7.8	14.1	7.5	8.9	22
VD1bis	-	7.1	7.9	14.4	7.6	9.0	23
VD2	-	10.3	12.7	35	12.0	17	57

REFERENCES

[1] Masha Mozayan Kharazi, "Une méthodologie de modélisation pour l'évaluation de l'étanchéité des enceintes de confinement des centrales nucléaires", *PhD dissertation*, 2013

[2] T. Thénint, V. Le Corvec and S. Ghavamian, "Study of the containment history of the VeRCoRs mock-up and prediction of the leakage rate under pressurization tests", *Vercors Workshop 2015*

[3] T. Thénint *et al.*, "Evaluation of aging structural response and leakage rate of Vercors mock-up (2016), *3rd Conference on Technological Innovations in Nuclear Civil Engineering*, TINCE 2016, Paris

[4] *Code_Aster reference and utilisation documentation*: http://code-aster.org/doc/v12/en/

[5] "Relation de comportement BETON_BURGER_FP pour le fluage de béton". R7.01.35. Documentation de Code_Aster

[6] F. Benboudjema, "Contribution à l'analyse des déformations différées dans les matériaux cimentaires et de ses effets dans les ouvrages de Génie Civil", *Mémoire de l'obtention de l'habilitation à diriger des recherche*, ENS Cachan. 2012
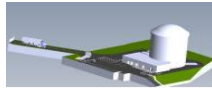
Finite element analysis of a pre-stressed mock-up reactor containment - the VeRCoRs 2018 benchmark case (Themes 2 and 3)

Kim M. Calonius[*]

[*]VTT Technical Research Centre of Finland Ltd, Finland, e-mail: kim.calonius@vtt.fi

ABSTRACT

The numerical analyses were successful in the sense that the models worked, simulations were completed, and the behaviour seemed realistic in general sense. The improved calculation model of the test containment created by VTT brought the results closer to both the experimental results. Compared to the test results, the model has globally less compression after the post-tensioning. The effect of pressurization is more evident in the test than in the calculations. VTT has initially overestimated the concrete cracking substantially. The new results do not directly indicate less amount of cracking, but with a closer examination of the FE results, it can be concluded that there might not be any cracks at all that extend through the whole thickness of the wall. In case the concrete is assumed highly saturated, the calculated permeable flow can be considered to match the experimentally measured one.

INTRODUCTION

As part of EDF's continuous effort on the safety and life extension of its Nuclear Power Plants, an experimental mock-up of a reactor containment building at 1/3 scale has been built near Paris (France) [1]. The main objectives of the project are to study the behaviour at early age, the evolution of the leak tightness under the effect of aging and the behaviour under severe accident conditions. VTT took part in the first international calculation benchmark called VeRCoRs 2015 and focused mainly on cracking and leakage under a test pressure of 0.52 MPa abs [2, 3].

This paper presents results of finite element analysis of the pre-stressed mock-up reactor containment mentioned above.

FINITE ELEMENT MODEL

The FE models presented VTT is three-dimensional (Figure 1). It uses shell elements for the concrete structure. The tendons are modelled with truss elements and the coupling to the concrete shell element model is performed using connector elements. The soft reinforcement is included as layers in the shell elements (not shear reinforcement).
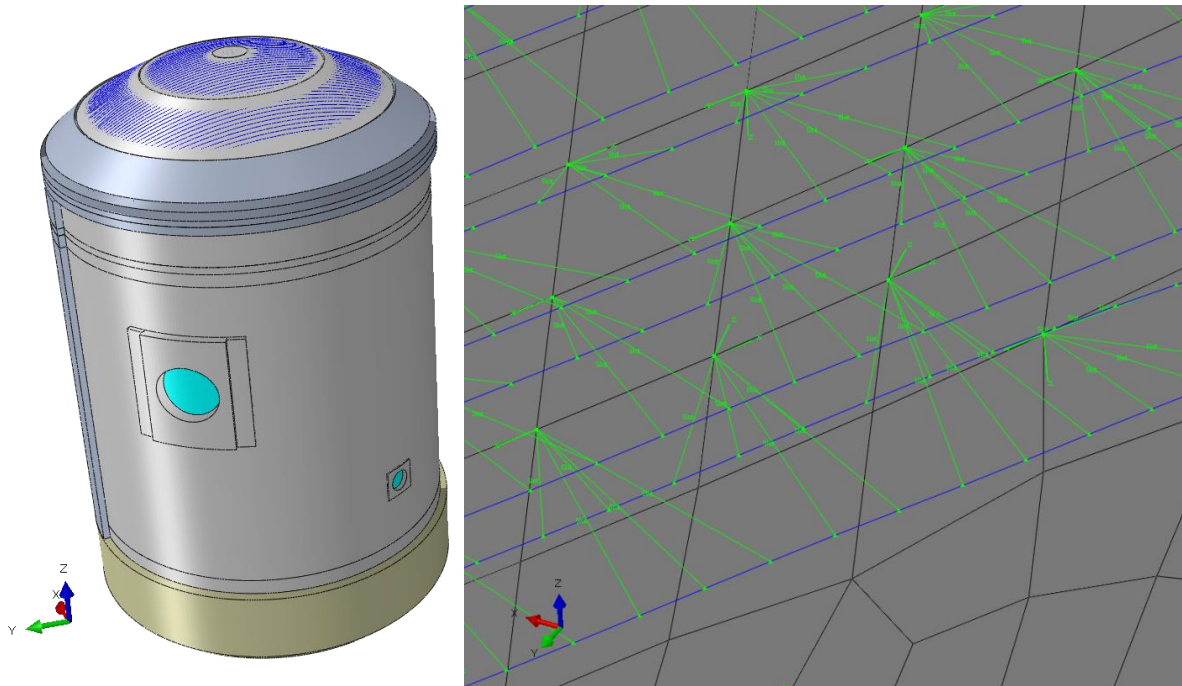
Figure 1. FE model and a detail on the right showing the connector elements in green colour.

The mean concrete Young's modulus is taken at the end of post-tensioning date as $E = 39\ 050$ MPa. The concrete in the VTT model is modelled using the Abaqus Concrete Damage Plasticity feature [4]. The analyses have been conducted using Abaqus code [4].

The loads in the VTT model are post-tensioning and pressurization. Time dependent loads are not yet included in the VTT model. The new analyses are reported in a separate research report [5]. The following improvements have been done to the previous model of VTT that was used for the benchmark calculations presented in the VeRCoRS workshop in March 2016:

- Interaction between the tendons and concrete has been modelled with connector elements.

- Prestressing has been modelled explicitly with connector elements.

- Wall thickness off-sets in the shell elements have been redefined.

- Material property values have been changed to better correspond with the real ones.

- The main penetrations have been modelled slightly more in detail. The shell element off-sets are modelled in more detail and the hatches have been modelled. In the previous model, inner pressure was not applied in the circular hole areas.

- The mechanical interaction in the junction between the cylinder and base slab has been modelled in more detail. However, the base slab is now model with shell elements while in the previous model it was modelled with solid elements.

STRAIN AND STRESS RESULTS

The VTT model is analysed nonlinearly with explicit time integration. Required results in the current benchmark are strain and stress at end of erection, end of post-tensioning and 0.52 MPa abs. pressure. Moreover, an estimate of crack properties in the inner containment was expected to be delivered. Some tendon strain results are shown in Figure 2.
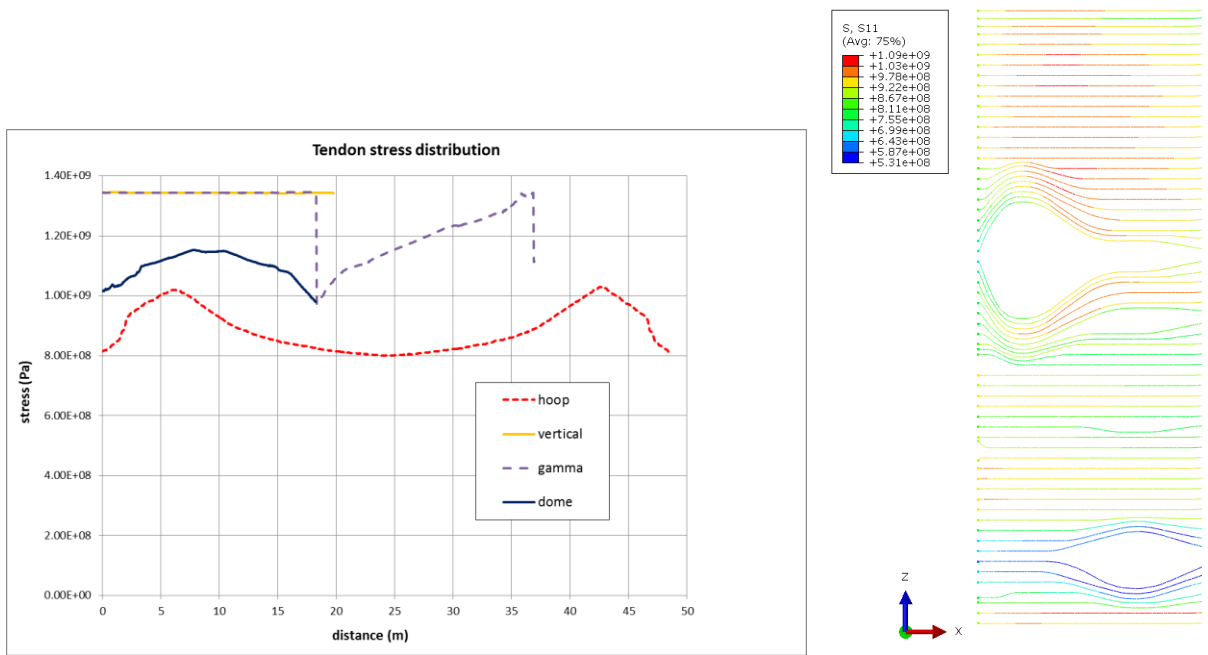
Figure 2. Tendon stresses in the FE model during overpressure in some selected general field tendons (left) and a distribution plot of tendon stresses (Pa) in a selected region.

Long term strains are calculated according to EC2 for the cylindrical wall with thickness of 400 mm. Due to small resources, this value is adopted to all the gauge positions. The long term effects have been added to the FE results after FE simulation. In the future, they will be included in the model for instance as a change of Young's modulus or with thermal expansion analogy. Dead weight is not taken into account. Since the strains are zeroed before the first pressure test, the results do not include the immediate strains due to tensioning, but only part of the long-term strains. The measured strains at the start of VD1 are surprisingly large in compression. Eurocode does not give that high compressive long-term strains. According to EC2, the creep and shrinkage at VD1 in the cylindrical wall are approx 100 microns, but the measured ones are over 300 microns in some locations.

Since the long term effects are not included in the FE model, the results are identical for both VD1 bis and VD2. The result is the difference in strains before the pressure application and during the test pressure. Principal stresses in the cylindrical wall during overpressure are shown in Figure 4. Strain results sent to EDF are shown in Figure 3.

Gusset			Cylindrical part (mid-height)			Equipm. hatch			DOME		
	F1IV	131		P1EV	66		M3EV	50		I1_194_EM	245
	FIIT	7		P1ET	132		M3ET	-29		I1_94_EM	180
	F2EV	-37		P2IV	56		M4IV	55		I2_194_IM	195
	F2ET	4		P2IT	145		M4IT	140		I2_94_IM	220
	G1IV	131		H1EV	48		M7EV	-32		J1EM	206
	G1IT	30		H1ET	139		M7ET	41		J1ET	91
	G2EV	-7		H2IV	60		M8IV	76		J2IM	76
	G2ET	31		H2IT	136		M8IT	162		J2IT	26
				H5EV	63						
				H5ET	156						
				H6IV	61						
				H6IT	116						

Figure 3. Strain results sent to EDF (same results for both VD1 bis and VD2).

inner surface	mid-plane	outer surface
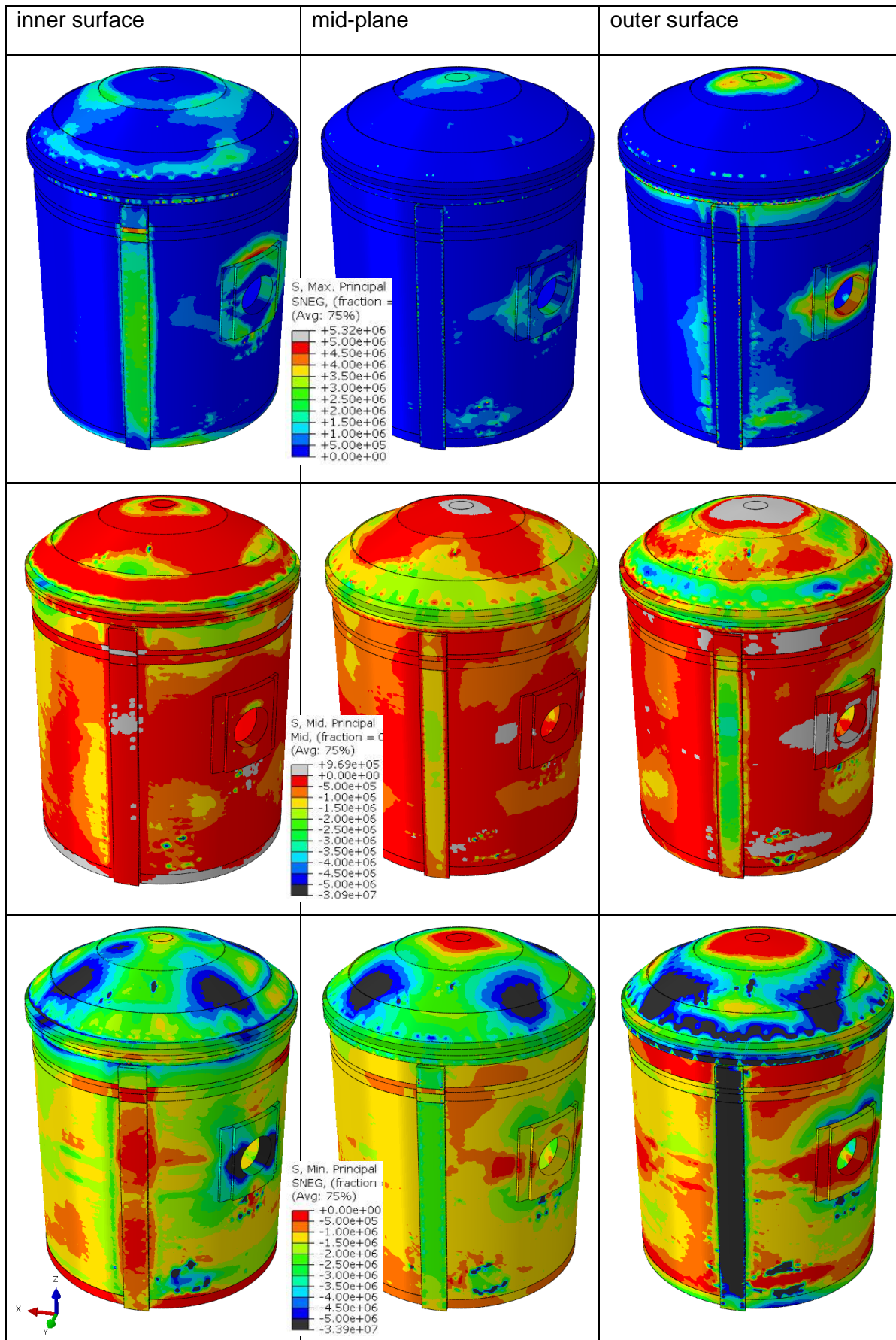
Figure 4. Principal stresses in the cylindrical wall during overpressure (from 200 gr to 400 gr).

CRACKING EVALUATION

In this section an estimate of the crack density, length and width is performed. The estimation of the crack width is based on the FE analysis. A crack in the concrete may develop if the maximum principal stress exceeds zero in the model. The maximum crack width is determined by multiplying the strain magnitude with the characteristic element length in the areas where the stress in the same direction exceeds zero. Only the results during the overpressure are considered, since the leakage was measured during the pressure test. Only through-wall cracks are considered. It is assumed here, that the cracks will only grow in radial direction, i.e. they will not extend from one location to another. A model with solid elements for the concrete would give more detailed results and the cracking would be easier to evaluate visually from the field output results.

By viewing the hoop and vertical stress distributions of VTT model in, it can be seen that there are hardly any locations where the stress clearly exceeds zero at both inner and outer surface. This suggests that there cannot be any hoop or vertical through-wall cracks. According to calculated strains, there are not any location with high tensile strain at both inner and outer surface.

By viewing the maximum principal stresses in Figure 3 (the topmost plots), it can be seen that only in the left and right side of the equipment hatch the stress clearly exceeds zero throughout the thickness of the wall. The maximum principal strain varies from approximately 30 μm/m (0.003%) to 100 μm/m (0.01%) through the thickness of the wall. Tensile damage which is one output parameter of the CDP material model is one way to estimate cracking. It suggests that there might be through-wall cracking below the equipment hatch, to the right from the tendon pilaster near the gusset and at some even smaller areas in the dome. The high strains in small spot-like areas near the pilaster are probably unrealistic results due to numerical problems. They are left without consideration here.

Based on this examination of the stress and strain results, the only through-wall cracks are located on the both sides of the equipment hatch. To be conservative, it is assumed, that there are two cracks which are both 2 m long and the crack width is formed within 3 elements. Thus, the crack width is 0.01% multiplied by the size of three elements (0.3 m), which gives 0.00003 m or 0.003 mm. The evaluated cracks are shown in Figure 5.

Area	Inner face		Outer face		Through-wall		
	total length	max opening	total length	max opening	total length	max opening	spacing
gusset	2000 mm	0.1 mm	2000 mm	0.1 mm	2000 mm	0.01 mm	100 mm
hatch area	2000 mm	0.1 mm	2000 mm	0.1 mm	2000 mm	0.01 mm	100 mm
cylindrical part (wall)	5000 mm	0.01 mm	5000 mm	0.01 mm	2000 mm	0.005 mm	100 mm
dome	1000 mm	0.01 mm	1000 mm	0.01 mm	1000 mm	0.005 mm	100 mm

Figure 5. Evaluated cracks in the structure.

LEAKAGE ESTIMATION

The leakage through the containment has two significant mechanisms, gas flow through cracks and permeable flow through concrete. Gas flow estimation through cracks follows the assumptions according to for instance Rizkalla et al. [6]. This is described in the previous benchmark paper [3]. The model employed in this study is the Badoux model [7]. The permeable flow through the concrete is solved here by [8, 9].

The few cracks predicted by the FE analysis described above are too narrow for leakage estimation. It is thus concluded that the leakage will be merely due to permeable flow through the porosity of the concrete (shown in Figure 6). From the experimental results, it can be assumed, that the main leakage mechanism also in the real test containment is the permeable flow. Only the gusset has through-wall cracks that are wide enough for leakage. VTT model does not consider the gusset area detailed enough to assess cracking and leakage. From the experimental results given after the previous benchmark, it is seen that the degree of saturation in the test containment during the pressure test was still considerably high.

Global air leakage at the end of 4,2 bar (rel) level (Nm^3/h)				Local air leakage at 4,2 bar (rel.)		
			Area	VD1	VD1bis	VD2
1st Pressure test ('Pre-op')	7.7		gusset	1	1	1
2nd Pressure test ('VC1')	9.5		hatch area	1	1	1
3rd Pressure test ('VD1')	3		cylindrical part (wall)	0.5	0.5	0.5
4th Pressure test ('VD1 bis')	3		dome	0.5	0.5	0.5
5th Pressure test ('VD2')	3					

Figure 6. Estimated leakage.

CONCLUSIONS

The numerical analyses were successful in the sense that the models worked, simulations were completed, and the behaviour seemed realistic in general sense. The improved calculation model of the test containment created by VTT brought the results closer to both the experimental results. Compared to the test results, the model has globally less compression after the post-tensioning. The effect of pressurization is more evident in the test than in the calculations. VTT has initially overestimated the concrete cracking substantially. The new results do not directly indicate less amount of cracking, but with a closer examination of the FE results, it can be concluded that there might not be any cracks at all that extend through the whole thickness of the wall. In case the concrete is assumed highly saturated, the calculated permeable flow can be considered to match the experimentally measured one.

The real structure has been more in compression globally than the simulation model. The main factor for the compression of concrete is the prestressing, so there possibly is still something wrong in the simulation of prestressing or in the prestressing test data that was provided. Furthermore, the strain measurements suggest that cracks can develop only in some special locations with geometrical disturbances.

Some of the long-term effects have been taken into account simply by calculating them separately according to Eurocode and accordingly modifying the FE results afterwards. In the future, they should be more or less included in the FE model itself.

REFERENCES

[1] Corbin, M. and Garcia M. International Benchmark VeRCoRs 2015 - Overview, synthesis and lessons learnt. (2016).

[2] Calonius, K., Nilsson, T., Elison, O. and Lehmann, S. EDF VERCORS Project – Benchmark 1: Themes 1, 2 and 3. Research Report VTT-R-00016-16. (2016).

[3] Calonius, K., Nilsson, T., Elison, O. and Lehmann, S. Theme 2 and 3 of the international benchmark VeRCoRs, paper for the VeRCoRs Workshop in Les Renardières, France, 7-9 March 2016.

[4] DS SIMULIA, Abaqus Analysis User's Manual Version 6.14, (2014).

[5] Calonius, K. VERCORS Project – Benchmark 1: Themes 2 and 3 – improved model. VTT Research Report VTT-R-01041-17. (2017).

[6] S. M. Rizkalla, B. L. Lau and S. H. Simmonds, "Air leakage characteristics in reinforced concrete," Journal of Structural Engineering, vol. 10, pp. 1149-1162, 1984.

[7] M. Badoux, N. Fellay, "Swissmetro - Gas permeability of cracked concrete slabs," in MAGLEV'2002, topic 5, Lausanne, Switzerland, 2002.

[8] F. A. L. Dullien, Porous Media, Fluid Transport and Pore Structure, 2nd edition, San Diego, California: Academic Press, Inc., 1992.

[9] A. Abbas, M. Carcasses and J-P. Ollivier , "Gas permeability of concrete in relation to its degree of saturation," Materials and structures, vol. 32, no. 1, pp. 3-8, 1999.

Predictive probabilistic analysis of the long term ageing of concrete effect on the behaviour of NCBs during pressurization tests: Mechanical and tightness analysis

D. E.-M. Bouhjiti[†*], J. Baroth[††], F. Dufour[††] and B. Masson[†††]

[†] Grenoble INP Partnership Foundation – industrial chair PERENITI, Grenoble, France.
[*] Corresponding author: David.bouhjiti@3sr-grenoble.fr / david.elmahdi.bouhjiti@gmail.com
[††] Univ. Grenoble Alpes, CNRS, Grenoble INP, 3SR, F-38000, Grenoble, France
Julien.baroth@3sr-grenoble.fr/frederic.dufour@3sr-grenoble.fr
[†††] Electricité de France (EDF-SEPTEN), Lyon, France
Benoit.masson@edf.fr

ABSTRACT

This contribution aims at defining a Stochastic Finite Elements Method to deal with concrete ageing in large concrete structures; particularly Nuclear Containment Buildings. The behaviour of concrete is described using a staggered Thermo-Hydro-Mechanical+Leakage approach within a viscoelastic framework. The existence of early cracks is accounted for explicitly by reducing, locally at their position, the tensile rigidity $E_d = (1 - d_{ja})E_0$ assuming that the early age damage d_{ja} does not increase in time thanks to the prestressing loads. The air permeability of concrete is computed using a new strain-based permeability law which accounts for the loading and unloading cycles during the pressurization and a residual permeability where cracks have developed. After quantifying the variability of the most influential inputs (mainly the prestressing and pressurization loads, drying and permeability properties), the THM-L model is coupled to a non-intrusive Polynomial Chaos Expansion based strategy. The Gauss-Quadrature method is used to define the various polynomial coefficients and, once the meta-model defined, Crude Monte Carlo Method is applied to achieve probabilistic analysis. The proposed SFEM is applied and validated using a Representative Structural Volume based analysis of the VeRCoRs mock-up. The obtained results show good agreement with in situ measurements variance and demonstrate the need for probabilistic approaches for a realistic and accurate prediction of concrete ageing in large structures.

INTRODUCTION

The long term ageing of prestressed concrete structures refers principally to their delayed behaviour due to drying and creep phenomena. These elements are responsible for prestressing losses and air tightness decrease in the concrete volume. There accurate prediction is, therefore, a critical step for the assessment of concrete structures' serviceability and durability.

In most existing works, the modelling of concrete's ageing in large structures is based on a deterministic approach [1]. That includes homogeneous thermal, hydric and mechanical (THM-L) boundary conditions and constant concrete hydric, viscoelastic and permeability properties. Yet, at the structural scale, these hypotheses remain strong as the scattering of THM-L boundary conditions and the intrinsic variability of concrete properties have a non-negligible effect on the observed THM-L response [2][3][4]. As a consequence, deterministic approaches lack the physical representativeness of the global structural behaviour as there meaning remains local for a particular defined boundary conditions and a given set of values of concrete properties. To overcome such limitations and enhance the predictiveness of models, a probabilistic framework is required. However, given the necessary

computational time for such non-linear system of equations, the use of Crude Monte Carlo based on Finite Elements Analyses (FEA) remains hard to achieve. Alternative methods need to be defined for practicality and feasibility purposes (such as Surface Response based Methods (SRM) [5]). Accordingly, this paper is divided into three parts:

- **The first one** recalls the weakly coupled THM-L model [6][7] within a viscoelastic framework (the effect of early age damage on the global behaviour overlooked).

- **The second one** presents the selected non-intrusive stochastic approach for probabilistic analysis and global sensitivity analysis. Herein, the Polynomial Chaos Expansion (PCE) method [5] is used to define a meta-model of the saturation rate and delayed strains [8].

- **The third and final part** is an application of the previously presented methodology to the VeRCoRs mock-up [9] at the scale of Representative Structural Volumes (RSV). After introducing their geometries and the various Probability Density Functions (PDF) of the most influential parameters, the obtained polynomial surface responses are used to achieve uncertainty propagation. Predictive numerical results are eventually compared to in situ observations and the pertinence of the stochastic approach is assessed qualitatively and quantitatively.

In this work, all developments and calculations are performed using Code_Aster solver and Mfront law generator [10].

WEAKLY COUPLED THM-L MODEL

For the long term ageing phase, concrete is supposed chemically stable (the hydration process is supposed over and concrete is fully erect). Calculations are pursued from the THM state obtained at early age [3][6]. The staggered THM-L approach consists of solving, in order, the thermal, hydric, mechanical and hydraulic problems [2][4]:

- **Thermal model:** It consists of solving the classical heat equation using Neumann boundary conditions (1).

$$\frac{\partial T}{\partial t} - \frac{\lambda_c}{\rho_c\, C_c^p} \operatorname{div}\left(\overrightarrow{\operatorname{grad}}(T)\right) = 0$$
$$-\mathbf{q}.\,\mathbf{n} = h_{eq,th}(T_\Gamma - T_{ext}) \tag{1}$$

T the temperature field, ρ_c the concrete's density, λ_c, C_c^p the thermal conductivity and capacity of concrete repsectively, $h_{eq,th}$ the thermal exchange coefficient accounting for convective and radiation

- **Hydric model:** The drying problem is computed using also the heat equation involving a non-linear diffusivity factor (2). The boundary conditions are expressed in terms of the relative humidity.

$$\frac{\partial C}{\partial t} - \operatorname{div}\left(A e^{B\,C}\, \frac{T}{T_0}\, e^{-\frac{E_a^W}{R}\left(\frac{1}{T}-\frac{1}{T_0}\right)} \overrightarrow{\operatorname{grad}}(C)\right) = 0$$
$$-\mathbf{q}.\,\mathbf{n} = h_{eq,w}(RH - RH_{ext}) \tag{2}$$
$$RH = e^{-\frac{\left(\left(\frac{C}{\varphi_V}\right)^{\frac{1}{b_w}}-1\right)^{1-b_w}}{a_w}} \qquad RH_{ext} = 163.61\, \frac{r}{r+0.62}\, e^{-\frac{17.5\, T_{ext}}{241.2+T_{ext}}}$$

C the water content field, A, B fitting parameters defining the diffusivity factor $D(C, T) = A e^{B\,C}\, \frac{T}{T_0}\, e^{-\frac{E_a^W}{R}\left(\frac{1}{T}-\frac{1}{T_0}\right)}$, $h_{eq,w}$ the hydric exchange coefficient, φ_V total capillary volume, $S_r = \frac{C}{\varphi_V}$ the saturation rate, a_w, b_w fitting parameters of the desorption curve, r the mixing ratio of water in the dry air.

- **Mechanical model:** The total strain is decomposed into five components (3):

$$\boldsymbol{\varepsilon_{TOT}} = \boldsymbol{\varepsilon_{ELAS}} + \boldsymbol{\varepsilon_{TH}} + \boldsymbol{\varepsilon_{DS}} + \boldsymbol{\varepsilon_{BC}} + \boldsymbol{\varepsilon_{DC}} \tag{3}$$

$\boldsymbol{\varepsilon_{ELAS}}$ the elastic strain tensor, $\boldsymbol{\varepsilon_{TH}} = \alpha_{TH}\,(T - T_{ref})\mathbf{I_d}$ the thermal strain tensor, α_{th} the coefficient of thermal expansion, $\boldsymbol{\varepsilon_{DS}} = \alpha_{DS}\,(C - C_{ref})\mathbf{I_d}$ the drying shrinkage strain tensor, α_{DS} the coefficient of drying shrinkage, $\boldsymbol{\varepsilon_{BC}}, \boldsymbol{\varepsilon_{DC}}$ the basic and drying creep strain tensors.

Basic and drying creep terms are computed using the revisited Burgers model in [2] where the strain and stress tensors are divided into spherical and deviatoric parts to account for creep Poisson effects.

And the crack opening values are directly deduced from (4):

$$w_{ck} = h_{EF} \frac{d_{ja}}{1 - d_{ja}} \frac{<\sigma_I>_+}{E_0} \tag{4}$$

$<\sigma_I>_+$ the residual tensile stress in the concrete volume in the principal direction, d_{ja} the damage variable computed at early age.

- **Leakage model:** The equivalent permeability of concrete is expressed locally as shown in (5) [7]:

$$k_{eq} = (k_F)^{\left(\frac{<d_r - d_{lim}>_+}{1 - d_{lim}}\right)^\delta} (k_D)^{1 - \left(\frac{<d_r - d_{lim}>_+}{1 - d_{lim}}\right)^\delta} \tag{5}$$

k_F the Poiseuille's flow mode accounting for the crack's roughness and shape effects on the permeability, k_D the darcy's flow mode accounting for the effects of saturation, pressure and damage on the mass permeability. d_r, d_{lim}, δ are permeability law parameters to ensure a smooth transition from a diffuse to a localized state of permeability.

And the hydraulic system to solve writes (6):

$$\frac{\partial P_{air}}{\partial t} - \text{div}\left(\frac{k_{eq}}{\mu_{air}} P_{air} \overrightarrow{\text{grad}}(P_{air})\right) = 0$$

$$\overrightarrow{q_{flux}}(\Gamma) = -\frac{k_{eq}}{\mu_{air}} \overrightarrow{\text{grad}_\Gamma}(P_{air}) \tag{6}$$

PCE-BASED PROBABILISTIC STRATEGY

Let's consider $\mathcal{M}$ a computational model whose input parameters are represented by a random vector $X = \{X_{1 \leq i \leq N}\}$. The model's random outputs Y verify $Y = \{Y_{1 \leq j \leq N'}\} = \mathcal{M}(X)$. Given the physical nature of our problem, Y is assumed to have a finite variance and can be fully defined using a Hilbertian representation (7). Several choices are possible for the expansion basis. Herein, a particular focus is granted to Polynomial Chaos Expansion (PCE) in which the terms are multivariate orthonormal polynomials [8]. The selection of the polynomial basis $\{P_{i \in \mathbb{N}}\}$ to be associated with each random parameter X_i depends on its marginal PDF $f_i(x_i)$. For instance, and under the hypothesis of independent random variables $\{X_i\}$, standard normal distributions $X_i \sim \aleph(0,1)$ lead to the use of Hermite polynomials $\{He_i\}$ and uniform distributions $X_i \sim U(-1,1)$ lead to the use of Legendre polynomials $\{Le_i\}$.

$$\mathbf{Y} = M(\mathbf{X}) = \sum_{k=0}^{+\infty} y_k \psi_k(\mathbf{X}) \approx \widehat{M}(\mathbf{X}) = \sum_{\sum \alpha_i = 0}^{Q} y_\alpha \psi_\alpha(\mathbf{X}) \tag{7}$$

$\{\Psi_{k \in \mathbb{N}}\}$ a numerable set of random variables forming the Hilbertian basis and $\{y_{k \in \mathbb{N}}\}$ are coordinates within that basis. $\psi_{\alpha = \{\alpha_{1 \leq i \leq N}\}}(\mathbf{x}) = \prod_{i=1}^{N} P_{\alpha_i}(x_i)$ a countable orthonormal basis to represent the random response $\mathbf{Y}$. $\alpha = \{\alpha_{1 \leq i \leq N}\}$ a global index referring to the order of each polynomial α_i associated with the parameter's realization x_i.

As an infinite sum is numerically out of reach, equation (7) is approximated by a truncated expression at a given degree Q. The resultant number of terms in (7) become $\binom{N + Q}{Q} = \frac{(N+Q)!}{N!Q!}$ which increases polynomially with N and Q (curse of dimensionality). Orders around 3 to 5 are considered in practice [11].

The identification of the polynomial coefficients y_α can be achieved by regression. This however, does not take advantage of the orthonormality rule of the basis $\{\psi_{\alpha = \{\alpha_{1 \leq i \leq N}\}}; \alpha_i \in \mathbb{N}\}$ unlike projection methods where each coordinate y_α writes (8):

$$y_\alpha = \int_{D_X} \Psi_\alpha(\mathbf{x}) f_X(\mathbf{x}) \mathcal{M}(\mathbf{x})\, d\mathbf{x} \approx \sum_{j_1=1}^{S_1} \cdots \sum_{j_N=1}^{S_N} w_{j_1}^1 \cdots w_{j_N}^N \Psi_{\{\alpha_1,\ldots,\alpha_N\}}\left(\mathbf{x_{1,j_1}}, \ldots, \mathbf{x_{N,j_N}}\right) \mathcal{M}\left(\mathbf{x_{1,j_1}}, \ldots, \mathbf{x_{N,j_N}}\right) \qquad (8)$$

$f_X(\mathbf{x}) = \prod_{i=1}^N f_{X_i}(x_i)$ the joint PDF of the random vector $\mathbf{X}$. The problem then is reduced to the evaluation of the previous integration using classical integration methods, in particular Gauss-Quadrature-Method [10]: $(x_{k,j_k}; w_{j_k}^k)$ the integration points and the associated weights with respect to the distribution f_{X_k}. For an order Q of the PCE, Q+1 integration points are required. The numerical cost (model calls) is then $(Q+1)^N$.

Once the model's response M($\mathbf{X}$) is approximated using the PCE terms in (7-8), the resultant explicit metamodel $\widehat{M}(\mathbf{X})$ can be used to achieve uncertainty propagation using Crude Monte Carlo Method (CMCM) at low cost. Naturally the validity domain of such approach is conditioned by the extent of the selected integration points in (8).

APPLICATION: RSV-BASED ANALYSIS OF THE VERCORS MOCK-UP

The application of the probabilistic THM model described above directly to the full scale 3D model of the VeRCoRs mock-up (Figure 1a) would take unreasonable computational time. Given the structural design of NCBs and geometrical symmetries, a RSV-based approach is preferred herein. It consists of simulating each structural volume apart from the others (Figure 1b). The mechanical boundary conditions are then defined so as to take into account the structural rigidity of the absent volume. In this work, these boundaries are simplified and consist mainly of axisymmetric boundaries on the lateral edges and uniform vertical displacements on upper and lower ones. The errors induced by such hypothesis on the stress distribution in particular areas such as the gusset and O-ring [2] are accounted for directly when defining the probabilistic distribution of prestressing and pressurization loads within the concrete volume (Table 1).

(a) Full 3D

(b) RSVs

Gusset (1 lift - 15°) Wall (1 lift - 15°) ¼ of EAH (3 lifts - 30°) Dome+O-ring (4 lifts - 15°)
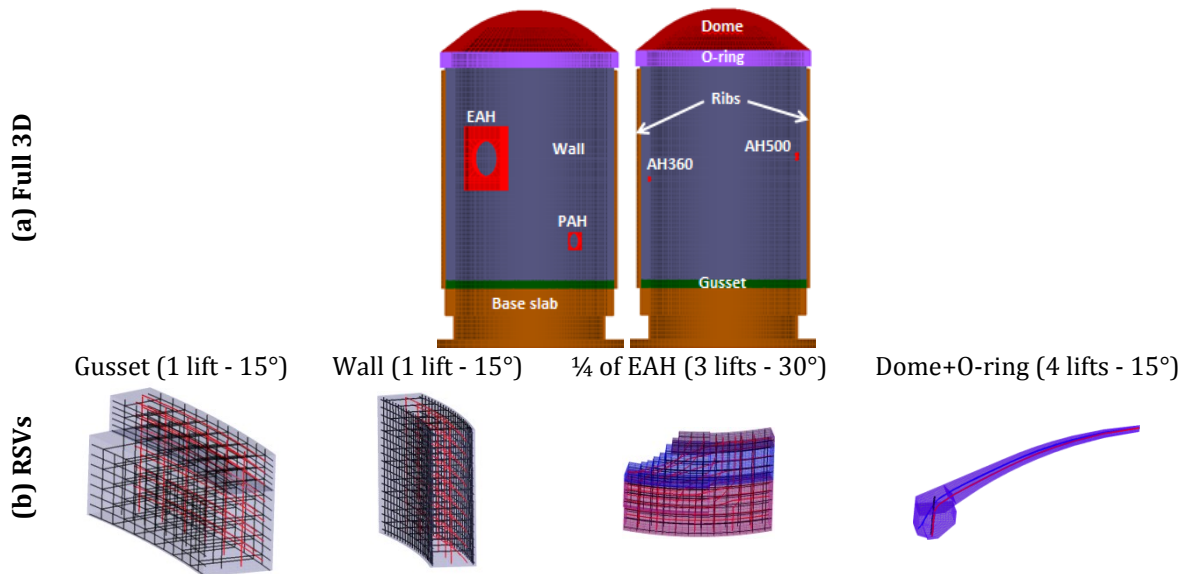
Figure 2. Rheological model of the drying and basic creep components

Based on a previous sensitivity analysis [6], it has been demonstrated that the most influential parameters with regards to concrete ageing are the drying parameters B, C_{ref}, the mechanical parameters $\sigma_{PRES}, \sigma_{PREC}, \alpha_{DS}$ and [4] the permeability factors (intrinsic permeability k_0 and roughness effects). Those inputs seem to have more influence on the model's variance than the viscoelastic properties or thermo-hydric boundaries. Accordingly, the distributions in Table 2 are considered for the influential inputs.

Eventually, coupling the PCE method and the THM calculations at the RSV scale leads to the following results (for the sake of succinctness, hydric and mechanical results are limited to the gusset's saturation rate and strain evolution in time during the pressurization phase):

- The mean saturation rate of concrete at the VeRCoRs gusset level (Figure 3a) is expected to evolve from 80 % ($\pm6\%$) to 65 % ($\pm12\%$) within 6 years of drying under usual operational loads

(Temperature of 35°C±40%). The chances of the saturation rate to be less than 40 % (the diffusivity factor in (2) is only valid for relative humidity values higher than 40 %) are of $P(S_r<=0.4)=0.13$. For such configuration, the drying model needs to be revisited as the concrete's hydric transfer properties are no longer defined by water particles diffusivity but by the air vapour's. Unfortunately in situ measurements of the saturation rate are restricted. So, no comparison between the model's response and the observations on site is performed. However, the model's accuracy is evaluated through the strain (vertical and tangential components) estimation. Indeed, the total strain is dependent on the water content field (particularly drying shrinkage and creep) and can be used to assess the pertinence of both drying and mechanical calculations.

Table 1. Results from a full 3D-ELAS FE analysis of the VeRCoRs mock-up during prestressing (accounting for realistic cables' deviations, instantaneous losses) and pressurization (relative pressure of 4.2 bars) phases

RSVs	Prestressing ($\sigma_{PRES} \leq 0$)				Pressurisation ($\sigma_{PRES} \geq 0$)			
	Vertical		Tangential		Vertical		Tangential	
	μ (MPa)	CoV* (%)	μ (MPa)	CoV* (%)	μ (MPa)	CoV* (%)	μ (MPa)	CoV* (%)
Gusset***	4.6	45	0.8	38	2.6	66	1.0	53
Wall	6.0	24	9.0	30	3.5	26	6.0	34
EAH	6.4	70	8.0	58	2.9	85	6.5	64
Dome**	1.8	95	6.4	57	0.9	137	3.4	95
VeRCoRs	4.2	62	7.5	48	2.4	71	4.7	65

*CoV: Coefficient of Variation. ** For the dome (spherical coordinate system): vertical = tangential and tangential=circumferential. *** For the gusset stresses are defined by inverse analysis of the observed strain increments during the tensioning and pressurization phases. Given the strong heterogeneousness of the restraining effects due to early age damage and the different mechanical behaviour of concrete at the casting joints, such randomness is hard to achieve numerically.

Table 2. Probability Density Functions of the influential parameters

| Parameter	Unit	Mean	CoV (%)	Distribution	Number of Gauss points
B	-	0.05	20	Uniform	
C_{ref}	Liter/m³	132	20	Lognormal	
σ_{PRES}	MPa	Table 1		Lognormal	4
σ_{PREC}				Lognormal	
α_{DS}	μm/m/(liter/m³)	7.1	10	Lognormal	
k_0	m²	5.4 10^{-17}	50	Lognormal	

- In Figure 2b-c, the mean and the confidence intervals of the tangential $\varepsilon_T^{RES} = \varepsilon_{TOT}^T(t = t_{PRES})$ and vertical $\varepsilon_V^{RES} = \varepsilon_{TOT}^V(t = t_{PRES})$ total strains (respectively) are shown during the pressurization phases (PO: 1.3 yrs, VC:1.51 yrs, VD1:2.6 yrs, VD1': 2.61 yrs, VD2: 3.67 yrs, VD3: 4.75 yrs, VD4: 5.81 yrs, VD4': 5.86 yrs, VD4'': 6.01 yrs). Based on the measurements from sensors F1to4 and G1to4, the model shows good agreement with the observed strains during the first two pressurization tests. In the tangential direction, the first mean estimate is rather underestimated by the model whereas the second is well predicted (gaps less than 180 μm/m). In the vertical direction, the mean estimate is first underestimated and for the second overestimated (gaps less than 150 μm/m). However, one should note that, for such assessment, it is assumed that the 8 sensors that are used are representative of the gusset's global behaviour. This hypothesis remains unverified. In terms of variance, in situ measurements show a coefficient of variation around 70 % whereas the used CoVs in Table 2 lead to a 120 % and 80 % variation during the first and second pressurization tests respectively. Finally, one can notice that the performed predictive probabilistic analysis allows the identification of a confidence interval bounding in situ measurements. This enhances the predictiveness of the used FE model and leads to a global assessment of concrete behaviour in the gusset level. One is informed that similar results are obtained for the wall's, EAH's and dome's RSV.

- In Figure 3, the mean and the confidence intervals of the total leakage rate (Poiseuille's and Darcy's) through the VeRCoRs mock-up are shown. Calculations are performed at the RSV scale under the following hypotheses (Figure 1):
- Only the gusset is supposed to develop early age cracks.
- After prestressing, the number of cracks is supposed constant throughout the lifespan of the

mock-up (demonstrated numerically in [3]).

- The air leakage through porosity lines and punctual defects have been added a posteriori (they are not included in the FE model).

- The Poiseuille's flow is estimated based on the number of cracks identified at early age using a predictive stochastic approach [12].

- Only the mechanical boundary conditions at the gusset level have been calibrated based on strain measurements on site (Table 1).
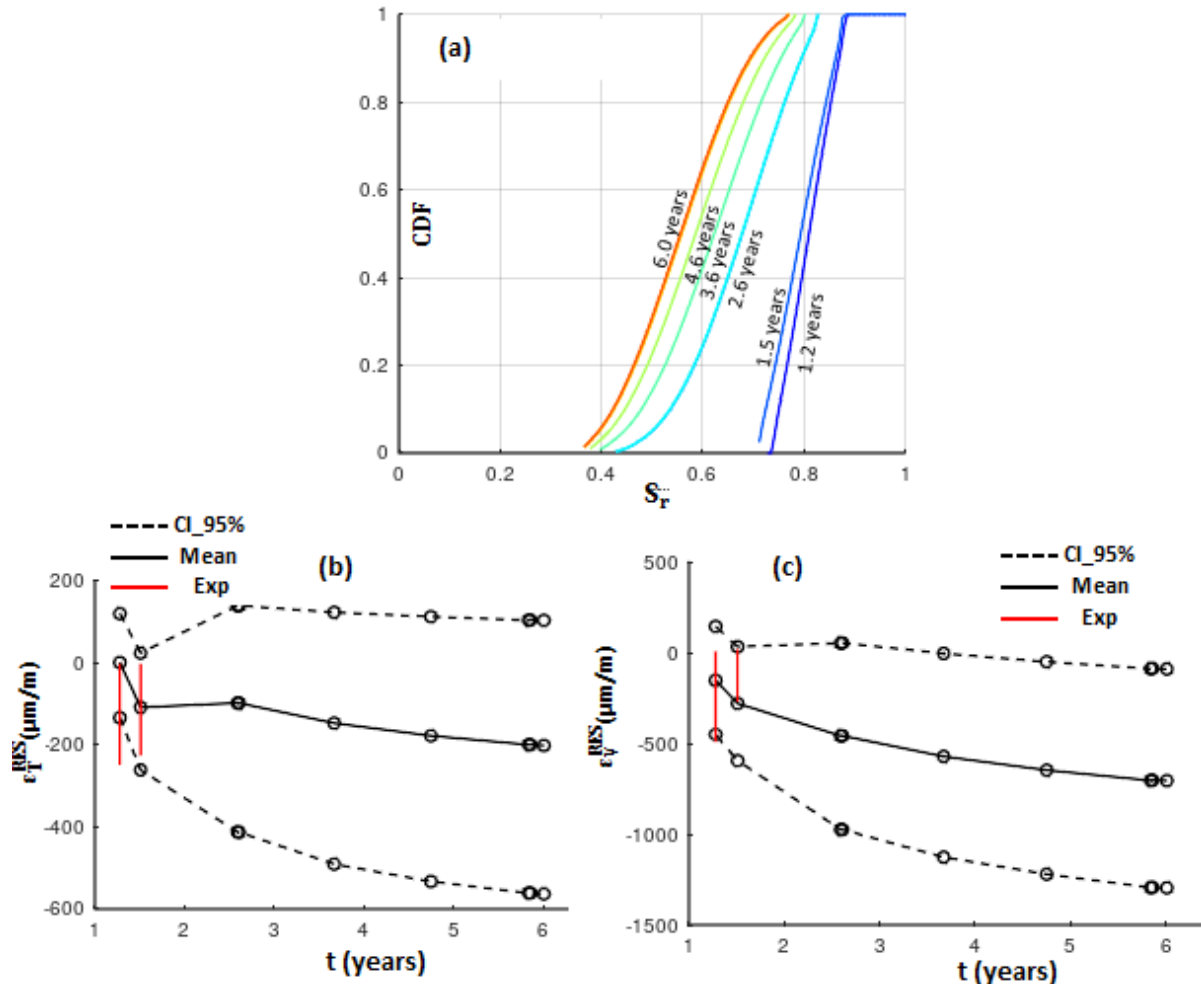
Figure 2. (a) Cumulative Density function of the mean saturation rate in the VeRCoRs gusset (b) The tangential strain at the gusset level during the pressurization phases (c) The vertical strain at the gusset level during the pressurization phases (sensors G1-4/F1-4)
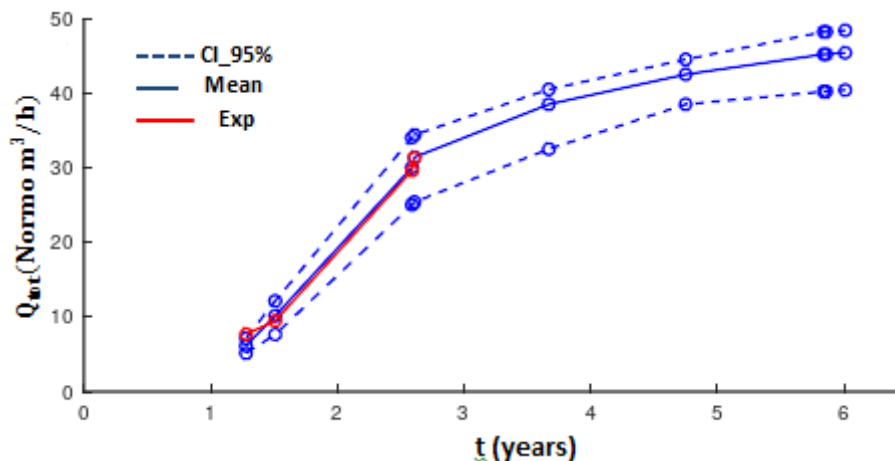
Figure 3. Estimation of the total air leakage rate through the VeRCoRs mock-up.

The obtained results show good agreement with in situ observations. Nevertheless, it is worth

mentioning that, by comparing each leakage mode separately, the model underestimates the air leakage through cracks and overestimates the one through the concrete mass. But such analysis remains strongly dependent on the precision of the localized leakage rates (a priori highly uncertain). So, it is preferred herein to assess the model's predictiveness based on the total air leakage rate. Quantitatively, the VeRCoRs mock-up air leakage rate is expected to reach 45 Normo m^3/h by the end of its operational lifespan.

CONCLUSION

Eventually, the suggested approach is recommended for NCBs probabilistic structural analysis within a reasonable computational cost (for the VeRCoRs mock-up, the cumulated computation time is of 40 days per RSV – such time can be greatly reduced by using a proper parallelization technique).

REFERENCES

[1] M. Corbin, M. Garcia, ''Benchmark VERCORS report'', (2015)

[2] D. E.-M. Bouhjiti, M. Boucher, M. Briffaut, F. Dufour, J. Baroth, B. Masson, ''Accounting for realistic Thermo-Hydro-Mechanical boundary conditions whilst modeling the ageing of concrete in nuclear containment buildings: Model validation and sensitivity analysis'', *Eng. Struct*, **166**, 314–338 (2018)

[3] D. E.-M. Bouhjiti, M. Blasone, J. Baroth, F. Dufour, B. Masson, S. Michel-Ponnelle, ''Statistical modeling of cracking in large concrete structures under Thermo-Hydro-Mechanical loads: Application to Nuclear Containment Buildings. Part 2: Sensitivity analysis'', Nuc. Eng. Des., **334**, 1-23 (2018)

[4] D. E.-M. Bouhjiti, J. Baroth, F. Dufour, B. Masson, ''Prediction of air permeability in large RC structures using a stochastic FE THM modeling strategy'', *Proc. of Euro-C Int. Conf.* (2018)

[5] G. Blatman, B. Sudret, ''An adaptive algorithm to build up sparse polynomial chaos expansions for stochastic FE analysis'', Prob. Eng. Mech., **25**, 2, 183-197 (2010)

[6] D. E.-M. Bouhjiti, J. Baroth, M. Briffaut, F. Dufour, B. Masson, ''Statistical modeling of cracking in large concrete structures under Thermo-Hydro-Mechanical loads: Application to Nuclear Containment Buildings. Part 1: Random field effects (Reference analysis)'', Nuc. Eng. Des., **333**, 196-223 (2018)

[7] D. E.-M. Bouhjiti, M. Ezzedine El Dandachy, F. Dufour, S. Dal Pont, M. Briffaut, J. Baroth, B. Masson, '' New continuous strain-based description of concrete's damage-permeability coupling'', Num. & Ana. Meth. in Geom., In press. (2018)

[8] B. Sudret, ''Global Sensitivity analysis using polynomial chaos expansions'', *Reliab. Eng. Safety*, **93**, 7, 964-979 (2008)

[9] VeRCoRs project description and data available at: https://fr.xing-events.com/OLD-EDF-vercors-project.html / https://www.conference-service.com/EDF-VeRCoRs-Benchmark-2018/welcome.cgi

[10] Code_aster® software: www.code-aster.org/Mfront® software : www.tfel.sourceforge.net

[11] J. Baroth, D. Breysse, F. Schoefs, ''Construction Reliability: Safety, Variability and Sustainability'', (2011)

[12] S. Michel-Ponnelle, D. Bouhjiti, F. Dufour, B. Masson, J. Baroth, M. Briffaut, ''Modélisation des aléas et incertitudes associés au comportement Thermo-Hydro-Mécanique des enceintes de confinement'', *Journées des Utilisateurs Salomé-Méca*, (2018)

Session VeRCoRs
(workshop & TINCE)

- **VeRCoRs program : what is going on, what will go on**

  B. Masson, M. Corbin & J. Niepceron (EDF – Direction Technique)

- **How to characterize the airtightness of containment structures. Overview of monitoring techniques tested on VeRCoRs Mock Up**

  Jean-Marie Henault [1], Pauline Laviron[1], Solenne Desforges[2], Denis Vautrin[1], Alexis Courtois[2], Benjamin Martin[3], Alexis Legrix[4]
 *([1]EDF R&D PRISME, Chatou, [2]EDF DPIH DTG, Lyon, [3]EDF DI TEGG, Aix en Provence, [4]EDF R&D MMC, Moret Sur Loing – France)*

- **VeRCoRs digital twin and its tools**

  G. Boulant[1], C. Toutlemonde[2], F. Hamon[1], J-P. Mathieu[2]
  [1]EDF-R&D, EDF Lab Paris – Saclay - 7 bvd Gaspard Monge - 91120 Palaiseau, Fr
  [2]EDF R&D, EDF Lab Les Renardières – Avenue des Renardières - 77250 Ecuelles, Fr
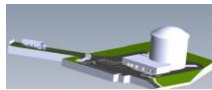
VeRCoRs program : what is going on, what will go on

Benoit Masson*, Manuel Corbin and Julien Niepceron

EDF Direction Technique, 19, rue Pierre Bourdeix, 69007 Lyon (France)
*Corresponding Author, benoit.masson@edf.fr:

Abstract: This paper summaries the aims of the VeRCoRs project: demonstrate the adequate behavior of a nuclear containment in case of severe accident, improve our understanding of the leakage and its evolution with the ageing, and collect experimental data necessary for the development and validation of numerical models. In order to perform those objectives a mockup at 1/3 scale, widely instrumented with numerous different type sensors was built on the R&D site of EDF in Les Renardières in 2016. This scale allows us to see in the future by accelerating all the ageing phenomena. Besides the ageing measurements (strains, temperatures, hygrometry, humidity of the concrete) and the samples testings (strength, modulus, …), pressure test are carried out as if this building would be part of the nuclear fleet of EDF. Since three years of measurements collected in the databank, it is confirmed that the ageing phenomena are significantly accelerated. The first pressure test has confirmed the representativeness of the mockup, and the leakage rate has increased in the same proportions than a real containment. Some new results has been gathered thanks to optic fiber measurements, leakage collecting boxes, gas pressure in the concrete, have led to a better knowledge of the leakage way in a prestressed wall. The creep, especially before the heating of the mock-up is not at all those attended, but confirm that the thermal activation is important.

Keywords: Ageing, Containment building, Mockup, Leakage

Introduction

The passive leak-tightness function of the French 1300-1450 MWe NPP reactor building is provided by a reinforced and pre-stress concrete inner wall without steel liner, an outer reinforced wall assuring the protection against external effects. The leak through the internal wall is collected in the annular space being permanently maintained slightly below atmospheric pressure.
The technical objective, in term of leak-tightness, is to maintain the rate of gas escape under a legal criterion. The compliance with the rule is evaluated by measuring the quantity of air leak, obtained during a periodical pressure test at ambient temperature.

Numerical models are up to now not sufficiently mature and accurate to predict the evolution of the leakage rate during these pressure tests, nor during standard design-basis accidents. In the frame of NPP life extension perspective, the project of building a reduced scale containment mock-up seemed to be a good way to obtain reliable results. The main objectives were the following:
- to demonstrate in an indisputable way the adequate behaviour of inner wall in situation of severe accident (high pressure and high temperature during two weeks);
- to have a better understanding of the leakage and its evolution with the ageing of the structure. The ageing of the mock-up will be accelerated by the scale effects

(reduced thickness, faster drying, faster shrinkage); which allows to anticipate the behavior of the real containments.
- to collect experimental data necessary for the development and validation of numerical models.

The 1/3 scale was chosen to anticipate on the containment behaviour with an accelerating factor of time. As the wall thickness will be reduced, the drying of the structure will be then faster. These will result in faster drying shrinkage and drying creep, which are supposed to be the main phenomena explaining the leak rate evolution. As the thickness is reduced by a factor 1/3, the time accelerating factor is hoped to be 9. As a consequence, extended end-of-life conditions (60 years) of a full size structure may be reproduced on the mock-up only after about 7 years.

In order to facilitate the transfer of the results from the experimental case to the NPP cases, the mock-up has to be as close as possible to the real containment building. That's why it integrates all complexities of the containment structure.

The mock-up or precisely the inner containment building, was built between May 2014 and August 2015 which according to the scale factor of 9 fits well with the real containment building erection time.

The main characteristics of the mock-up are stated below (Fig 1 and Tab 1):

	1/3 scale model	Full scale
Height from gusset to the top [m]	20.79	62.38
Internal radius of cylinder [m]	7.30	21.90
Thickness of cylinder [m]	0.40	1.20
Internal radius of the dome (tore) [m]	2.67	8.00
Internal radius of the dome (center) [m]	10.67	32.00
Thickness of the dome [m]	0.30	0.90
Free volume inside containment [m^3]	3 160	85 350

Fig 1: Scheme of the mockup   Tab 1: Characteristics of the mockup

The pressurization test were intended to be held with the same periodicity as a real containment, but with a time scale of 1/9. So, the pre commissioning test was held in December 2015, the first operational test, after about one year for a real containment, in January 2016 for the mock-up, and the decennial tests (for real containment), every 13 month. However for practical reasons, the decennial test will be held from now every 12 month. A simulation of a severe accident, with an increase of the internal pressure with air and steam is considered at the end of the research program.

To achieve the objectives of the project, VeRcOrs has been wisely and extensively instrumented furthermore numerous sample of concrete, steel rebars, tendons were sampled to characterize the materials. Measurements were taken from the first concreting and will be perform up to the end of the project, without discontinuities. The monitoring system is composed of:
- 1 meteorological station

- for the ambient air measure : 10 thermometers, 10 relative humidity sensors, 1 atmospheric pressure gage, 1 flow meter
- 12 pendulums (4 plumb lines with each 3 tables of aiming at different heights on 4 vertical lines)
- 4 vertical Invar wires
- 336 Embedded strain sensors
- 211 Thermo-sensors PT100
- 2 km of optic fiber
- 31 TDR (Time Domain Reflectometry) sensors
- 30 « pulse » sensors (permeability measurement)
- 6 dynamometers for instrumented tendons
- 160 strain gauges on rebars

Results of the program up to now

The daily measurements (strain, temperatures, and hygrometry) are available on a very large number of sensor (only few strain gauges are damaged and 80% of the optical fibre length in the wall is operable). The measurement of the global air leakage during the first four tests (pre commissioning, first test, first decennial test and second decennial test) is very accurate and the local measurements of the leakage (with collecting boxes placed on the wall and flow meter to measure the leakage) gives us lot of answer concerning the leakage through the wall. The mock-up, for ageing, for structural behavior and for patterns of leakage defects, is representative of a real containment.
In the next items, we will give you the most interesting results.

Digital twin

When we think of Digital Twin it is often mixed up with BIM (Building Information Modelling). BIM helps to design, to build and perhaps to operate the building, however the purpose of the Digital Twin is far more ambitious. It can use a part of the BIM (drawings, modelling, …), but is ultimate goal is to collect all the data (principally measurements on the structure and on samples, but visual inspections too and other kinds of results interesting for the structure), from the beginning of the erection, in the correct format, to gather the different finite element models and calculations and to aggregate this elements, calculations and data, so that the engineer could easily perform studies with variable hypothesis to better understand the ageing of the structure.
The DT emerged from the necessity to collaborate seamlessly between the specialists of the construction, the measurement, the materials experts and the calculation engineers. The design of the DT was not defined before the beginning of the project, it has significantly progressed from the first air test so that we now have an operating and efficient DT. We are now going to use the DT on real containment buildings.

Materials knowledges

To have a perfect understanding of the mock-up, the materials (cement, concrete, steel rebars, ten-dons) have to be very well defined. This is why numerous (more than 1200) samples were collected. Several laboratories (more than 40 laboratories in the international COST 1404 project for example, more than 10 in the MACENA project which the aim was the behavior in case of severe accident) have tested the samples, at early age, after ageing, and in different environmental conditions. A very large data base has been build and is still gather data today. All those data is highly valuable for the scientific community and has allowed to complete and improve the material behaviours laws.

Accelerating ageing factor

Fig 2: Accelerating factor in tangential direction

Fig 3: Accelerating factor in vertical direction

Ageing is identified by the delayed strains on the prestressed concrete structures. The expected accelerated factor for delayed strains was 9, based on the Eurocode rules for creep and shrinkage. Modelling gave us other factors, depending of the different creep and shrinkage laws, with lower values (the minor value given was 4). For the aim of the mock-up and the duration of the research program, it is very important to know the real factor, based on the delayed deformations.

To obtain the accelerating factor, a comparison is performed of the measurements of three real containments and VeRCoRs from the end of prestressing, in both tangential and vertical directions. On the graph below (Fig 2 & 3), the accelerating factor is taken to be 10 for VeRCoRs (yellow curves). It can be noticed that the yellow curves matches well with the greens (our reference). The effect of dead load, that reduce the stress and so the shrinkage in vertical direction for the mock-up, appears not to be significant.

This accelerating factor confirm that creep and shrinkage, and their relationships with water content and temperature, are not perfectly known. Indeed, some models and creep laws gave us values about of 4 or 7, and the Eurocode 9. We intend to continue our work to better understand their interdependency.

Ways of leak

Several types of measurements give us some information.

- Some pulse sensors, used to measure the gas pressure in the wall, located at different places in the thickness of the wall, show us a typical leakage through a porous medium, with an increasing of the pressure in the wall correlated with the distance from the side were pressure is applied. But some other indicated that the leakage found shortcuts in the wall. These sensors were located close to the sheath of the tendons, as it is assumed that this kind of singularity is a weak point (steel sheath is not perfectly adherent). Some tests have been performed in Grenoble INPG which show same phenomena for the rebars.

- Optic fibers are embedded in the wall, at three different thickness. This kind of device allows to see the strains, and the cracks, or more precisely the evolution of the cracks, through the wall. The graph below (Fig 4) represents a horizontal section of the containment wall and in blue, red and green, the evolutions of strain measured with the OF. Where there is an evolution on the three levels, it could be cracks going through the full depth. The black dotted lines indicate leaking cracks, and the length of the line is representative of the leakage.

Fig 4: Strain measured by OF in the depth and leakage measured with boxes

- The leakage on the wall is located by spraying soap water on the wall, and measured thanks to a leak-tight box connected to flow meter on the area where the leakage is targeted. There is a good correlation between the signals perceived by the OF showing a peak of strain through the full depth of the wall, and detected leaking cracks located thank to collecting box, however sometimes signals obtained from OF doesn't necessary lead to leaking cracks. As an explanation it may possible that for small opening the leak either a) find an easier path, b) or the crack isn't a full depth crack.

- A concrete sample has been saturated with deuterium, and placed in a tomographic device. A water pressure was applied on a face, and the progression of the water in the sample highlighted by tomography. It has appeared that the permeability was higher (so the leakage was higher) along the rebar.

To conclude about the leak, it definitely appears that the leakage, that goes majority directly through the wall, can use sometimes tortuous ways, for example along the tendons or the rebars, and probably in the areas with poor concrete quality (low cement rate, honeycombing …). More investigations must be perform to better understand and quantify this phenomenon.

Technologies benchmarking

The high density of sensors and theirs locations on the structure allow to compare different technologies that gives in theory the same measurement. To validate that the location of a OF sensor vertically on the wall gives the same results as the vertical invar wire or as the integrate measurement of the vertical vibrating wires embedded in the wall, three OF sensors have been anchored on the wall (Fig 5). The results are not coherent, it is possible that the anchorage methodology has to be improved. Another idea is to glue the OF directly on the wall.


**Fig 5-a: Position of the added FO sensor (in blue) regarding the Invar wire (in green); 5-b: anchorage**

Fig 5-c: displacements measured by invar wire (full curve) and by FO sensors (dashed curve)

Non destructive evaluations

The "Non Destructive Evaluation of containment nuclear plant structures" project (ENDE) is a French project developed with 8 partners. This project aims to control the containment of structures by Non Destructive Testing with ultrasonic, electromagnetic and electric methods. It consists to transfer the NDE technics achieved in laboratory to on site measurements. In situ measurements involved some constraints such as: the proximity of reinforcements and the properties gradients in the concrete. The testing were implemented on the VeRCoRs mock up (Fig 6), during testing stages or in normal running.

Fig 6: a) VeRCoRs containment mock-up developed by EDF, b) Ultrasonic surface wave non-contact scanner, c) Resistivity measurement, d) Diffused utrasonic waves monitoring

The results are widely described by the ENDE project, for example in [1] and [2]. As a conclusion, NDE methods can be successfully used on a nuclear power plant. To improve our understanding of the ageing and leakage phenomenon it is mandatory have to pursue research:
- On determining if a crack is a full depth crack or not on walls up to 1,2 m thickness.
- The knowledge of the water content or humidity in the wall is still not possible. However, it is possible to measure the humidity in the first centimeters of the wall and afterwards, with a numerical model, to deduce the humidity in the entire wall.

Bio healing

Bio healing research is very promising. Tests performed on samples, that the leakage through concrete cracks, could be reduced up to 70%. It has been decided to evaluate this possibility on the mock-up. The bio healing process started 8 weeks before the test, on a vertical crack and on a horizontal construction joint (at each batch of concrete), that were leaking on the test performed the year before. The two areas were just above the gusset. For the vertical cracks, no improvement has been seen. For the horizontal defect, the decrease of the leakage rate was up to 8 times. The research has to continue to understand those promising results, which could be a good way to enhance the leak tightness of the concrete structures.

Prediction of the leakage

The prediction of the leakage is one of the most important aim of the Vercors mockup. A first benchmark has been organized in 2016, and the results have shown a large dispersion of the results, with differences of about 200 times in the predictions, nonetheless nobody gave an accurate results. For the next benchmark, it is expected to obtain more accurate results. Moreover, EDF has developed a methodology that has been very close to the test results, but the physic of the models used has to be consolidated. If the global prediction is satisfying, further progress will have to be performed in order to reach a higher accuracy on each specific areas of the mock-up.

What is going on now

About the measurement devices, the mock-up is still open for new comers to evaluate a new sensor technology, as for OF strain sensor. The next step is to test OF glued directly on the wall to compare with invar wire.

About the NDE technology, further progress are on-going in the concrete moisture content (or water content) measurements. Surface sensor measurements can be quite accurate in the prediction of the water content through the thickness of the wall. This humidity gradient knowledge is of prior importance to calibrate the creep and shrinkage models. Another axis of work is to develop the cracking sensor based on sonic waves, which gave us some hopeful results. NDE technologies are more than necessary in a context of ageing structures.

This is why large samples will be build, with well-known defects, to evaluate sensors that other companies have to propose. The targeted fields are: carbonation, cracks, permeability, stiffness, strength, delamination, corrosion. If the results obtained are valid on the sample, the technology will be evaluated on VeRCoRs and used and eventually on real structures.

The next steps for the experimental program are the periodic pressure tests, every year (thanks to the accelerating factor of 10, so the test performed every ten years on a real containment are performed every year on VeRCoRs). There will be 5 more tests and at the end an ultimate test with air and steam pressure, to simulate a severe accident, could be done. This is not sure, because the representativeness of this kind of test must be demonstrated before the test would be performed.

To better understand the leakage phenomena, the execution of tests at low pressure, with some parts of the containment coated with removable coating, is studied.

Conclusion

The VeRCoRs project is now running as planned, as the mock-up has demonstrated his representativeness. Several research programs have used the mock-up (COST TU 1404 [4], ENDE, MACENA [5], …) which makes VeRCoRs concrete the most studied and documented concrete in the world. Two benchmark were done, so that the different teams can compare theirs results and improve their calculation.

VeRCoRs is still open for tests, especially for NDE tests, because these kind of methodologies will be increasingly useful to demonstrate the capacity of the structure to resist to a severe accident at the end of its life, especially for containments that are not equipped with monitoring devices.

The knowledge gathered on VeRCoRs, regarding materials, laws behaviors and the understanding of the leakage phenomenon, will be very useful to manage the lifetime of the containments, besides the digital twin that will be developed for the real containments.

It is likely that other benchmarks will be proposed, both on ageing, severe accident or NDE methodologies.

REFERENCES

[1] *"Non Destructive Evaluation of the durability and damages of concrete in nuclear power plants"* in 12th European Conference on Non-Destructive Testing (12th ECNDT)

[2] *"Non-destructive evaluation of containment walls in Nuclear Power Plants"* in 43rd Annual Review of progress in Quantitative Non-destructive evaluation, vol 36

[3] VeRCoRs website where data and results of the first benchmark are available: https://fr.amiando.com/EDF-vercors-project.html.

[4] COST TU 1404 website: more than 40 laboratories have made tests and evaluations on the VeRCoRs concrete: https://www.tu1404.eu

[5] MACENA website: https://espaces-collaboratifs-production.grenet.fr/share/page/site/MACENA/documentlibrary

How to characterize the airtightness of containment structures. Overview of monitoring techniques tested on VeRCoRs Mock Up

Jean-Marie Henault[1*]**, Pauline Laviron**[1]**, Solenne Desforges**[2]**, Denis Vautrin**[1]**, Alexis Courtois**[2]**, Benjamin Martin**[3]**, Alexis Legrix**[4]

[1]EDF R&D PRISME, 6 quai Watier, 78401 Chatou, France
[2]EDF DPIH DTG, 12 rue St Sidoine, Lyon, France
[3]EDF DI TEGG, 905 avenue du Camp de MLenthe 13100 Aix en Provence, France
[4]EDF R&D MMC, avenue des Renardières - Ecuelles, 77818 Moret Sur Loing, France
[*]Corresponding Author, E-mail: jean-marie.henault@edf.fr

Abstract: This paper deals with the different monitoring techniques performed on Vercors Mock Up to assess the leak tightness of the building during several pressure tests at about 5 bar. It addresses the different methods and shows some recent and promising results.

Keywords: monitoring, NDE, NDT, concrete, leak tightness, leakage rate, crack, containment, VeRCoRs Mock Up

Introduction

As part of EDF's continuous effort on the safety and life extension of its Nuclear Power Plants (NPPs) fleet, a large experimental mock-up of a double containment wall building at 1/3 scale has been built at "EDF Lab Les Renardières" near Paris (France).The mock up, completed at the end of 2015, is finely instrumented so that its behaviour is monitored from the beginning of the construction. The main objectives of the VeRCoRs project are to study the evolution of the airtightness under the effect of ageing and the behaviour under severe accident conditions for which the thermo-mechanical loading is maintained for several days

One of the aims of the VeRCoRs project is the assessment of the leakage rate over time. Once a year, an Integrated Leakage Rate Test (ILRT) is performed on VeRCoRs mock-up, pressurizing it at 5.2 bar. Thanks to the data provided by ILRTs, the evolution of the leak tightness under design pressure is monitored. Additional information is needed when it comes to model and predict the future containment leakage rate. For this challenging task, the modelling teams would require other data concerning the thermal-hydro-mechanical evolution of the structure.

To achieve this goal, the mock up is massively instrumented compared to real EDF's NPPs: hundreds of traditional sensors were embedded in concrete, like temperature Pt100 sensors, strain vibrating wire gauges, or surface-mounted, like pendulums, invar wires associated with LVDT sensors and dynanometers. In addition, more innovative sensors were installed like water content sensors and temperature and strain optical fiber sensors. All this instrumentation was presented in details in 0.

The paper focuses on methods used on VeRCoRs to assess leakage rate during pressure test. After describing traditional techniques used on real NPPs and reproduced on VeRCoRs, new monitoring systems tested on the mock-up are presented.

Traditional techniques

<u>Overall leakage rate measurements</u>
In France, each PWR undergoes ILRTs performed at intervals to determine the total leakage of the pre-stressed concrete containment and thus confirm the structure's ability to contain an overpressure which might arise during certain fault conditions. The ILRT is equivalent to the Type A test defined in the US regulations 10CFR50 Appendix J and in French codes RCC-G, ETC-C and RCC-CW.

During ILRT, the pressure is gradually increased (Figure 1). Once reached the ILRT pressure, the pressurized air entrance valve is shut down. A stabilization period is necessary for temperature and humidity to reach a steady state in the containment volume, in order to get accurate measurements. The global leak rate is measured by the so-called "absolute pressure decay method" which consists in measuring pressure decrease of the dry air contained in the containment and correcting them based on mean temperature and hygrometry variations. To proceed, the law of ideal gases is used as mentioned in the part M of the RCC CW code. The uncertainty of the global leakage rate is about 1%.
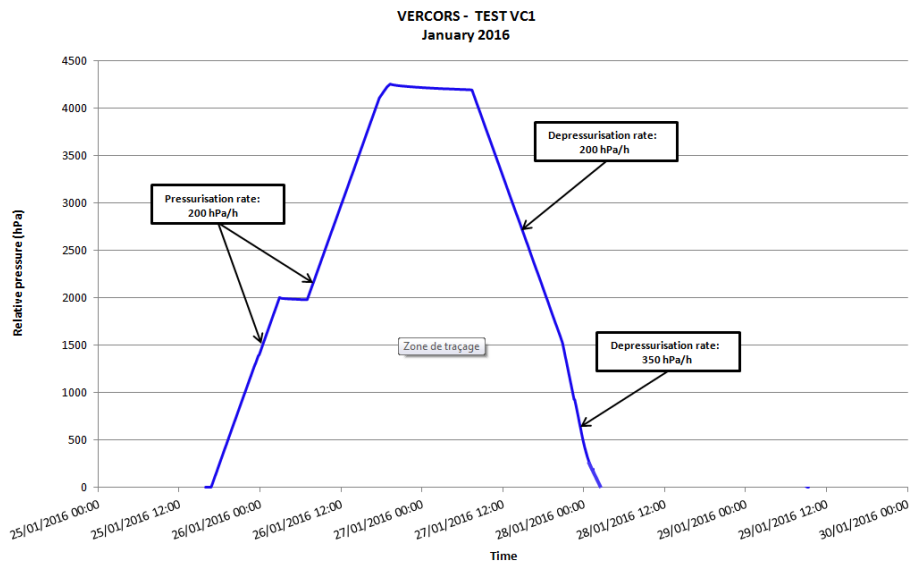

**Figure 1: pressure cycle for VERCORS ILRT.**
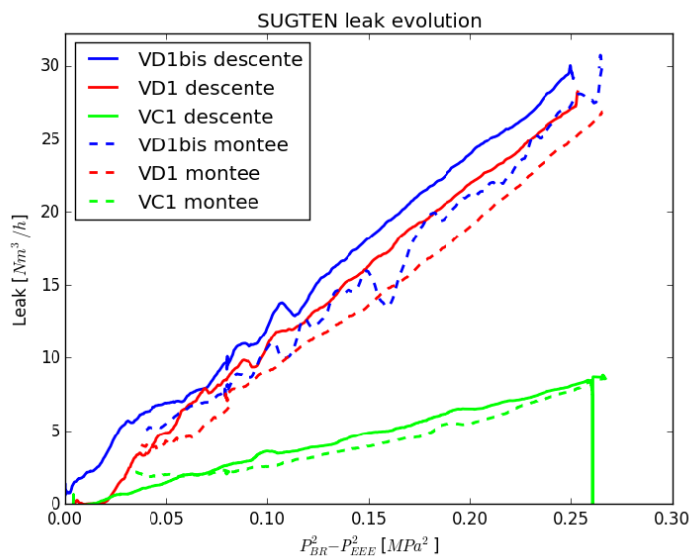
Figure 2: SUGTEN measurements during VERCORS ILRTs.

Another measurement system, called SUGTEN, allows to collect the air flow going from the pressurized concrete vessel to the space between the inner and the outer walls of the mock up. This method is similar to a laboratory permeability test, in which the concrete wall is the specimen. In steady state conditions and considering a constant permeability, the measured flow rate plotted as a straight line against the difference between the squares of pressure. This kind of curve is useful to detect some significant changes in the "overall" permeability due to new cracks appearing during the test. So far, the SUGTEN results shows linear curve (Figure 2), so we can assume that no significant damage occur during a test. But we observe also an evolution of the curves from one test to another, implying that the overall permeability of the structure is increasing with time.

Local measurements of leaks on the structure
The previous methods allow accessing an overall leakage rate. Additional measurements are carried out to collect local leaks.
During the ILRT, once reached the maximal pressure, some technician teams enter the space between the two walls. Their objectives is to detect, localize and quantify local leaks coming out from the containment wall. The method used is very simple. Technicians spray the wall locally with water mixed with soap. In the presence of a leak, bubbles form at the surface of the wall (Figure 3.a). Then technicians place a collecting box on the leaking zone and measure the flow rate with an adapted flowmeter (Figure 3.b). If the leaking zone extension is greater than the collecting box dimension, the measured flow rate is linearly extrapolated to assess to flow rate of the whole leaking zone. The advantage is to save time to be able to inspect the maximum surface of the structure. The drawback is to increase the uncertainties which can reach up to 100%. For each leaking zone, type of flaw, localization and flow rate evaluation are registered. On VeRCoRs, the whole surface is inspected. On real NPPs, it is not the case because some zones in the space between the two walls are not accessible and because the surface to inspect is much greater and the time is short. All the local leak measurements can be reported on a map to have an overview of the inspection (Figure 3.c).

(a)   (b)   (c)
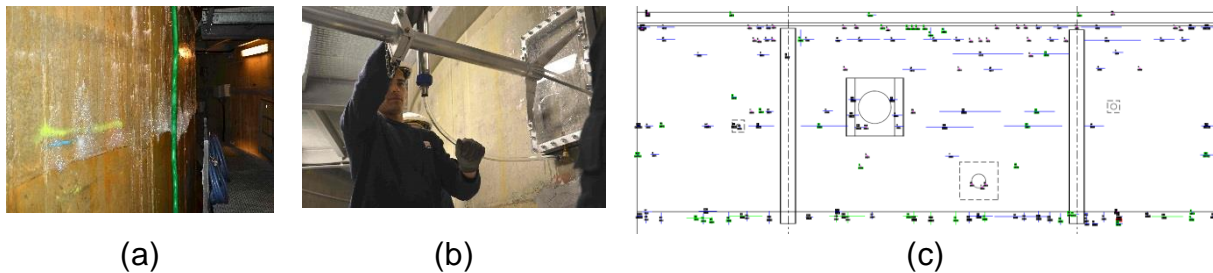
Figure 3: (a) leaking zones revealed by soap bubbling, (b) flow rate measurement with collecting box and flowmeter (c) local leakage mapping.

New techniques tested on VeRCoRs

To complete these global and local traditional techniques, new ones are tested on VeRCoRs, with two objectives:
- validating techniques to optimize the inspection on real NPPs,
- better understanding the leakage phenomenon on VeRCoRs.

Acoustic Emission
The acoustic emission technique is a passive method, well known for different applications. It is used to detect leaks in pipelines or pressurize vessels. It is also used to detect and localize cracks in concrete or in prestressed cables in civil engineering structure. This technique is tested on VeRCoRs to detect and localize leaking zones. It consists in measuring the vibrations induced by the air flow through the wall thickness and propagating inside concrete

when the containment building is under pressure. The objective is to localize the areas on the external wall with high leakage rates. More precisely, we aim at distinguishing between three levels of leakage rates (low or inexistent, moderate and high).

For that purpose, several sensors (accelerometers) are fixed to the external concrete wall. Given the very low level of vibrations, high-sensitivity sensors must be used. The measurement signals are then amplified and collected on computers. Acquisitions are made all along the pressure cycle, but the signals of interest are those acquired during the pressure steps, at 2 and 4 bars. Indeed, during these periods, the measurement conditions are constant and the ambient noise level is lower since the pressurizer is not working.

For now, the measurement signals are analyzed in the frequency domain. The frequencies of interest range from about 1 to 20kHz. For each sensor and each pressure step, the amplitude spectrum is computed for each measurement and we finally consider the median spectrum. It is then compared to a reference spectrum which is computed from measurements performed before the IRLT.

An example is presented in Figure 4. It corresponds to the ILRT conducted on VERCORS in 2017. A scheme of the containment building is shown and two areas are considered. Inspection and local leakage measurements showed that in the first area, no leakage was present whereas the second area includes a leaking point with a significant leakage rate (more than 500 L/h). For one sensor in each zone, we present the reference spectrum and the spectra corresponding two the pressure steps at 2 and 4 bars. In the first case, no significant evolution of the spectrum with the internal pressure is visible whereas in the second case, the amplitude of the spectrum increases with the internal pressure on a large frequency band. Further analysis showed that with this technique, leakages with flow rates greater than 200 L/h were detectable at distances of 5 meters.
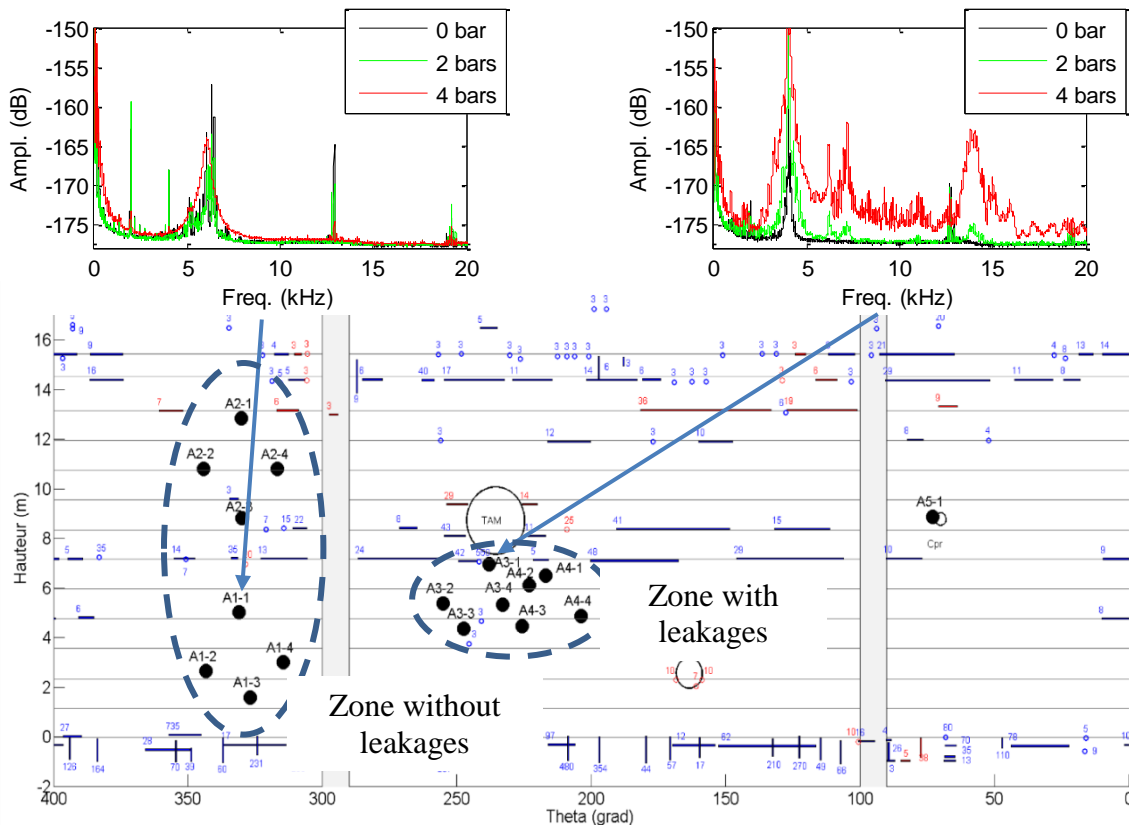
Figure 4: Evolution of the amplitude spectrum for two sensors located in two different areas (with and without leakage). Measurements obtained during the IRLT conducted on VERCORS in 2017.

Further research are currently conducted in order to produce an industrialized system enabling to inspect the whole external wall of a containment building. Research work is also conducted in order to better interpret the measurements. This technique could be used on real NPPs to

optimize the inspection. The acoustic emission results could reveal some zones of interests where the leakage is large and where the technician teams could be sent primary to make inspection and local flow rate measurements.

Crack evaluation with fiber optic

Vertical cracking was observed by visual inspection on the concrete surface in the gusset zone at the early age of the structure. This cracking phenomenon is explained by means of mechanics consideration as this specific zone is the junction between the raft and the cylindrical part. During the first two ILRTs in November 2015 and January 2016, only a few leaks appear at these crack locations. But, during the VD1 ILRT in March 2017, the global leakage rate increased a lot and many new leaks came from these cracks. To quantify the crack opening and to know more about the crack paths through the wall, it was decided to make specific Rayleigh measurements in the fiber optic cable embedded in the gusset, during the VD2 ILRT in March 2018. Moreover, to improve our knowledge on the relationship between cracking and leaking, collecting boxes equipped with automatic flowmeters were installed to monitor continuously several vertical cracks in the gusset during the VD2 ILRT (Figure 5).


Figure 5: Flowrate monitoring installation of a vertical leaking crack in the gusset.

As described in 0, fiber optic cables were embedded in concrete and connected to Raman and Brillouin interrogators to measure temperature and strain profiles in the structure. For the VD2 ILRT, a complementary Rayleigh interrogator was installed in the space between the two walls of the containment building and connected to 5 horizontal loops of the fiber optic cable embedded in the gusset zone (Figure 6). This interrogator enables to measure automatically strain profile in the optical fiber. It has a short range but is very sensitive and highly resolved. It was proved to be able to monitor cracks in terms of detection, localization and even opening quantification 0. In measured strain profiles, cracks appear as peaks. The peak shape represents the mechanical transfer function of the optical fiber cable in concrete. And the peak area corresponds to the crack opening. Based on 0, a data processing was developed to analyze the strain profiles automatically. Results in peak detection and quantification are greatly dependent on baseline evaluation in strain profiles. A morphological filter was found to be the most efficient to fit the baseline. Then, peaks are localized by maxima detection. A control step is performed by checking the peak shape. The theoretical peak shape could be approached by an exponential function corresponding to the Mechanical Transfer Function from the concrete to the optical fiber through the coating of the cable. The peaks which fit badly are removed. Finally, crack opening is estimated by calculating the area of the peak. An example is shown on Figure 7.
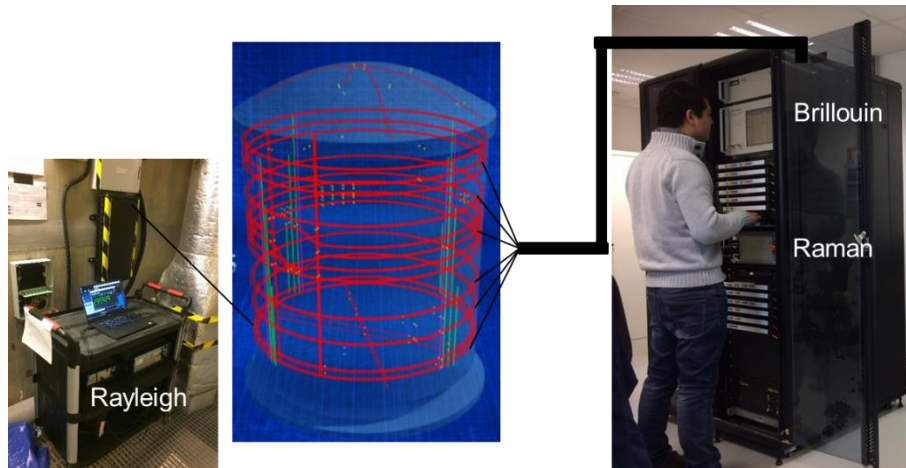
Figure 6: Fiber optic installation on VeRCoRs.
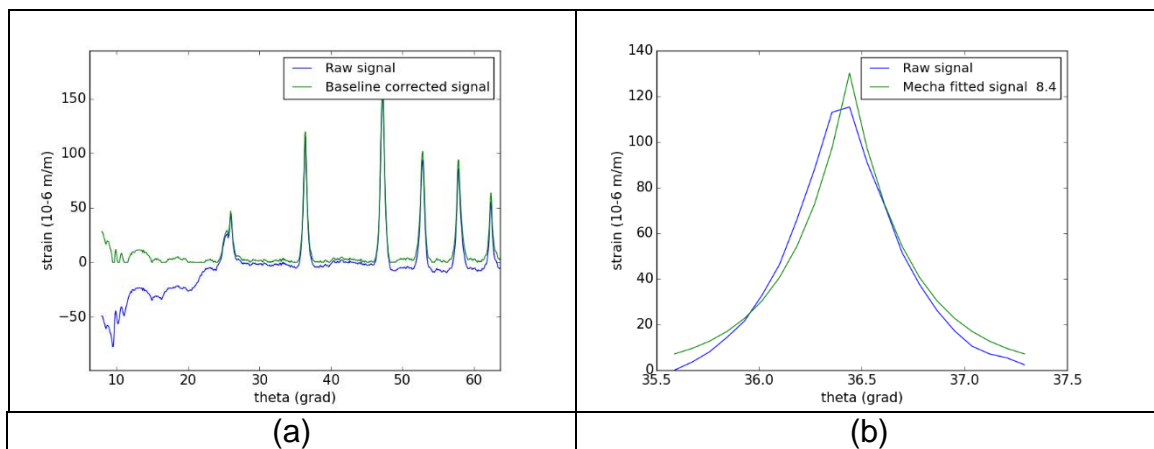
Figure 7: (a) Example of Rayleigh measurements before and after baseline correction and (b) peak shape control and area calculation leading to a crack opening of 8.4 µm.

Figure 8.a presents the localization of the fiber optic cables in the wall in the gusset zone. Figure 8.b and 8.c present, in two ways of visualization, the results of localization and quantification of cracks thanks to Rayleigh measurements in the cables located at level -0.2m. They are compared with local flow rate measured at the outer face of the structure during the inspection. The Rayleigh results show that the crack opening values are not uniform around the gusset. The maximum value is about 15µm. The two displays reveal that almost all cracks are through cracks and that they leak. Like crack opening, flow rate values are not uniform around the gusset zone. Moreover, the correlation between crack opening and flow rate values is not obvious which confirms that the leakage through cracks in concrete is a complex phenomenon.

For the monitored cracks equipped with automatic flowmeter, it is possible to get the relationship between local flowrate, crack opening and pressure. The results obtained for a specific crack is presented on Figure 9. It reveals that flowrate and crack opening have a close evolution with pressure. A log-log analysis shows that, for the example, the dependency is proportional to $\Delta P^{1.6}$. These data are of great importance to the modelling teams who are in charge of modelling and predicting the containment leakage rate.
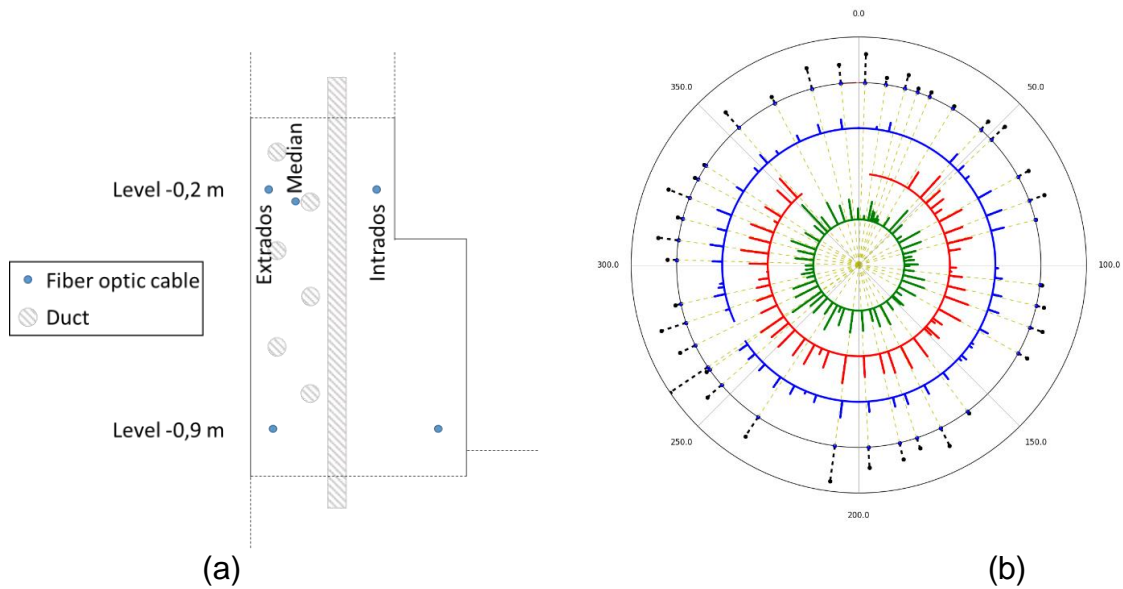
Figure 8: (a) localization of the fiber optic cable in the gusset zone. (b) and (c) mapping of cracks obtained with Rayleigh measurements at level -0.2m at 3 different depths (straight lines), compared with local flow rate measurement (dotted lines). Blue zones correspond to dead zone for Rayleigh measurements due to measuring noise or fiber cut, grey zones correspond to the two buttresses.
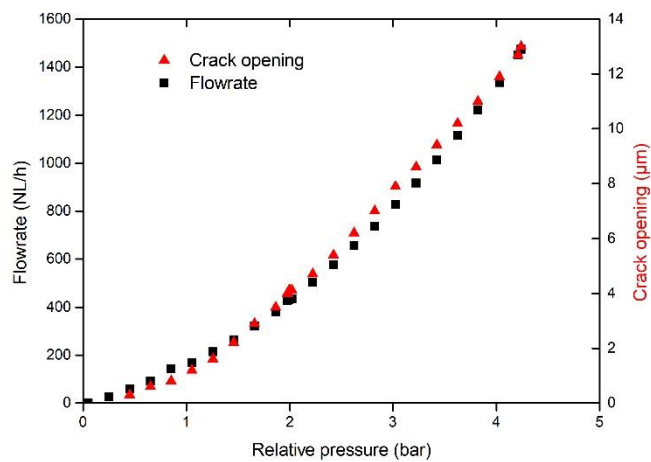
Figure 9: Flowrate and crack opening in function of relative pressure during the VD2 ILRT. The crack opening is obtained with the Rayleigh measurements for the crack at level -0.2m, at the median depth, and at 208 grad.

Conclusion

Airtightness of NPPs containment is an industrial issue for EDF. That is the reason why monitoring techniques are deployed on site to characterize global and local leakage. The VeRCoRs Mock-up is equipped with traditional techniques but also with new ones. Acoustic Emission is tested to optimize the localization of leaking zones. Fiber optic connected with a very high resolved strain interrogator enables to get crack mapping in the structure. Complementary automated flow measurements enables to determine the correlation between crack opening, local flowrate and pressure. This will help to better understand the leakage phenomenon on VeRCoRs, and will feed numerical modelling used for the prediction of the evolution of the leak-tightness in relation with ageing.

REFERENCES

[1] OUKHEMANOU et al., VeRCoRs Mock-Up: Comprehensive Monitoring System for Reduced Scale Containment Model. *Proceedings of the Technical Innovation in Nuclear Civil Engineering (TINCE), Paris, France*, 2016.

[2] HENAULT J.-M., Approche méthodologique pour l'évaluation des performances et de la durabilité des systèmes de mesure répartie de déformation. Application à un câble à fibre optique noyé dans le béton, PhD thesis, Université Paris-Est, 2013.

[3] BUCHOUD E., Détection, localisation et quantification de déplacements par capteurs à fibre optique, PhD thesis, Université de Grenoble, 2014.

VeRCoRs Digital Twin and its Tools

Guillaume Boulant[1], Charles Toulemonde[2], François Hamon[1], Jean-Philippe Mathieu[2*]

[1]EDF R&D, EDF Lab Paris – Saclay - 7 bvd Gaspard Monge - 91120 PALAISEAU, FR
[2]EDF R&D, EDF Lab Les Renardières – Avenue des Renardières - 77250 ECUELLES, FR
[*]Corresponding Author, E-mail: jean-philippe.mathieu@edf.fr

Abstract: This paper and presentation will describe the technical choices and the methodology currently set-up at EDF to create a "Digital-Twin" of VERCORS, namely: a "best-estimate" finite element model and associated scientific studies embedded in a global information system that gathers all the information and data about VERCORS. This approach is based on several computer tools that are different access levels to VERCORS, depending on the requirements of the user in terms of technical efficiency versus user-friendly interface. This organization allow a seamless dialog between teams dedicated to monitoring, concrete material surveillance, and prediction of the ageing and its effect. After having presented this setup and each of its tools, some insights in the benefits and the drawbacks of such an approach will be discussed as a prospect.

Keywords: VERCORS, mockup, digital twin, measurements, modelling, ageing

Introduction

To continue operation of its Nuclear Power Plants fleet under the optimal safety conditions, EDF launched, among others, a specific program related to civil engineering named VERCORS in the beginning of the 2010's (Masson & Corbin, 2016). VERCORS consists on the construction of a highly instrumented experimental facility that is 1/3 the size of the containment of a double-walled containment building of a French 1300MW power plant. This mockup inner wall construction was completed in 2015 at "EDF Lab Les Renardières" near Paris. The scale factor and operating conditions (assuming that drying is the main mechanism causing ageing) allows for the acceleration of ageing of this structure with a factor close to 10 times.

Thus, VERCORS allows EDF to pursue two simultaneous objectives: (i) It will provide an experimental demonstration of the inherent safety of double-walled containment building under accidental situation (LOCA) at the horizon of the fourth decennial safety assessment campaign of the power plants with double-walled containments, (ii) This facility is a unique tool to improve the knowledge on the aging mechanisms of such type of structure for the benefit of EDF as well as for the civil engineering community worldwide. In addition, three international benchmarks about civil works calculations have been recently performed: 1) on early age behavior, 2) on ageing under normal operating conditions and 3) performance under accidental situations.

A major objective of the VERCORS project is to progress on the characterization of the ageing process of the containment building, and especially on the capability to elaborate predictive models of ageing process effect on the leak rate evolution. To be fulfilled, this objective requires to federate several technical and scientific domains, the most easily identifiable being civil engineering, measurements, physics and computational physics into a consistent informational framework (Mathieu & Masson, 2017). The core functions of this

framework are (i) the capitalization of data that are considered as relevant to analyze the ageing process and (ii) a consistent set of tools to analyze these data and to elaborate ageing models.

The first function is embodied by the SYSACC system described just after, while the second function is embodied by the ARMORIC platform described in a next section. These core functions are completed by an end user interface, named CERVIN, to get a large access to the data.

SYSACC: Centralized data management and an application programming interface (API)

The system SYSACC capitalizes the knowledge of the project that is considered as relevant for analysing the ageing. Figure 1 provides a diagram that identifies the different functions of the system and the associated data flows:
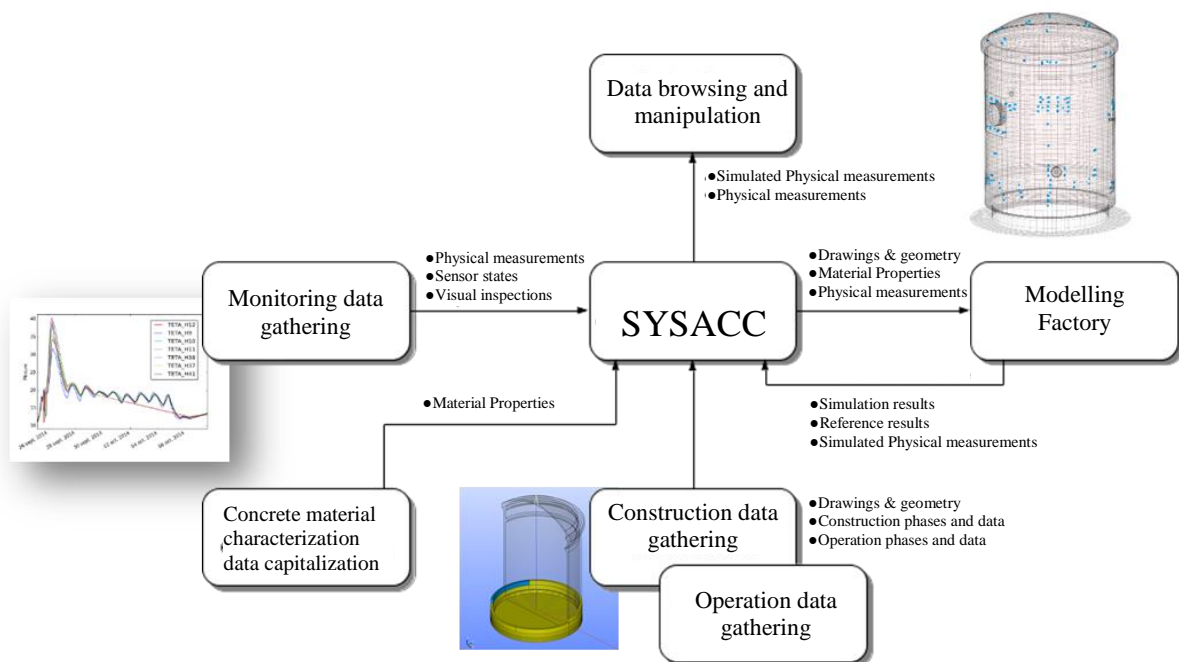
Figure 1: Main functions of the SYSACC system

The system is designed to handle several kinds of data:
- construction phases description (timing, structural work, pre-stressing sequences)
- Building construction details (casting sections, on site concrete properties, tendons, rebar, drawings)
- Operating phases description and results (visual inspections, ILRTs, global and local leak rates)
- Building auscultation and Structural Health Monitoring (sensors description, measures)
- Concretes material properties characterisation (laboratory tests)

In the global demarche towards a digital twin, it is also designed to handles other results, like "virtual measurements" that would result from the use of the other tools described in the next section.

The system SYSACC has interactions with other systems. The diagram presented below in gives a schematic representation of the global architecture of the VERCORS software framework and of the interface between its components. One can identify:

- The CERVIN web interface that uses the system to give graphical representations of monitoring data, measurements and material properties
- The ARMORIC platform that uses the system together with the SALOME-MECA (SALOME + Code_Aster (EDF R&D, 2018)) simulation platform to drive computational physics studies.
- The components ZET and KOALA that both feeds the system with metering data. They manage the data collections and data flows toward the central system. One should notice that they are
- The component CADEEX that manage the material and experimental data of EDF R&D projects, like the VERCORS project.
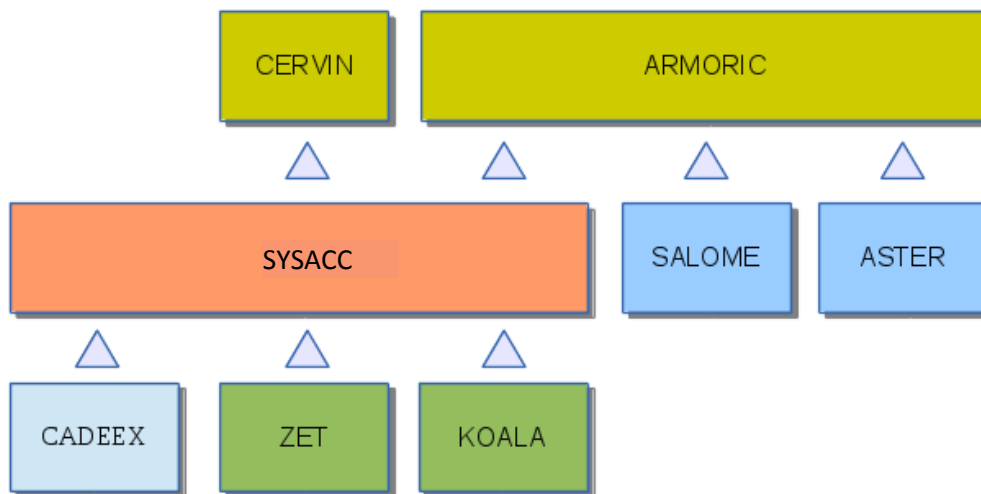
Figure 2 : Interaction between the different systems inside the VERCORS digital ecosystem

The system has different user interface. As already indicated above, one user interface of the system SYSACC is the CERVIN web application. This application is "monitoring oriented" and then restricted to measurements data (sensors and measures) and material properties (physical properties of materials around the sensors), and their "virtual" counterpart in the digital twin framework.

Natively, the system SYSACC comes with a Text User Interface (TUI) based on the Python language (Python Software Foundation, 2018) that provides the user with a Domain Specific Language (DSL) to fully interact with all data. The code below shows a simple example of the set of instructions for plotting the time series associated to temperature sensors in the concrete basement raft:

```
# Get the sensors of type PT100 thermocouple embedded in the basement raft
(code of the concrete basement raft: 1)

listSensors = recupererCapteurs(type = "PT100",
                                zone_fonctionnelle = 1)

# Select the first element of the list of sensor
capteur = listSensors[0]

# Get the measures associated to this sensor since february 2018
datafile = capteur.listerMesures(date_debut = "2018-02-12 12:00:00")
```

Figure 3 : Example of a set of TUI instructions of the SYSACC system

The DSL could be harsh to manipulate data for most civil engineers (the user needs to be familiar with some basic Python language), but it is the key for interfacing with other systems,

especially the ARMORIC platform. Indeed, the DSL can be considered as an Application Programming Interface (API): the ARMORIC platform can directly interact with the whole system through the use of this DSL.

ARMORIC, a platform dedicated to experimental data analysis and to computation

ARMORIC is a set of tools dedicated to study the containment buildings, and mainly aimed at helping the scientific approach on the VERCORS mock-up. ARMORIC manipulates both experimental data and computation tools to produce digital twins of the buildings. In this section a brief overview of the ARMORIC platform is given, then the needs for such a platform are explained. The organisation of the development is then described, as ARMORIC is a software which development will involve people that are not software developers. Finally examples of ARMORIC functionalities and studies are presented.

The context of the advanced studies on nuclear buildings explains the need for such a platform. Available experimental data on a mock-up like VERCORS becomes a huge and complex system now. If you want to really understand what is going on, you have to cross the analysis of different data that can be either experimental data or computation results. It hardly seems possible to make a complete analysis of complex phenomena like delayed strains or leak through a reinforced pressurised concrete wall if this analysis only come from experiments or from computation. In order to better understand reality, you have to build a framework that helps you to analyse both of them.

Advanced numerical studies are more and more complex. It takes time and more than one person to develop and to setup properly. Advanced numerical studies have the same technical properties as modern software codes, they need the same kind of standardisation rules to be developed in an efficient way and to reach their goal in the shortest time. A complex numerical study can be viewed as a software function or as a set of software functions.

In order to be able to develop tools that work for every building of the same kind, data and algorithms have to be managed in different spaces and with different methods. No dedicated "data" must remain in the algorithmic part of the studies.

Such complex studies might also evolve with time, they need backups, and they will not be developed by a single person. For these reasons it was necessary to propose a real framework and to develop a platform.

ARMORIC architecture has been thought in order to answer the needs of the advanced studies on containment buildings. This architecture has been designed to build a platform of standard modular tools. The different functionalities of ARMORIC work in the same way, parameters are given by the user in a parameter file.

These functionalities are numerous: there are at the present time at least fifty functions in ARMORIC platform. In order to really understand the meaning of the function an explicit name is given to every function. The beginning of the name determines the family of the functions: demo (for the functions that have been developed for a sake of demonstration), pre (for pre-processing), solver (for the functions that solve or compute problems), post (for post-processing)

When a piece of algorithm is used by at least two functionalities, it is placed in a common library. That piece of code can be shared and improved by every developer. The libraries are sorted and structured by type. There are libraries of different kinds: physics, geometry and meshing tools, post-processing, pre-processing, studies, data analysis, tests, parameter management...

The digital twins of the building are the result of complex studies. These studies need the use of a large number of functions: post-processing of experimental data, pre-processing of a computation, computation itself and then post-processing of the computational results.

In order to respect the architecture of the platform, it is necessary to determine a technical

organisation. An infrastructure is provided to help the developers do their job: release content, task and project management, code versioning, automatic tests. The rules and the infrastructure are not sufficient.

In order to really succeed in developing the platform, technical periodic meetings have to be organised to explain and discuss the different aspects of the development. Some developers with particular skills in code development and a good knowledge in technical problems addressed by the users also have to be used as mentors for other ones, and to help at the integration of the work of less experienced developers. It is also important to keep an animation of the collective: twice a year, developers and users are gathered during two days into Hackathon-like sessions that are specifically aimed at addressing common issues.

After having exposed the needs and principles of the platform, in order to better explain its nature, a few examples of the ARMORIC functionalities will be provided.

As a first example of an ARMORIC pre-processing function, a function has been developed to produce standardised parametric meshes of containment buildings (the meshes that are provided to the second benchmark participants were produced using ARMORIC). These meshes are quite complex and cannot be made with interactive tools, it is necessary to develop dedicated scripts. These scripts can be complex because the geometry of containment building is quite complex (cables, singularities), furthermore if you want to build a parametric full-hexahedral mesh: one can observe in Figure 4 an example of such a function call in ARMORIC workflow.


```
[pre_mesh_containment]
containment_names        =
vercors
simulations   =   thermic,
mechanics
refinments    =    coarse,
average
          fine
output_path = /v_benchmark
filename_base = mesh
output_formats = med,unv
```
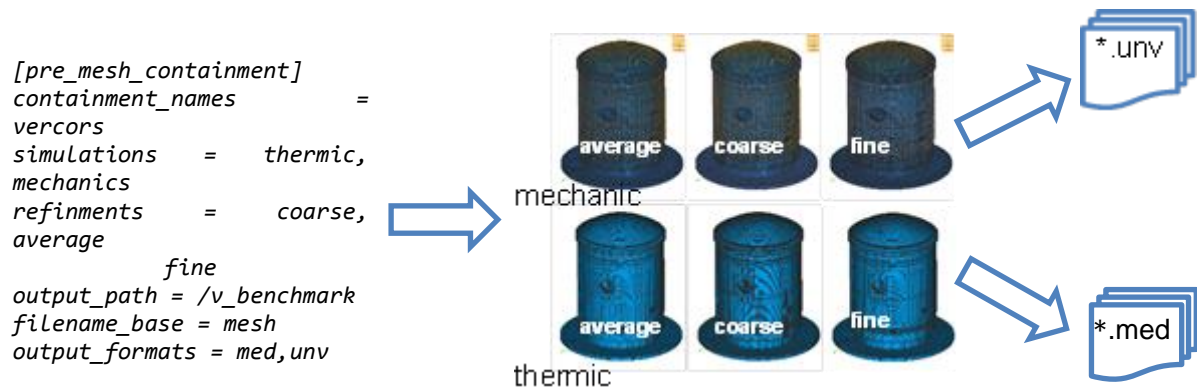
Figure 4 : Input code to ARMORIC that was used to produce the twelve Finite-Element (FE) meshes that were provided to participant to the VERCORS benchmark. This code produces : 2x2x3 meshes of different natures (with or without tendons meshed for mechanical or thermal/hydric modeling), different refinements (example for thermic mesh : fine – 1.436 Mnodes, average – 742Knodes, coarse – 353Knodes), and different output formats (med, unv).

As a second example of an ARMORIC function dedicated to experimental data, a function has been developed to clean up and extract the data of a series of sensors. TDR sensors are sensors that measure some electromagnetic property of the concrete that is related to water saturation. The relation between these quantities has been capitalised into an algorithm and it has been automatically applied to every sensors in order to estimate the evolution of water saturation in the building wall with time. Thanks to this function water content is now accurately guessed and its influence on other phenomena (leaks, delayed strains...) can now be taken into account more properly in a smooth process.

A final example can be given with a computational function base on finite elements. That function prepares *Code_Aster* input files and launches the computation on EDF's clusters or on the user workstation. That function works because it is based on the mesh produced before and also because it uses the right experimental data smoothly (like the one previously described on water saturation), see (Haelewyn, et al., 2017) (Mathieu, et al., 2018) for example

ARMORIC is a platform that has been developed to organise and capitalise both experimental

and simulation studies made on containment buildings. It is used to perform advanced studies on VERCORS mock-up. Thanks to ARMORIC studies can be developed faster and their quality are improved and controlled on a regular basis.

CERVIN: a WEB interface for measurement analysis

Previously, the system SYSACC which capitalizes the knowledge of the project has been presented. It uses a Python interface. This programming language is a guarantee of the robustness of the database and its perpetuation. Moreover, it is essential to simplify the connection with other tools such as ARMORIC and CERVIN.

However, this kind of interface can put off users because it requires to have bases in Python language. In addition, the requests to the SYSACC are done peer the Linux or Windows terminal server which can't be considered as a really friendly user interface. In July 2016, a specific Hackathon session was organized to think about the access and the analysis of data from the mock up VERCORS.

The conclusions were that it is needed to establish a simple and fast tool allowing all the users to access the data whatever operating system they use (Linux, Windows, Android ...). The tool has to be user-friendly to promote exchanges between the EDF users or outsiders.
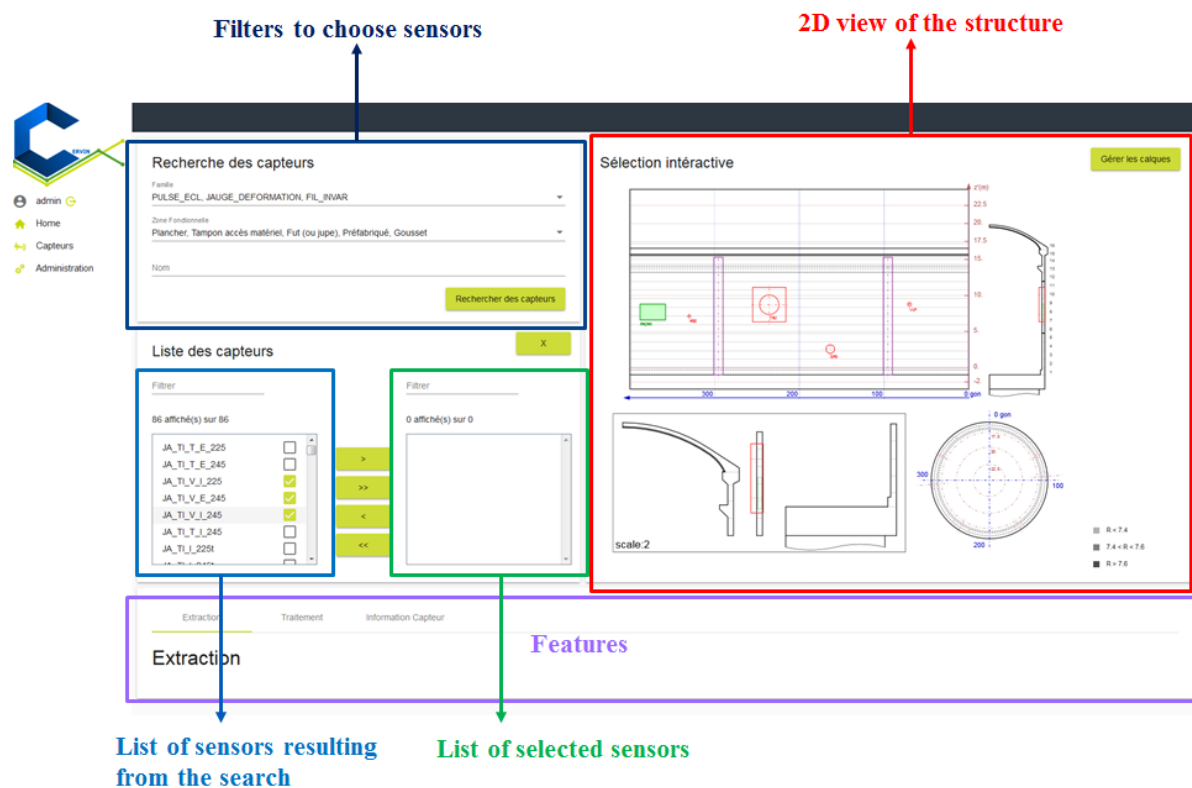

Figure 5: Home page of CERVIN to extract or visualize data from VERCORS

Consequently, it was chosen to provide a web tool to fulfill these objectives. Its name is CERVIN : (*Comportement des Enceintes de Réacteurs: Visualisation Interactive* / **C**ontainm**E**nt of **R**eactors : **V**isualisation & **I**nteractivity for **N**uclear). This section presents the features of the web tool and the futures improvement to fully integrate it in the digital twin environment.

To access to the tool, the URL of CERVIN must be entered in any web browser (FireFox, Chrome…). The connection is done by the classical way for EDF users, using EDF internal safety protocols. For external users the access will be done by their mail and password: one have to consider that working with IT department of a large company like EDF is mandatory to develop such tools in accordance with company's safety policy. The home page of CERVIN is illustrated in Figure 5.

CERVIN is composed into four main components that each provides specific features:

- Data Selection: This feature allows the user to specify which sensors they want to use or

study during their session. In order to identify the sensor, the user can indicate a sensor family (vibrating wire gage, optic fiber, PT100 thermocouple...), the name of a sensor or its belonging to a specific geometric area of the mock-up (Gusset, Dome, Concrete Basement Raft ...)

- <u>Visualization of the position of the sensor</u>: The CERVIN tool incorporates a 2D view of VERCORS where it is possible to visualize the position of the selected sensors. Each sensor has a specific color. Their coordinates are accessible as well as a color code according to their position in the wall thickness of the internal containment building.
- <u>Data extraction</u>: The previously selected data are extracted from the SYSACC database according to a given time range. In addition, the time period can be define from specific events such as the pre-stressing phases or ILRTs (*Visites Decennales: VD*). Three kinds of data can be extracted in CSV format:
  - The raw measure provided directly by the sensor.
  - The smoothed measure obtained by eliminating outliers of the raw measurement.
  - The processed measure calculated from smoothed measure. It is usually the quantities of interest
- <u>Visualization of the data</u>: this action allows the user to visualize the evolution of the measured quantities (temperature, strain ...) in the form of a graph. As the previous feature, it is possible to plot raw, smoothed and processed measures. Several settings are available at the graph (color, thickness, etc.). The data can be saved in a CSV file and the graph can be exported in SVG format.
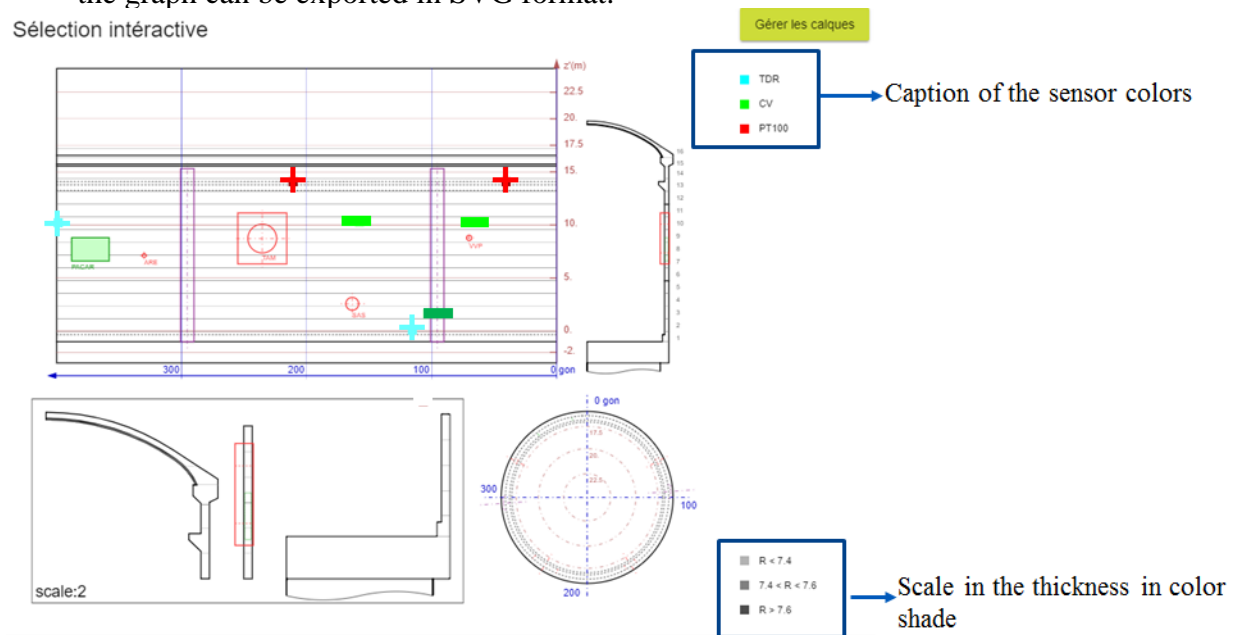

Figure 6: Visualization of the localization of the sensors on 2D view.

Some improvements will be done before the end of this year to:
- Introduce the numerical results from the digital twin. It will be possible to compare predictions from the "best-estimate" model and experimental results;
- integrate post-treatments of optical fiber and leaks measurements;
- plot 2D view of the field of numerical and experimental quantities

The development of the first functional "beta" WEB interface took less than a year. The first version is now achieved. Obviously, the development of CERVIN interface has been possible because of the efficiency and robustness of the underground tools such as SYSACC and then ARMORIC. CERVIN is a Proof Of Concept based on VERCORS. In the future, CERVIN will include features of ARMORIC and it will become the main interface of the digital twin

for civil engineers. It is also planned that its evolution could be used on nuclear sites by engineers to monitor the structures and to compare simulations with measurement in order to provide information that will be used for refurbishment operations and safety improvements.
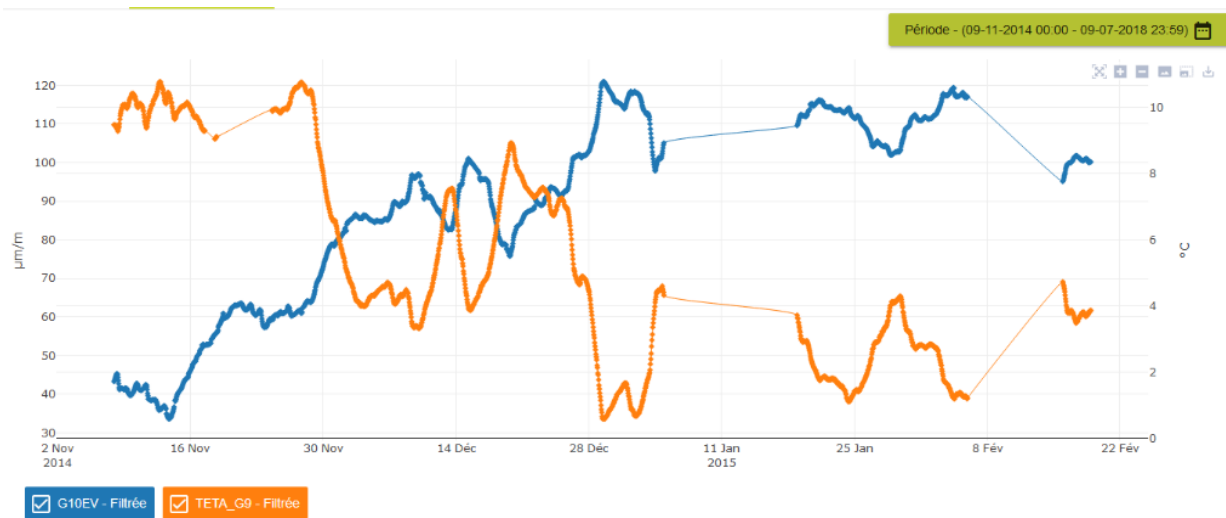
Figure 7: Example of curves plotted by the tool for two different sensors (PT100 thermocouples: time Vs Temperature, Vibrating Wire Gages: time VS strain)

Conclusion and prospects

It is quite important to insist on the fact that, according to the VERCORS team experience, no "digital twin" effort can be built in a durable manner without starting at the beginning: managing the data and establishing a unified data model, which was done by designing the SYSACC system before the first concreting. It is planned to test and provide feedback to EDF about the economical and the organizational aspects of such an approach based on the planned 7 years of VERCORS operation.

The costs are immediate and they are to be found on the organizational aspects: it is a matter of interfaces between the different technical and scientific disciplines which do not always share the same habits, the same tools or the same definition of concepts: as a matter of fact, men and tools must be able to access the information and to understand each other without further explanation and it can be done in an integrated informational approach based on computer tools: at one point there has to be a common language between every teams: for instance in this common space, file formats, tools and standards are chosen "open" and clearly specified whenever possible.

The benefits seem to be worth the effort: monitoring with innovative tools, studying ageing and interpreting its effects, comparing large experimental data set. These actions are eased providing new insights into the understanding of ageing mechanisms. Concerning VERCORS, prospects will concern the extension of such an approach to "real" containment buildings where others challenges will be faced : management of "paper" information for existing ones, integration of such tools within Building Information Modeling toolboxes for future ones.

Acknowledgment

EDF R&D teams want to thank their engineering team's colleagues for their support in building these tools. Many researchers and engineers are involved in this project, from EDF and third parties companies and laboratories and should be acknowledged.

References

EDF R&D. (2018). Salome_Meca platform. Retrieved from www.code_aster.org: https://www.code-aster.org/spip.php?article302

Haelewyn, J., Sémété, P., Mathieu, J.-p., Escoffier, F., Michel-Ponnelle, S., & Hamon, F. B. (2017). A numerical clone for VeRCoRs mock-up. Congrès Français de Mécanique. Lille. Retrieved from https://cfm2017.sciencesconf.org/129562

Masson, B., & Corbin, M. (2016). VERCORS mockup – first experimental results and synthesis of the benchmark. In RILEM (Ed.), International RILEM Conference on Materials, Systems and Structures in Civil Engineering, 1, p. 79. Lyngby.

Mathieu, J.-P., & Masson, B. (2017). The VERCORS Project - An Effort to Observe Containment Building Ageing and an Opportunity to Develop Digital Twins. In IAEA (Ed.), International Conference on Nuclear Power Plant Life Management (PLiM) for Long Term Operations (LTO). Lyon.

Mathieu, J.-P., Charpin, L., Sémété, P. T., Boulant, G., Haelewyn, J., & Hamon, F. (2018). Temperature and humidity-driven ageing of the VeRCoRs mock-up. Proceedings of the Conference on Computational Modelling of Concrete and Concrete Structures (EURO-C 2018) (p. 215). Bad Hofgastein: CRC Press.

Python Software Foundation. (2018, 07 13). Python website homepage. Retrieved from Python website: https://www.python.org/